Technische Universität München

Fakultät für Mathematik

Lehrstuhl für Numerische Mathematik

Reduced Basis Methods for Option Pricing and Calibration

Olena Burkovska

Vollständiger Abdruck der von der Fakultät für Mathematik der Technischen Universität München zur Erlangung des akademischen Grades eines

Doktors der Naturwissenschaften (Dr. rer. nat.)

genehmigten Dissertation.

Vorsitzender:		Univ.-Prof. Dr. Boris Vexler
Prüfer der Dissertation:	1.	Univ.-Prof. Dr. Barbara Wohlmuth
	2.	Univ.-Prof. Dr. Bernard Haasdonk Universität Stuttgart

Die Dissertation wurde am 04.04.2016 bei der Technischen Universität München eingereicht und durch die Fakultät für Mathematik am 20.06.2016 angenommen.

Abstract

In this thesis, a reduced basis framework for the pricing of European and American options is developed. The underlying problems are described by parametrized time-dependent variational (in-)equalities. Corresponding reduced problem formulations are introduced, a posteriori error estimates are derived, and the construction of suitable reduced spaces is worked out. The efficiency of the resulting method is demonstrated in the context of calibrating to market data and by comparing it with existing methods used in practice.

Zusammenfassung

In dieser Arbeit wird eine Reduzierte-Basis-Methode für die Bewertung von europäischen und amerikanischen Optionen entwickelt. Die zugrunde liegenden Probleme werden durch parametrisierte zeitabhängige Variationsungleichungen beschrieben. Dazugehörige reduzierte Problemformulierungen werden eingeführt, a posteriori Fehlerabschätzungen werden hergeleitet und geeignete reduzierte Räume werden konstruiert. Die Effizienz der resultierenden Methode wird demonstriert anhand der Kalibrierung an Marktdaten und durch den Vergleich mit verbreiteten Methoden aus der Praxis.

Acknowledgments

I want to start by expressing my sincere gratitude to my supervisor Prof. Barbara Wohlmuth for introducing me to this interesting topic of research and for her guidance and continuous support during all stages of the Ph.D. Her vast expertise and passion for research were truly inspiring for me and had a significant impact on my personal and professional development. Furthermore, I am thankful for her encouragement in many situations, which was a great support.

I owe my gratitude to Prof. Boris Vexler for his assistance and valuable advice, and for always having an open door for me. Moreover, I greatly appreciate his support with the funding application for the last months of the doctorate. I also acknowledge the financial support of the German Research Foundation (DFG) through the International Research Training Group (IGDK) 1754 Munich–Graz "Optimization and Numerical Analysis for Partial Differential Equations with Nonsmooth Structures".

I thank Prof. Bernard Haasdonk for introducing me to the theory of the Reduced Basis Method and for generously sharing his time and ideas during our collaboration and my research visits in Stuttgart. I have learned very much through this work, which immensely helped me in forming this thesis.

As a part of the IGDK 1754 program, I had the pleasure to conduct several research visits at the Technische Universität Graz. I sincerely thank Prof. Olaf Steinbach for providing me a warm welcome in his research group and for having time for valuable discussions, which have opened new perspectives on my research topic.

To gain an insight into the area of mathematical finance, I could rely on the help of experts in this area. For this, I am very grateful to Prof. Kathrin Glau, Mirco Mahlstedt, and Max Gaß. Our fruitful meetings, extensive collaboration, and their expertise and advice greatly helped me in shaping the application-oriented part of this work.

In addition, there are many colleagues and collaborators who were available for questions and stimulating discussions. In particular, I would like to thank Julien Salomon for a fruitful collaboration and productive conversations during the SIAM CSE conference, Linus Wunderlich for pleasant companionship during workshops and interesting discussions on the Reduced Basis Method, and Shubhangi Gupta for her

friendship and support. My special thanks go to Konstantin Pieper for many discussions on various topics of mathematics, his constant support, and encouragement.

Furthermore, I would like to thank my colleagues from the Chair of Numerical Mathematics and from the IGDK 1754 doctoral school for a friendly and cooperative atmosphere. I particularly enjoyed the time spent on the IGDK 1754 students' workshops, where I had the possibility to learn new mathematical techniques in a friendly environment.

Finally, I want to express a deep sense of gratitude to my mother, who has always stood by me like a pillar of strength in times of need. To her I owe for the constant love, encouragement, and never-ending support.

Contents

1 Introduction

Modeling financial processes is one of the most dynamically developing branches of science today. In particular, this relates to the option pricing theory, which has been consistently gaining attention from the engineers and the mathematicians since the 70's when the Black-Scholes formula was derived.

One of the central objectives of this branch of research is the evaluation of the fair price of an option. Options are derivative contracts, which means that their price derivation is based on the price of another economical resource. They allow their owner to sell or to buy the underlying asset (e.g., stocks) for a specified price before or at some time in the future. The options are categorized into different types, depending on the function they perform. The most popular types are European and American options. The latter one, in fact, remains the most complex to value. From the mathematical point of view, these financial products can be described by means of probabilistic methods as well as by deterministic ones, including parametrized partial differential equations (PDEs), where the parameter reflects the properties of the model. One of the simplest and widely know models, which attempts to evaluate the theoretical value of an option, is the Black-Scholes model [BS73]. Although this model is widely used in the option pricing theory, it presents major limitations, such as, e.g., an assumption of a constant volatility. To overcome these limitations, a variety of other models, like, e.g., the constant elasticity of variance (CEV) or the Heston models, have been developed, which mimic the market behavior more realistically. These models are inherently more complex than the Black-Scholes model. Evidently, to deal with the complexity of these models, it becomes imperative to develop suitable numerical approximation techniques. While the finite elements method (FEM), finite differences (FD), or finite volumes (FV) are the canonic numerical methods for PDEs, their application to financial modeling, [AP05b; HRS$^+$13; Sey09], is still considered relatively new in comparison to the standard Monte Carlo methods, (binomial) tree methods or semi-analytic formulae. Often, more simple, but less realistic models are favored in practical applications due to the low computational cost. Consequently, the development and utilization of methods for efficient evaluation of option prices, yet in complex models, is of current interest in research, which is one of the motivations for the present work.

The objective of this thesis is to develop a parametric model order reduction framework, based on the reduced basis method (RBM) for an efficient and accurate computation of the solution of option pricing models. Focus is particularly laid on the

American options which we model as parabolic variational inequalities, discussed in more detail below. The basic idea is to construct the reduced-order model, which can approximate the original high fidelity problem (i.e., the detailed problem) for different variations of the parameter values. The reduced-order model is constructed based on an appropriate low-dimensional approximation solution space by exploiting the parameter dependency of the problem.

The RBM is not a new method, and its beginning can be traced back to the pioneering works of Almroth, Noor, Peters [ASB78; Noo81; NP80] and others for structural engineering applications. More recent developments in RB methods can be found in [GMN$^+$07; GP05; PRV$^+$02; VPR$^+$03] and the references therein. Over the years since, a strong mathematical theory has been developed for the RB methods with a particular focus on sharp and reliable a posteriori error bounds, and the utilization of the standard POD and greedy procedures for the basis construction, see, e.g., [Gre05; Haa13; HO08b; Rov03; VPR$^+$03].

The distinctive difference of the RBM to other reduced-order modeling (ROM) techniques lies in the fact that the method seeks to exploit the physical properties of the system by studying the parametric nature of the problem. That is, the reduced space which is used for an approximation, is chosen such that it represents all possible variations of the model with respect to the parameter. The efficiency of the method is gained by the so-called offline-online decomposition of the computational routine. In short, this splitting separates the parameter-independent computations from the parameter dependent ones. The first phase is computationally expensive, but performed only once, while the latter one is computationally cheap and can be executed multiple times for different instances of an input parameter. This is a significant feature of the method, which allows to perform computations in a real-time and/or multi-query context.

The significant interest of the method has been also in its realization in the wide range of applications, including, e.g., the Stokes problem, linear elasticity and contact problems [BAF16; GV11; MQR08; Rov03; RV07; Ver03]. So far only little attention has been paid to the applications in finance. The recent works include, e.g., [FCG06; PGB15; Pir12; SS08; SS14; SSS14], which are primarily focused on exploiting POD techniques. The first studies with the RBM, where the attention was on the choice of the basis functions, include the work [CLP11] for jump-diffusion models. Subsequently, in [Pir11] it has been extended to the basket options. In [Pir12] it was shown to be a variant of the POD. In the recent paper [MU14] the application of the reduced basis method to more complex models, e.g., with parameter functions as an initial condition, has been investigated. The method also formed the basis of several textbooks and tutorials, [Haa11; Haa16; HRS16; PR06; QMN16] as well as software libraries, e.g., [DHK$^+$12; RBm13].

We point out that previously mentioned studies considered only the linear case of European options, even though the most frequently traded are American options. By

their early exercise property these derivative securities are formulated as an optimal stopping problems, which are, in turn, described by parabolic variational inequalities (PVI). The subject of variational inequalities (VI) has a well developed theory and wide range of applications, especially for obstacle and contact problems. For example, for American options, the pay-off functional acts as an obstacle. To impose the contact condition one uses an inequality constraint. This, however, adds an additional non-linearity that has to be resolved. We refer to [BL82; DL72; IK08; KS00; Lio72; LS67] for the general theory of stationary and instationary variational inequalities. For the numerical treatment a wide range of literature is available, see, e.g., [BHR78; Glo08; GLT81; KO88]. An extensive survey for the treatment of the finite-dimensional variational inequalities is given in [FP03].

We note that the contact condition can be enforced by means of the Lagrange multiplier method, which transforms the original variational inequality into a mixed problem in saddle point form. It can be treated by active set methods, such as the primal-dual active set strategy (PDAS) [HIK02]. For an overview of discretization schemes for such type of problems, we refer to [Woh11].

Employing the reduced basis method to stationary variational inequalities has been initiated by the works [HSW11; HSW12], where the main theoretical results for the reduced problem were discussed together with the derivation of a posteriori error estimates. The interest in such problems has increased, which led to further research in [GU14; GU15; ZBV16]. Despite the interesting mathematical nature of the problem, the non-linearity of the model is reflected in the difficulty of the construction of the reduced bases. On one hand, one has to guarantee the inf-sup stability of the constructed pair of the reduced spaces. One can follow the standard approach of enrichment by supremizers. This, for example, has been used extensively for the treatment of the pressure term in the Stokes problem or for non-coercive problems, see, e.g., [GV11; NMR15; Rov03; RV07; VPR$^+$03]. On the other hand, one has to enforce the positivity of the reduced Lagrange multiplier and thereby the approximation of the space of Lagrange multipliers becomes more involved.

The inequality constraints also complicate the derivation of a posteriori error estimates. Specifically, the estimation of the inequality residual is not straightforward and requires a careful treatment. This is also reflected in only partial offline-online decomposition of the a posteriori error estimates. This question was addressed in [ZBV16] for the elliptic variational inequalities and in [BKG$^+$15] in the context of optimal control problems with variational inequalities. In this work the authors consider the problem in the so-called primal formulation, which is obtained by introducing an additional "slack" variable. For this formulation they derive simpler error estimates, which are computable in an offline-online fashion. The extension of the RBM to the parabolic case is studied in the works [BAF16; BHS$^+$15; GU14; GU15; HSW13]. In [GU14; GU15] the parabolic variational inequalities in the space-time framework has been discussed. There the authors provide a well-posedness result

and derive a posteriori error estimates for the problem with a relaxed coercivity assumption.

The research in this thesis focuses on two objectives. The first is to construct the generalized reduced basis framework for the parabolic variational inequalities which arise in option pricing. Here we extend an earlier developed methodology for the elliptic variational inequalities, summarized in the aforementioned work [HSW12] to the parabolic case. In particular, we deal with the well-posedness of the reduced problem, the construction of the reduced basis spaces, and a posteriori error estimates. We remark, that in contrast to the space-time parabolic variational inequalities [GU14; GU15], we follow the standard time-stepping approach, where the reduction is performed for the spatial coordinate. For the derivation of a posteriori error estimates we utilize techniques used for elliptic variational inequalities [HSW12] together with the estimates for parabolic problems, see, e.g., [GP05; GRV12]. Most of these results for coercive problems were reported in [BHS+15]. In addition to it, to cover a larger class of models, an extension to weakly coercive problems, i.e., where only the Gårding inequality is satisfied, is presented.

In contrast to the elliptic case, the construction of the reduced spaces for parabolic variational inequalities is more complex because of the time dependence. For the construction of the primal space we still can follow the standard POD-Greedy algorithm, [Haa13; HO08b]. However, for the dual reduced space this is not applicable because of the non-negativity constraint. Instead we consider the new combination of the POD-Angle-Greedy procedure, which has been first introduced in [HSW13] and generalized in [BHS+15]. It unifies the known POD-Greedy algorithm for the primal space and the Angle-Greedy algorithm for the Lagrange multiplier space. An alternative approach based on the non-negative matrix factorization (NNMF) [LS99] was described in [BAF16], where it has been compared to the SVD procedure. In this thesis we also provide a numerical comparison of the performance of both approaches, the NNMF and the POD-Angle-Greedy algorithm.

The second objective of the thesis is the application and the empirical investigation of the RBM to problems in finance. In particular, we consider the problem of calibration on option prices, which requires the solution of a least-squares minimization problem. This is one of the typical applications of the RBM, where many query evaluations of the high-fidelity solutions are required. While, a lot of research has been carried out on the application of model reduction techniques in calibration on option prices, most of them deal with the linear case of European options, [Pir09; SS14]. We present a unified model reduction approach, which covers not only the European, but also the more complex case of the American options. In this part of the work, we investigate the capacity of the RBM and compare it to alternative model reduction approaches, which are popular in financial practice. The numerical findings highlight the potential of the RBM in application to problems in finance, allowing to achieve a computational saving for complex problems. A substantial part of the thesis is

also allocated to the discussion of the Heston option pricing model. This includes the modeling details, boundary conditions and influence of the parameters. We remark, that this model is favorable in calibration on option prices, see, e.g., [AGG10; GGM+12; MPS14; SST04], due to its ability to replicate market behavior better than some other models.

The content of this thesis is organized as follows. In Chapter 2 we give a brief overview of the option pricing theory and terminology used throughout this thesis. In particular, we consider the derivation of the Black-Scholes and Heston models. We focus on the Heston model, where we provide a detailed summary of the model setting for different types and styles of options.

Next we introduce the reduced basis methodology in Chapter 3. First we derive the abstract parametrized weak and discrete weak formulations, which constitute the parametrized linear parabolic PDE. The conditions for the existence and uniqueness of the continuous and discrete solutions for the Heston and the Black-Scholes models are discussed. We recall the main characteristics of the RBM for linear parabolic problems, which include the a posteriori error estimates, well-posedness of the reduced problem, offline-online decomposition of the computational routine, and the construction of the reduced spaces. Finally, we present numerical results for the application of the RBM to price European options in the Heston model. Some of these experiments have been published already in a similar form in [BHS+15].

In Chapter 4 we extend the RBM methodology to the case of American options, which are mathematically modeled as parabolic variational inequalities. We discuss the well-posedness of the weak and discrete weak formulations. By means of Lagrange multipliers, we study the problem in a saddle-point form. We derive the RBM based on the discrete formulation. We focus especially on the derivation of a posteriori error estimates and the construction of suitable reduced basis spaces. Finally, we test the theoretical findings with suitable numerical experiments, the results of which have appeared in our earlier work [BHS+15].

In Chapter 5 we apply the RBM to a realistic market problem. We consider the calibration problem on option prices, where we compare the RBM method to some existing model reduction methods, which include the de-Americanization method and the calibration using closed-form solutions. We use synthetic and real market data sets to demonstrate the performance of different model reduction methods.

We complete this work with concluding remarks and perspectives on future work, which are given in Chapter 6.

2 Models in Option Pricing

2.1 Introduction

With this introductory chapter, we provide basic definitions and an overview of the theory of option pricing with some standard mathematical models. For a more detailed introduction; see, e.g., [AP05b; HRS$^+$13; Hul03; Jam03; LL96; Sey09; WDH93; Wil01].

The central question in the option pricing theory is: given a value of an option at its expiration day, $\tau = T$, how to define a fair price of an option today, $\tau = 0$? To answer this question, many models and techniques were developed, among them the famous Black-Scholes model, which was derived by Fischer Black and Myron Scholes in 1973 [BS73]. Despite being the most popular, the model also has some limitations. One of the main ones is the assumption of a constant volatility, which, in most of the situations, is not fulfilled by market behavior. In 1993 another model was proposed by Steven Heston [Hes93], which assumes a stochastic nature of the volatility and is based on the dynamics of both, the stock price and the volatility.

In this Chapter we provide a mathematical description of both models, specify appropriate boundary conditions and present their closed-form solutions. In particular, in Section 2.2–Section 2.3, we briefly outline the definition of options and stock price processes. In Section 2.4, we discuss the derivation of the Black-Scholes equation and present the Black-Scholes formula for pricing European options. The limitations of the model are considered in Section 2.5. These shortcomings give raise to an introduction of an alternative stochastic volatility model, presented in Section 2.6. We discuss, in great details, several choices of the boundary conditions in Section 2.6.2 for European and in Section 2.6.4 for American options in the Heston model.

2.2 Options

Initially, we recall some basic definitions of financial instruments.

Derivative securities, or shortly *derivatives*, are contracts, whose value depends on an underlying asset and an investor's decision. An *underlying asset* or just *underlying* can be stocks, bonds, currencies etc. We denote the price of an asset by $S = \{S_\tau : \tau \geq 0\}$, where τ is time.

An *option* is a derivative contract which permits its owner a right, but not an

obligation, to buy (a *call option*) or to sell (a *put option*), an underlying asset at a prespecified fixed *strike price* $K \geq 0$ before or at a certain time $T \geq 0$, called *maturity*. An option is issued by a *writer*, usually a bank, to a *holder*, who purchases an option.

There are two common types of options, the European and the American ones. European options can be exercised only at maturity. These options are the simplest ones and are also called *plain vanilla* options. By contrast, American options, which belong already to the category of complex options, allow an owner to exercise an option at any time prior to the maturity date. In turn, these options are also the most prevalent in the market. For American options we need to know not only the value of an option, but also when it is best to exercise it, which is a hard task.

There are other types of options, e.g., *path-dependent* options, the value of which depends not only on the value of an asset price at maturity, but also on the history of an asset price.

At an expiration day T, the value of an option is known and called a *pay-off*. The pay-offs for call and put options are defined as

$$\mathcal{H}(S) = \begin{cases} (S-K)_+, & \textit{call}, \\ (K-S)_+, & \textit{put}, \end{cases} \tag{2.2.1}$$

with $(\cdot)_+ := \max(\cdot, 0)$.

Provided a pay-off of an option and a price of an underlying S_0, the task of "option pricing" is to determine a fair price of an option today, i.e., at $\tau = 0$. Later in the chapter, a mathematical interpretation of this problem is given. Graphically, the prices of the call and put options for different S_0 can be presented as in Figure 2.1.

For a call (put), an option is said to be *in the money*, if $S > K$ ($S < K$); *out of the money*, if $S < K$ ($S > K$); and *at the money*, if $S = K$, for all $\tau < T$. Different types and combinations of options can be considered, which include more involved strategies and lead to more complicated pay-offs, e.g., digital options, straddles, strangles, butterfly spreads, see, e.g., [Jam03; WDH93; Wil01].

In general, as we will see later, the value of an option P depends on the maturity time T, strike K, and some set of parameters $\boldsymbol{\mu}$, which are determined by the model used to price an option.

In this thesis, we focus on two option pricing models: the constant volatility Black-Scholes model, and its extension, the stochastic volatility Heston model.

2.3 Stock Price Process

The stock price process is modeled by a Brownian motion. This concept was already introduced in early works on option pricing, in the beginning of the 20th century. L.

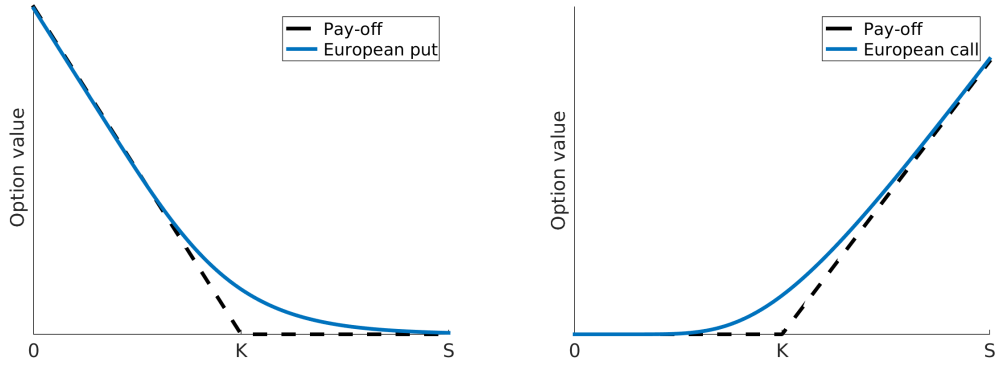

Figure 2.1: The values of a European put (left) and call (right) options at $\tau = 0$ and their corresponding pay-offs.

Bachelier was the first to use a stochastic process (a Brownian motion) to model stock options. The work was a part of his dissertation "Théorie de la spéculation" [Bac00].

The price process of an asset is described by a stochastic process on the time horizon $0 \leq \tau \leq T$. In general, we are not interested in the asset price itself, but in the *return* of an asset price, which describes the relative measure of the change in the price, dS/S. Mathematically, it is represented by the following stochastic differential equation (SDE):

$$\frac{dS}{S} = \mu d\tau + \sigma dW. \tag{2.3.1}$$

The return of an asset (2.3.1) is composed of two terms, the deterministic part $\mu d\tau$, and the stochastic part σdW. The deterministic contribution represents a return on money invested in a risk-free bank, where μ is called a *drift*, an average rate of growth of the asset price. The remaining term σdW is a stochastic contribution, which models a random change in the price due to to some unexpected external events. It is driven by a *Wiener process* (or a standard Brownian motion) W and a *volatility* σ, which measures a range of fluctuations of the returns. We discuss the notion of volatility in more details in Section 2.5.1. For simplicity, we assume, that both σ and μ are constants. For a rigorous mathematical interpretation of (2.3.1) and an introduction to stochastic calculus, see, e.g., [KS91; LL96].

A Wiener process (or a standard Brownian motion) is a real-valued continuous stochastic process $W = \{W_\tau : \tau \geq 0\}$, with the following properties:

(i.) $W_0 = 0$,

(ii.) W_τ has independent increments, i.e., for all $0 \leq \tau_1 < \tau_2 \leq \tau_3 < \tau_4$, $W_{\tau_2} - W_{\tau_1}$ and $W_{\tau_4} - W_{\tau_3}$ are independent stochastic variables,

(iii.) $W_\tau - W_s$ is normally distributed, i.e., for $0 \leq s < \tau$, $W_\tau - W_s \sim \mathcal{N}(0, \tau - s)$ with mean $\mathrm{E}[W_\tau - W_s] = 0$ and variance $\mathrm{Var}[W_\tau - W_s] = \mathrm{E}[(W_\tau - W_s)^2] = \tau - s$.

(iv.) W_τ has continuous trajectories almost surely.

The SDE (2.3.1) admits the unique solution

$$S_\tau = S_0 e^{\left(\mu - \sigma^2/2\right)\tau + \sigma W}. \tag{2.3.2}$$

The above solution is a log-normally distributed random variable, which follows a *geometric Brownian motion* (the exponential of a Brownian motion).

We note that the random term in (2.3.1) plays a crucial role in the modeling of the asset price. Indeed, if we eliminate the term by setting $\sigma = 0$, then the price of an asset $S_\tau = S_0 e^{\mu\tau}$ is fully deterministic, which is not true in real markets.

The SDE (2.3.1) is a particular case of a more general SDE (*Itô process*),

$$dX = a(X, \tau)d\tau + b(X, \tau)dW, \quad X_0 = Z, \tag{2.3.3}$$

where $a : \mathbb{R} \times \mathbb{R} \to \mathbb{R}$ is a drift coefficient and $b : \mathbb{R} \times \mathbb{R} \to \mathbb{R}$ is a diffusion coefficient. The solution $X = \{X_\tau : \tau \geq 0\}$ of (2.3.3) is called a *diffusion*. The result of existence and uniqueness of such a solution, under particular regularity assumptions on $a(X, \tau)$ and $b(X, \tau)$, can be found in [LL96, Theorem 3.5.3].

Next we present the Itô formula, which is one of the most fundamental tools in stochastic calculus.

Lemma 2.3.1 (Itô formula)**.** *Let $X = \{X_\tau : \tau \geq 0\}$ follow the Itô process* (2.3.3)*, and let $f(\tau, x) \in C^2([0, \infty) \times \mathbb{R})$. Then for $Y := f(\tau, X)$ the following holds*

$$dY = \left(\frac{\partial f}{\partial x}a + \frac{\partial f}{\partial \tau} + \frac{1}{2}\frac{\partial^2 f}{\partial x^2}b^2\right)d\tau + \frac{\partial f}{\partial x}b\ dW. \tag{2.3.4}$$

The proof of this result can be found in, e.g., [KS91, Section 3.3.A].

The equation (2.3.3), driven by a Wiener process, serves as a basis for a very large class of financial models, called *diffusion models*, which includes also the Black-Scholes model, which is discussed in the next section.

2.4 Black-Scholes Model

The Black-Scholes model is based on the following set of assumptions:

(i) The stock price follows a geometric Brownian motion (2.3.1) with constant parameters μ and σ.

(ii) Short selling of securities is permitted, i.e., the seller may sell the assets, which he may not own.

(iii) The underlying is not paying dividends.

(iv) Security trading is continuous and there are no transaction costs associated with a portfolio.

(v) There are no arbitrage possibilities, meaning no opportunity to make a riskless profit. This is a very crucial assumption for nearly all pricing models. In practice, only very small arbitrage opportunities are observed in the prices.

(vi) The risk-free interest rate r is constant for all maturities, i.e., an interest rate of risk-free investment or loan is known and constant.

Some of these assumptions can be relaxed, e.g., allowing r and σ to vary over time, or adding dividends. This leads to more complex models.

There are numerous derivations of the Black-Scholes partial differential equation. We present here the approach from, e.g., [Hul03; Top05; Wil01]. Consider the dynamics of the stock price (2.3.1),

$$dS = \mu S d\tau + \sigma S dW. \tag{2.4.1}$$

Let $P = P(S, \tau)$ to be the price of an option, e.g., a call option. Using Itô's formula (2.3.4), we write

$$dP = \left(\frac{\partial P}{\partial S} \mu S + \frac{\partial P}{\partial \tau} + \frac{1}{2} \sigma^2 S^2 \frac{\partial^2 P}{\partial S^2} \right) d\tau + \frac{\partial P}{\partial S} \sigma S dW. \tag{2.4.2}$$

Both SDEs (2.4.1) and (2.4.2) are driven by the random term dW. Our goal is to express a value of an option P in a fully deterministic manner. For this, we construct another variable (portfolio) Π. The portfolio Π is represented as a 'correct' combination of S and P terms

$$\Pi = \Delta_1 P + \Delta_2 S. \tag{2.4.3}$$

As we will see below, choosing appropriately Δ_1 and Δ_2 will allow us to eliminate the randomness in the model and to present it in a deterministic manner.

Incorporating (2.4.1) and (2.4.2), the change of the portfolio $d\Pi$ in a time interval dt can be written

$$d\Pi = \Delta_1 \left(\frac{\partial P}{\partial S} \mu S + \frac{\partial P}{\partial \tau} + \frac{1}{2} \sigma^2 S^2 \frac{\partial^2 P}{\partial S^2} \right) d\tau + \Delta_2 \mu S d\tau + \left(\Delta_1 \frac{\partial P}{\partial S} \sigma S + \Delta_2 \sigma S \right) dW. \tag{2.4.4}$$

By setting Δ_1 and Δ_2 as follows, we eliminate the random term dW in (2.4.4):

$$\Delta_1 := -1, \qquad \Delta_2 := \frac{\partial P}{\partial S}. \tag{2.4.5}$$

Then (2.4.4) reduces to

$$d\Pi = -\left(\frac{\partial P}{\partial \tau} + \frac{1}{2}\sigma^2 S^2 \frac{\partial^2 P}{\partial S^2}\right) d\tau. \tag{2.4.6}$$

The portfolio earns a risk-free interest rate r for a short period of time (i.e., an amount Π, invested in riskless asset, growths exponentially with the constant interest rate)

$$d\Pi = r\Pi d\tau. \tag{2.4.7}$$

From (2.4.3), (2.4.6) and (2.4.7), we obtain

$$-\left(\frac{\partial P}{\partial \tau} + \frac{1}{2}\sigma^2 S^2 \frac{\partial^2 P}{\partial S^2}\right) d\tau = r\left(-P + \frac{\partial P}{\partial S} S\right) d\tau, \tag{2.4.8}$$

and finally

$$\frac{\partial P}{\partial \tau} + \frac{1}{2}\sigma^2 S^2 \frac{\partial^2 P}{\partial S^2} + rS\frac{\partial P}{\partial S} - rP = 0. \tag{2.4.9}$$

Equation (2.4.9) is the Black-Scholes or Black-Scholes-Merton partial differential equation. A linear partial differential operator of elliptic type associated with it is

$$\mathcal{L}^{\mathrm{BS}} P := \frac{1}{2}\sigma^2 S^2 \frac{\partial^2 P}{\partial S^2} + rS\frac{\partial P}{\partial S} - rP. \tag{2.4.10}$$

Note that the assumption (iii), in general, can be weakened. Then assuming that the asset pays out a dividend q, the Black-Scholes operator can be rewritten as following, [AP05b, Section 2.3],

$$\mathcal{L}^{\mathrm{BS}} P := \frac{1}{2}\sigma^2 S^2 \frac{\partial^2 P}{\partial S^2} + (r-q)S\frac{\partial P}{\partial S} - rP. \tag{2.4.11}$$

In the compact form the Black-Scholes equation can be expressed as

$$\frac{\partial P}{\partial \tau} + \mathcal{L}^{\mathrm{BS}} P = 0. \tag{2.4.12}$$

To specify a particular type of a derivative, appropriate terminal and boundary conditions should be established. For the European call we have

$$P(T) = \mathcal{H}(S) = (S-K)_+, \tag{2.4.13a}$$

$$\lim_{S\to\infty} P(\tau, S) = S, \quad P(\tau, 0) = 0. \tag{2.4.13b}$$

And for the European put,

$$P(T) = \mathcal{H}(S) = (K - S)_+, \tag{2.4.14a}$$

$$\lim_{S\to\infty} P(\tau, S) = 0, \quad P(\tau, 0) = Ke^{-r(T-\tau)}. \tag{2.4.14b}$$

We provide a short interpretation of these conditions. For a call option, when $S \to \infty$, it is more likely that we exercise the option and its value will tend to the value of an asset. When $S \to 0$, the option becomes worthless and falls to zero. For a put option, when $S \to \infty$, the option is unlikely to be exercised and its value becomes 0. For $S \to 0$ the value of an option is a present value of amount K received at time T.

2.4.1 Put-Call Parity

European put and call options with the same strikes K and maturities T can be related to each other via a put-call parity relation (2.4.15)

$$P_C + Ke^{-r(T-\tau)} = P_P + S. \tag{2.4.15}$$

It means, that given the price of the European call P_C, the price of the European put P_P can be directly deduced from it and vice versa, see e.g., [Hul03; Wil01]. This relation is often used in practice, making it sufficient to compute only one type of an option.

2.4.2 Black-Scholes Formula

Assuming constant coefficients σ and r in the Black-Scholes equation (2.4.12), an exact explicit formula for evaluating European options can be derived, [BS73]. Let $N(\cdot)$ be a cumulative distribution function (CDF) of a standard normal distribution,

$$N(x) = \frac{1}{\sqrt{2\pi}} \int_{-\infty}^{x} e^{-\frac{1}{2}z^2} dz. \tag{2.4.16}$$

Then the price for the European call in the Black-Scholes model is given by

$$P(\tau, S) = SN(d_1) - Ke^{-r(T-\tau)}N(d_2), \tag{2.4.17}$$

where

$$d_1 = \frac{\log(\frac{S}{K}) + (r + \frac{\sigma^2}{2})(T - \tau)}{\sigma\sqrt{T - \tau}}, \quad d_2 = d_1 - \sigma\sqrt{T - \tau}. \tag{2.4.18}$$

Similarly, due to a put-call parity (2.4.15), the European put option can be expressed

$$P(\tau, S) = -SN(-d_1) + Ke^{-r(T-\tau)}N(-d_2). \tag{2.4.19}$$

2.4.3 American Options

We extend our considerations to American type of options. In particular, we start our discussion with American puts. Despite the fact that these options are more complex than European ones, due to the inequality constraints and no closed-form formula for the solution, they are more frequently used in the market.

As it was mentioned already in Chapter 2.2, American options can be exercised at any time before their expiration date, which implies that the owner has more rights compared to the European case, thereby making American options more valuable. Hence, the price of an American put option is always larger than the price of an equivalent European one,

$$P^{AO} \geq P^{EO}. \tag{2.4.20}$$

However, for an American call, one can prove that on non-dividend paying stocks, American and European calls have the same price [Hul03]. In addition, the price of an American put can not fall below its pay-off $\mathcal{H}(S) := (K - S)_+$,

$$P(\tau, S) \geq \mathcal{H}(S). \tag{2.4.21}$$

If, for instance, $P(\tau, S)$ would be less than the pay-off, $P(\tau, S) < \mathcal{H}(S)$, this would mean that one can purchase the asset and the option and immediately exercise it, which would lead to an immediate profit with a zero initial investment. This case then would contradict to a non-arbitrage argument, Section 2.2. Hence, the condition (2.4.21) is always true.

We can see that the condition (2.4.21) naturally decomposes the strip $(\tau, S) \in [0, T] \times \mathbb{R}_+$ into two parts: the region where (2.4.21) becomes an equality, and the part where only a strict inequality holds; see Figure 2.2. These regions are determined by a so-called *early-exercise curve*[1] and characterized by the following inequalities:

$$P(\tau, S) > \mathcal{H}(S), \quad S > S_f(\tau), \quad \tau \in [0, T), \tag{2.4.22}$$

$$P(\tau, S) = \mathcal{H}(S), \quad S \leq S_f(\tau), \quad \tau \in [0, T]. \tag{2.4.23}$$

The curve $S_f(\tau)$ is changing over time and is not known a priori. A problem of such kind is called a moving boundary problem (for a static case a free boundary problem).

The curve $S_f(\tau)$ has also an economic meaning, telling us that there exist a particular time τ^* (an *optimal stopping time*), when it is the best to exercise the option. It is clear, that for $S > S_f$, exercising the put option would lead to an immediate loss $(K - S - P < 0)$. To eliminate the possible loss, it is rational to continue to hold an option. In this way, the region $S > S_f$ is called a *continuation region*. For the case, $S < S_f$, the holder can create a profit and stops to hold the option by exercising it. This region is called a *stopping region*.

[1] In some literature the name "critical stock price" is used, e.g., [JLL90].

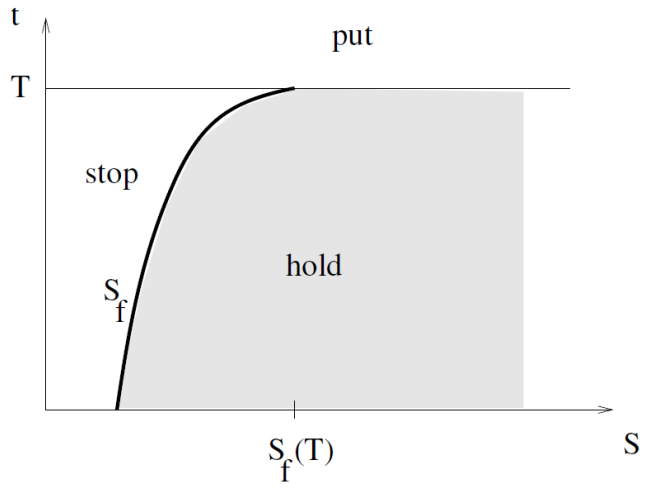

Figure 2.2: Schematic representation of an early exercise curve S_f with continuation and stopping regions. Source: [Sey09].

Next we consider a problem in the PDE framework. The price of an American put P satisfies the Black-Scholes equation in the continuation region

$$\frac{\partial P}{\partial \tau} + \mathcal{L}^{\mathrm{BS}} P = 0, \quad S > S_f, \quad \tau \in [0, T], \tag{2.4.24}$$

with the terminal condition

$$P(T, S) = \mathcal{H}(S). \tag{2.4.25}$$

We prescribe a fixed and free boundary conditions for $\tau \in [0, T]$

$$\lim_{S \to \infty} P(\tau, S) = 0, \tag{2.4.26a}$$

$$\frac{\partial P}{\partial S}(\tau, S_f(\tau)) = -1, \tag{2.4.26b}$$

$$P(\tau, S_f(\tau)) = K - S_f(\tau), \tag{2.4.26c}$$

$$P(S, \tau) = \mathcal{H}(S), \quad S < S_f(\tau). \tag{2.4.26d}$$

Then, the price of an American put option in the Black-Scholes model is a solution of the free-boundary value problem (2.4.24)–(2.4.26). The difficulty of solving this problem is associated with an unknown boundary $S_f(\tau)$. From a numerical point of view, it is nicer to work with another formulation (2.4.27), where the unknown boundary $S_f(\tau)$ does not show up explicitly. This is described below:

Problem 2.4.1. *The price of an American put option in the Black-Scholes model is a solution of the following system of inequalities*

$$\frac{\partial P}{\partial \tau} + \mathcal{L}^{\mathrm{BS}} P \leq 0, \qquad (\tau, S) \in [0, T) \times \mathbb{R}_+, \tag{2.4.27a}$$

$$P \geq \mathcal{H}(S), \qquad (\tau, S) \in [0, T) \times \mathbb{R}_+, \tag{2.4.27b}$$

$$\left(\frac{\partial P}{\partial \tau} + \mathcal{L}^{\mathrm{BS}} P\right)(P - \mathcal{H}(S)) = 0, \qquad (\tau, S) \in [0, T) \times \mathbb{R}_+, \tag{2.4.27c}$$

$$P(T, S) = \mathcal{H}(S), \qquad S \in \mathbb{R}_+. \tag{2.4.27d}$$

The derivation of this result can be found in [BL82; JLL90]. The weak form of the set of inequalities (2.4.27) results in a variational inequality problem, which is studied in Chapter 4.

2.5 Limitations of the Black-Scholes Model

Despite its popularity, the Black-Scholes model has several limitations in capturing real market behavior. The model makes a strong assumption that the stock returns are normally distributed with a constant variance. In most of the situations, the market violates this assumption, a clear evidence of it is the stock market crash in 1987.

Extensive research has been done to extend the Black-Scholes model to a model with a non-constant volatility. As a result several models emerged, where the volatility can be either some deterministic function of time and stock price $\sigma(\tau, S)$, e.g., the constant elasticity of variance (CEV) model, or a completely random variable, e.g., the Heston model. The first one belongs to the class of a so-called local volatility models, while the second one is related to stochastic volatility models.

In the case of local volatility models, the local volatility function represents an averaging over all possible instantaneous volatilities. These models are frequently applied to price exotic options. In turn, stochastic volatility models are more complex than the local volatility ones, however, they are more capable to replicate the realistic dynamics of an underlying.

The early studies on stochastic volatility models include [Gar76; Hes93; HW87; JS87; Sco97; SS91; Wig87]. The models in [HW87; JS87; Sco97; Wig87] did not provide an analytical solution and used numerical techniques to evaluate an option price. The analytical approach was considered in [SS91] with an assumption that the stock price and volatility processes are uncorrelated. Later, Heston generalized the approach to a model, where these two quantities are correlated with a non-zero correlation parameter, and provided a semi-analytic formula, [Hes93]. This

model became very popular and nowadays extensively used by both practitioners and researchers.

2.5.1 Stochastic Volatility

We start by introducing a concept of volatility, which is used to measure standard deviation of the trading price series. In practice, the volatility can not be observed directly, but it can be measured statistically, for example, by taking a look on its past history.

There are several notions of the volatility, such as *actual*, *historical (realized)*, *implied* and *forward* volatility, [Wil01]. The measure of the randomness in an asset return at any time is defined by an actual volatility; and at some fixed period of time in the past by a historical volatility. The forward volatility is associated with the future time of the stock price movements. The implied volatility is defined from option prices observed in the market. To calculate an implied volatility one needs to insert all available data, S, T, K and r, in the option pricing model, e.g., the Black-Scholes model, and to solve it with respect to the volatility parameter σ. Since implied volatility is less fluctuating than the option prices, it is also common for traders to work with implied volatilities itself instead of option prices, e.g., for calibration.

One of the features of the implied volatility is the so called volatility *'smile'* or *'skew'*. It shows that the implied volatility as a function of K is not constant, as in the Black-Scholes settings. Indeed, it generates a curve which has a shape of a smile. This is one of the evidences how market behavior violates the Black-Scholes settings.

Another empirical evidence can be recalled from the stock market crash in October 1987. We present it here as it is described in [Gat06]. On Figure 2.3, the log returns over 15 years of SPX (the Standard & Poor's 500 index) are depicted. It can be seen the stock price empirically exhibits a so-called *volatility clustering*, when large/small price changes follow large/small price changes. This property is also known as *a mean reverting* property of the volatility, [Gat06]. This is one of the characteristics, which can not be described by a constant volatility.

In Figure 2.4, the frequency distribution of SPX daily log returns is plotted. The distribution is fat-tailed and highly peaked compared to a normal distribution, which is assumed for the behavior of the stock price in the Black-Scholes model. This can be a characteristic of the combination of distributions with different variances.

This example serves as a good motivation to consider the volatility as a mean reverting random variable. The Heston model, introduced in the next section, incorporates this feature of the volatility in the modeling of the option price.

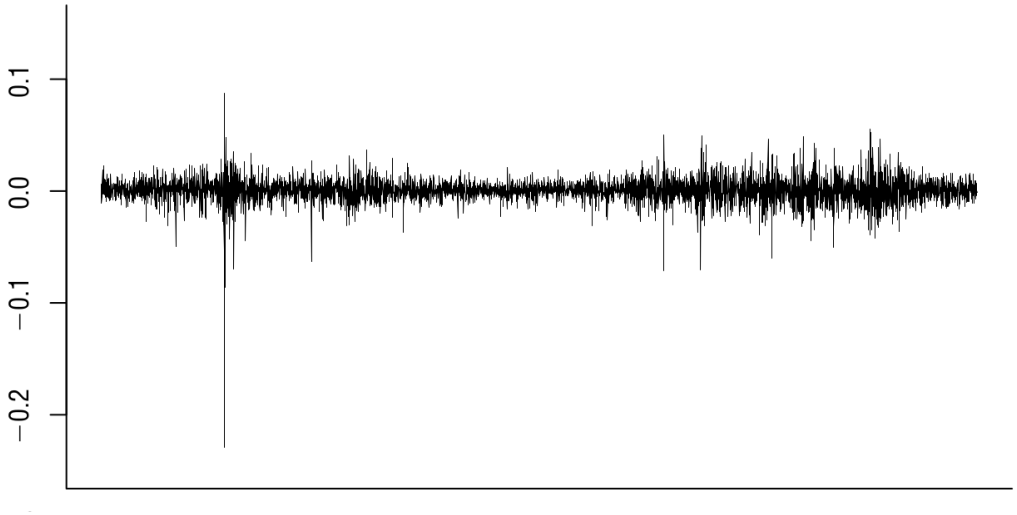

Figure 2.3: SPX daily log returns from 31.12.1984, to 31.12.2004. Source: [Gat06].

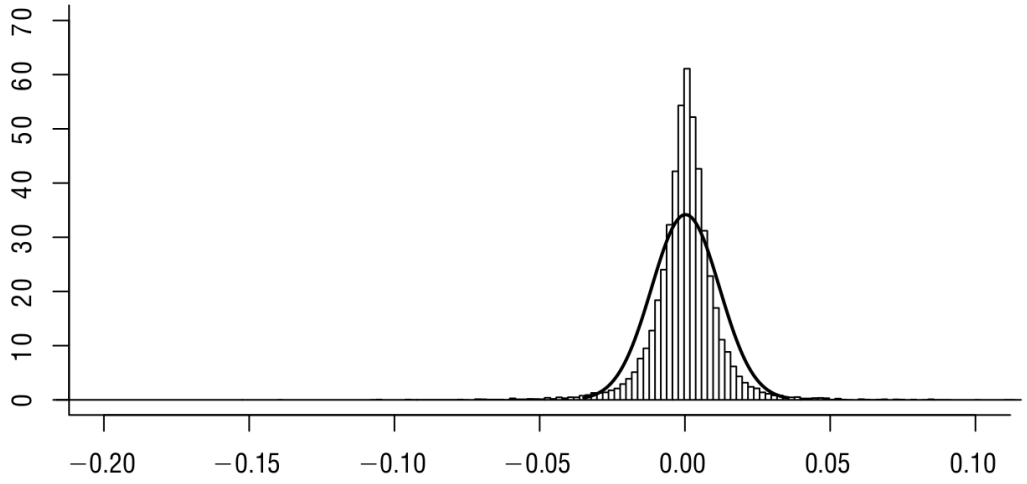

Figure 2.4: Frequency distribution of (77 years) SPX daily log returns compared with the normal distribution. Source: [Gat06].

2.6 Heston Stochastic Volatility Model

The Heston model [Hes93] is described by the following stock price and volatility dynamics

$$dS = \mu S d\tau + \sqrt{\nu} S dW^1, \tag{2.6.1a}$$

$$d\nu = \kappa(\gamma - \nu)d\tau + \xi\sqrt{\nu} dW^2, \tag{2.6.1b}$$

The dynamics of the stock price follows a geometric Brownian motion as for the Black-Scholes model (2.4.1). The non-constant instantaneous variance $\nu := \{\nu_t : \tau \geq 0\}$ is driven by a mean-reverting square root process (known as Cox-Ingersoll-Ross (CIR) process) with a long-run variance $\gamma > 0$, rate of mean reversion $\kappa > 0$ and a volatility of variance (also called volatility of volatility) $\xi > 0$. The Wiener processes W^1 and W^2 are correlated with the correlation parameter $\rho \in [-1, 1]$.

For the Heston model, the so-called *Feller condition* is often assumed in the literature. It implies, that the variance process (2.6.1b) is strictly positive if the parameters obey the following condition, see, e.g., [JKW+11],

$$2\kappa\gamma > \xi^2. \tag{2.6.2}$$

It is uncommon and, in some cases, not desirable that the parameters violate this condition. In most situations the parameters are chosen in such a way, that the Feller condition is fulfilled.

2.6.1 Heston Partial Differential Equation

The derivation of the partial differential equation for the Heston model (2.6.1) is similar to the derivation of the Black-Scholes model. In our presentation we closely follow [Gat06]. Consider a portfolio of one option P, Δ_1 units of stock S and Δ_2 units of another asset U, such that,

$$\Pi = P + \Delta_1 S + \Delta_2 U. \tag{2.6.3}$$

The change in the portfolio value in a time interval $d\tau$ is

$$d\Pi = dP + \Delta_1 dS + \Delta_2 dU. \tag{2.6.4}$$

Applying the multidimensional version of Itô's formula [KS91, Theorem 3.6] to dP and dU we obtain

$$dP = \frac{\partial P}{\partial \tau}d\tau + \frac{\partial P}{\partial S}dS + \frac{\partial P}{\partial \nu}d\nu + \frac{1}{2}\nu S^2\frac{\partial^2 P}{\partial S^2}d\tau + \frac{1}{2}\xi^2\nu\frac{\partial^2 P}{\partial \nu^2}d\tau + \xi\nu\rho S\frac{\partial^2 P}{\partial \nu \partial S}d\tau, \tag{2.6.5a}$$

$$dU = \frac{\partial U}{\partial \tau}d\tau + \frac{\partial U}{\partial S}dS + \frac{\partial U}{\partial \nu}d\nu + \frac{1}{2}\nu S^2\frac{\partial^2 U}{\partial S^2}d\tau + \frac{1}{2}\xi^2\nu\frac{\partial^2 U}{\partial \nu^2}d\tau + \xi\nu\rho S\frac{\partial^2 U}{\partial \nu \partial S}d\tau. \tag{2.6.5b}$$

Incorporating (2.6.5) to (2.6.4), provides

$$d\Pi = dP + \Delta_1 dS + \Delta_2 dU = \left(\frac{\partial P}{\partial \tau} + \frac{1}{2}\nu S^2 \frac{\partial^2 P}{\partial S^2} + \frac{1}{2}\xi^2 \nu \frac{\partial^2 P}{\partial \nu^2} + \xi\nu\rho S \frac{\partial^2 P}{\partial \nu \partial S}\right) d\tau$$
$$+ \Delta_2 \left(\frac{\partial U}{\partial \tau} + \frac{1}{2}\nu S^2 \frac{\partial^2 U}{\partial S^2} + \frac{1}{2}\xi^2 \nu \frac{\partial^2 U}{\partial \nu^2} + \xi\nu\rho S \frac{\partial^2 U}{\partial \nu \partial S}\right) d\tau$$
$$+ \left(\frac{\partial P}{\partial S} + \Delta_2 \frac{\partial U}{\partial S} + \Delta_1\right) dS + \left(\frac{\partial P}{\partial \nu} + \Delta_2 \frac{\partial U}{\partial \nu}\right) d\nu. \tag{2.6.6}$$

The random terms dS and $d\nu$ create a risk in the portfolio. To eliminate the risk, we set

$$\Delta_2 = \frac{-\frac{\partial P}{\partial \nu}}{\frac{\partial U}{\partial \nu}}, \qquad \Delta_1 = -\frac{\partial P}{\partial S} - \Delta_2 \frac{\partial U}{\partial S}. \tag{2.6.7}$$

Following the steps as for the Black-Scholes model in the preceding section, we require a portfolio to earn a risk-free interest rate r: $d\Pi = r\Pi d\tau$. Then (2.6.6) reduces to

$$d\Pi = \left(\frac{\partial P}{\partial \tau} + \frac{1}{2}\nu S^2 \frac{\partial^2 P}{\partial S^2} + \frac{1}{2}\xi^2 \nu \frac{\partial^2 P}{\partial \nu^2} + \xi\nu\rho S \frac{\partial^2 P}{\partial \nu \partial S}\right) d\tau$$
$$+ \Delta_2 \left(\frac{\partial U}{\partial \tau} + \frac{1}{2}\nu S^2 \frac{\partial^2 U}{\partial S^2} + \frac{1}{2}\xi^2 \nu \frac{\partial^2 U}{\partial \nu^2} + \xi\nu\rho S \frac{\partial^2 U}{\partial \nu \partial S}\right) d\tau$$
$$= r\Pi d\tau = r(P + \Delta_1 S + \Delta_2 U) d\tau.$$

Grouping P and U terms, we obtain

$$\frac{\frac{\partial P}{\partial \tau} + \frac{1}{2}\nu S^2 \frac{\partial^2 P}{\partial S^2} + \frac{1}{2}\xi^2 \nu \frac{\partial^2 P}{\partial \nu^2} + \xi\nu\rho S \frac{\partial^2 P}{\partial \nu \partial S} + rS\frac{\partial P}{\partial S} - rP}{\frac{\partial P}{\partial \nu}} \tag{2.6.8}$$
$$= \frac{\frac{\partial U}{\partial \tau} + \frac{1}{2} v S^2 \frac{\partial^2 U}{\partial S^2} + \frac{1}{2}\xi^2 v \frac{\partial^2 U}{\partial \nu^2} + \xi\nu\rho S \frac{\partial^2 U}{\partial \nu \partial S} + rS\frac{\partial U}{\partial S} - rU}{\frac{\partial U}{\partial \nu}}. \tag{2.6.9}$$

The left-hand side is a function of P and the right-hand side is a function of U, which makes the equality possible only when both sides are equal to some function $f(\tau, \nu, S)$. We chose $f = -\kappa(\gamma - \nu) + \lambda(\tau, \nu, S)$ as in [Gat06], where $\lambda(\tau, \nu, S)$ is a price of volatility risk, such that $\lambda(\tau, \nu, S) = \lambda\nu$, [Hes93]. Then the pricing PDE of the Heston model has the following form

$$\frac{\partial P}{\partial \tau} + \frac{1}{2} v S^2 \frac{\partial^2 P}{\partial S^2} + \xi\nu\rho S \frac{\partial^2 P}{\partial \nu \partial S} + \frac{1}{2}\xi^2 v \frac{\partial^2 P}{\partial \nu^2} + rS\frac{\partial P}{\partial S} + [\kappa(\gamma - \nu) - \lambda\nu]\frac{\partial P}{\partial \nu} - rP = 0. \tag{2.6.10}$$

We can write $\kappa(\gamma - \nu) - \lambda\nu = \kappa\gamma - (\kappa + \lambda)\nu = (\kappa + \lambda)(\frac{\kappa}{\kappa+\lambda}\gamma - \nu)$. Then by considering $\kappa' = \kappa + \lambda$, and $\gamma' = \frac{\kappa}{\kappa+\lambda}\gamma$, the parameter λ can be eliminated [Hes93; WAW01].

Therefore, without loss of generality it suffices to set $\lambda = 0$ and consider only $\xi, \rho, \gamma, \kappa$ and r as model parameters.

We define a spatial differential operator corresponding to the Heston model as follows

$$\mathcal{L}^{\mathrm{H}} P := \frac{1}{2}\nu S^2 \frac{\partial^2 P}{\partial S^2} + \xi\nu\rho S \frac{\partial^2 P}{\partial \nu \partial S} + \frac{1}{2}\xi^2 \nu \frac{\partial^2 P}{\partial \nu^2} + rS\frac{\partial P}{\partial S} + \kappa(\gamma - \nu)\frac{\partial P}{\partial \nu} - rP. \quad (2.6.11)$$

Then equation (2.6.10) can be written in the compact form

$$\frac{\partial P}{\partial \tau} + \mathcal{L}^{\mathrm{H}} P = 0. \quad (2.6.12)$$

Analogously to the derivation of the Black-Scholes equation, a standard call or a put type of an option in the Heston model is characterized by the terminal condition (2.4.13a) or (2.4.14a).

Remark 2.6.1. *Assuming that the volatility is constant in the Heston model, we have $\xi = 0$ and $\nu = \gamma$, and the Heston PDE reduces to the Black-Scholes one with $\nu = \sigma^2 = \gamma$. Thereby, the Heston model can be considered as an extension of the standard Black-Scholes model.*

2.6.2 European Options

For the parabolic PDE (2.6.10) to be solved with specified terminal conditions, we need to impose appropriate boundary conditions. The Heston model has a complex structure and there are several specifications of the boundary conditions in the literature for both European and American (Section 2.6.4) options. The choice may depend on several aspects and we discuss several different settings, which exist in the literature.

For the case of European call options the commonly used boundary conditions, cf. [Hes93; HF10; WAW01], are given by

$$\lim_{S\to\infty} \frac{\partial P}{\partial S}(\tau, \nu, S) = 1, \quad (2.6.13a)$$

$$P(\tau, \nu, 0) = 0, \quad (2.6.13b)$$

$$\lim_{\nu\to\infty} P(\tau, \nu, S) = S, \quad (2.6.13c)$$

$$\frac{\partial P}{\partial \tau}(\tau, 0, S) + \widetilde{\mathcal{L}}^{\mathrm{H}} P(\tau, 0, S) = 0, \quad (2.6.13d)$$

with the operator $\widetilde{\mathcal{L}}^{\mathrm{H}}$ defined as

$$\widetilde{\mathcal{L}}^{\mathrm{H}} P = rS\frac{\partial P}{\partial S} + \kappa\gamma\frac{\partial P}{\partial \nu} - rP. \quad (2.6.14)$$

We interpret these conditions as follows: For a large stock price S, we have a Neumann boundary condition (2.6.13a), which says that the option price grows linearly w.r.t. S. When the stock is worthless, $S = 0$, it is natural to assume that the value of the call is also worthless (2.6.13b). With increasing volatility ν, the option price is also increasing, but it remains bounded by the stock price S (2.6.13c). One of the main difficulties for the Heston model appears at the boundary $\nu = 0$, where no boundary conditions can be established and the degeneracy of the PDE occurs. We assume that the equation is satisfied on the line $\nu = 0$ (2.6.13d).

The boundary conditions described above are the ones proposed by Heston [Hes93]. However, this is not a unique way to prescribe boundary conditions for the European call option. Other variations of the boundary conditions exist. In particular, in [Gal08] the following boundary conditions are provided

$$\lim_{S\to\infty} \frac{\partial P}{\partial S}(\tau,\nu,S) = 1, \tag{2.6.15a}$$

$$P(\tau,\nu,0) = 0, \tag{2.6.15b}$$

$$\lim_{\nu\to\infty} \frac{\partial P}{\partial \nu}(\tau,\nu,S) = 0, \tag{2.6.15c}$$

$$\frac{\partial P}{\partial \tau}(\tau,0,S) + \kappa\gamma \frac{\partial P}{\partial \nu}(\tau,0,S) = 0. \tag{2.6.15d}$$

The conditions (2.6.15a), (2.6.15b) and (2.6.15d) remain the same as in (2.6.13). The condition (2.6.15d) is identical to (2.6.13d) with an additional assumption of zero interest rate, $r = 0$. The only different condition is (2.6.15c), which tells that for a large volatility, the option price tends to be constant.

An alternative setting is provided in [ZFV98],

$$\lim_{S\to\infty} P(\tau,\nu,S) = S, \tag{2.6.16a}$$

$$\frac{\partial P}{\partial \tau}(\tau,\nu,0) + \frac{\xi^2\nu}{2}\frac{\partial^2 P}{\partial \nu^2}(\tau,\nu,0) + \kappa(\gamma-\nu)\frac{\partial P}{\partial \nu}(\tau,\nu,0) - rP(\tau,\nu,0) = 0, \tag{2.6.16b}$$

$$\lim_{\nu\to\infty}\left(\frac{\partial P}{\partial \tau}(\tau,\nu,S) + \frac{1}{2}vS^2\frac{\partial^2 P}{\partial S^2}(\tau,\infty,S) + rS\frac{\partial P}{\partial S}(\tau,\infty,S) - rP(\tau,\infty,S)\right) = 0, \tag{2.6.16c}$$

$$\frac{\partial P}{\partial \tau}(\tau,0,S) + rS\frac{\partial P}{\partial S}(\tau,0,S) + \kappa\gamma\frac{\partial P}{\partial \nu}(\tau,0,S) - rP(\tau,0,S) = 0. \tag{2.6.16d}$$

As we can see, the Heston PDE is satisfied at the boundaries, resulting in the boundary conditions (2.6.16b)–(2.6.16d).

In turn, for European put options, the following set of conditions has been studied in [DF12],

$$\lim_{S\to\infty} \frac{\partial P}{\partial S}(\tau,\nu,S) = 0, \tag{2.6.17a}$$

$$P(\tau,\nu,0) = Ke^{-r(T-\tau)}, \tag{2.6.17b}$$

$$\lim_{\nu\to\infty} \frac{\partial P}{\partial \nu}(\tau,\nu,S) = 0, \tag{2.6.17c}$$

$$\frac{\partial P}{\partial \tau}(\tau,0,S) = 0. \tag{2.6.17d}$$

The interpretation of these conditions are similar to the American put options, which will be discussed later.

2.6.3 Closed-Form Solution for European Options

One of the main advantages of the Heston model is an existence result of the closed-form solution for European options. This is particularly important for calibration purposes, when multiple evaluations of an option price need to be performed with a small computational effort.

We present a representation formula of a closed-form solution for an European call option presented in the original work by L. Heston using the method of characteristic functions, for details of the derivation see [Hes93]. The solution is guessed in the following form

$$P_C(t,\nu,S) = SF_1 - Ke^{-rt}F_2, \tag{2.6.18}$$

where $t = T - \tau$ is the time to maturity and F_j $(j = 1, 2)$ are cumulative distribution functions (in the $\ln(K)$ variable). They satisfy the log-transformed PDE $(x = \ln S)$ (2.6.10) and can be evaluated via characteristic functions as follows

$$F_j(t,\nu,x;\ln(K)) = \frac{1}{2} + \frac{1}{\pi}\int_0^\infty \Re\left[\frac{e^{-\phi\ln(K)} f_j(t,\nu,x;\phi)}{i\phi}\right] d\phi, \tag{2.6.19}$$

where f_j are the characteristic functions of F_j, $j = 1, 2$, defined as

$$f_j(t,\nu,x;\phi) = e^{C_j(t;\phi)+D_j(t;\phi)\nu+i\phi x}, \tag{2.6.20}$$

$$C_j(t;\phi) = r\phi it + \frac{\kappa\gamma}{\xi^2}\Big\{(b_j - \rho\xi\phi i + d_j)t - 2\ln\left[\frac{1-g_j e^{d_j t}}{1-g_j}\right]\Big\}, \tag{2.6.21}$$

$$D_j(t;\phi) = \frac{b_j - \rho\xi\phi i + d_j}{\xi^2}\left[\frac{1-e^{d_j t}}{1-g_j e^{d_j t}}\right], \tag{2.6.22}$$

with auxiliary quantities

$$g_j = \frac{b_j - \rho\xi\phi i + d_j}{b_j - \rho\xi\phi i - d_j}, \qquad d_j = \sqrt{(\rho\xi\phi i - b_j)^2 - \xi^2(2u_j\phi i - \phi^2)}, \tag{2.6.23}$$

$$u_1 = \frac{1}{2}, \quad u_2 = \frac{-1}{2}, \qquad b_1 = \kappa - \rho\xi, \quad b_2 = \kappa. \tag{2.6.24}$$

Given the closed-form solution for the price of an European call we can use the put-call parity (2.4.15) to determine the price of an European put with the same strike and maturity.

We note that the integrals in (2.6.19) can not be computed directly and require an appropriate quadrature scheme, hence the Heston's solution is only semi-analytical.

2.6.4 American Put Options

We extend our considerations to American put options in the Heston model. Similar arguments as for the Black-Scholes model, Problem 2.4.1, are used here.

Problem 2.6.1. *The price of an American put option in the Heston model is a solution of the following system of inequalities*

$$\frac{\partial P}{\partial \tau} + \mathcal{L}^{\mathrm{H}} P \leq 0, \qquad (\tau, \nu, S) \in [0, T) \times \mathbb{R}^2_+ \tag{2.6.25a}$$

$$P \geq \mathcal{H}(S), \qquad (\tau, \nu, S) \in [0, T) \times \mathbb{R}^2_+ \tag{2.6.25b}$$

$$\left(\frac{\partial P}{\partial \tau} + \mathcal{L}^{\mathrm{H}} P\right)(P - \mathcal{H}(S)) = 0, \qquad (\tau, \nu, S) \in [0, T) \times \mathbb{R}^2_+ \tag{2.6.25c}$$

$$P(T, \nu, S) = \mathcal{H}(S), \qquad (\nu, S) \in \mathbb{R}^2_+, \tag{2.6.25d}$$

with appropriate boundary conditions.

Analogously to European call options, presented previously, several variations of the boundary conditions are found in the literature. The boundary conditions which are common in the literature, see, e.g., [CP99; KSW12], are

$$\lim_{S \to \infty} P(\tau, \nu, S) = \lim_{S \to \infty} \mathcal{H}(S) = 0, \tag{2.6.26a}$$

$$P(\tau, \nu, 0) = \mathcal{H}(0), \tag{2.6.26b}$$

$$\lim_{\nu \to \infty} \frac{\partial P}{\partial \nu}(\tau, \nu, S) = 0, \tag{2.6.26c}$$

$$P(\tau, 0, S) = \mathcal{H}(S). \tag{2.6.26d}$$

They can be described as follows, see, e.g., [CP99]: when the stock price is $S = 0$, it remains at zero, (2.6.1a), and an immediate exercise of the option is the best in this

case, which leads to a profit of $K - S$. For a large stock price, $S \to \infty$, the option is far out of the money and becomes worthless. For $\nu \to \infty$, it is expected that the price of the option is insensitive to the change of the volatility. For ν falling to 0, the asset becomes deterministic and an option is immediately exercised.

As before, the main difficulty and point of discussion appears for the boundary $\nu = 0$, due to the degeneracy of the Heston PDE. For this boundary, one may use a homogeneous Neumann boundary condition, [CP99; DF12],

$$\lim_{S\to\infty} P(\tau, \nu, S) = 0, \tag{2.6.27a}$$

$$P(\tau, \nu, 0) = \mathcal{H}(0), \tag{2.6.27b}$$

$$\lim_{\nu\to\infty} \frac{\partial P}{\partial \nu}(\tau, \nu, S) = 0, \tag{2.6.27c}$$

$$\frac{\partial P}{\partial \nu}(\tau, 0, S) = 0. \tag{2.6.27d}$$

In addition, Clarke et al., [CP99], propose to replace the condition (2.6.27a) with the gradient condition (2.6.28), "which was found in practice to be a better approximation at large volatilities":

$$\lim_{S\to\infty} \frac{\partial P}{\partial \nu}(\tau, \nu, S) = 0. \tag{2.6.28}$$

This modification was taken into account in subsequent research and as a result the following set of conditions appears in [HH15; IT08; IT09; Oos03]:

$$\lim_{S\to\infty} \frac{\partial P}{\partial \nu}(\tau, \nu, S) = 0, \tag{2.6.29a}$$

$$P(\tau, \nu, 0) = \mathcal{H}(0), \tag{2.6.29b}$$

$$\lim_{\nu\to\infty} \frac{\partial P}{\partial \nu}(\tau, \nu, S) = 0. \tag{2.6.29c}$$

For the boundary $\nu \to 0$, it is assumed that the Heston problem (2.6.25) is fulfilled on $\nu = 0$,

$$\begin{cases} \frac{\partial P}{\partial \tau} + \widetilde{\mathcal{L}}^{\mathrm{H}} P \leq 0, \quad P \geq \mathcal{H}(S), \\ \left(\frac{\partial P}{\partial \tau} + \widetilde{\mathcal{L}}^{\mathrm{H}} P\right)(P - \mathcal{H}(S)) = 0, \end{cases} \tag{2.6.29d}$$

where the operator $\widetilde{\mathcal{L}}^{\mathrm{H}}$ is defined in (2.6.14).

Note that in [Oos03], instead of the boundary condition (2.6.29d), the condition (2.6.27d) is used.

In [OO13] the same setting of the boundary conditions (2.6.29) is used, despite a small modification. Instead of the first order derivative terms for $\nu, S \to \infty$, the second derivative asymptotic boundary condition is employed (2.6.30)

$$\lim_{\nu,S\to\infty} \frac{\partial^2 P}{\partial S \partial \nu}(\tau, \nu, S) = 0. \tag{2.6.30}$$

In [FLM+11], all boundary conditions are set up to be the value of the pay-off function,

$$\lim_{\substack{\nu,S\to 0 \\ \nu,S\to\infty}} |P(\tau, \nu, S) - \mathcal{H}(S)| = 0. \tag{2.6.31}$$

In [ZFV98], for $S \to \infty$ one uses $P(\tau, \nu, S) = 0$. The remaining boundary conditions ($\nu, S \to 0$, $\nu \to \infty$) are obtained by taking an asymptotic limit in the Heston PDE (2.6.16b)–(2.6.16d), similarly to the case of European options.

2.7 Log-Transformation and Localization of the Problem

The Black-Scholes (2.4.10) and Heston (2.6.11) operators have variable coefficients in the stock price direction. For convenience of numerical simulation and for eliminating the degeneracy of the PDE when $S = 0$, a standard way is to perform a log-transformation of a stock variable by introducing a new variable $x := \log(S/K)$. In addition, a transformation of the time axis $t := T - \tau$ allows us to consider a forward problem instead of a backward one.

Denote $w(t, x) := P(T - t, Ke^x)$ to be an option's price in the new variables. The pay-off function for a call or put option transforms to $\chi(x) := \mathcal{H}(Ke^x)$,

$$\chi(x) = \begin{cases} (Ke^x - K)_+, & \textit{call}, \\ (K - Ke^x)_+, & \textit{put}. \end{cases} \tag{2.7.1}$$

Define $L := L^s$, $s \in \{\mathrm{BS}, \mathrm{H}\}$ to be a spatial operator for the Black-Scholes ($s = \mathrm{BS}$) or Heston ($s = \mathrm{H}$) models with respect to the log-transformation of the stock-price. It corresponds to an operator $\mathcal{L}^s$, $s = \{\mathrm{BS}, \mathrm{H}\}$ in (2.4.10), (2.6.11), and is defined as follows:

$$L^{\mathrm{BS}} w = \frac{1}{2}\sigma^2 \frac{\partial^2 w}{\partial x^2} + \left(r - \frac{1}{2}\sigma^2\right)\frac{\partial w}{\partial x} - rw, \tag{2.7.2}$$

$$L^{\mathrm{H}} w = \frac{1}{2}\nu \frac{\partial^2 w}{\partial x^2} + \xi\nu\rho \frac{\partial^2 w}{\partial \nu \partial x} + \frac{1}{2}\xi^2 \nu \frac{\partial^2 w}{\partial \nu^2} + \kappa(\gamma - \nu)\frac{\partial w}{\partial \nu} + \left(r - \frac{1}{2}\nu\right)\frac{\partial w}{\partial x} - rw. \tag{2.7.3}$$

In a case of a dividend payment, similarly to (2.4.11), the log-transformed Black-Scholes operator is defined as follows

$$L^{\mathrm{BS}}w = \frac{1}{2}\sigma^2\frac{\partial^2 w}{\partial x^2} + (r - \frac{1}{2}\sigma^2 - q)\frac{\partial w}{\partial x} - rw. \tag{2.7.4}$$

Above operators are of diffusion-convection-reaction type. In a compact form the Heston operator (2.7.3) can be re-written as

$$L^{\mathrm{H}}w = \nabla \cdot \mathbf{A}\nabla w - \mathbf{b} \cdot \nabla w - rw, \tag{2.7.5a}$$

with $\nabla := \left(\frac{\partial}{\partial \nu}, \frac{\partial}{\partial x}\right)^T$, diffusion matrix $\mathbf{A}$ and velocity vector $\mathbf{b}$

$$\mathbf{A} := \frac{1}{2}\nu \begin{bmatrix} \xi^2 & \rho\xi \\ \rho\xi & 1 \end{bmatrix}, \qquad \mathbf{b} := \begin{bmatrix} -\kappa(\gamma - \nu) + \frac{1}{2}\xi^2 \\ -r + \frac{1}{2}\nu + \frac{1}{2}\xi\rho \end{bmatrix}. \tag{2.7.5b}$$

We introduce a spatial domain $\Omega_\infty := (-\infty, \infty)$ for the Black-Scholes model and $\Omega_\infty := (0, \infty) \times (-\infty, \infty)$ for the Heston model.

With the use of these notations, we can reformulate the option pricing problems for European and American options as follows.

Problem 2.7.1. *The price of the European call/put option in the Black-Scholes or Heston model is a solution of the following problem*

$$\frac{\partial w}{\partial t} - L^s w = 0, \qquad \text{in} \quad (0, T] \times \Omega_\infty, \tag{2.7.6a}$$

$$w_0(x) = \chi(x), \qquad \text{in} \quad \Omega_\infty, \tag{2.7.6b}$$

with $s \in \{\mathrm{BS}, \mathrm{H}\}$ and subject to the corresponding boundary conditions.

Problem 2.7.2. *The price of the American put option in the Black-Scholes or Heston model is a solution of the system of inequalities*

$$\frac{\partial w}{\partial t} - L^s w \geq 0, \qquad \text{in} \quad (0, T] \times \Omega_\infty, \tag{2.7.7a}$$

$$w \geq \chi, \qquad \text{in} \quad (0, T] \times \Omega_\infty, \tag{2.7.7b}$$

$$\left(\frac{\partial w}{\partial t} - L^s w\right)(w - \chi) = 0, \qquad \text{in} \quad (0, T] \times \Omega_\infty, \tag{2.7.7c}$$

$$w_0(x) = \chi(x), \qquad \text{in} \quad \Omega_\infty, \tag{2.7.7d}$$

with $s \in \{\mathrm{BS}, \mathrm{H}\}$ and subject to the corresponding boundary conditions.

In order to perform a numerical simulation, we localize the problem to a bounded domain Ω. It is defined as $\Omega := (x_{\min}, x_{\max}) \subset \mathbb{R}$ for the Black-Scholes model and $\Omega := (\nu_{\min}, \nu_{\max}) \times (x_{\min}, x_{\max}) \subset \mathbb{R}^2$ for the Heston model, with $x_{\min} < 0 < x_{\max}$ and $0 < \nu_{\min} < \nu_{\max}$.

If not stated otherwise, we assume that the Feller condition (2.6.2) is satisfied, such that the variance process is strictly positive. Taking $\nu_{\min} > 0$ allows us to avoid the degeneracy of the Heston PDE at $\nu = 0$ and preserve the matrix $\mathbf{A}$ in (2.7.5b) to be uniformly positive definite.

Next, we impose boundary conditions on the truncated boundaries of the domain Ω. The boundary conditions (2.4.13b), (2.4.14b) for European call and put options in the Black-Scholes model transforms accordingly with respect to the new variable.

The truncated boundary conditions for the European call option in the Heston model follows from (2.6.13) and are prescribed as in [WAW01]:

$$\Gamma_1 : \nu = \nu_{\min} \qquad w(t, \nu_{\min}, x) = Ke^x N(d_1) - Ke^{-rt} N(d_2), \tag{2.7.8a}$$

$$\Gamma_2 : \nu = \nu_{\max} \qquad w(t, \nu_{\max}, x) = Ke^x, \tag{2.7.8b}$$

$$\Gamma_3 : x = x_{\min} \qquad w(t, \nu, x_{\min}) = \lambda w(t, \nu_{\max}, x_{\min}) + (1 - \lambda) w(t, \nu_{\min}, x_{\min}), \tag{2.7.8c}$$

$$\lambda = \frac{\nu - \nu_{min}}{\nu_{\max} - \nu_{\min}},$$

$$\Gamma_4 : x = x_{\max} \qquad \frac{\partial w}{\partial x}(t, \nu, x_{\max}) := \mathbf{A}\nabla w \cdot \mathbf{n} = \frac{1}{2}\nu K e^x. \tag{2.7.8d}$$

The boundary condition at $\nu = \nu_{\min}$, $\nu_{\min} > 0$ and $\nu = \nu_{\max}$ are derived from the solution of the Black-Scholes equation (2.4.17), see [WAW01] and Remark (2.6.1). The cumulative distribution function $N(\cdot)$ is defined in (2.4.16). The quantities $d_{1,2}$ are defined in (2.4.18) with $\sigma = \sqrt{\nu}$, $\nu = \gamma$ and $\gamma = \nu_{\min}$ and $\gamma = \nu_{\max}$ respectively.

Alternatively, instead of a Neumann condition on $\Gamma_4 := \{x = x_{\max}\}$, one may impose a Dirichlet boundary condition as a linear interpolation between the values $\nu = \nu_{\min}$ and $\nu = \nu_{\max}$,

$$\Gamma_4 : x = x_{\max} \qquad w(t, \nu, x_{\max}) = \lambda w(t, \nu_{\max}, x_{\max}) + (1 - \lambda) w(t, \nu_{\min}, x_{\max}), \tag{2.7.9}$$

$$\lambda = \frac{\nu - \nu_{\min}}{\nu_{\max} - \nu_{\min}}.$$

For European put options in the Heston model, the truncated boundary conditions

follows from (2.6.17)

$$\frac{\partial w}{\partial \nu}(t, \nu_{\min}, x) = 0, \qquad \text{on} \quad \Gamma_1, \tag{2.7.10a}$$

$$\frac{\partial w}{\partial \nu}(t, \nu_{\max}, x) = 0, \qquad \text{on} \quad \Gamma_2, \tag{2.7.10b}$$

$$w(t, \nu, x_{\min}) = Ke^{-rt}, \qquad \text{on} \quad \Gamma_3, \tag{2.7.10c}$$

$$w(t, \nu, x_{\max}) = 0, \qquad \text{on} \quad \Gamma_4. \tag{2.7.10d}$$

For an American put in the Black-Scholes model we set

$$w(t, x) = \chi(x), \qquad \text{on} \quad \Gamma_3 \cup \Gamma_4. \tag{2.7.11}$$

The boundary conditions (2.6.26) for an American put in the Heston model on the truncated domain are replaced by

$$w(t, \nu, x) = \chi(x), \qquad \text{on} \quad \Gamma_1 \cup \Gamma_3 \cup \Gamma_4, \tag{2.7.12}$$

$$\frac{\partial w}{\partial \nu}(t, \nu_{\max}, x) = 0, \qquad \text{on} \quad \Gamma_2. \tag{2.7.13}$$

The alternative set of conditions (2.6.27) transforms into

$$w(t, \nu, x) = \chi(x), \qquad \text{on} \quad \Gamma_3 \cup \Gamma_4, \tag{2.7.14a}$$

$$\frac{\partial w}{\partial \nu}(t, \nu_{\min}, x) = 0, \qquad \text{on} \quad \Gamma_1, \tag{2.7.14b}$$

$$\frac{\partial w}{\partial \nu}(t, \nu_{\max}, x) = 0, \qquad \text{on} \quad \Gamma_2. \tag{2.7.14c}$$

3 RBM for Parametrized Linear Parabolic Equations

3.1 Introduction

In this chapter we consider an application of the reduced basis methods to European options or, generally speaking, to parametrized linear parabolic problems. The methodology was extensively studied in the literature, cf. [BMP$^+$12; GP05; Gre05; Haa16; HO08b; HRS16; Roz05; VPR$^+$03] and the references therein.

The reduced basis method is a model order reduction technique, which tries to exploit the parameter-dependence of the problem and is based on an approximation by low-dimensional spaces. These spaces are constructed by greedy procedures from a set of snapshots, i.e., solutions computed at different parameter values. For parabolic problems, an adapted version of the greedy strategy, the POD-Greedy procedure, is used, [Haa13; HO08b]. The efficiency of the method is then established with a so called offline-online decomposition of the computation routine.

We refer to some recent contributions of the reduced basis method in the context of option pricing. In [CLP11] a tailored RB approach is used to price options with diffusion and jump-diffusion models, which later was generalized to basket options [Pir11] and, in fact, was shown to be a variant of the Proper Orthogonal Decomposition method (POD) [Pir12]. In [MU14] the reduced basis method in a space-time framework was applied to price European options in the Heston model with parameter functions as initial condition. The reduced basis method for basket options in the Black-Scholes and Heston model in combination with sparse grids was explored in [PGB15].

In this chapter we recall the theoretical framework of the RBM for linear parabolic equations with an adaptation to the pricing of European options. In particular, we discuss the POD-Greedy procedure for the reduced basis construction as well as a posteriori error estimates. Several numerical tests at the end of the chapter provide a verification of the described approach.

The content of this chapter is structured as follows: In Section 3.2 we present the strong formulation of the model problem to price European options. In Section 3.3 we provide the weak and discrete weak formulations of the problem. In Section 3.4, we outline the main aspects of the reduced basis methodology for linear parabolic equations. In particular, we discuss a derivation of a posteriori error bounds (see

Section 3.4.2) and an algorithm for the construction of reduced basis spaces (see Section 3.4.3). An offline-online computational procedure, in a general framework as well as for particular examples of the Black-Scholes and Heston models, is summarized in Section 3.4.4. Numerical results, given in Section 3.5, illustrate the performance of the method for pricing European options in the Heston model.

3.2 Model Problem: European Options

Recall the problem formulation to price European options, introduced in Chapter 2. We present the problem in the context of a general framework, which can cover a larger class of applications, not necessarily in finance.

Let $\Omega \subset \mathbb{R}^d$, $d = 1, 2$, be an open bounded domain with Lipschitz continuous boundary $\partial\Omega$. Consider a second order linear differential operator

$$Lw := \nabla \cdot (\mathbb{K}\nabla w) - \mathbf{b} \cdot \nabla w - c_0 w, \tag{3.2.1}$$

where $\mathbb{K} : \Omega \to \mathbb{R}^{d\times d}$, $\mathbf{b} : \Omega \to \mathbb{R}^d$, $c_0 : \Omega \to \mathbb{R}$. We impose the following assumptions on the coefficients,

(*A*1) there exist constants $0 < k_1 \leq k_2$, such that $k_1|\xi|^2 \leq \mathbb{K}(\mathbf{x})\xi \cdot \xi \leq k_2|\xi|^2$, for all $\xi \in \mathbb{R}^d$, a.e. $\mathbf{x} \in \Omega$.

(*A*2) $\mathbb{K} := (\kappa_{i,j})_{i,j=1}^d$, $\mathbf{b} := (b_j)_{j=1}^d$, with $\kappa_{ij}, b_j, c_0 \in L^\infty(\Omega)$.

The first condition is often referred as *ellipticity* of the differential operator $\nabla\cdot(\mathbb{K}\nabla w)$ with ellipticity constant k_1.

Define the space-time cylinder $Q_\mathrm{T} := (0, T] \times \Omega$, $T > 0$ and the space-time surfaces $\Sigma_\mathrm{D} := (0, T] \times \Gamma_\mathrm{D}$, $\Sigma_\mathrm{N} := (0, T] \times \Gamma_\mathrm{N}$, where Γ_D and Γ_N denote the Dirichlet and Neumann portions of the boundary $\partial\Omega$, $\partial\Omega := \Gamma_\mathrm{D} \cup \Gamma_\mathrm{N}$, $\Gamma_\mathrm{D} \cap \Gamma_\mathrm{N} = \emptyset$, respectively.

We are dealing with the following initial and boundary value problem: Given $w_0 : \Omega \to \mathbb{R}$, $g : \Sigma_\mathrm{D} \to \mathbb{R}$ and $h : \Sigma_\mathrm{N} \to \mathbb{R}$, find $w : Q_\mathrm{T} \to \mathbb{R}$, satisfying

$$\frac{\partial w}{\partial t} - Lw = 0, \qquad \text{in} \quad Q_\mathrm{T}, \tag{3.2.2a}$$

$$w(0) = w_0, \qquad \text{on} \quad \Omega, \tag{3.2.2b}$$

$$w = g, \qquad \text{on} \quad \Sigma_\mathrm{D}, \tag{3.2.2c}$$

$$\frac{\partial w}{\partial n_L} = h, \qquad \text{on} \quad \Sigma_\mathrm{N}, \tag{3.2.2d}$$

where $\frac{\partial w}{\partial n_L}$ is a conormal derivative of w w.r.t. L, $\frac{\partial w}{\partial n_L} := \mathbb{K}\nabla w \cdot \mathbf{n}$. Note that we consider only a time independent linear operator L.

Such model covers a very large class of problems, e.g., convection-diffusion-reaction processes with also non-homogeneous right-hand side, where the term $-\nabla \cdot (\mathbb{K}\nabla w)$

describes the diffusion (with $\mathbb{K}$ being a diffusion/conductivity matrix), the term $\mathbf{b}\cdot\nabla w$ models the transport or convection process (with $\mathbf{b}$ being a velocity/convective field) and $c_0 w$ represents the reaction term (with a reaction rate c_0).

In particular, for the Black-Scholes and Heston models, recall the following settings from Section 2. The domain Ω is defined in (3.2.3a) and (3.2.3b) respectively.

$$\Omega := \{x \in \mathbb{R} : -\infty \leq x_{\min} \leq x \leq x_{\max} < \infty\}, \tag{3.2.3a}$$

$$\Omega := \{(\nu, x) \in \mathbb{R}^2 : 0 < \nu_{\min} \leq \nu \leq \nu_{\max} < \infty, \quad -\infty < x_{\min} \leq x \leq x_{\max} < \infty\}. \tag{3.2.3b}$$

The initial value w_0 is defined as the value of the pay-off functional $w_0 = \chi(x)$, $\chi(x) := (K - Ke^x)_+$ or $\chi(x) := (Ke^x - K)_+$, for a call or put option respectively, (2.7.1). The spatial operator L is defined in (2.7.4) and (2.7.5) for the Black-Scholes and Heston models respectively. The boundary data h and g together with the boundary portions Γ_{D}, Γ_{N} of $\partial\Omega$ are specified in Section 2.7.

3.3 Detailed Problem Formulation

In this section we present a variational formulation of (3.2.2), state a well-posedness result and discuss the discretization of the weak problem.

3.3.1 Mathematical Preliminaries

To recast the problem (3.2.2) in a weak form, we recall the notion of Bochner spaces, which are used to study time-dependent PDEs, see, e.g., [LM72a; LM72b; Zei90].

In the context of parabolic problems, a standard way to consider a space-time function u as a vector-valued function $u : [0, T] \to X$, defined on a time interval $[0, T]$, $0 < T < \infty$ with values in some Banach or Hilbert space X. Consider a Gelfand triple (or an "evolution triple") of Hilbert spaces $X \hookrightarrow H \hookrightarrow X'$, see, e.g., [Zei90, Section 23.4], with X' being the dual space of X. Denote by $(\cdot, \cdot)_X$ the scalar product on X with the corresponding norm $\|\cdot\|_X$. Define $\langle \cdot, \cdot \rangle_{X' \times X}$ to be a duality pairing of X with X'. For example, a standard choice for linear parabolic PDEs is

$$H := L^2(\Omega), \qquad H_0^1(\Omega) \subset X \subset H^1(\Omega).$$

Denote by $L^2(0, T; X)$ the space of all measurable functions $u : [0, T] \to X$, for which

$$\|u\|_{L^2(0,T;X)} := \left(\int_0^T \|u\|_X^2 dt \right)^{1/2} < \infty.$$

We define the Sobolev space $W(0, T; X)$ as follows:

$$W(0, T; X) := \left\{ u \in L^2(0, T; X) : u' = \frac{du}{dt} \in L^2(0, T; X') \right\},$$

where the time derivative $\frac{du}{dt}$ is understood as a generalized derivative on $(0,T)$, such that

$$\langle u'(t), v\rangle_{X'\times X} = \frac{d}{dt}\left(u(t), v\right)_H, \quad \forall v \in X. \tag{3.3.1}$$

The space $W(0,T;X)$ is endowed with the norm

$$\|u\|_{W(0,T;X)} := \|u\|_{L^2(0,T;X)} + \|u'\|_{L^2(0,T;X')}.$$

An alternative notation is

$$W(0,T;X) = L^2(0,T;X) \cap H^1(0,T;X'). \tag{3.3.2}$$

3.3.2 Variational Formulation

Introduce the following spaces

$$X = H^1(\Omega), \qquad V = H^1_{\Gamma_\mathrm{D}}(\Omega) := \{v \in X : \quad v|_{\Gamma_\mathrm{D}} = 0\}. \tag{3.3.3}$$

If not stated otherwise, we equipped these spaces with the following norms, $\|\cdot\|_X = \|\cdot\|_{H^1(\Omega)}$ and $\|\cdot\|_V = |\cdot|_{H^1(\Omega)}$, where the former is the full H^1-norm and the latter is the corresponding seminorm. We set $H := L^2(\Omega)$, and assume that $w_0 \in H$ and the Dirichlet boundary data $g \in L^2(0,T;H^{1/2}(\Gamma_\mathrm{D})) \cap H^{1/4}(0,T;L^2(\Gamma_\mathrm{D}))$. Introduce a linear continuous extension operator $\mathcal{R}$, which extends a non-homogeneous Dirichlet boundary conditions to the interior of the domain,

$$\mathcal{R} : L^2(0,T;H^{1/2}(\Gamma_\mathrm{D})) \cap H^{1/4}(0,T;L^2(\Gamma_\mathrm{D})) \to W(0,T;X). \tag{3.3.4}$$

Such operator can be defined, e.g., as the solution of the heat equation ($\partial\Omega \subset C^2$), [LM72b, Chapter 4, Section 15.5]. Define the Dirichlet lift function $u_L \in W(0,T;X)$ as $u_L = \mathcal{R}g$. For all $v \in V$ we now define $f(t)$ via the functional

$$\langle f(t), v\rangle_{V'\times V} = \int_{\Gamma_\mathrm{N}} h(t) v d\Gamma_\mathrm{N} - \frac{d}{dt}(u_L(t), v)_H - a(u_L(t), v). \tag{3.3.5}$$

Assuming that $h \in L^2(0,T,L^2(\Gamma_\mathrm{N}))$ and provided $u_L \in W(0,T;X)$, we have $f \in L^2(0,T;V')$. Next, we define a bilinear form $a : V \times V \to \mathbb{R}$, as

$$a(u,v) = \int_\Omega \left(\mathbb{K}\nabla u \cdot \nabla v + \mathbf{b}\cdot\nabla u v + c_0 u v\right) d\Omega. \tag{3.3.6}$$

We say that a bilinear form $a(\cdot,\cdot)$ is (*strongly*) *coercive* and *continuous*, if there exist $0 < \alpha_a \le \gamma_a < \infty$, such that

$$|a(u,v)| \le \gamma_a \|u\|_V \|v\|_V \qquad \forall u, v \in V, \qquad (\textit{continuity}) \tag{3.3.7a}$$

$$a(v,v) \ge \alpha_a \|v\|_V^2 \qquad \forall v \in V. \qquad (\textit{coercivity}) \tag{3.3.7b}$$

We also introduce a weaker condition than a strong coercivity, referred to as the Gårding inequality. We say, that the bilinear form satisfies the Gårding inequality if there exist $\alpha_a > 0$ and $0 \leq \lambda_a < \infty$, such that

$$a(v,v) \geq \alpha_a \|v\|_V^2 - \lambda_a \|v\|_{L^2(\Omega)}^2 \qquad \forall v \in V. \qquad (\textit{Gårding inequality}) \tag{3.3.7c}$$

Obviously, if the bilinear form is coercive, then it satisfies the Gårding inequality.

We define $u(t) := w(t) - u_L(t)$, $t \in (0,T)$, with $u(0) = u_0 := w(0) - u_L(0)$. Then we consider the following weak formulation of (3.2.2) with the homogeneous Dirichlet boundary conditions: Given $u_0 \in H$, $f \in L^2(0,T;V')$, find $u \in W(0,T;V)$, such that for a.e. $t \in (0,T)$ it holds

$$\frac{d}{dt}(u(t),v)_H + a(u(t),v) = \langle f(t), v\rangle_{V'\times V}, \quad \forall v \in V, \tag{3.3.8a}$$

$$u(0) = u_0. \tag{3.3.8b}$$

The well-posedness of the problem (3.3.8) is a well-know result; see e.g., [DL00, Chapter XVIII, §3], [QV94, Theorem 11.1.1, Remark 11.1.1] and is summarized in the following theorem.

Theorem 3.3.1. *Let V, H are given and form a Gelfand triple. Assume a bilinear form $a(\cdot,\cdot)$ is continuous and satisfies a Gårding inequality on V,* (3.3.7)*. Then, given $f \in L^2(0,T;V')$ and $u_0 \in H$, there exist a unique solution $u \in W(0,T;V)$ of* (3.3.8)*.*

Remark 3.3.1. *Note that under the assumptions (A1)–(A2), the bilinear form $a(\cdot,\cdot)$* (3.3.6) *is always continuous and satisfies a Gårding inequality, see, e.g., [QV94]. However a coercivity condition does not follow directly and requires additional investigations of the coefficients. In some cases, e.g., if*

$$c_0(\mathbf{x}) - \frac{1}{2}\nabla\cdot\mathbf{b}(\mathbf{x}) \geq \mu_0 > 0 \quad \textit{in } \Omega \qquad \mathbf{b}\cdot\mathbf{n} \geq 0 \quad \textit{on } \Gamma_{\mathrm{N}}, \tag{3.3.9}$$

then we can conclude that the bilinear form is coercive on V with $\|\cdot\|_V = |\cdot|_{H^1}$, see e.g., [QV94].

3.3.3 Parametrized Problem

We consider option pricing models which involve a set of different parameters. It is convenient to reformulate the problem (3.3.8) as a parametrized PDE. Denote by $\boldsymbol{\mu} = (\mu_1, \ldots, \mu_p)$ an input parameter vector, collecting all parameters of the model, and by $\mathcal{P} \subset \mathbb{R}^p$, a p-dimensional parameter set. Then for any $\boldsymbol{\mu} \in \mathcal{P}$ we consider

the following parametrized form of the problem (3.3.8): Given $f(\boldsymbol{\mu}) \in L^2(0,T;V')$, $u_0(\boldsymbol{\mu}) \in H$, find $u(\boldsymbol{\mu}) \in W(0,T;V)$ such that for a.e. $t \in (0,T)$ it holds

$$\frac{d}{dt}(u(t;\boldsymbol{\mu}),v)_H + a(u(t;\boldsymbol{\mu}),v;\boldsymbol{\mu}) = \langle f(t;\boldsymbol{\mu}),v\rangle_{V'\times V}, \quad \forall v \in V, \tag{3.3.10a}$$

$$u(0) = u_0(\boldsymbol{\mu}). \tag{3.3.10b}$$

For the well-posedness of the parametrized problem, we need to require that the parameter dependent bilinear form $a(\cdot,\cdot;\boldsymbol{\mu})$ remains continuous and coercive (or at least satisfies the Gårding inequality) for all values of the parameter $\boldsymbol{\mu} \in \mathcal{P}$, i.e., there exist positive constants $0 < \overline{\alpha}_a \leq \alpha_a(\boldsymbol{\mu})$, $0 < \gamma_a(\boldsymbol{\mu}) \leq \overline{\gamma}_a < \infty$, $0 \leq \lambda_a(\boldsymbol{\mu}) \leq \overline{\lambda}_a < \infty$, such that

$$|a(u,v;\boldsymbol{\mu})| \leq \gamma_a(\boldsymbol{\mu})\|u\|_V\|v\|_V \qquad \forall u,v \in V, \tag{3.3.11}$$

$$a(v,v;\boldsymbol{\mu}) \geq \alpha_a(\boldsymbol{\mu})\|v\|_V^2 - \lambda_a(\boldsymbol{\mu})\|v\|_{L^2(\Omega)}^2 \qquad \forall v \in V. \tag{3.3.12}$$

For all $\boldsymbol{\mu} \in \mathcal{P}$ the coercivity and continuity constants are, respectively, defined as

$$\gamma_a(\boldsymbol{\mu}) = \sup_{u\in V}\sup_{v\in V}\frac{a(u,v;\boldsymbol{\mu})}{\|u\|_V\|v\|_V}, \qquad \alpha_a(\boldsymbol{\mu}) = \inf_{u\in V}\frac{a(u,u;\boldsymbol{\mu}) + \lambda_a(\boldsymbol{\mu})\|u\|_{L^2(\Omega)}^2}{\|u\|_V^2}. \tag{3.3.13}$$

We note that the optimal choice of $\alpha_a(\boldsymbol{\mu})$ still depends on an admissible choice of $\lambda_a(\boldsymbol{\mu})$, which should fulfill

$$\lambda_a(\boldsymbol{\mu}) > -\inf_{u\in L^2(\Omega)}\frac{a(u,u;\boldsymbol{\mu})}{\|u\|_{L^2(\Omega)}^2}.$$

Due to the strict inequality, which can not be relaxed, there is still some freedom in the choice of $\lambda_a(\boldsymbol{\mu})$.

To simplify the presentation, in some cases we omit the parameter vector $\boldsymbol{\mu}$ in the notation of the parameter dependent quantities.

Parametrized form of the Black-Scholes and Heston models

Recall that in the case of the Black-Scholes model, $\boldsymbol{\mu} = (\sigma, q, r) \in \mathcal{P} \subset \mathbb{R}^3$ with $\sigma > 0$, $q, r \geq 0$ (see Section 2.4), and in the Heston model, $\boldsymbol{\mu} = (\xi, \rho, \gamma, \kappa, r) \in \mathcal{P} \subset \mathbb{R}^5$, with $\xi, \gamma, \kappa > 0$, $r \geq 0$, $\rho \in (-1, 1)$ (see Section 2.6).

We define the bilinear form $a(\cdot,\cdot;\boldsymbol{\mu}) := a^s(\cdot,\cdot;\boldsymbol{\mu})$, $s = \{\mathrm{BS}, \mathrm{H}\}$, for the Black-Scholes (3.3.14a) and Heston (3.3.14b) models. Note that $a(\cdot,\cdot,\boldsymbol{\mu})$ is given by (3.3.6), where $\mathbb{K} = \frac{1}{2}\sigma^2$, $\mathbf{b} = (\frac{1}{2}\sigma^2 + q - r)$, and $c_0 = r$ for the Black-Scholes and $\mathbb{K} = \mathbf{A}$ and

$c_0 = r$ for the Heston models:

$$a^{\mathrm{BS}}(u, v; \boldsymbol{\mu}) := \int_\Omega \left(\frac{1}{2}\sigma^2 \nabla u \cdot \nabla v + \left(\frac{1}{2}\sigma^2 + q - r \right) \nabla uv + ruv \right) d\Omega, \tag{3.3.14a}$$

$$a^{\mathrm{H}}(u, v; \boldsymbol{\mu}) := \int_\Omega \left(\mathbf{A}\nabla u \cdot \nabla v + \mathbf{b} \cdot \nabla uv + ruv \right) d\Omega, \tag{3.3.14b}$$

where

$$\mathbf{A} := \frac{1}{2}\nu \begin{bmatrix} \xi^2 & \rho\xi \\ \rho\xi & 1 \end{bmatrix}, \qquad \mathbf{b} := \begin{bmatrix} -\kappa(\gamma - \nu) + \frac{1}{2}\xi^2 \\ -r + \frac{1}{2}\nu + \frac{1}{2}\xi\rho \end{bmatrix}, \tag{3.3.15}$$

Note, we have $\nu \geq \nu_{\min} > 0$, $\rho \in (-1, 1)$ and, hence, $\mathbf{A}$ is uniformly positive definite on $\overline{\Omega}$.

It follows, from the admissible values of the parameters, that for both models the assumptions $(A1)$ and $(A2)$ are fulfilled. Hence, the bilinear forms (3.3.14) are continuous and satisfy the Gårding inequality, and the existence of a unique solution for the Black-Scholes and Heston models is guaranteed, see Theorem 3.3.1, Remark 3.3.1.

Moreover, for $r > 0$, $a^{\mathrm{BS}}(\cdot, \cdot)$ is also coercive, see Remark 3.3.1. However, the same is not true for $a^{\mathrm{H}}(\cdot, \cdot)$. In fact, if the coefficients of the Heston model are such that $r > \frac{1}{2}\kappa$ and, if (2.7.8d) is applied, also $\frac{1}{2}\xi\rho - r > 0$, then the bilinear form $a^{\mathrm{H}}(\cdot, \cdot)$ is coercive, Remark 3.3.1, see also [WAW01, Theorem 3.1].

3.3.4 Discretization

We introduce a high-fidelity approximation of (3.3.10). Upon the discrete problem we will later build our reduced basis approximation. In this context, the discrete problem is often referred as the *"detailed"* or *"truth"* one, and the original model problem (3.2.2) as the *"exact"* one.

Let $X_{\mathcal{N}} \subset X$ and $V_{\mathcal{N}} \subset V$ be finite-dimensional subspaces of X and V respectively, endowed with the basis

$$X_{\mathcal{N}} = \mathrm{span}\{\phi_i, \quad i = 1, \ldots, \mathcal{N}_X\}, \quad V_{\mathcal{N}} = X_{\mathcal{N}} \cap V = \mathrm{span}\{\phi_i, \quad i = 1, \ldots, \mathcal{N}_V\},$$

of the dimension $\dim(V_{\mathcal{N}}) = \mathcal{N}_V = \mathcal{N}$ and $\dim(X_{\mathcal{N}}) = \mathcal{N}_X$. The dimensions $\mathcal{N}, \mathcal{N}_X$ are assumed to be large enough, such that the error between the exact and discrete solution is negligible. The discrete spaces inherit the inner products and norms of the exact spaces, i.e., $(\cdot, \cdot)_{X_{\mathcal{N}}} = (\cdot, \cdot)_X$, $\| \cdot \|_{X_{\mathcal{N}}} = \| \cdot \|_X$, and analogously for $V_{\mathcal{N}}$.

For the temporal discretization, we apply a θ-scheme, with $\theta = 1$ for the implicit Euler, $\theta = 0$ for the explicit Euler and $\theta = 1/2$ for the Crank-Nicolson schemes. Since, for $1/2 \leq \theta \leq 1$ the scheme is unconditionally stable, see, e.g., [QV94], for further discussion we restrict ourselves to this choice of the parameter θ.

We divide the interval $[0,T]$ into I subintervals of equal length $\Delta t := T/I$ and $t^k := k\Delta t$, $0 < k \leq I$. For notational convenience, we introduce the following sets of indices

$$\mathbb{I} \equiv \{0,\dots,I-1\}, \quad \mathbb{I}_0 \equiv \mathbb{I} \cup \{I\} \tag{3.3.16}$$

The exact solution $u(t;\boldsymbol{\mu})$ is then approximated by $u_{\mathcal{N}}^{k+1}(\boldsymbol{\mu}) := u_{\mathcal{N}}(t^{k+1};\boldsymbol{\mu}) \in V_{\mathcal{N}}$,

$$u_{\mathcal{N}}^{k+1}(\boldsymbol{\mu}) = \sum_{j=1}^{\mathcal{N}} u_{\mathcal{N},j}^{k+1}(\boldsymbol{\mu})\phi_j, \quad u_{\mathcal{N},j}^{k+1}(\boldsymbol{\mu}) \in \mathbb{R}, \quad k \in \mathbb{I}.$$

Denote by $g_{\mathcal{N}}^k(\boldsymbol{\mu})$ the nodal interpolation of the Dirichlet data $g^k(\boldsymbol{\mu})$, $\boldsymbol{\mu} \in \mathcal{P}$, $k \in \mathbb{I}_0$, i.e., $g_{\mathcal{N}}^k(\boldsymbol{\mu}) = \mathcal{I}_{\mathcal{N}}(g^k(\boldsymbol{\mu}))$, where $\mathcal{I}_{\mathcal{N}}$ is the nodal interpolation operator. Denote by $X_{\mathcal{N}}^{\mathrm{D}} \subset X_{\mathcal{N}}$ the space of basis functions associated with the nodes on the Dirichlet boundary Γ_{D}. Then we introduce a discrete linear continuous extension operator $\mathcal{R}_{\mathcal{N}} : X_{\mathcal{N}}^{\mathrm{D}} \to X_{\mathcal{N}}$, and a discrete lift function $u_{L\mathcal{N}}^k(\boldsymbol{\mu}) = \mathcal{R}_{\mathcal{N}}(g_{\mathcal{N}}^k(\boldsymbol{\mu})) \in X_{\mathcal{N}}$. Furthermore, for all $\boldsymbol{\mu} \in \mathcal{P}$, $k \in \mathbb{I}$, we define the linear functional

$$\begin{aligned} f^{k+\theta}(v;\boldsymbol{\mu}) &= \int_{\Gamma_{\mathrm{N}}} \left(\theta h^{k+1}(\boldsymbol{\mu}) + (1-\theta)h^k(\boldsymbol{\mu})\right) v d\Gamma_{\mathrm{N}} \\ &- \frac{1}{\Delta t}\left(u_{L\mathcal{N}}^{k+1}(\boldsymbol{\mu}) - u_{L\mathcal{N}}^k(\boldsymbol{\mu}), v\right)_{L^2(\Omega)} - a\left(\theta u_{L\mathcal{N}}^{k+1}(\boldsymbol{\mu}) + (1-\theta)u_{L\mathcal{N}}^k(\boldsymbol{\mu}), v;\boldsymbol{\mu}\right). \end{aligned} \tag{3.3.17}$$

Problem 3.3.1 (Detailed problem)**.** *Given $\boldsymbol{\mu} \in \mathcal{P}$, $\theta \in [1/2,1]$, find $u_{\mathcal{N}}^{k+1}(\boldsymbol{\mu}) \in V_{\mathcal{N}}$, $k \in \mathbb{I}$, such that for all $v \in V_{\mathcal{N}}$ holds*

$$\frac{1}{\Delta t}\left(u_{\mathcal{N}}^{k+1}(\boldsymbol{\mu}) - u_{\mathcal{N}}^k(\boldsymbol{\mu}), v\right)_{L^2(\Omega)} + a\left(\theta u_{\mathcal{N}}^{k+1}(\boldsymbol{\mu}) + (1-\theta)u_{\mathcal{N}}^k(\boldsymbol{\mu}), v;\boldsymbol{\mu}\right) = f^{k+\theta}(v;\boldsymbol{\mu}), \tag{3.3.18a}$$

$$\left(u_{\mathcal{N}}^0(\boldsymbol{\mu}) - u^0(\boldsymbol{\mu}), v\right)_V = 0, \quad \forall v \in V_{\mathcal{N}}. \tag{3.3.18b}$$

Note that it is also possible to replace the Galerkin projection of the initial condition (3.3.18b) by an interpolation, for instance $u_{\mathcal{N}}^0(\boldsymbol{\mu}) = \mathcal{I}_{\mathcal{N}} u^0(\boldsymbol{\mu})$. This introduces an additional interpolation error in the detailed solution, but does not affect the following arguments.

Due to conformity of the spaces $V_{\mathcal{N}} \subset V$, the bilinear form remains continuous and coercive (or satisfies the Gårding inequality) on $V_{\mathcal{N}}$, with discrete constants,

$$\gamma_a^{\mathcal{N}}(\boldsymbol{\mu}) = \sup_{u\in V_{\mathcal{N}}} \sup_{v\in V_{\mathcal{N}}} \frac{a(u,v;\boldsymbol{\mu})}{\|u\|_V \|v\|_V}, \quad \alpha_a^{\mathcal{N}}(\boldsymbol{\mu}) = \inf_{u\in V_{\mathcal{N}}} \frac{a(u,u;\boldsymbol{\mu}) + \lambda_a^{\mathcal{N}}(\boldsymbol{\mu})\|u\|_{L^2(\Omega)}^2}{\|u\|_V^2}. \tag{3.3.19}$$

Note that for all $\boldsymbol{\mu} \in \mathcal{P}$, $\alpha_a^{\mathcal{N}}(\boldsymbol{\mu}) \geq \alpha_a(\boldsymbol{\mu}) > 0$ and $\gamma_a^{\mathcal{N}}(\boldsymbol{\mu}) \leq \gamma_a(\boldsymbol{\mu}) < \infty$. Then for a small enough time step $\Delta t < 1/(\theta\lambda_a^{\mathcal{N}}(\boldsymbol{\mu}))$, by a generalized Lax-Milgram argument, the detailed problem (3.3.18) admits a unique solution, [AP05b; QV94].

3.4 Reduced Basis Approximation

In this section we outline the RBM methodology for linear parabolic PDEs. In particular, we consider the application to European option pricing, as introduced before. We discuss the main properties of the reduced system, construction of the reduced bases, a posteriori error estimates, and offline-online computational procedures.

3.4.1 Formulation

Consider a finite set of parameters $\mathcal{P}_N = \{\boldsymbol{\mu}_1, \dots, \boldsymbol{\mu}_N\} \subset \mathcal{P}$, with $\boldsymbol{\mu}_i \neq \boldsymbol{\mu}_j$, $\forall i \neq j$, $N \in \mathbb{N}$. For selected parameters we compute high-fidelity solutions, by solving the detailed problem (3.3.18), and form a set of snapshots $S_N^u = \{u_{\mathcal{N}}^k(\boldsymbol{\mu}_1), \dots, u_{\mathcal{N}}^k(\boldsymbol{\mu}_S)\}$, $k \in \mathbb{I}_0$, $S \in \mathbb{N}$. The reduced basis $\Psi_N = \{\psi_1, \dots, \psi_N\} \subset S_N^u$ is composed of linearly independent functions, which are suitably constructed from the set S_N. Different algorithms can be used for the construction of the basis. The standard approach for linear parabolic problems is a POD-Greedy algorithm, presented in Section 3.4.3.

We approximate the high-dimensional space $V_{\mathcal{N}}$ by a low-dimensional reduced basis space V_N, $\dim(V_N) := N \ll \mathcal{N} := \dim(V_{\mathcal{N}})$, which is defined as

$$V_N := \operatorname{span}\{\psi_1, \dots, \psi_N\} \subset V_{\mathcal{N}}. \tag{3.4.1}$$

The computation of a reduced solution is obtained as a Galerkin projection on V_N, i.e., for all $\boldsymbol{\mu} \in \mathcal{P}$ and $k \in \mathbb{I}$

$$u_N^{k+1}(\boldsymbol{\mu}) := \sum_{j=1}^{N} u_{N,j}^{k+1}(\boldsymbol{\mu})\psi_j, \tag{3.4.2}$$

with a reduced basis coefficient vector $\mathbf{u}_N^{k+1} := \left(u_{N,j}^{k+1}(\boldsymbol{\mu})\right)_{j=1}^{N} \in \mathbb{R}^N$. Then the reduced problem reads as follows.

Problem 3.4.1 (Reduced problem)**.** *Given $\boldsymbol{\mu} \in \mathcal{P}$, $\theta \in [1/2, 1]$, find $u_N^{k+1}(\boldsymbol{\mu}) \in V_N$, $k \in \mathbb{I}$, such that for all $v_N \in V_N$ it holds*

$$\frac{1}{\Delta t}\left(u_N^{k+1}(\boldsymbol{\mu}) - u_N^k(\boldsymbol{\mu}), v_N\right)_{L^2(\Omega)} + a\left(\theta u_N^{k+1}(\boldsymbol{\mu}) + (1-\theta)u_N^k(\boldsymbol{\mu}), v_N; \boldsymbol{\mu}\right) = f^{k+\theta}(v_N; \boldsymbol{\mu}). \tag{3.4.3a}$$

The initial value is chosen as the orthogonal projection of $u_{\mathcal{N}}^0(\boldsymbol{\mu})$ on V_N, i.e., for all $v_N \in V_N$

$$\left(u_N^0 - u_{\mathcal{N}}^0, v_N\right)_V = 0. \tag{3.4.3b}$$

By the construction procedure, $V_N \subset V_\mathcal{N}$, and under the continuity and coercivity (or Gårding inequality) assumptions on the bilinear form $a(\cdot,\cdot;\boldsymbol{\mu})$, for all $\boldsymbol{\mu} \in \mathcal{P}$, the well-posedness of the reduced problem (3.4.3) is inherited from that of the high-fidelity one (3.3.18).

The next property is the reproduction of the solutions, which is a consistency property of the reduced basis scheme.

Proposition 3.4.1 (Reproduction of the solutions)**.** *If for some $\boldsymbol{\mu} \in \mathcal{P}$ and all $k \in \mathbb{I}$ $u_\mathcal{N}^{k+1}(\boldsymbol{\mu}) \in V_N$ with $u_\mathcal{N}^0(\boldsymbol{\mu}) \in V_N$, then $u_N^k(\boldsymbol{\mu}) = u_\mathcal{N}^k(\boldsymbol{\mu})$ for all $k \in \mathbb{I}_0$.*

Proof. We prove this property by induction. For $k = 0$, $u_\mathcal{N}^0 \in V_N$ and for $u_N^0 \in V_N$ we have by (3.4.3b), that $(u_N^0 - u_\mathcal{N}^0, v_N)_V = 0$ for all $v_N \in V_N$. Set $v_N = u_N^0 - u_\mathcal{N}^0$, then

$$\left(u_N^0 - u_\mathcal{N}^0, u_N^0 - u_\mathcal{N}^0\right)_V = 0,$$

which holds only for $u_N^0 = u_\mathcal{N}^0$. For the next induction step, we assume that $u_\mathcal{N}^k = u_N^k$. We chose $v_\mathcal{N} = v_N \in V_N \subset V_\mathcal{N}$ and obtain

$$\frac{1}{\Delta t}(u_\mathcal{N}^{k+1}(\boldsymbol{\mu}) - u_N^k(\boldsymbol{\mu}), v_N)_{L^2(\Omega)} + a(\theta u_\mathcal{N}^{k+1}(\boldsymbol{\mu}) + (1-\theta)u_N^k(\boldsymbol{\mu}), v_N; \boldsymbol{\mu}) = f^{k+\theta}(v_N; \boldsymbol{\mu}),$$

which implies that $u_\mathcal{N}^{k+1} \in V_N$ solves the reduced problem (3.4.3). Due to the uniqueness of the solution, we obtain $u_N^k = u_\mathcal{N}^k$, $\forall k \in \mathbb{I}$. □

3.4.2 A Posteriori Error Estimates

We now turn to the a posteriori error estimation for the reduced basis approximation.

Define for all $\boldsymbol{\mu} \in \mathcal{P}$ and $k \in \mathbb{I}_0$ the following error quantities

$$e_u^k(\boldsymbol{\mu}) := u_N^k(\boldsymbol{\mu}) - u_\mathcal{N}^k(\boldsymbol{\mu}), \tag{3.4.4a}$$

$$e_N^u(\boldsymbol{\mu}) := \left(e_u^k(\boldsymbol{\mu})\right)_{k\in\mathbb{I}_0}. \tag{3.4.4b}$$

For all $\boldsymbol{\mu} \in \mathcal{P}$, $\theta \in [1/2, 1]$, $k \in \mathbb{I}$ and $v \in V_\mathcal{N}$, define the residual associated with the reduced basis approximation

$$r^{k+\theta}(v;\boldsymbol{\mu}) := \frac{1}{\Delta t}(u_N^{k+1}(\boldsymbol{\mu}) - u_N^k(\boldsymbol{\mu}), v)_{L^2(\Omega)} + a(\theta u_N^{k+1} + (1-\theta)u_N^k, v; \boldsymbol{\mu}) - f^{k+\theta}(v;\boldsymbol{\mu}), \tag{3.4.5}$$

with the norm

$$\|r^{k+\theta}(\boldsymbol{\mu})\|_{V'} := \sup_{v\in V_\mathcal{N}} \frac{|r^{k+\theta}(v;\boldsymbol{\mu})|}{\|v\|_V}. \tag{3.4.6}$$

From the Riesz representation theorem there exist $\hat{r}^k(\boldsymbol{\mu}) \in V_{\mathcal{N}}$, such that for all $\boldsymbol{\mu} \in \mathcal{P}$ and $k \in \mathbb{I}$

$$(\hat{r}^{k+\theta}(\boldsymbol{\mu}), v)_V = r^{k+\theta}(v; \boldsymbol{\mu}), \quad \forall v \in V_{\mathcal{N}}, \tag{3.4.7}$$

$$\|\hat{r}^{k+\theta}(\boldsymbol{\mu})\|_V = \|r^{k+\theta}(\boldsymbol{\mu})\|_{V'}. \tag{3.4.8}$$

Let $a(\cdot, \cdot; \boldsymbol{\mu})$ be a (strongly) coercive bilinear form and for $v = (v^{k+1})_{k \in \mathbb{I}}$ and $\theta = [1/2, 1]$ we define the following discrete spatio-temporal norm

$$|||v|||_{\boldsymbol{\mu}} := \left(\|v^I\|^2_{L^2(\Omega)} + \alpha_a^{\mathcal{N}}(\boldsymbol{\mu}) \Delta t \sum_{k=0}^{I-1} \|v^{k+\theta}\|^2_V \right)^{1/2}, \tag{3.4.9}$$

where

$$v^{k+\theta} = \theta v^{k+1} + (1-\theta) v^k.$$

Recall Young's inequality, i.e., for $\varepsilon, a, b \in \mathbb{R}$, the following holds

$$ab \leq \frac{a^2}{2\varepsilon^2} + \frac{\varepsilon^2 b^2}{2}. \tag{3.4.10}$$

The following classical relation will be useful for the derivation of the error bounds,

$$(a-b, a)_{L^2(\Omega)} = \frac{1}{2}\|a\|^2_{L^2(\Omega)} - \frac{1}{2}\|b\|^2_{L^2(\Omega)} + \frac{1}{2}\|a-b\|^2_{L^2(\Omega)}, \quad \forall a, b \in L^2(\Omega). \tag{3.4.11}$$

Then we obtain the following result for the error bound, introduced first in [GP05] and generalized in [HO08b].

Theorem 3.4.2 (A posteriori error estimates)**.** *For all $\boldsymbol{\mu} \in \mathcal{P}$, $k \in \mathbb{I}$, $\theta \in [1/2, 1]$, we have the following error bound for the primal error*

$$|||e_N^u(\boldsymbol{\mu})|||_{\boldsymbol{\mu}} \leq \Delta_N^u(\boldsymbol{\mu}) := \left(\|e_u^0(\boldsymbol{\mu})\|^2_{L^2(\Omega)} + \frac{\Delta t}{\alpha_a^{\mathcal{N}}(\boldsymbol{\mu})} \sum_{k=0}^{I-1} \|r^{k+\theta}(\boldsymbol{\mu})\|^2_{V'} \right)^{1/2}. \tag{3.4.12}$$

Proof. The proof is a modification of [Gre05, Proposition 11, Section 4.8] for $\theta = 1$ and [Gre05, Proposition 19, Appendix B] for $\theta = 1/2$.

Using the Problem 3.3.1, (3.4.5), we obtain

$$\left(e_u^{k+1} - e_u^k, v\right)_{L^2(\Omega)} + \Delta t \; a(e_u^{k+\theta}, v) = \Delta t \; r^{k+\theta}(v), \quad \forall v \in V_{\mathcal{N}}, \tag{3.4.13}$$

where $e_u^{k+\theta} := \theta e_u^{k+1} + (1-\theta) e_u^k$. Then choosing the test function $v = e_u^{k+\theta}$ and using the coercivity assumption of $a(\cdot, \cdot)$, we obtain

$$\left(e_u^{k+1} - e_u^k, e_u^{k+\theta}\right)_{L^2(\Omega)} + \alpha_a^{\mathcal{N}} \Delta t \|e_u^{k+\theta}\|^2_V \leq \Delta t \; r^{k+\theta}(e_u^{k+\theta}). \tag{3.4.14}$$

Using (3.4.11), the first term on the left-hand side can be estimated as

$$\begin{aligned}\left(e_u^{k+1}-e_u^k, e_u^{k+\theta}\right)_{L^2(\Omega)} &= \frac{\theta}{2}\left(\|e_u^{k+1}\|^2_{L^2(\Omega)} - \|e_u^k\|^2_{L^2(\Omega)} + \|e_u^{k+1}-e_u^k\|^2_{L^2(\Omega)}\right)\\ &+ \frac{(\theta-1)}{2}\left(\|e_u^k\|^2_{L^2(\Omega)} - \|e_u^{k+1}\|^2_{L^2(\Omega)} + \|e_u^k-e_u^{k+1}\|^2_{L^2(\Omega)}\right)\\ &= \frac{1}{2}\|e_u^{k+1}\|^2_{L^2(\Omega)} - \frac{1}{2}\|e_u^k\|^2_{L^2(\Omega)} + \frac{(2\theta-1)}{2}\|e_u^{k+1}-e_u^k\|^2_{L^2(\Omega)}.\end{aligned}$$

Then (3.4.14) can be written as

$$\begin{aligned}&\frac{1}{2}\|e_u^{k+1}\|^2_{L^2(\Omega)} - \frac{1}{2}\|e_u^k\|^2_{L^2(\Omega)} + \alpha_a^{\mathcal{N}}\Delta t\ \|e_u^{k+\theta}\|^2_V\\ &= \Delta t\ r^{k+\theta}(e_u^{k+1}) + \frac{(1-2\theta)}{2}\|e_u^{k+1}-e_u^k\|^2_{L^2(\Omega)}.\end{aligned} \tag{3.4.15}$$

Taking into account that $(1-2\theta)\leq 0$, for $\theta\in[1/2,1]$, and applying Young's inequality, with $\varepsilon^2=\alpha_a^{\mathcal{N}}(\boldsymbol{\mu})$, the right-hand side of (3.4.15) can be bounded as

$$\begin{aligned}\Delta t\ r^{k+\theta}(e_u^{k+\theta}) + \frac{(1-2\theta)}{2}\|e_u^{k+1}-e_u^k\|^2_{L^2(\Omega)} &\leq \Delta t\|r^{k+\theta}\|_{V'}\ \|e_u^{k+\theta}\|_V\\ &\leq \frac{\Delta t}{2\alpha_a^{\mathcal{N}}}\|r^{k+\theta}\|^2_{V'} + \frac{\Delta t\ \alpha_a^{\mathcal{N}}}{2}\|e_u^{k+\theta}\|^2_V.\end{aligned}$$

Combining the last estimate with (3.4.15), we obtain

$$\frac{1}{2}\|e_u^{k+1}\|^2_{L^2(\Omega)} + \frac{\alpha_a^{\mathcal{N}}}{2}\Delta t\|e_u^{k+\theta}\|^2_V \leq \frac{\Delta t}{2\alpha_a^{\mathcal{N}}}\|r^{k+\theta}\|^2_{V'} + \frac{1}{2}\|e_u^k\|^2_{L^2(\Omega)}.$$

Making a summation from $k=0,\ldots,I-1$, and multiplying by 2, we obtain a telescopic sum, which leads to

$$\|e_u^I\|^2_{L^2(\Omega)} + \alpha_a^{\mathcal{N}}\Delta t\sum_{k=0}^{I-1}\|e_u^{k+\theta}\|^2_V \leq \frac{\Delta t}{\alpha_a^{\mathcal{N}}}\sum_{k=0}^{I-1}\|r^{k+\theta}\|^2_{V'} + \|e_u^0\|^2_{L^2(\Omega)}.$$

Taking the square root on both sides of the last inequality, we obtain the necessary result. □

For all $\boldsymbol{\mu}\in\mathcal{P}$, denote $\alpha_a^{\mathrm{LB}}(\boldsymbol{\mu})$ a lower bound of the discrete coercivity constant $\alpha_a^{\mathcal{N}}(\boldsymbol{\mu})$. If for all $\boldsymbol{\mu}\in\mathcal{P}$ this bound is computable, with the computational cost independent of $\mathcal{N}$, then we can substitute $\alpha_a^{\mathcal{N}}(\boldsymbol{\mu})$ with $\alpha_a^{\mathrm{LB}}(\boldsymbol{\mu})$ in Δ_N^u and obtain an efficient computation of an a posteriori error bound in an offline-online fashion, with the online cost independent of $\mathcal{N}$.

In the case, when the bilinear form $a(\cdot,\cdot;\boldsymbol{\mu})$ is not coercive, but satisfies the Gårding inequality and Δt is sufficiently small, i.e., $\Delta t < 1/(2\lambda_a^{\mathcal{N}}(\boldsymbol{\mu}))$, we can obtain a similar result. In particular, for the special case of an implicit Euler scheme, $\theta = 1$, the error bound is given as follows

$$|||e_N^u(\boldsymbol{\mu})|||_{\boldsymbol{\mu}} \leq \Delta_N^u(\boldsymbol{\mu}),$$

$$\Delta_N^u(\boldsymbol{\mu}) := \left(\|e_u^0(\boldsymbol{\mu})\|^2_{L^2(\Omega)} + \frac{\Delta t}{\alpha_a^{\mathcal{N}}(\boldsymbol{\mu})} \sum_{k=0}^{I-1} \left(1 - 2\lambda_a^{\mathcal{N}}(\boldsymbol{\mu})\Delta t\right)^k \|r^{k+1}(\boldsymbol{\mu})\|^2_{V'} \right)^{1/2}, \tag{3.4.16}$$

where r^{k+1} is defined as in (3.4.5) with $\theta = 1$, and the discrete spatio-temporal norm is defined as

$$|||v|||^2_{\boldsymbol{\mu}} := \left(1 - 2\lambda_a^{\mathcal{N}}(\boldsymbol{\mu})\Delta t\right)^I \|v^I\|^2_{L^2(\Omega)} + \alpha_a^{\mathcal{N}}(\boldsymbol{\mu})\Delta t \sum_{k=0}^{I-1} \left(1 - 2\lambda_a^{\mathcal{N}}(\boldsymbol{\mu})\Delta t\right)^k \|v^{k+1}\|^2_V. \tag{3.4.17}$$

The derivation of this result is equivalent to the one, presented for the variational inequalities in Chapter 4, and hence, for compactness of the presentation we omit it here. Note, when the bilinear form $a(\cdot,\cdot;\boldsymbol{\mu})$ is coercive for all $\boldsymbol{\mu} \in \mathcal{P}$, then $\lambda_a^{\mathcal{N}}(\boldsymbol{\mu}) = 0$, and we recover the case (3.4.12).

3.4.3 Reduced Basis Construction

The reduced basis generation procedure remains one of the main components of the construction of the reduced basis approximation spaces, which influences the approximation quality and efficiency of the method. In the context of the parametrized PDEs, the most common are the POD (*Proper Orthogonal Decomposition*) method and the *greedy* strategies.

The POD method is used to reduce the dimensionality of the given data set (e.g., set of snapshots) by decomposing it onto a set of orthonormal basis vectors, called POD modes, retaining the essential information of the data. Different notions of the method can be found, e.g., Principal Component Analysis (PCA), Karhunen-Loève expansion or Hotelling transformation.

The greedy procedure is an iterative method which, at each iteration step, selects the worst resolved parameter and constructs the corresponding new basis vector. The selection procedure is based on a suitable error criterion, which can be either a true projection error (a *strong* greedy algorithm) or an a posteriori error bound (a *weak* greedy algorithm). The computation of the true error involves the evaluation of the expensive high-fidelity solutions and results in a high computational cost. Hence, the availability of efficiently computable a-posteriori error bounds becomes crucial for preserving the efficiency of the method.

Both greedy and POD algorithms have some distinctive properties. While the POD method is optimal in a least square sense, i.e., it minimizes the L^2-projection error, the greedy approach minimizes a maximal projection error. In terms of efficiency, a weak greedy method is much less computationally costly than a POD method, however it always requires a computable error bound.

In the context of parabolic PDEs, the application of only greedy or POD procedures may not be sufficient for an efficient basis construction procedure. Due to the inclusion of a time dimension, the POD method requires the computation of a large snapshot matrix for all time steps, which can result in a high computational cost. By contrast, a greedy loop for both parameter and time, e.g., [GP05; Gre05], may not capture all important information associated with a time trajectory. The common procedure is to use a combined strategy: a greedy search in a parameter space and a POD method in the temporal direction. This results in a combined algorithm, called POD-Greedy [Haa13; HO08b]. Additionally, under certain conditions the algorithm admits an exponential convergence rate, see [Haa13].

POD-Greedy Algorithm

Given a set of snapshots $v_1, \dots, v_n \in V_{\mathcal{N}}$, the POD basis of rank $l > 0$ is the set of orthonormal basis functions $\phi_1, \dots, \phi_l$ which solve the minimization problem

$$\begin{aligned} \mathrm{POD}_l(\{v_i\}_{i=1}^n) := \operatorname*{arg\,min}_{\phi_1,\dots,\phi_l} \sum_{i=1}^{n} \omega_i \|v_i - \sum_{j=1}^{l} (v_i, \phi_j)_V \phi_j\|_V^2, \\ \text{subject to} \quad (\phi_i, \phi_j)_V = \delta_{i,j}, \qquad i,j = 1,\dots,l, \end{aligned} \tag{3.4.18}$$

where ω_i are some positive weights, e.g., $\omega_i = 1$.

The POD-Greedy procedure is presented in Algorithm 3.1 and can be described as follows: Find the worst resolved parameter using a greedy loop with some error measure $E_N(\boldsymbol{\mu})$ (Step 3), compute the corresponding snapshot trajectory $\{u_{\mathcal{N}}^k(\boldsymbol{\mu}),\ k \in \mathbb{I}_0\}$ (Step 6), project the whole trajectory onto the current reduced basis space, and, using POD with respect to time, compress the projection error into the first m POD modes (Step 7). We restrict our attention to a single POD mode, i.e., $m = 1$.

In the algorithm, Π_{V_N} denotes the orthogonal projection on V_N with respect to the inner product $(\cdot,\cdot)_V$. The selection of the parameter in Step 3 requires an error measure $E_N(\boldsymbol{\mu})$, which can be chosen as, e.g., the projection error (3.4.19a), the L^2-error (3.4.19b), the space-time error (3.4.19c), or the error bound (3.4.19d). Note that for the case of $E_N(\boldsymbol{\mu}) = E_u^{\mathrm{proj}}(\boldsymbol{\mu})$, Algorithm 3.1 does not involve any reduced

Algorithm 3.1 POD-Greedy Algorithm

Input: Maximum number of iterations $N_{\max} > 0$, training sample set $\mathcal{P}_{\text{train}} \subset \mathcal{P}$, target tolerance ε_{tol}

Output: RB basis Ψ_N, RB space V_N

1: compute initial basis Ψ_0, $V_0 = \text{span}\{\Psi_0\}$
2: **for** $N = 1, \ldots, N_{\max}$ **do**
3: $\quad [\varepsilon_N^{\text{train}}, \boldsymbol{\mu}_N] = \arg\max_{\boldsymbol{\mu} \in \mathcal{P}_{\text{train}}} E_{N-1}(\boldsymbol{\mu})$
4: $\quad$ **if** $\varepsilon_N^{\text{train}} < \varepsilon_{\text{tol}}$ **then return**
5: $\quad$ **end if**
6: $\quad$ compute $\{u_{\mathcal{N}}^k(\boldsymbol{\mu}_N)\}_{k \in \mathbb{I}_0}$
7: $\quad \psi_N = \text{POD}_1\left(\left\{u_{\mathcal{N}}^k(\boldsymbol{\mu}_N) - \Pi_{V_{N-1}}\left(u_{\mathcal{N}}^k(\boldsymbol{\mu}_N)\right)\right\}_{k \in \mathbb{I}_0}\right)$
8: $\quad \Psi_N = \Psi_{N-1} \cup \{\psi_N\}$, $V_N = \text{span}\{\Psi_N\}$
9: **end for**

basis simulation procedure.

$$E_u^{\text{proj}}(\boldsymbol{\mu}) := \left(\Delta t \sum_{k=0}^{I} \|u_{\mathcal{N}}^k(\boldsymbol{\mu}) - \Pi_{V_N}(u_{\mathcal{N}}^k(\boldsymbol{\mu}))\|_V^2\right)^{1/2}, \tag{3.4.19a}$$

$$E_u^{\text{true}}(\boldsymbol{\mu}) := \left(\Delta t \sum_{k=0}^{I} \|e_u^k(\boldsymbol{\mu})\|_V^2\right)^{1/2} = \left(\Delta t \sum_{k=0}^{I} \|u_N^k(\boldsymbol{\mu}) - u_{\mathcal{N}}^k(\boldsymbol{\mu})\|_V^2\right)^{1/2}, \tag{3.4.19b}$$

$$E_u^{\boldsymbol{\mu}}(\boldsymbol{\mu}) := |||e_N^u(\boldsymbol{\mu})|||_{\boldsymbol{\mu}} = |||(u_N^k(\boldsymbol{\mu}) - u_{\mathcal{N}}^k(\boldsymbol{\mu}))_{k \in \mathbb{I}_0}|||_{\boldsymbol{\mu}}, \tag{3.4.19c}$$

$$E_u^{\text{apost}}(\boldsymbol{\mu}) := \Delta_N^u(\boldsymbol{\mu}), \tag{3.4.19d}$$

where $\Delta_N^u(\boldsymbol{\mu})$ is defined in (3.4.12) or in (3.4.16).

Remark 3.4.1. *Different choices of an initial basis Ψ_0 can be used. One may consider, e.g., Ψ_0 as an orthonormalization of a detailed solution $u_{\mathcal{N}}^{k'}(\boldsymbol{\mu}')$ for arbitrary chosen $\boldsymbol{\mu}' \in \mathcal{P}_{\text{train}}$ and $k' \in \mathbb{I}_0$. Alternatively, taking the orthonormalization of the set of all different initial data $u_{\mathcal{N}}^0(\boldsymbol{\mu})$ for varying $\boldsymbol{\mu} \in \mathcal{P}_{\text{train}}$ can give already a good initial reduced basis, [HO08b].*

The POD-Greedy algorithm produces also an error sequence

$$\varepsilon_N^{\text{train}} := \max_{\boldsymbol{\mu} \in \mathcal{P}_{\text{train}}} E_N(\boldsymbol{\mu}), \quad N = 1, \ldots, N_{\max},$$

often referred as the "training" error. In general, this error may not be a reliable quality measure of the reduced basis approximation, due to the possible over fitting effect, i.e., when $\max_{\boldsymbol{\mu} \in \mathcal{P}} E_N(\boldsymbol{\mu}) \gg \varepsilon_N^{\text{train}}$. Such situations can happen, e.g., when the training set $\mathcal{P}_{\text{train}}$ is not sufficiently large. To exclude these possibilities, one

may evaluate the error $\varepsilon_N^{\text{test}} := \max_{\boldsymbol{\mu}\in\mathcal{P}_{\text{test}}} E_N(\boldsymbol{\mu})$ on an independent finite test set $\mathcal{P}_{\text{test}} \subset \mathcal{P}$ (e.g., set of randomly distributed parameter values) with $|\mathcal{P}_{\text{test}}| \gg |\mathcal{P}_{\text{train}}|$.

We point out that he basis generation procedure is a computationally expensive routine and belongs to the offline computational phase, which we describe in the next section.

3.4.4 Offline-Online Computational Procedure

The efficiency of the reduced basis method relies on the assumption of affine parameter dependence of bilinear and linear forms. If the assumption is fulfilled, the computational procedure can be split into so-called *offline* and *online* routines. This decomposition brings a significant computational speed-up for solving the reduced system and allows to perform simulations in a real-time and multi-query context.

An affine parameter dependence (or *parameter-separability*) of bilinear and linear forms implies that for every $\boldsymbol{\mu} \in \mathcal{P}$ there exist functions $\Theta_q^a : \mathcal{P} \to \mathbb{R}$, for $q = 1, \dots, Q_a$ and $\Theta_q^{f,k} : \mathcal{P} \to \mathbb{R}$, for $q = 1, \dots, Q_f$, $k \in \mathbb{I}$, such that

$$a(u, v; \boldsymbol{\mu}) = \sum_{q=1}^{Q_a} \Theta_q^a(\boldsymbol{\mu}) a_q(u, v), \qquad f^k(v; \boldsymbol{\mu}) = \sum_{q=1}^{Q_f} \Theta_q^{f,k}(\boldsymbol{\mu}) f_q^k(v), \tag{3.4.20}$$

where the bilinear and linear forms $a_q : V \times V \to \mathbb{R}$, $f_q^k : V \to \mathbb{R}$, $k \in \mathbb{I}$ are parameter independent. In addition, we assume a parameter separability of the initial condition,

$$u_0(\boldsymbol{\mu}) = \sum_{q=1}^{Q_u} \Theta_q^u(\boldsymbol{\mu}) u_{0q}, \tag{3.4.21}$$

with $\Theta_q^u : \mathcal{P} \to \mathbb{R}$, $q = 1, \dots, Q_u$. Obviously, for all $\boldsymbol{\mu} \in \mathcal{P}$ the discrete initial condition $u_{\mathcal{N}}^0(\boldsymbol{\mu})$ will enjoy the same property (3.4.21) with parameter independent components $u_{\mathcal{N},q}^0$.

For the functional $f^{k+\theta}(v; \boldsymbol{\mu})$, defined in (3.3.17), the affine parameter dependence is inherited from the affine separability of $h^k(\boldsymbol{\mu})$ and $u_{L\mathcal{N}}^k(\boldsymbol{\mu})$, $\boldsymbol{\mu} \in \mathcal{P}$, $k \in \mathbb{I}_0$. Assume, that there exist $\Theta_q^{n,k}, \Theta_q^{m,k} : \mathcal{P} \to \mathbb{R}$, such that both functions can be represented as

$$h^k(\boldsymbol{\mu}) = \sum_{q=1}^{Q_n} \Theta_q^{n,k}(\boldsymbol{\mu}) h_q^k, \qquad u_{L\mathcal{N}}^k(\boldsymbol{\mu}) = \sum_{q=1}^{Q_m} \Theta_q^{m,k}(\boldsymbol{\mu}) \ell_q^k. \tag{3.4.22}$$

Remark 3.4.2. *In fact, an affine decomposition of the lift function $u_{L\mathcal{N}}^k(\boldsymbol{\mu})$ depends on affine decomposition of the Dirichlet data $g_{\mathcal{N}}^k(\boldsymbol{\mu})$, $k \in \mathbb{I}_0$. Indeed, assuming that $g_{\mathcal{N}}^k$ admits an affine decomposition, $g_{\mathcal{N}}^k(\boldsymbol{\mu}) = \sum_{q=1}^{Q_g} \Theta_q^{g,k}(\boldsymbol{\mu}) g_{\mathcal{N},q}^k$, and incorporating linearity of an extension operator $R_{\mathcal{N}}$, we obtain that $u_{L\mathcal{N}}^k(\boldsymbol{\mu}) = R_{\mathcal{N}} g_{\mathcal{N}}^k(\boldsymbol{\mu}) = \sum_{q=1}^{Q_g} \Theta_g^{g,k}(\boldsymbol{\mu}) R_{\mathcal{N}} g_{\mathcal{N},q}^k$, where $\ell_q^k := R_{\mathcal{N}}(g_{\mathcal{N},q}^k)$.*

Define the following quantities

$$n_q^k(v) := (h_q^k, v)_{L^2(\Gamma_N)}, \qquad q = 1, \dots, Q_n, \tag{3.4.23a}$$

$$m_q^k(v) := (\ell_q^k, v)_{L^2(\Omega)}, \qquad q = 1, \dots, Q_m, \tag{3.4.23b}$$

$$s_{q,q'}^k(v) := a_{q'}(\ell_q^k, v)_{L^2(\Omega)}, \qquad q = 1, \dots, Q_n, \quad q' = 1, \dots, Q_a. \tag{3.4.23c}$$

Then the functional $f^{k+\theta}(v; \boldsymbol{\mu})$, $k \in \mathbb{I}$, in (3.3.17), admits the following affine representation

$$\begin{aligned} f^{k+\theta}(v; \boldsymbol{\mu}) = &\sum_{q=1}^{Q_n} \left\{ \theta \Theta_q^{n,k+1}(\boldsymbol{\mu}) n_q^{k+1}(v) + (1-\theta)\Theta_q^{n,k}(\boldsymbol{\mu}) n_q^k(v) \right\} \\ &- \frac{1}{\Delta t} \sum_{q=1}^{Q_m} \left\{ \Theta_q^{m,k+1}(\boldsymbol{\mu}) m_q^{k+1}(v) - \Theta_q^{m,k}(\boldsymbol{\mu}) m_q^k(v) \right\} \\ &- \sum_{q'=1}^{Q_a} \Theta_{q'}^a(\boldsymbol{\mu}) \sum_{q=1}^{Q_m} \left\{ \theta \Theta_q^{m,k+1}(\boldsymbol{\mu}) s_{q,q'}^{k+1}(v) + (1-\theta)\Theta_q^{m,k}(\boldsymbol{\mu}) s_{q,q'}^k(v) \right\}. \end{aligned} \tag{3.4.24}$$

Recall, that for every $\boldsymbol{\mu} \in \mathcal{P}$, $k \in \mathbb{I}$, the reduced solution can be expanded as $u_N^{k+1}(\boldsymbol{\mu}) := \sum_{j=1}^N u_{N,j}^{k+1}(\boldsymbol{\mu}) \psi_j \in V_N$, with $V_N = \text{span}\{\Psi_N\}$, where $\Psi_N = \{\psi_1, \dots, \psi_N\}$ is an orthonormal basis, constructed by, e.g., Algorithm 3.1. Denote the reduced basis coefficient vector by $\mathbf{u}_N^k := (u_{N,1}^k, \dots, u_{N,N}^k)^T \in \mathbb{R}^N$. Choosing a test function $v_N = \psi_i$, $1 \le i \le N$, in (3.4.3), and invoking the parameter-separability of the bilinear and linear forms, the reduced Problem 3.4.1 can be written in the following algebraic form

$$\left(\frac{1}{\Delta t} \mathbf{M}_N + \theta \mathbf{A}_N(\boldsymbol{\mu}) \right) \mathbf{u}_N^{k+1}(\boldsymbol{\mu}) = \left(\frac{1}{\Delta t} \mathbf{M}_N + (\theta - 1) \mathbf{A}_N(\boldsymbol{\mu}) \right) \mathbf{u}_N^k(\boldsymbol{\mu}) + \mathbf{f}_N^{k+\theta}(\boldsymbol{\mu}), \tag{3.4.25}$$

with the initial condition $\mathbf{M}_N^V \mathbf{u}_N^0(\boldsymbol{\mu}) = \mathbf{U}_N^0(\boldsymbol{\mu})$, where the reduced quantities $\mathbf{A}_N \in \mathbb{R}^{N \times N}$, $\mathbf{M}_N \in \mathbb{R}^{N \times N}$, $\mathbf{M}_N^V \in \mathbb{R}^{N \times N}$, $\mathbf{U}_N^0 \in \mathbb{R}^N$ are the defined as follows

$$\mathbf{A}_N(\boldsymbol{\mu}) := \sum_{q=1}^{Q_a} \Theta_q^a(\boldsymbol{\mu}) \mathbf{A}_{N,q}, \qquad \mathbf{M}_N := \left((\psi_j, \psi_i)_{L^2(\Omega)} \right)_{i,j=1}^N, \tag{3.4.26}$$

$$\mathbf{U}_N^0(\boldsymbol{\mu}) := \sum_{q=1}^{Q_u} \Theta_q^u(\boldsymbol{\mu}) \mathbf{u}_{N,q}^0, \qquad \mathbf{M}_N^V := \left((\psi_j, \psi_i)_V \right)_{i,j=1}^N, \tag{3.4.27}$$

with

$$\mathbf{A}_{N,q} := (a_q(\psi_j, \psi_i))_{i,j=1}^N \in \mathbb{R}^{N \times N}, \qquad \mathbf{u}_{N,q}^0 := \left((u_{\mathcal{N},q}^0, \psi_i)_V \right)_{i=1}^N \in \mathbb{R}^N. \tag{3.4.28a}$$

The reduced vector $\mathbf{f}_N^{k+\theta}(\boldsymbol{\mu}) := \left(f^{k+\theta}(\psi_i;\boldsymbol{\mu})\right)_{i=1}^N \in \mathbb{R}^N$, according to (3.4.24), involves the computation of the following reduced quantities

$$\mathbf{n}_{N,q}^k := \left(n_q^k(\psi_i)\right)_{i=1}^N, \qquad q = 1,\dots,Q_n, \tag{3.4.28b}$$

$$\mathbf{m}_{N,q}^k := \left(m_q^k(\psi_i)\right)_{i=1}^N, \qquad q = 1,\dots,Q_m, \tag{3.4.28c}$$

$$\mathbf{s}_{N,q,q'}^k := \left(s_{q,q'}^k(\psi_i)\right)_{i=1}^N, \qquad q = 1,\dots,Q_m, \qquad q' = 1,\dots,Q_a. \tag{3.4.28d}$$

Due to the inclusion $V_N \subset V_\mathcal{N}$, the reduced basis functions $\{\psi_j\}_{j=1}^N \subset V_N$ can be expanded in a detailed basis $\{\phi_i\}_{i=1}^\mathcal{N} \subset V_\mathcal{N}$ of the high-fidelity problem, i.e., $\psi_j = \sum_{i=1}^\mathcal{N} \psi_{i,j}\phi_i$. Define the coefficient matrix

$$\boldsymbol{\Psi}_N := (\psi_{i,j})_{i,j=1}^{\mathcal{N},N} \in \mathbb{R}^{\mathcal{N}\times N}, \tag{3.4.29}$$

and introduce the following high-fidelity matrices and vectors

$$\mathbf{M} := \left((\phi_j,\phi_i)_{L^2(\Omega)}\right)_{i,j=1}^\mathcal{N}, \quad \mathbf{A}_q := (a_q(\phi_j,\phi_i))_{i,j=1}^\mathcal{N}, \qquad \mathbf{M}_V := ((\phi_j,\phi_i)_V)_{i,j=1}^\mathcal{N}$$

$$\widetilde{\mathbf{M}} := \left((\phi_j,\phi_i)_{L^2(\Omega)}\right)_{i,j=1}^{\mathcal{N},\mathcal{N}_X}, \quad \widetilde{\mathbf{A}}_q := (a_q(\phi_j,\phi_i))_{i,j=1}^{\mathcal{N},\mathcal{N}_X},$$

$$\mathbf{n}_q^k := \left(n_q^k(\phi_i)\right)_{i=1}^\mathcal{N}, \qquad \mathbf{m}_q^k := \left(m_q^k(\phi_i)\right)_{i=1}^\mathcal{N}, \qquad \mathbf{s}_{q,q'}^k := \left(s_{q,q'}^k(\phi_i)\right)_{i=1}^\mathcal{N}.$$

Denote the coefficient vector of the parameter independent lift functions ℓ_q^k, (3.4.22), $\mathbf{u_L}_q^k := (\ell_{q,1}^k,\dots,\ell_{q,\mathcal{N}_X}^k)^T \in \mathbb{R}^{\mathcal{N}_X}$. Then we can express $\mathbf{m}_q^k$, $\mathbf{s}_{q,q'}^k$ as $\mathbf{m}_q^k = \widetilde{\mathbf{M}}\mathbf{u_L}_q^k$ and $\mathbf{s}_{q,q'}^k = \widetilde{\mathbf{A}}_{q'}\mathbf{u_L}_q^k$.

The reduced matrices and vectors can be expressed via high-fidelity ones as follows

$$\mathbf{M}_N = \boldsymbol{\Psi}_N^T\mathbf{M}\boldsymbol{\Psi}_N, \quad \mathbf{A}_{N,q} = \boldsymbol{\Psi}_N^T\mathbf{A}_q\boldsymbol{\Psi}_N, \qquad \mathbf{M}_N^V = \boldsymbol{\Psi}_N^T\mathbf{M}_V\boldsymbol{\Psi}_N, \tag{3.4.30a}$$

$$\mathbf{n}_{N,q}^k = \boldsymbol{\Psi}_N^T\mathbf{n}_q^k, \qquad \mathbf{m}_{N,q}^k = \boldsymbol{\Psi}_N^T\widetilde{\mathbf{M}}\mathbf{u_L}_q^k, \qquad \mathbf{s}_{N,q,q'}^k = \boldsymbol{\Psi}_N^T\widetilde{\mathbf{A}}_{q'}\mathbf{u_L}_q^k, \tag{3.4.30b}$$

and $\mathbf{u}_{N,q}^0 = \boldsymbol{\Psi}_N^T\mathbf{M}_V\mathbf{u}_q^0$, where $\mathbf{u}_q^0$ denotes the coefficient vector of $u_{\mathcal{N},q}^0$.

The offline-online procedure is set up as follows: In the offline stage, we compute snapshots $S_N^u = \{u_\mathcal{N}^k(\boldsymbol{\mu}_1),\dots,u_\mathcal{N}^k(\boldsymbol{\mu}_N)\}$, $k \in \mathbb{I}_0$, and construct a reduced basis $\Psi_N = \{\psi_1,\dots,\psi_N\} \subset S_N^u$, as well as compute all parameter independent quantities (3.4.30). Then for every new instance parameter $\boldsymbol{\mu} \in \mathcal{P}$, we perform an online routine. Namely, we assemble all precomputed quantities into the reduced ones, e.g., $\mathbf{A}_N(\boldsymbol{\mu})$, $\mathbf{f}_N^{k+\theta}(\boldsymbol{\mu})$, and solve the reduced problem (3.4.25).

An offline routine involves a calculation of computationally expensive matrices and vectors corresponding to a high-fidelity problem of dimension $\mathcal{N}_X$. However, it needs

to be performed only once. By contrast, an online stage is executed multiple times for different values of the parameter $\boldsymbol{\mu} \in \mathcal{P}$, yet with the cheaper computational cost, which is independent of $\mathcal{N}_X$.

We remark, that an offline-online procedure applies also to the calculation of the error estimates, which are used either for the construction of the reduced basis spaces offline or for the certification of the method in an online routine. For both situations an efficient evaluations of the error bounds is significant. We provide the description of this procedure in the next chapter in the context of variational inequalities and omit it here for to avoid redundancy.

We comment on the computational complexity of both routines. Computation of N snapshots in the offline stage requires $\mathcal{O}(NI(\mathcal{N}_X)^p)$ operations, where I is the number of time-steps and p is some number, determined by the solver used for the detailed problem ($p \leq 3$). The cost of construction of all parameter independent matrices and vectors is $\mathcal{O}((Q_a+1)N^2\mathcal{N} + Q_nN\mathcal{N} + Q_mN(\mathcal{N}_X) + Q_mQ_aN(\mathcal{N}_X))$. As we can see, the total offline cost is dominated by the snapshots computation cost $\mathcal{O}(NI(\mathcal{N}_X)^p)$. In the online routine, given $\boldsymbol{\mu} \in \mathcal{P}$, we assign all parameter dependent matrices and vectors with the cost $\mathcal{O}((Q_a+1)N^2 + IN(Q_n+Q_m+Q_aQ_n))$ and solve a dense reduced system with complexity $O(IN^3)$. We can see, that the total cost of the online computational procedure, which involves the dimension of the reduced system N and a number of time steps I, is independent of the detailed dimension $\mathcal{N}_X \gg N$.

Empirical Interpolation Method

Computational efficiency of the reduced basis method strongly depends on the affine parameter dependence of the problem. For non-affine problems, the efficiency of the method may be highly deteriorated. To recover a parameter separability in this case, one may employ a so-called *empirical interpolation method* (EIM), first introduced in [BMN$^+$04] and later extended for non-affine and nonlinear parabolic problems, e.g., [DHO12; GMN$^+$07; Gre05]. A similar approach, called *discrete empirical interpolation method* (DEIM), which is based on the POD method, was introduced in [CS09; CS10].

In this section we outline the main idea of the EIM method and refer to [MNP$^+$09] for more details and a theoretical study. Assume that the function $g : \Omega \times \mathcal{P} \to \mathbb{R}$, $g(\boldsymbol{\mu}) \in C^0(\overline{\Omega})$, $\boldsymbol{\mu} \in \mathcal{P}$ does not admit an affine decomposition with respect to the parameter $\boldsymbol{\mu}$. The idea of EIM relies on an assumption of sufficient regularity of the parameter induced manifold $\mathcal{M}_g$,

$$\mathcal{M}_g := \{g(\boldsymbol{\mu}) : \quad \boldsymbol{\mu} \in \mathcal{P}\}.$$

which makes it then possible to approximate $g(z;\boldsymbol{\mu})$, $\boldsymbol{\mu} \in \mathcal{P}$, $z \in \Omega$ by a linear combination of snapshots $g(\cdot,\boldsymbol{\mu}_1), \ldots, g(\cdot,\boldsymbol{\mu}_M)$ at well-chosen parameters $\boldsymbol{\mu}_1, \ldots, \boldsymbol{\mu}_M \in \mathcal{P}$.

Define the approximation space X_M as

$$X_M := \operatorname{span}\{g(\cdot;\boldsymbol{\mu}_1),\dots,g(\cdot;\boldsymbol{\mu}_M)\} = \operatorname{span}\{q_1,\dots,q_M\}.$$

Then for all $\boldsymbol{\mu}\in\mathcal{P}$ and $z\in\Omega$ we look for an approximation $g_M(z;\boldsymbol{\mu})\in X_M$ of $g(z;\boldsymbol{\mu})$, which is defined as

$$g_M(z;\boldsymbol{\mu}) = \mathcal{I}_M g(z;\boldsymbol{\mu}) = \sum_{j=1}^{M} c_j(\boldsymbol{\mu}) q_j(z), \quad z\in\Omega. \tag{3.4.31}$$

The approximation is performed via an interpolation operator $\mathcal{I}_M$, which is exact in M interpolation points $\zeta_1,\dots,\zeta_M\in\Omega$ (often referred to as *"magic points"* [MNP$^+$09]), i.e.,

$$\mathcal{I}_M g(\zeta_i;\boldsymbol{\mu}) = g(\zeta_i;\boldsymbol{\mu}), \quad i=1,\dots,M. \tag{3.4.32}$$

Let $T_M=\{\zeta_1,\dots,\zeta_M\}$ be a set of interpolation points. Then for $\boldsymbol{\mu}\in\mathcal{P}$, to find an interpolant $\mathcal{I}_M g(z;\boldsymbol{\mu})$ we have to determine the coefficients $c_j(\boldsymbol{\mu})\in\mathbb{R}$ by solving the following linear system

$$\sum_{j=1}^{M} c_j(\boldsymbol{\mu}) q_j(\zeta_i) = g(\zeta_i;\boldsymbol{\mu}), \quad i=1,\dots,M. \tag{3.4.33}$$

The last system (3.4.33) can be written in a matrix form

$$\mathbf{Q}_M \mathbf{c}_M(\boldsymbol{\mu}) = \mathbf{g}_M(\boldsymbol{\mu}), \qquad \forall\boldsymbol{\mu}\in\mathcal{P}, \tag{3.4.34}$$

where $\mathbf{Q}_M := (q_j(\zeta_i))_{i,j=1}^M \in \mathbb{R}^{M\times M}$, $\mathbf{c}_M(\boldsymbol{\mu}) := (c_j(\boldsymbol{\mu}))_{j=1}^M \in \mathbb{R}^M$ and $\mathbf{g}_M(\boldsymbol{\mu}) := (g(\zeta_i;\boldsymbol{\mu}))_{i=1}^M \in \mathbb{R}^M$.

In order to solve the system (3.4.33), one should construct the basis functions $q_j(z)\in X_M$ and determine the set of interpolation points T_M. In the standard EIM, the construction of both ingredients is based on a greedy strategy. The summary of the procedure is presented in Algorithm 3.2. In this case the matrix $\mathbf{Q}_M$ is lower triangular with $(\mathbf{Q}_M)_{ij}=1$ for $i=j$, and hence invertible, [BMN$^+$04; GMN$^+$07]. For every instance $\boldsymbol{\mu}\in\mathcal{P}$, the system (3.4.34) is solved in an online computational routine with the cost $\mathcal{O}(M^2)$, generally with M being relatively small.

We comment on an approach, that is similar to EIM, which is referred to as DEIM [CS09; CS10] (*discrete empirical interpolation method*). To avoid a confusion, DEIM is not the discrete version of Algorithm 3.2 and has some differences compared to EIM. In particular, the construction of the basis vectors is performed not via a greedy iterative procedure, but using a POD method. The selection of the interpolation points follows the same greedy routine as in Algorithm 3.2. In this case the interpolation matrix $\mathbf{Q}_M$ is full and the cost of solving a system (3.4.34) in general scales

Algorithm 3.2 EIM Algorithm

Input: maximum number of interpolation points $M_{\max} > 0$, training sample set $\mathcal{P}_{\text{train}} \subset \mathcal{P}$, target tolerance ε_{tol}

Output: set of basis functions $X_M = \{q_1, \dots, q_M\}$, and interpolation points $T_M = \{\zeta_1, \dots, \zeta_M\}$

1: set $\boldsymbol{\mu}_1 = \arg\max_{\boldsymbol{\mu} \in \mathcal{P}_{\text{train}}} \|g(\cdot; \boldsymbol{\mu})\|_{L^\infty(\Omega)}$
2: define $\zeta_1 = \arg\max_{z \in \Omega} |g(z; \boldsymbol{\mu}_1)|$
3: set $q_1 = g(z; \boldsymbol{\mu}_1)/g(\zeta_1; \boldsymbol{\mu}_1)$
4: **for** $m = 2, \dots, M_{\max}$ **do**
5: $\quad [\varepsilon_m, \boldsymbol{\mu}_m] = \arg\max_{\boldsymbol{\mu} \in \mathcal{P}_{\text{train}}} \|g(\cdot; \boldsymbol{\mu}) - \mathcal{I}_{m-1} g(\cdot; \boldsymbol{\mu})\|_{L^\infty(\Omega)}$
6: $\quad$ **if** $\varepsilon_m < \varepsilon_{\text{tol}}$ **then return**
7: $\quad$ **end if**
8: $\quad$ compute $\delta(z) = g(z; \boldsymbol{\mu}_m) - \mathcal{I}_{m-1} g(z; \boldsymbol{\mu}_m)$
9: $\quad \zeta_m = \arg\max_{z \in \Omega} |\delta(z)|$
10: $\quad q_m(z) = \delta(z)/\delta(\zeta_m)$
11: **end for**

to $\mathcal{O}(M^3)$. However, due to the parameter independence of $\mathbf{Q}_M$ during the online routine, the matrix $\mathbf{Q}_M$ can be factorized in the offline phase with the cost $\mathcal{O}(M^3)$ (by using, e.g., LU-decomposition), and then all subsequent online computations can be performed with the $\mathcal{O}(M^2)$ computation cost.

Offline-Online Decomposition for the Black-Scholes and Heston Models

In this subsection we comment on affine parameter dependence of the Black-Scholes and Heston models. The bilinear form in the Black-Scholes model, $a(\cdot, \cdot; \boldsymbol{\mu}) = a^{\text{BS}}(\cdot, \cdot; \boldsymbol{\mu})$, defined in (3.3.14a), admits the affine decomposition

$$a^{\text{BS}}(u, v; \boldsymbol{\mu}) = \sum_{q=1}^{3} \Theta_q^a(\boldsymbol{\mu}) a_q^{\text{BS}}(u, v),$$

with

$$\Theta_1^a = \frac{\sigma^2}{2}, \qquad a_1^{\text{BS}}(u, v) = (\nabla u, \nabla v)_{L^2(\Omega)}, \tag{3.4.35a}$$

$$\Theta_2^a = \frac{1}{2}\sigma^2 + q - r, \qquad a_2^{\text{BS}}(u, v) = (\nabla u, v)_{L^2(\Omega)}, \tag{3.4.35b}$$

$$\Theta_3^a = r, \qquad a_3^{\text{BS}}(u, v) = (u, v)_{L^2(\Omega)}. \tag{3.4.35c}$$

For the Heston model $a(\cdot, \cdot; \boldsymbol{\mu}) = a^{\text{H}}(\cdot, \cdot; \boldsymbol{\mu})$, defined in (3.3.14b), can be written as

$$a^{\text{H}}(u, v; \boldsymbol{\mu}) = \sum_{q=1}^{6} \Theta_q^a(\boldsymbol{\mu}) a_q^{\text{H}}(u, v),$$

with parameter functions

$$\Theta_1^a = \frac{1}{2}\xi^2, \qquad \Theta_2^a = \frac{1}{2}\xi\rho, \qquad \Theta_3^a = \frac{1}{2}, \tag{3.4.36a}$$

$$\Theta_4^a = -\kappa\gamma + \frac{1}{2}\xi^2, \qquad \Theta_5^a = \kappa, \qquad \Theta_6^a = -r, \tag{3.4.36b}$$

and bilinear forms

$$a_1^{\mathrm{H}}(u,v) = \left(\nu \begin{bmatrix} 1 & 0 \\ 0 & 0 \end{bmatrix} \nabla u, \nabla v\right)_{L^2(\Omega)}, \tag{3.4.36c}$$

$$a_2^{\mathrm{H}}(u,v) = \left(\nu \begin{bmatrix} 0 & 1 \\ 1 & 0 \end{bmatrix} \nabla u, \nabla v\right)_{L^2(\Omega)} + \left(\begin{bmatrix} 0 \\ 1 \end{bmatrix} \cdot \nabla u, v\right)_{L^2(\Omega)}, \tag{3.4.36d}$$

$$a_3^{\mathrm{H}}(u,v) = \left(\nu \begin{bmatrix} 0 & 0 \\ 0 & 1 \end{bmatrix} \nabla u, \nabla v\right)_{L^2(\Omega)} + \left(\nu \begin{bmatrix} 0 \\ 1 \end{bmatrix} \cdot \nabla u, v\right)_{L^2(\Omega)}, \tag{3.4.36e}$$

$$a_4^{\mathrm{H}}(u,v) = \left(\begin{bmatrix} 1 \\ 0 \end{bmatrix} \cdot \nabla u, v\right)_{L^2(\Omega)}, \tag{3.4.36f}$$

$$a_5^{\mathrm{H}}(u,v) = \left(\nu \begin{bmatrix} 1 \\ 0 \end{bmatrix} \cdot \nabla u, v\right)_{L^2(\Omega)}, \tag{3.4.36g}$$

$$a_6^{\mathrm{H}}(u,v) = \left(\begin{bmatrix} 0 \\ 1 \end{bmatrix} \cdot \nabla u, v\right)_{L^2(\Omega)} - (u,v)_{L^2(\Omega)}. \tag{3.4.36h}$$

The affine decomposition of the linear form $f^{k+\theta}(\cdot;\boldsymbol{\mu})$ for both Black-Scholes and Heston models follows directly from the affine decomposition of the Dirichlet and Neumann boundary data, defined in Section 2.7, see Remark 3.4.2. However, for some cases, e.g., for the European call option in the Heston model with the boundary conditions specified as in (2.7.8), the function $g_{\mathcal{N}}^{k+1}(z,\boldsymbol{\mu})$, $z=(\nu,x)\in\Omega\subset\mathbb{R}^2$ is not affine w.r.t. the parameter r, see (2.7.8a), (2.4.16). Hence, the lift function $u_{L\mathcal{N}}^{k+1}(\boldsymbol{\mu})$ is also not parameter separable and the cost of an online routine depends on the dimension of the high-fidelity problem, $\mathcal{N}_X$.

To recover the online $\mathcal{N}$-independence, the (D)EIM strategy can be employed. We replace $g_{\mathcal{N}}^{k+1}(z;\boldsymbol{\mu})$ by an affine approximation $g_M^{k+1}(z;\boldsymbol{\mu})$, $z\in\Gamma_{\mathrm{D}}$. The notable difference in this case, is the inclusion of the time variable. To apply the (D)EIM procedure, described above, one of the possibilities could be to treat the time variable as an additional parameter instance $\widetilde{\boldsymbol{\mu}} := (t^{k+1},\boldsymbol{\mu})$, $k\in\mathbb{I}$, residing in a time-parameter domain $\widetilde{\mathcal{P}} := (0,T)\times\mathcal{P}$, see, e.g., [DHO12; GMN$^+$07; Gre05]. Then $g_M(z;\widetilde{\boldsymbol{\mu}}) := g_M^{k+1}(z;\boldsymbol{\mu})$, $k\in\mathbb{I}$ can be represented as

$$g_M(z;\widetilde{\boldsymbol{\mu}}) = \sum_{m=1}^{M} c_m(\widetilde{\boldsymbol{\mu}}) q_m(z), \quad z\in\Gamma_{\mathrm{D}},$$

satisfying M interpolation constraints

$$g_M(\zeta_i;\widetilde{\boldsymbol{\mu}}) = g_{\mathcal{N}}(\zeta_i;\widetilde{\boldsymbol{\mu}}), \quad \zeta_i \in \Gamma_{\mathrm{D}}, \quad i = 1,\dots,M. \tag{3.4.37}$$

The basis functions q_m are constructed by, e.g., the POD algorithm from snapshots $\{g_{\mathcal{N}}(\widetilde{\boldsymbol{\mu}}_1),\dots,g_{\mathcal{N}}(\widetilde{\boldsymbol{\mu}}_M)\}$, $\widetilde{\boldsymbol{\mu}}_i \in \widetilde{\mathcal{P}}_{\mathrm{train}}$. Then for every $\boldsymbol{\mu} \in \mathcal{P}$, a system of interpolation equations (3.4.37) is solved in the online computational phase, with the cost $\mathcal{O}(IM^2)$, which depends on the number of time steps I.

Using the linearity of the extension operator, we can recover an affine decomposition of the lift function $u_{L\mathcal{N}}^{k+1}(\boldsymbol{\mu})$, $\boldsymbol{\mu} \in \mathcal{P}$, $k \in \mathbb{I}$,

$$u_{L\mathcal{N}}^{k+1}(\boldsymbol{\mu}) = \mathcal{R}_{\mathcal{N}}(g_{\mathcal{N}}^{k+1}(\boldsymbol{\mu})) \approx \sum_{m=1}^{M} c_m(t^{k+1},\boldsymbol{\mu}) q_m^L,$$

where $q_m^L := \mathcal{R}_{\mathcal{N}}(q_m) \in X_{\mathcal{N}}$.

3.5 Numerical Results

In this section we present numerical results of the application of the RBM to the model problem of pricing European options in the Heston model, described in Section 3.2. Due to the existence of the Black-Scholes analytic formula and its relatively cheap evaluation, we do not perform numerical experiments for pricing European options in this model.

We define the approximation spaces $X_{\mathcal{N}}$, $V_{\mathcal{N}}$ to be the standard conforming piecewise linear finite element spaces. More precisely, consider a triangulation $\mathcal{T}_{\mathcal{N}}$ of Ω, consisting of J simplices $T_{\mathcal{N}}^j$, $1 \le j \le J$, such that $\overline{\Omega} = \cup_{T_{\mathcal{N}} \in \mathcal{T}_{\mathcal{N}}} \overline{T}_{\mathcal{N}}$, where $\Omega \in \mathbb{R}^d$, $d = 1, 2$ is a polygonal domain. We use standard conforming nodal first order finite element spaces, defined as

$$X_{\mathcal{N}} := \{v \in X : \quad v_{|T_{\mathcal{N}}^j} \in \mathbb{P}^1(T_{\mathcal{N}}^j), 1 \le j \le J\}, \quad V_{\mathcal{N}} = X_{\mathcal{N}} \cap V. \tag{3.5.1}$$

We associate the basis function $\phi_i \in X_{\mathcal{N}}$ with its Lagrange node $m_i \in \overline{\Omega}$, i.e., $\phi_i(m_j) = \delta_{i,j}$, for $i, j = 1,\dots,\mathcal{N}_X$, $\mathcal{N}_X = \mathcal{N} + \mathcal{N}_{\mathrm{D}}$, where a number $\mathcal{N}$ corresponds to the interior nodes of Ω and $\mathcal{N}_{\mathrm{D}}$ refers to the nodes on Γ_{D}. For a time discretization, we choose $\theta = 1/2$ corresponding to the Crank-Nicolson method. The time domain $[0, T]$ is discretized with a uniform mesh of step size $\Delta t := T/I$. The spatial computational domain $\Omega = (\nu_{\min}, \nu_{\max}) \times (x_{\min}, x_{\max})$ consist of $\mathcal{N}_X = 49 \times 97 = 4753$ nodes. Recall, that for the Heston model the model parameter vector is $\boldsymbol{\mu} = (\xi, \rho, \gamma, \kappa, r) \in \mathcal{P}$.

We consider the European call and put options with the pay-off functions $\chi(x) := (K - Ke^x)_+$ and $\chi(x) := (Ke^x - K)_+$, respectively. The boundary conditions for the call options are chosen as in (2.7.8), and for the put as in (2.7.10). The strike price K can be considered as a scaling factor, and we set $K = 1$.

To generate the snapshots and to build the reduced basis we use a finite subset $\mathcal{P}_{\text{train}} \subset \mathcal{P}$, which is, if not specified, composed of equidistantly distributed points. To validate and test the reduced model, we use a random test subset $\mathcal{P}_{\text{test}} \subset \mathcal{P}$.

3.5.1 European Call Option in the Heston Model

We start our consideration with the pricing of the European call options in the Heston model. We consider $T = 1$, $I = 20$, $\nu_{\min} = 0.0025$, $\nu_{\max} = 0.5$, $x_{\min} = -5$, $x_{\max} = 5$. The parameter domain is chosen as follows

$$\mathcal{P} \equiv [0.6, 0.9] \times [0.21, 0.9] \times [0.16, 0.25] \times [3, 5] \times [0.01, 0.2] \subset \mathbb{R}^5. \tag{3.5.2}$$

To motivate the application of the reduced basis approach, first, we demonstrate the variability of the solution in parameter and time. In Figure 3.1 the detailed solution for a fixed parameter value $\boldsymbol{\mu}^\star = (0.4, 0.55, 0.06, 2.5, 0.0198)$ is presented at the final time $t = T = 1$ (left) and an evolution over time (right). The variation of the solution with respect to different values of the parameter is depicted in Figure 3.2. While some of the parameters are varying, the others are fixed and taking their values from the reference parameter vector $\boldsymbol{\mu}^\star$.

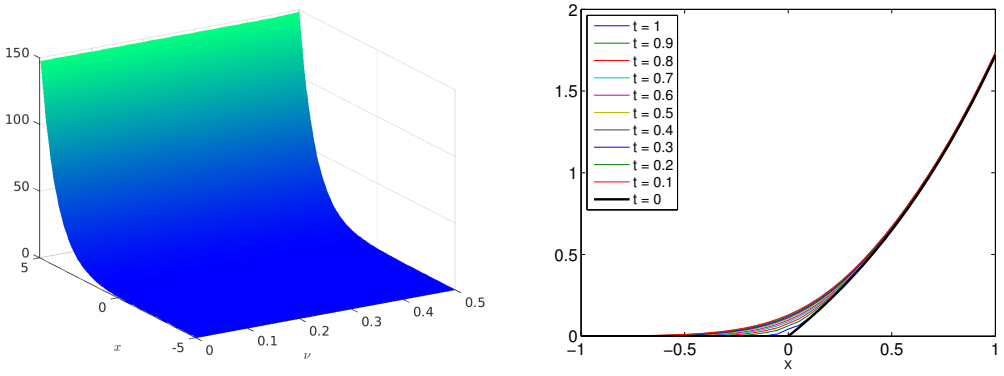

Figure 3.1: Left: The value of the European call option in the Heston model for $\boldsymbol{\mu}^\star = (0.4, 0.55, 0.06, 2.5, 0.0198)$ at $t = T = 1$. Right: A time evolution of the option price for $\boldsymbol{\mu}^\star$, extracted at $\nu = 0.1683$.

The next step is a computation of the snapshots for different $\boldsymbol{\mu}_i \in \mathcal{P}_{\text{train}}$. We apply the reduced basis approach for different dimensions of the parameter domain $\mathcal{P} \subset \mathbb{R}^d$, $d = 2, 3, 4, 5$, in particular, we consider $\boldsymbol{\mu} = (\gamma, \kappa) \in \mathbb{R}^2$, $\boldsymbol{\mu} = (\gamma, \kappa, r) \in \mathbb{R}^3$, $\boldsymbol{\mu} = (\rho, \gamma, \kappa, r) \in \mathbb{R}^4$ and $\boldsymbol{\mu} = (\xi, \rho, \gamma, \kappa, r) \in \mathbb{R}^5$. For each choice of $\boldsymbol{\mu}$, the remaining parameter values are assumed to be fixed and taken from the default parameter

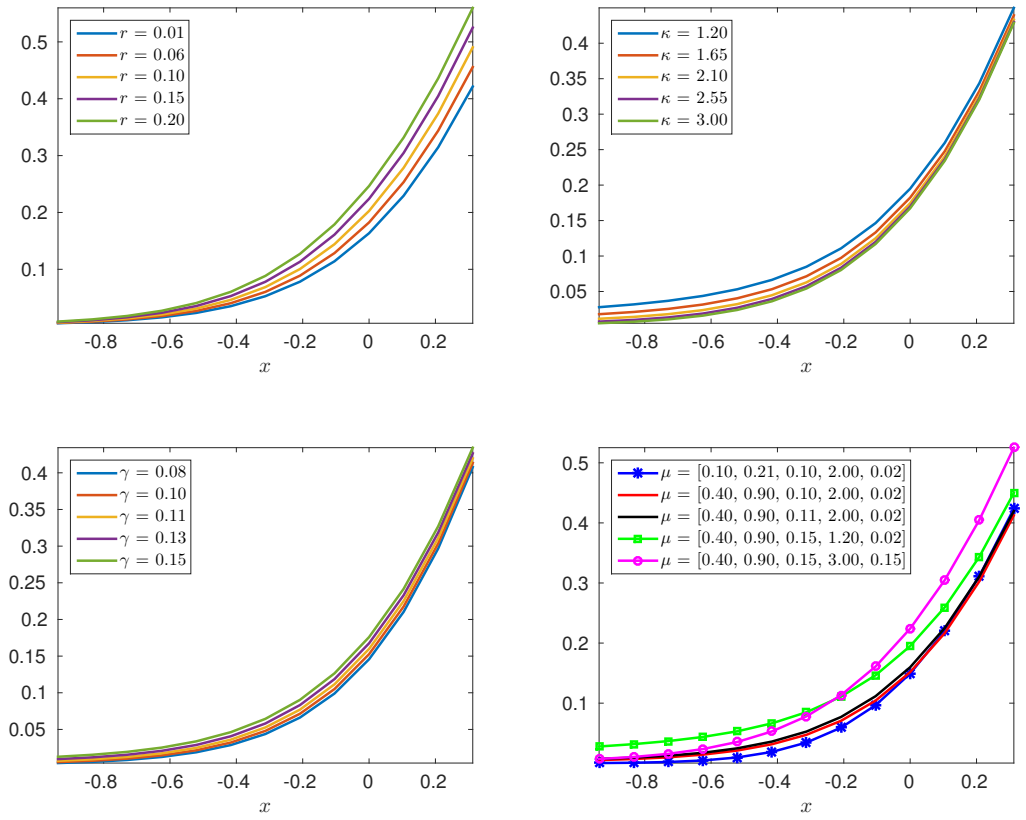

Figure 3.2: Snapshots of the solution for different parameter values, extracted at the fixed volatility $\nu = 0.1683$ and maturity $T = 1$.

vector $\boldsymbol{\mu}^\star = (0.3, 0.21, 0.095, 2, 0.0198)$. Then the POD-Greedy Algorithm 3.1, with $E_u^{\text{true}}(\boldsymbol{\mu})$ (see (3.4.19b)) as a selection criterion, is used to construct the reduced basis space V_N.

In the first test, we consider $\boldsymbol{\mu} = (\kappa, \gamma)$ and $|\mathcal{P}_{\text{train}}| = 15^2 = 225$ equidistantly distributed points. The first six orthonormal reduced basis vectors produced by the POD-Greedy algorithm are presented in Figure 3.3.

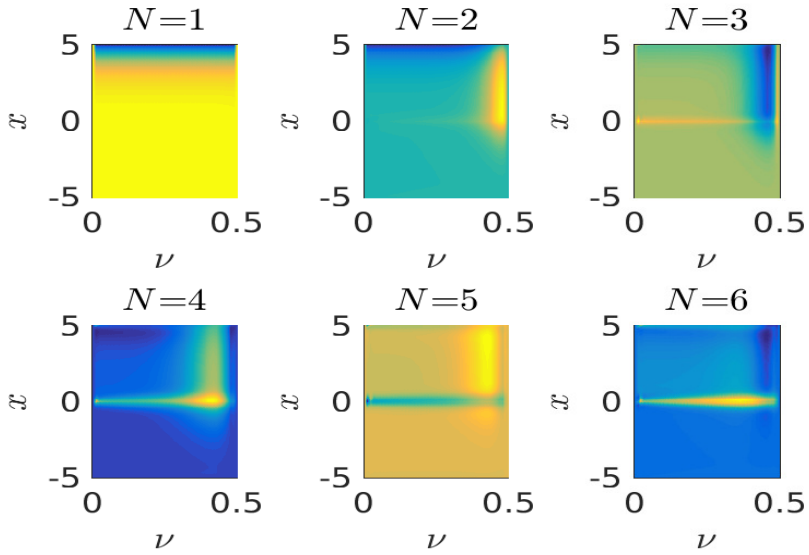

Figure 3.3: First six vectors of the reduced basis $\{\psi_k\}_{k=1}^N \subset \Psi_N$, $\boldsymbol{\mu} = (\gamma, \kappa)$.

To quantify the approximation quality of the reduced basis method, we investigate the error decay when increasing the dimension of the reduced system. For each reduced model, we consider the "training" error, i.e., the error produced by the basis construction algorithm: $\max_{\boldsymbol{\mu}\in\mathcal{P}_{\text{train}}} \{E_u^{\text{true}}(\boldsymbol{\mu})\}$ over N. We can observe, as expected, an exponential decay of the error, Figure 3.4 (left). To study the reliability of the constructed reduced basis, we, in addition, compute the "testing" error $\max_{\boldsymbol{\mu}\in\mathcal{P}_{\text{test}}} \{E_u^{\text{true}}(\boldsymbol{\mu})\}$ over an independent random test set $|\mathcal{P}_{\text{test}}| = 400$. We observe that the "training" and "testing" errors are almost the same, that suggests the reliability of the constructed reduced basis space. The selected parameters produced by the POD-Greedy algorithm are depicted in Figure 3.4 (right). By the "frequency of the selection" of the parameters, we mean how often the same parameter is chosen during the basis generation. Larger circles indicate training parameters which are chosen more often during the POD-Greedy procedure. We can observe that the selected parameters are distributed over a whole parameter domain, which indicates that POD-Greedy tries to exploit all possible parameter variations.

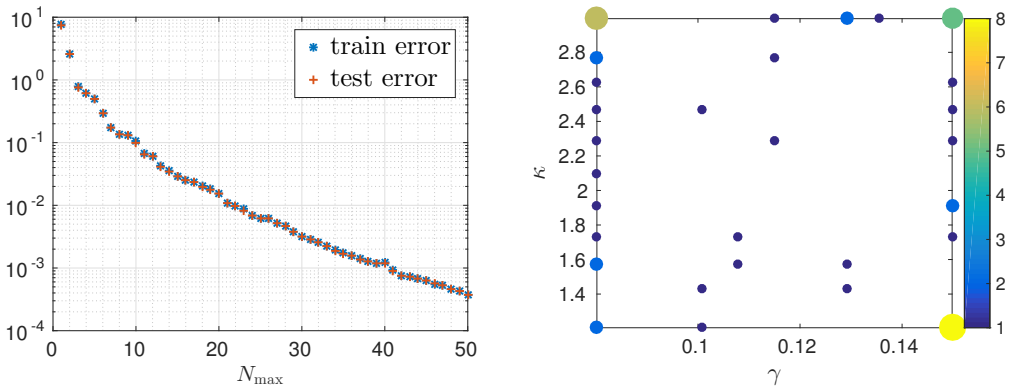

Figure 3.4: Left: Evolution of $\max_{\boldsymbol{\mu}\in\mathcal{P}_{\text{train / test}}}\{E_u^{\text{true}}(\boldsymbol{\mu})\}$ for the European call option in the Heston model produced by Algorithm 3.1 with $\boldsymbol{\mu} = (\gamma, \kappa)$, $|\mathcal{P}_{\text{train}}| = 15^2 = 225$, $|\mathcal{P}_{\text{test}}| = 400$. Right: Plot of the selected parameters $\boldsymbol{\mu}_1, ..., \boldsymbol{\mu}_N \in \mathcal{P}_{\text{train}}$ and their frequency of the selection.

The analogous results for other choices of $\boldsymbol{\mu} = (\gamma, \kappa, r)$, $\boldsymbol{\mu} = (\rho, \gamma, \kappa, r)$ and $\boldsymbol{\mu} = (\xi, \rho, \gamma, \kappa, r)$ are presented in Figure 3.5 and Figure 3.6, respectively. For these

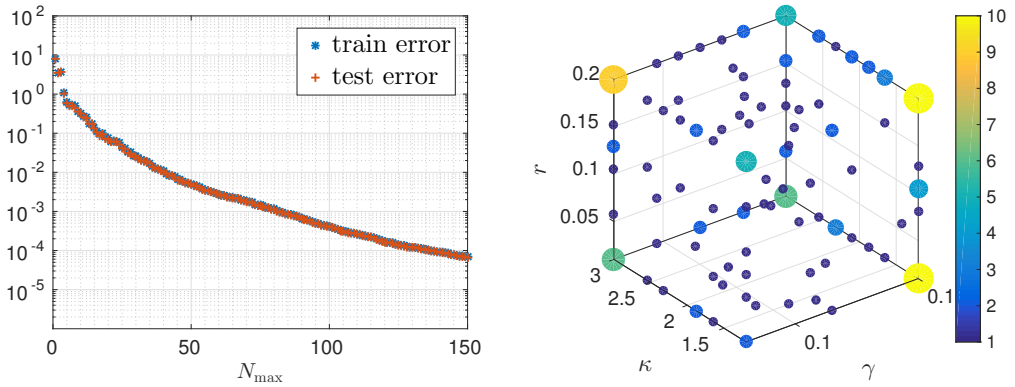

Figure 3.5: Left: Evolution of $\max_{\boldsymbol{\mu}\in\mathcal{P}_{\text{train / test}}}\{E_{L^2}^{\text{true}}(\boldsymbol{\mu})\}$ for the European call option in the Heston model produced by Algorithm 3.1 with $\boldsymbol{\mu} = (\gamma, \kappa, r)$, $|\mathcal{P}_{\text{train}}| = 9^3 = 729$, $|\mathcal{P}_{\text{test}}| = 1024$. Right: Plot of the selected parameters $\boldsymbol{\mu}_1, ..., \boldsymbol{\mu}_N \in \mathcal{P}_{\text{train}}$ and their frequency of the selection.

cases we observe similar performance of the reduced basis method. In particular, we can see the exponentially decaying behavior of the error, however with much slower convergence for the larger dimension of the parameter domain. This can be explained by the increasingly complex parameter dependence of the model. Additionally, for the

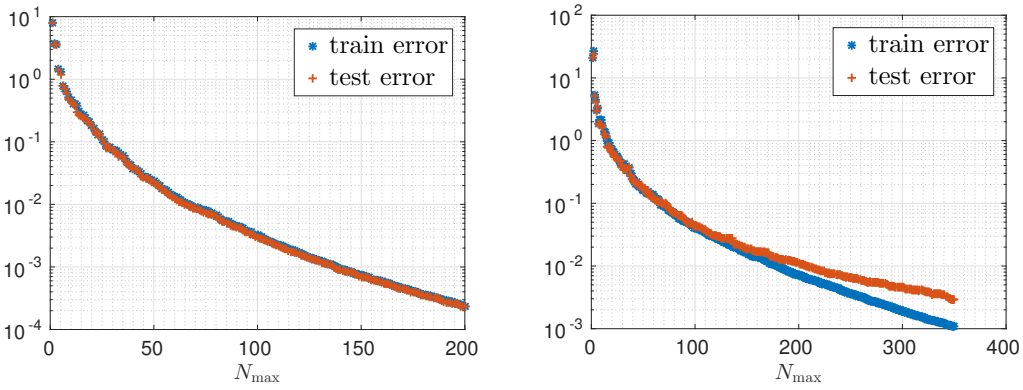

Figure 3.6: Left: Evolution of $\max_{\boldsymbol{\mu}\in\mathcal{P}_{\text{train / test}}} \{E_u^{\text{true}}(\boldsymbol{\mu})\}$ for the European call option in the Heston model produced by Algorithm 3.1 with $\boldsymbol{\mu} = (\rho, \gamma, \kappa, r)$, $|\mathcal{P}_{\text{train}}| = 7^4 = 2401$, $|\mathcal{P}_{\text{test}}| = 3000$ (left) and with $\boldsymbol{\mu} = (\xi, \rho, \gamma, \kappa, r)$, $|\mathcal{P}_{\text{train}}| = 6^5 = 7776$, $|\mathcal{P}_{\text{test}}| = 10000$ (right).

last example, $\boldsymbol{\mu} = (\xi, \rho, \gamma, \kappa, r)$, see Figure 3.6 (right), we can notice a larger deviation between the "training" and "testing" errors. This observation can be justified by the fact that, possibly, the size of the training set $\mathcal{P}_{\text{train}}$ is not sufficiently large. In this situation, a larger training set is required. The problem, which may occur here, is that we do not know a priori how large the training set should be. While too large dimension of $\mathcal{P}_{\text{train}}$ results in a very expensive offline routine, too coarse $\mathcal{P}_{\text{train}}$ may not be sufficient to capture the parameter dependence of the model, as we could already observe experimentally. Different strategies can be proposed to overcome this difficulty. One of them, is to consider the adaptive training set partitioning, see, e.g., [HDO11; HO08a], where initially one starts with the coarse training set and adaptively refines $\mathcal{P}_{\text{train}}$ within the iterations of the greedy loop. Such a procedure has similarities to the adaptive finite element method.

3.5.2 European Put Options in the Heston Model

Due to the availability of closed-form solutions, in practice, it is sufficient to evaluate only, e.g., put options and then, using the put-call parity relation, to obtain the corresponding call prices. However, for the numerical approximation of the underlying PDE we are not aware of the error produced by the put-call parity relation. Several sources, such as different boundary conditions, can cause an additional error. For this reason, we consider an application of the reduced basis method to the European put option as well. For comparative purposes with the American put options, studied in the next chapter, we restrict ourselves to similar settings. Namely, we consider $T = 2$, $I = 250$ and $\nu_{\min} = 10^{-5}$, $\nu_{\max} = 3$, $x_{\min} = -5$, $x_{\max} = 5$. The parameter

domain is set to

$$\mathcal{P} \equiv [0.1, 0.9] \times [-0.95, 0.95] \times [0.01, 0.5] \times [0.1, 5] \times [0.0001, 0.8] \subset \mathbb{R}^5. \qquad (3.5.3)$$

The snapshot of the detailed solution for $\boldsymbol{\mu} = (0.64, 0.21, 0.16, 0.1, 0.07)$ at maturity $T = 2$ and its time evolution are depicted in Figure 3.7.

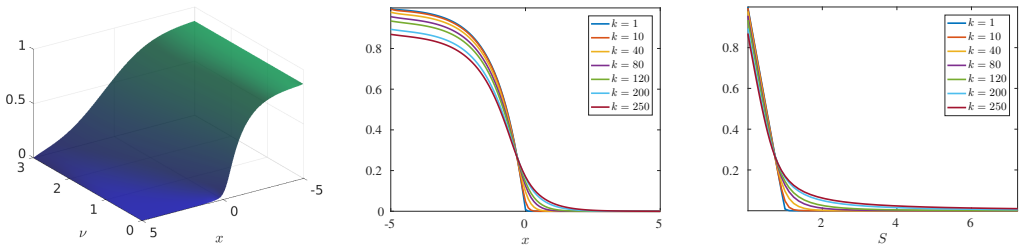

Figure 3.7: The value of the European put option $u^I_{\mathcal{N}}(\boldsymbol{\mu})$ in the Heston model at $T = 2$ for $\boldsymbol{\mu} = (0.64, 0.21, 0.16, 0.1, 0.07)$ (left). The time evolution of the solution in the log-transformed variable x (middle) and in the original stock price variable $S = Ke^x$ (right) (zoomed).

Similarly to the European call options, we construct the reduced model for the put options. In particular, we consider different variations of the parameter: $\boldsymbol{\mu} = (\xi, \rho, \gamma) \in \mathcal{P} \subset \mathbb{R}^3$ and $\boldsymbol{\mu} = (\xi, \rho, \gamma, \kappa, r) \in \mathcal{P} \subset \mathbb{R}^5$. The remaining parameters are set to the values of the reference parameter vector $\boldsymbol{\mu}^\star = (0.2, -0.2, 0.16, 0.1, 0.07)$. We apply the POD-Greedy algorithm with E_u^{true} as the selection criterion. The training errors, produced by the algorithm for different scenarios are depicted in Figure 3.8. As previously, we observe that the convergence of the RBM becomes slower with increasing the dimension of the parameter domain, which again confirms a non-trivial parameter dependence of the model.

We close this chapter with the efficiency study of the method. In particular, we consider the following measures of the computational times.

- t_1: Computation time for the trajectory of a single detailed solution for a given parameter value $\boldsymbol{\mu} \in \mathcal{P}$. This includes the time $t_{1,1}$ to assemble the detailed system and the time $t_{1,2} := t_1 - t_{1,1}$ to solve the high-fidelity problem.

Online phase

- t_2: Computation time to assemble the reduced system and to solve the reduced problem for a given $\boldsymbol{\mu} \in \mathcal{P}$.

- t_1/t_2: Asymptotic speed-up of the online routine while using the reduced basis method.

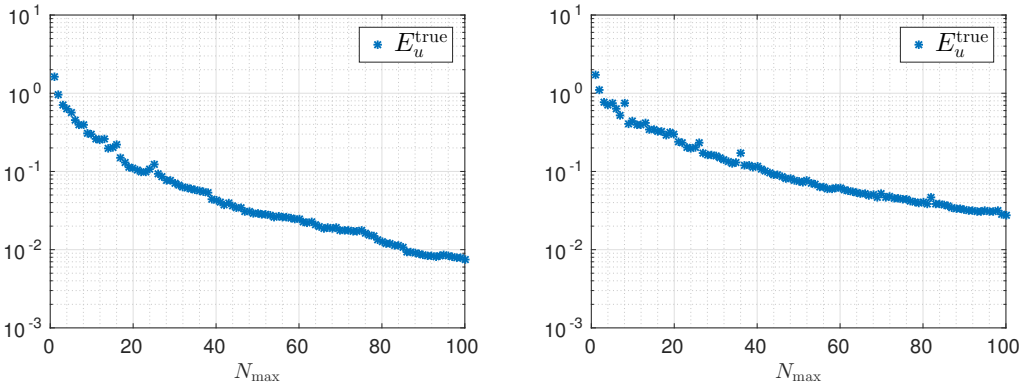

Figure 3.8: Left: Evolution of $\max_{\boldsymbol{\mu}\in\mathcal{P}_{\text{train}}}\{E_u^{\text{true}}(\boldsymbol{\mu})\}$ for the European put option in the Heston model produced by Algorithm 3.1 with $\boldsymbol{\mu} = (\xi, \rho, \gamma)$, $|\mathcal{P}_{\text{train}}| = 7^3 = 343$ (left) and with $\boldsymbol{\mu} = (\xi, \rho, \gamma, \kappa, r)$, $|\mathcal{P}_{\text{train}}| = 4^5 = 1024$ (right).

Offline phase

- t_3: Computation time for the construction of the reduced bases using Algorithm 3.1 with $E_N(\boldsymbol{\mu}) = E_u^{\text{true}}(\boldsymbol{\mu})$ as a selection criterion.
- t_4: Computation time to construct the parameter independent reduced data.
- t_5: Computation time for evaluation of the snapshots, i.e., the time for computing the detailed solutions $u_{\mathcal{N}}^k(\boldsymbol{\mu})$, for all $\boldsymbol{\mu} \in \mathcal{P}_{\text{train}}$. This cost depends on the size of $\mathcal{P}_{\text{train}}$.

The measurements of the run-time performance corresponding to the previous two examples of the European put options are summarized in Table 3.1.

	$N_{\max}$	$\lvert\mathcal{P}_{\text{train}}\rvert$	t_1	t_2	t_3	t_4	t_5	t_1/t_2
$\boldsymbol{\mu} = (\xi, \rho, \gamma)$	100	343	33.11	0.0682	9140	0.084	4018	485.9
$\boldsymbol{\mu} = (\xi, \rho, \gamma, \kappa, r)$	100	1024	31.94	0.0613	27192	0.0835	12977	521

Table 3.1: Run-time measurements (in seconds) of the reduced basis method for different $N_{\max}$ and for different model parameter settings.

We notice that the performance of the RBM in the online stage is very similar for both scenarios and provides more than 400 times speed-up compared to the FEM. However, due to the different dimensions of the parameter domain, the computational effort of the offline routine differs significantly.

Note that the time t_1 includes not only the solution time for the detailed problem, but also the matrix assembly time $t_{1,1}$, which is in the present case equal to $t_{1,1} = 26.21$ seconds on average. Hence, the asymptotic speed-up for only solving the problem is $t_{1,2}/t_2 \approx 101.17$ for the first case and $t_{1,2}/t_2 \approx 93.47$ for the second case. In the multi-query context, using the affine-decomposition, if given, the assembly time can be neglected for the computation of the asymptotic speed-up.

4 RBM for Parametrized Parabolic Variational Inequalities

4.1 Introduction

In this chapter we extend the reduced basis methodology to more complex models, in particular to ones used to price American options. Mathematically, this leads to solving a variational problem with inequality constraints in a weak form, referred to as a variational inequality problem.

In general, abstract variational inequalities provide a solid framework to study many different kind of processes, e.g., in engineering, physics, and finance. The study of abstract variational inequalities goes back to the works of A. Signorini [Sig59] and G. Fichera [Fic63]. Since then extensive research has been done; for more details on the theoretical study as well as different areas of application we refer to, e.g., [BL82; DL72; KO88; KS00; LS67]. The numerical analysis of variational inequalities is very broad and an overview can be found in some classical sources [Glo08; GLT81].

The goal of this chapter is to provide a general framework for accurately and efficiently solving parameterized time dependent variational inequalities with the reduced basis method. This work involves an extension and combination of the reduced basis methodology for the linear parabolic problems (Chapter 3) and stationary variational inequalities [HSW12]. The method is presented here in the context of option pricing; however it can cover a large class of applications, as mentioned previously. Much of the content of this chapter follows [BHS$^+$15; HSW13].

As discussed previously, we consider the examples of pricing American options in the Black-Scholes and Heston models (see Chapter 2). The numerical solution of these problems can be accomplished with standard techniques, such as finite differences, see, e.g., [HF10; IT08; IT09] or finite elements; see, e.g., [AP05b; FLM$^+$11; HRS$^+$13; KSW12; WAW01; ZFV98].

For the development of the reduced basis method we reformulate the problem in a saddle point form. We refer to, e.g., [BFB13; BHR78; Woh11] for the numerical treatment of such type of problems.

The application of the reduced basis method for parabolic variational inequalities considered in a space-time framework can be found in [GU14; GU15]. The works on stationary variational inequalities include [HSW12] and [ZBV16], where in the latter one the variational inequality is treated by a primal-dual approach.

The chapter is organized as follows: In Section 4.2 we present the model formulation to price American options. In Section 4.3 we pose the problem in a variational and a discrete variational form and discuss the existence and uniqueness of the weak and discrete solutions. In Section 4.4 we develop the reduced basis methodology for time dependent variational inequalities. Here, we discuss the main properties, such as well-posedness of the reduced system. In Section 4.5 we derive a posteriori estimates for the reduced basis error. In particular, in Section 4.5.1 we state some preliminary results needed for the further analysis and in Section 4.5.2 we present the a posteriori error bounds. Finally, in Section 4.6 we present algorithms which can be used for the construction of the reduced basis. Section 4.7 discusses the algorithmic aspects of the method, namely, the practical and efficient implementation of the reduced problem and a posteriori error bounds. We close the chapter with Section 4.8, where, using numerous examples of pricing American options in the Black-Scholes and Heston models, we provide an empirical illustration of the developed methodology.

4.2 Model Problem: American Put Options

We recall Problem 2.7.2 for pricing American put options restated in the log-transformed variables. We follow the same setting as introduced in Section 3.2. Namely, we consider an open bounded domain $\Omega \subset \mathbb{R}^d$, $d = 1, 2$, cf. (3.2.3), with Lipschitz continuous boundary $\partial\Omega = \Gamma_{\mathrm{D}} \cap \Gamma_{\mathrm{N}}$ and the space-time cylinder $Q_{\mathrm{T}} = (0, T] \times \Omega$, $T > 0$ with space-time boundaries $\Sigma_{\mathrm{D}} := (0, T] \times \Gamma_{\mathrm{D}}$, $\Sigma_{\mathrm{N}} := (0, T] \times \Gamma_{\mathrm{N}}$. Then the problem for finding the price w of an American put option can be written as

$$\frac{\partial w}{\partial t} - Lw \geq 0, \qquad \text{in} \quad Q_{\mathrm{T}}, \tag{4.2.1a}$$

$$w \geq \chi, \qquad \text{in} \quad Q_{\mathrm{T}}, \tag{4.2.1b}$$

$$\left(\frac{\partial w}{\partial t} - Lw\right)(w - \chi) = 0, \qquad \text{in} \quad Q_{\mathrm{T}}, \tag{4.2.1c}$$

$$w(0) = w_0, \qquad \text{on} \quad \Omega, \tag{4.2.1d}$$

with the pay-off $\chi(x) := (Ke^x - K)_+$ and $w_0 = \chi(x)$. The problem (4.2.1) is subject to the corresponding Dirichlet and Neumann boundary conditions (see Section 2.7) which are defined for the Black-Scholes model in (4.2.2a) and for the Heston model in (4.2.2b), respectively.

$$w = g = \chi, \qquad \text{on} \quad \Sigma_{\mathrm{D}}, \qquad \Sigma_{\mathrm{N}} = \emptyset, \tag{4.2.2a}$$

$$w = g = \chi, \qquad \text{on} \quad \Sigma_{\mathrm{D}}, \qquad \frac{\partial w}{\partial n_L} = h = 0, \quad \text{on} \quad \Sigma_{\mathrm{N}}. \tag{4.2.2b}$$

4.3 Detailed Problem Formulation

4.3.1 Variational Formulation

To pose the problem (4.2.1) in a weak form, we make use of the separable Hilbert spaces X, V and H, introduced in Section 3.3, i.e., $X = H^1(\Omega)$, $V = \{v \in X : v|_{\Gamma_D} = 0\}$ and $H = L^2(\Omega)$, with $\|\cdot\|_X = \|\cdot\|_{H^1(\Omega)}$ and $\|\cdot\|_V = |\cdot|_{H^1(\Omega)}$.

As before, in order to tackle non-homogeneous boundary conditions, we introduce the Dirichlet lift function $u_L \in W(0,T;X)$, defined by an extension operator (3.3.4), and set $u(t) := w(t) - u_L(t)$, $t \in (0,T)$, with $u(0) = u_0 := w(0) - u_L(0)$. We denote the modified pay-off functional by $\widetilde{\chi}(t) := \chi - u_L(t)$ and introduce the closed convex subset $K(t)$ of V as

$$\mathcal{K}(t) = \{v \in V : \quad v \geq \widetilde{\chi}(t) \quad \text{in } \Omega\}, \quad \text{a.e. } t \in [0,T], \tag{4.3.1}$$

where the inequality is understood pointwise almost everywhere. We assume the function $\widetilde{\chi}(t)$ is such that $K(t) \neq \emptyset$ for almost all $t \in [0,T]$. Define the linear continuous operator $\mathcal{A} \in \mathcal{L}(V;V')$ induced by the bilinear form $a : V \times V \to \mathbb{R}$, such that $a(u,v) = (\mathcal{A}u, v)$ for all $v, u \in V$.

Consider the following variational formulation of the problem (4.2.1) with homogeneous Dirichlet boundary conditions: Given $u_0 \in \mathcal{K}$, find $u \in W(0,T;V)$, such that $u(t) \in \mathcal{K}(t)$ for almost all $t \in [0,T]$, and satisfies

$$\left\langle \frac{d}{dt}u(t), v - u(t) \right\rangle_{V' \times V} + a(u(t), v - u(t)) \geq \langle f(t), v - u(t)\rangle_{V' \times V}, \quad \forall v \in \mathcal{K}(t), \tag{4.3.2a}$$

$$u(0) = u_0, \tag{4.3.2b}$$

where $f \in L^2(0,T;V')$, and is defined in (3.3.5). To obtain a solution of (4.3.2), we use a result on the existence of *strong* solutions according to [DL72; GLT81; Lio72]. For this result an additional assumption is needed, namely that $f' \in L^2(0,T;V')$, where $f' = \frac{df}{dt}$. In fact, assuming additionally $u_L' \in W(0,T;X)$, and since there are only homogeneous Neumann boundary conditions, the regularity $f' \in L^2(0,T;V')$ can be guaranteed in this context. Note additionally, that the result on strong solutions will guarantee a higher regularity of the time derivative of u, such that the duality pairing for the time derivative in (4.3.2) can be replaced by the L^2-inner product.

The following result establishes the existence and uniqueness of the solution of (4.3.2); see e.g., [GLT81, Chapter 6, Theorem 2.1], [DL72, Chapter 1, Theorem 5.1], [Lio72, Chapter 2, Theorem 2.1].

Theorem 4.3.1. *Let V, H be given and form the Gelfand triple. Assume that the bilinear form $a(\cdot,\cdot)$ is continuous and satisfies the Gårding inequality on V and $f, f' \in$*

$L^2(0,T;V')$, where $f' = \frac{df}{dt}$. Moreover, assume, $u_0 \in \mathcal{K}(0)$, $\mathcal{K}(t) \neq \emptyset$, $t \in [0,T]$, and $f(0) - \mathcal{A}u_0 \in H$. Then the problem (4.3.2) admits a unique solution u, which, in addition, satisfies: $u \in L^2(0,T;V)$, $u' \in L^2(0,T;V) \cap L^\infty(0,T;H)$.

Parametrized Problem

To present a parametrized form of the problem (4.3.2), as before, we denote by $\boldsymbol{\mu} \in \mathcal{P}$ an input parameter vector from a p-dimensional parameter space $\mathcal{P} \subset \mathbb{R}^p$. For any $\boldsymbol{\mu} \in \mathcal{P}$, we define a parametrized version of $\mathcal{K}(t)$:

$$\mathcal{K}(t;\boldsymbol{\mu}) = \{v \in V : \quad v \geq \widetilde{\chi}(t;\boldsymbol{\mu}) \quad \text{in } \Omega\}, \quad \text{a. e. } t \in [0,T].$$

Then the parametrized version of the variational problem (4.3.2), reads as follows: For a given $\boldsymbol{\mu} \in \mathcal{P}$, $u_0(\boldsymbol{\mu}) \in \mathcal{K}(\boldsymbol{\mu})$, $f(\boldsymbol{\mu}), f'(\boldsymbol{\mu}) \in L^2(0,T;V')$, find $u(\boldsymbol{\mu}) \in W(0,T;V) \cap \mathcal{K}(\boldsymbol{\mu})$, such that for all $v \in \mathcal{K}(t;\boldsymbol{\mu})$ holds

$$\left\langle \frac{d}{dt}u(t;\boldsymbol{\mu}), v - u(t;\boldsymbol{\mu}) \right\rangle_{V'\times V} + a(u(t;\boldsymbol{\mu}), v - u(t;\boldsymbol{\mu});\boldsymbol{\mu}) \geq \langle f(t;\boldsymbol{\mu}), v - u(t;\boldsymbol{\mu})\rangle_{V'\times V} \tag{4.3.3a}$$

$$u(0) = u_0(\boldsymbol{\mu}), \tag{4.3.3b}$$

As before, to guarantee the well-posedness of the parametrized problem, we need to require that the bilinear form remains continuous and coercive (or satisfies a Gårding inequality) for all $\boldsymbol{\mu} \in \mathcal{P}$, with the coercivity constant $\alpha_a(\boldsymbol{\mu})$ (the Gårding constant $\lambda_a(\boldsymbol{\mu})$) and the continuity $\gamma_a(\boldsymbol{\mu})$ constant, defined in (3.3.13).

4.3.2 Discretization

In this section we present an abstract framework for the discrete approximation of the parabolic variational inequality (4.3.3). Upon this formulation we will build the reduced basis approximation.

For the temporal discretization we consider a finite differences approach. In particular, we apply an implicit Euler scheme. Recall, that the interval $[0,T]$ is divided into I subintervals of equal length $\Delta t := T/I$ and $t^k := k\Delta t$, $0 < k \leq I$. We use sets of indices $\mathbb{I}$, $\mathbb{I}_0$, specified in (3.3.16). For all $\boldsymbol{\mu} \in \mathcal{P}$, $k \in \mathbb{I}_0$, we denote the semi-discrete solution $u^{k+1}(\boldsymbol{\mu}) := u(t^{k+1};\boldsymbol{\mu})$ and introduce a semi-discretization of the convex sets

$$\mathcal{K}^{k+1}(\boldsymbol{\mu}) = \{v \in V : \quad v \geq \widetilde{\chi}^{k+1}, \quad \text{in } \Omega\}. \tag{4.3.4}$$

Then we arrive in the following semi-discrete formulation of (4.3.3).

Problem 4.3.1 (Semi-discrete Problem)**.** *Given $\boldsymbol{\mu} \in \mathcal{P}$ and $u^0(\boldsymbol{\mu}) = u_0(\boldsymbol{\mu})$, find $u^{k+1}(\boldsymbol{\mu}) \in \mathcal{K}^{k+1}(\boldsymbol{\mu})$, $k \in \mathbb{I}$, such that for all $v \in \mathcal{K}^{k+1}(\boldsymbol{\mu})$ holds*

$$\frac{1}{\Delta t}\left(u^{k+1}(\boldsymbol{\mu}) - u^k(\boldsymbol{\mu}), v - u^{k+1}(\boldsymbol{\mu})\right)_{L^2(\Omega)} + a(u^{k+1}(\boldsymbol{\mu}), v - u^{k+1}(\boldsymbol{\mu}); \boldsymbol{\mu}) \geq f^{k+1}(v - u^{k+1}(\boldsymbol{\mu}); \boldsymbol{\mu}), \quad (4.3.5)$$

with $f^{k+1}(\cdot; \boldsymbol{\mu})$ defined as in (3.3.17) for $h \equiv 0$ and $\theta = 1$, i.e.,

$$f^{k+1}(v; \boldsymbol{\mu}) = -\frac{1}{\Delta t}\left(u^{k+1}_{L\mathcal{N}}(\boldsymbol{\mu}) - u^k_{L\mathcal{N}}(\boldsymbol{\mu}), v\right)_{L^2(\Omega)} - a(u^{k+1}_{L\mathcal{N}}(\boldsymbol{\mu}), v; \boldsymbol{\mu}). \quad (4.3.6)$$

The above scheme is unconditionally stable, [Glo08, Chapter 6, Section 3.2], and often used in practice.

Alternatively, one may use a weighted θ-scheme, $\theta \in [0, 1]$. Let $\omega \in \{1, \theta\}$ and recall an index

$$\cdot^{k+\theta} = \theta \cdot^{k+1} + (1 - \theta)\cdot^k, \quad \theta \in [0, 1]. \quad (4.3.7)$$

Denote the semi-discrete convex cone by

$$\mathcal{K}^{k+\omega}(\boldsymbol{\mu}) = \{v \in V : \quad v \geq \widetilde{\chi}^{k+\omega}, \quad \text{in } \Omega\}. \quad (4.3.8)$$

Then we consider an alternative semi-discrete problem.

Problem 4.3.2. *Given $\boldsymbol{\mu} \in \mathcal{P}$, $\omega \in \{1, \theta\}$, $\theta \in [0, 1]$, $u^0(\boldsymbol{\mu}) = u_0(\boldsymbol{\mu})$, find $u^{k+\omega}(\boldsymbol{\mu}) \in \mathcal{K}^{k+\omega}(\boldsymbol{\mu})$, $k \in \mathbb{I}$, such that for all $v \in \mathcal{K}^{k+\omega}(\boldsymbol{\mu})$ holds*

$$\frac{1}{\Delta t}\left(u^{k+1}(\boldsymbol{\mu}) - u^k(\boldsymbol{\mu}), v - u^{k+\omega}(\boldsymbol{\mu})\right)_{L^2(\Omega)} + a(u^{k+\theta}(\boldsymbol{\mu}), v - u^{k+\omega}(\boldsymbol{\mu}); \boldsymbol{\mu}) \geq f^{k+\theta}(v - u^{k+\omega}(\boldsymbol{\mu}); \boldsymbol{\mu}), \quad (4.3.9)$$

with $f^{k+\theta}(\cdot; \boldsymbol{\mu})$ defined as in (3.3.17) for $h \equiv 0$ and $\theta \in [0, 1]$.

The index ω encodes at which time step the constraints are imposed. For $\omega = 1$, we impose the constraints at the $k+1$ time step, as in (4.3.8). For $\omega = \theta$, the constraints are established at the $k+\theta$ time step. Obviously, for $\theta = \omega = 1$, we obtain the implicit Euler scheme and (4.3.5) and (4.3.9) become equivalent formulations. However, other situations may occur, for instance, (a) $\omega = 1$, $\theta \in [0, 1]$ or (b) $\omega = \theta = 1/2$. In the first case, according to [GLT81, Chapter 6, Section 3.2], the scheme is referred as "scheme I" and there it is proven unconditional stability for $\theta = 1$. For $\theta = \frac{1}{2}$ only a conditional stability is shown. In the second case, according to [Glo08, Chapter III, Section 4] the scheme (4.3.5) is referred as a Crank-Nicolson scheme and unconditionally stable. However, in this case u^{k+1} may not belong to $\mathcal{K}^{k+1}$, and the scheme is not recommended if the continuous solution is lacking regularity in time.

We restrict our attention to the case $\omega = 1$, and $\theta \in [1/2, 1]$. For the a posteriori error analysis, we will only consider $\omega = \theta = 1$.

Saddle Point Formulation

It is well-known that stationary variational inequalities with a symmetric bilinear form can equivalently be reformulated as constrained minimization problems. In turn, using the method of Lagrange multipliers, these problems can be reformulated as saddle point problems. This leads to search for the solution of the minimization problem in a linear space, instead of a closed convex set.

In our setting we are dealing with the time dependent problems and, generally, non symmetric bilinear forms, which means that the variational inequality cannot be characterized as constrained minimization problem. However, we can still use the notion of the saddle point problem.

Let W be a Hilbert space endowed with an inner product $(\cdot,\cdot)_W$ and norm $\|\cdot\|_W$ and let $M \subset W$ be a nonempty closed convex cone. Furthermore, define a parameter independent, continuous bilinear form on $W \times V$, $b : W \times V \to \mathbb{R}$ with continuity constant γ_b, i.e.,

$$|b(\eta, v)| \leq \gamma_b \|\eta\|_W \|v\|_V. \tag{4.3.10}$$

We say, that $b(\cdot,\cdot)$ is inf-sup stable on $W \times V$, if there exist $\beta_0 > 0$, such that

$$\beta := \inf_{\eta \in W} \sup_{v \in V} \frac{b(\eta, v)}{\|v\|_V \|\eta\|_W} \geq \beta_0 > 0. \tag{4.3.11}$$

The pair of spaces (V, W) satisfying (4.3.11) are referred to as a *"stable"* pair.

For the particular case $W = V'$, which we consider in our numerical experiments, we define $b(\cdot,\cdot)$ to be a duality pairing $b(\eta, v) := \langle \eta, v \rangle_{V' \times V}$, and the cone M to be a "dual cone", cf., e.g., [IM91], and expressed as

$$M := \{\eta \in W : \quad b(\eta, v) \geq 0, \quad v \in V^+\}, \tag{4.3.12}$$

where $V^+ := \{v \in V : \quad v \geq 0\}$.

For $\boldsymbol{\mu} \in \mathcal{P}$ and $k \in \mathbb{I}$, we introduce the functional $g^{k+1} \in W'$,

$$g^{k+1}(\eta; \boldsymbol{\mu}) := b(\eta, \widetilde{\chi}^{k+1}) = b(\eta, \chi) - b(\eta, u_L^{k+1}(\boldsymbol{\mu})).$$

We also assume, that the convex set $\mathcal{K}^{k+1}(\boldsymbol{\mu})$, $\boldsymbol{\mu} \in \mathcal{P}$, $k \in \mathbb{I}$, can be expressed in terms of the cone M, i.e,

$$\mathcal{K}^{k+1}(\boldsymbol{\mu}) = \{v \in V : \quad b(\eta, v) \geq g^{k+1}(\eta; \boldsymbol{\mu}), \quad \eta \in M\}. \tag{4.3.13}$$

Then the problem (4.3.9) can be written in the following semi-discrete saddle point form.

Problem 4.3.3. *For a given $\boldsymbol{\mu} \in \mathcal{P}$, $\theta \in [1/2, 1]$, $u^0(\boldsymbol{\mu}) \in V$ find $(u^{k+1}(\boldsymbol{\mu}), \lambda^{k+1}(\boldsymbol{\mu})) \in V \times M$, $k \in \mathbb{I}$, such that for all $v \in V$, $\eta \in M$ it holds*

$$\frac{1}{\Delta t}\left(u^{k+1}(\boldsymbol{\mu}) - u^k(\boldsymbol{\mu}), v\right)_{L^2(\Omega)} + a(u^{k+\theta}(\boldsymbol{\mu}), v; \boldsymbol{\mu}) - b(\lambda^{k+1}(\boldsymbol{\mu}), v) = f^{k+\theta}(v; \boldsymbol{\mu}), \tag{4.3.14a}$$

$$b(\eta - \lambda^{k+1}(\boldsymbol{\mu}), u^{k+1}(\boldsymbol{\mu})) \geq g^{k+1}(\eta - \lambda^{k+1}(\boldsymbol{\mu}); \boldsymbol{\mu}). \tag{4.3.14b}$$

The following theorem establishes the well-posendess of Problem 4.3.3.

Theorem 4.3.2. *Let for all $\boldsymbol{\mu} \in \mathcal{P}$, $k \in \mathbb{I}$, $a(\cdot, \cdot; \boldsymbol{\mu})$ be continuous and satisfy the Gårding inquality on V, $f^{k+1}(\boldsymbol{\mu}) \in V'$, $\Delta t < 1/(\theta \lambda_a(\boldsymbol{\mu}))$ and $\mathcal{K}^{k+1}(\boldsymbol{\mu}) \subset V$, $\mathcal{K}^{k+1}(\boldsymbol{\mu}) \neq \emptyset$. In addition, assume that $b(\cdot, \cdot)$ is inf-sup stable on $W \times V$, that is* (4.3.11) *holds. Then the following statements are true:*

(i) *there exist a unique solution $(u^{k+1}(\boldsymbol{\mu}), \lambda^{k+1}(\boldsymbol{\mu})) \in V \times W$ of Problem 4.3.3,*

(ii) *the formulations* (4.3.9) *and* (4.3.14) *are equivalent, which means, if the pair $(u^{k+1}(\boldsymbol{\mu}), \lambda^{k+1}(\boldsymbol{\mu}))$ is a solution of Problem 4.3.3, then $u^{k+1}(\boldsymbol{\mu})$ is a solution of Problem 4.3.1 and vice versa.*

Proof. The proof can be found in, e.g., [BHR78, Theorem 2.1], [Woh11, Lemma 2.1] for the second statement. □

We often refer to $u^{k+1}(\boldsymbol{\mu}) \in V$ as a primal solution and to the Lagrange multiplier $\lambda^{k+1}(\boldsymbol{\mu})$ as a dual one; similarly for the spaces V and W.

Spatial Discretization

For the spatial discretization of the saddle-point problem (4.3.14), we consider conforming finite dimensional approximation spaces $X_\mathcal{N} \subset X$, $V_\mathcal{N} \subset V$ and $W_\mathcal{N} \subset W$, given in terms of the basis functions ϕ_p and χ_q,

$$X_\mathcal{N} = \operatorname{span}\{\phi_p,\ p = 1, \ldots, \mathcal{N}_X\}, \quad V_\mathcal{N} = X_\mathcal{N} \cap V = \operatorname{span}\{\phi_p,\ p = 1, \ldots, \mathcal{N}_V\},$$
$$W_\mathcal{N} = \operatorname{span}\{\chi_q,\ q = 1, \ldots, \mathcal{N}_W\}.$$

The dimensions of the spaces are $\dim(X_\mathcal{N}) = \mathcal{N}_X$, $\dim(V_\mathcal{N}) = \mathcal{N}_V$ and $\dim(W_\mathcal{N}) = \mathcal{N}_W$, with $\mathcal{N}_X$, $\mathcal{N}_V$, $\mathcal{N}_W$ being sufficiently large, such that the approximation error is small enough. As before, these spaces inherit the inner products and norms of the exact spaces, i.e., $(\cdot, \cdot)_{X_\mathcal{N}} = (\cdot, \cdot)_X$, $\|\cdot\|_{X_\mathcal{N}} = \|\cdot\|_X$ and in similar manner for the other spaces.

The discrete Lagrange multiplier cone $M_{\mathcal{N}} \subset W_{\mathcal{N}}$ is defined as follows

$$M_{\mathcal{N}} = \operatorname{span}_+\{\chi_q\}_{q=1}^{\mathcal{N}_W} := \Big\{\eta \in W_{\mathcal{N}} : \quad \eta = \sum_{q=1}^{\mathcal{N}_W} \alpha_q \chi_q, \quad \alpha_q \geq 0\Big\}. \tag{4.3.15}$$

Remark 4.3.1. *Note that we do not necessary require the conformity of the discrete cone, $M_{\mathcal{N}} \subset M$. In particular, in our numerical simulations we use discontinuous dual biorthogonal basis functions for the discretization of $W_{\mathcal{N}}$ (see [Woh00; Woh01; Woh11]). This results in $M_{\mathcal{N}} \not\subset M$, i.e., with respect to the Lagrange multiplier the method is not conforming.*

For a given $\boldsymbol{\mu} \in \mathcal{P}$ and $k \in \mathbb{I}$, the solution pair $(u^{k+1}(\boldsymbol{\mu}), \lambda^{k+1}(\boldsymbol{\mu})) \in V \times M$ is then approximated by $(u_{\mathcal{N}}^{k+1}(\boldsymbol{\mu}), \lambda_{\mathcal{N}}^{k+1}(\boldsymbol{\mu})) \in V_{\mathcal{N}} \times M_{\mathcal{N}}$, where

$$u_{\mathcal{N}}^{k+1}(\boldsymbol{\mu}) = \sum_{p=1}^{\mathcal{N}_V} u_{\mathcal{N},p}^{k+1}(\boldsymbol{\mu})\phi_p, \qquad \lambda_{\mathcal{N}}^{k+1}(\boldsymbol{\mu}) = \sum_{q=1}^{\mathcal{N}_W} \lambda_{\mathcal{N},q}^{k+1}(\boldsymbol{\mu})\chi_q.$$

For $\boldsymbol{\mu} \in \mathcal{P}$, $k \in \mathbb{I}_0$ the Dirichlet lift function $u_L^k(\boldsymbol{\mu}) \in X$ is approximated by the discrete functions $u_{L\mathcal{N}}^{k+1}(\boldsymbol{\mu})$; see Section 3.3.4. Accordingly, for the modified pay-off $\widetilde{\chi}^k \in V$ we consider an approximation $\widetilde{\chi}_{\mathcal{N}}^k(\boldsymbol{\mu}) = \sum_{p=1}^{\mathcal{N}_V} \widetilde{\chi}_{\mathcal{N},p}^k(\boldsymbol{\mu})\phi_p$. The initial condition $u_{\mathcal{N}}^0$ is chosen as $u_{\mathcal{N}}^0(\boldsymbol{\mu}) = \widetilde{\chi}_{\mathcal{N}}^0(\boldsymbol{\mu})$. Then we consider the following fully discrete saddle point formulation of Problem 4.3.3.

Problem 4.3.4 (Detailed saddle point problem)**.** *For a given $\boldsymbol{\mu} \in \mathcal{P}$, $\theta \in [1/2, 1]$, $u_{\mathcal{N}}^0(\boldsymbol{\mu}) \in V_{\mathcal{N}}$, find $u_{\mathcal{N}}^{k+1}(\boldsymbol{\mu}) \in V_{\mathcal{N}}$, $\lambda_{\mathcal{N}}^{k+1}(\boldsymbol{\mu})) \in M_{\mathcal{N}}$, $k \in \mathbb{I}$, such that for all $v \in V_{\mathcal{N}}$, $\eta \in M_{\mathcal{N}}$ it holds*

$$\frac{1}{\Delta t}\left(u_{\mathcal{N}}^{k+1}(\boldsymbol{\mu}) - u_{\mathcal{N}}^{k}(\boldsymbol{\mu}), v\right)_{L^2(\Omega)} + a\left(u_{\mathcal{N}}^{k+\theta}(\boldsymbol{\mu}), v; \boldsymbol{\mu}\right) - b(\lambda_{\mathcal{N}}^{k+1}(\boldsymbol{\mu}), v) = f^{k+\theta}(v; \boldsymbol{\mu}), \tag{4.3.16a}$$

$$b(\eta - \lambda_{\mathcal{N}}^{k+1}(\boldsymbol{\mu}), u_{\mathcal{N}}^{k+1}(\boldsymbol{\mu})) \geq g^{k+1}(\eta - \lambda_{\mathcal{N}}^{k+1}(\boldsymbol{\mu}); \boldsymbol{\mu}), \tag{4.3.16b}$$

with

$$f^{k+\theta}(v; \boldsymbol{\mu}) = -\frac{1}{\Delta t}\left(u_{L\mathcal{N}}^{k+1}(\boldsymbol{\mu}) - u_{L\mathcal{N}}^{k}(\boldsymbol{\mu}), v\right)_{L^2(\Omega)} - a(u_{L\mathcal{N}}^{k+\theta}(\boldsymbol{\mu}), v; \boldsymbol{\mu}). \tag{4.3.17}$$

As previously, the continuity and coercivity properties of the bilinear forms (or Gårding inequality) are carried over to the discrete spaces. That is, $a(\cdot, \cdot; \boldsymbol{\mu})$ is continuous and coercive on $V_{\mathcal{N}}$ (or satisfies the Gårding inequality) with the corresponding discrete continuity $\gamma_a^{\mathcal{N}}(\boldsymbol{\mu})$ and coercivity constants $\alpha_a^{\mathcal{N}}(\boldsymbol{\mu})$ (with $\lambda_a^{\mathcal{N}}(\boldsymbol{\mu})$), defined in (3.3.19), and $b(\cdot, \cdot)$ is continuous on $W_{\mathcal{N}} \times V_{\mathcal{N}}$ with continuity a constant $\gamma_b^{\mathcal{N}}(\boldsymbol{\mu})$.

Proposition 4.3.3. *Let $V_\mathcal{N} \subset V$, $W_\mathcal{N} \subset W$ and the conditions of Theorem 4.3.2 hold. Assume that $b(\cdot,\cdot)$ is inf-sup stable on $W_\mathcal{N} \times V_\mathcal{N}$: that is, there exists a constant β_0 independent of the mesh size, such that*

$$\beta_\mathcal{N} := \inf_{\eta \in W_\mathcal{N}} \sup_{v \in V_\mathcal{N}} \frac{b(\eta, v)}{\|v\|_V \|\eta\|_W} \geq \beta_0 > 0. \tag{4.3.18}$$

Then for every $\boldsymbol{\mu} \in \mathcal{P}$, $k \in \mathbb{I}$, there exists a unique solution $(u_\mathcal{N}^{k+1}(\boldsymbol{\mu}), \lambda_\mathcal{N}^{k+1}(\boldsymbol{\mu}))$ of Problem 4.3.4.

Proof. The proof directly follows from Theorem 4.3.2. See also, e.g., [BHR78, Theorem 4.4]. □

Upon Problem 4.3.4 we build the reduced basis method, described in the next section. To guarantee the well-posedness of the detailed problem (4.3.16), we always assume that $V_\mathcal{N}$ and $W_\mathcal{N}$ are chosen such that the discrete inf-sup condition is fulfilled.

4.4 Reduced Basis Approximation

In this section we present a reduced basis scheme for parabolic variational inequalities and give an existence and uniqueness result together with other properties of the reduced system.

4.4.1 Formulation

We consider a finite subset $\mathcal{P}_N := \{\boldsymbol{\mu}_1, \ldots, \boldsymbol{\mu}_N\} \subset \mathcal{P}$ with $\boldsymbol{\mu}_i \neq \boldsymbol{\mu}_j$, $\forall i \neq j$, $N \in \mathbb{N}$. The primal and dual sets of snapshots are denoted by $S_N^u := \{u_\mathcal{N}^k(\boldsymbol{\mu}_1), \ldots, u_\mathcal{N}^k(\boldsymbol{\mu}_S)\}$ and $S_N^\lambda := \{\lambda_\mathcal{N}^k(\boldsymbol{\mu}_1), \ldots, \lambda_\mathcal{N}^k(\boldsymbol{\mu}_S)\}$, $k \in \mathbb{I}_0$, $S \in \mathbb{N}$. Using a suitable algorithm, we construct the reduced primal Ψ_N and dual Ξ_N bases using S_N^u and S_N^λ,

$$\Psi_N := \{\psi_1, \ldots, \psi_{N_V}\} \subset V_\mathcal{N}, \quad \Xi_N := \{\xi_1, \ldots, \xi_{N_W}\} \subset W_\mathcal{N}.$$

Numerical algorithms to build these two sets will be discussed in Section 4.6. Then the detailed primal and dual spaces are approximated by low-dimensional reduced spaces $V_N \subset V_\mathcal{N}$ and $W_N \subset W_\mathcal{N}$, defined as

$$V_N := \operatorname{span}\{\psi_i, \quad 1 \leq i \leq N_V\}, \qquad W_N := \operatorname{span}\{\xi_j, \quad 1 \leq j \leq N_W\}.$$

The reduced basis approximation M_N of the detailed cone $M_\mathcal{N}$ is defined as

$$M_N = \operatorname{span}_+\{\xi_j\}_{j=1}^{N_W} := \Big\{ \sum_{j=1}^{N_W} \alpha_j \xi_j, \quad \alpha_j \geq 0 \Big\}. \tag{4.4.1}$$

For the construction of the reduced space, we assume $\xi_j \in M_{\mathcal{N}}$, and hence $M_N \subseteq M_{\mathcal{N}}$. We define the reduced basis solution pair $\left(u_N^{k+1}(\boldsymbol{\mu}), \lambda_N^{k+1}(\boldsymbol{\mu})\right) \in V_N \times M_N$, $\boldsymbol{\mu} \in \mathcal{P}$, $k \in \mathbb{I}$, where

$$u_N^{k+1}(\boldsymbol{\mu}) = \sum_{p=1}^{N_V} u_{N,j}^{k+1}(\boldsymbol{\mu})\psi_p, \qquad \lambda_N^{k+1}(\boldsymbol{\mu}) = \sum_{q=1}^{N_W} \lambda_{N,q}^{k+1}(\boldsymbol{\mu})\xi_q. \tag{4.4.2}$$

Then the reduced problem reads as follows.

Problem 4.4.1 (Reduced problem)**.** *Given $\boldsymbol{\mu} \in \mathcal{P}$, $\theta \in [1/2, 1]$, find $u_N^{k+1}(\boldsymbol{\mu}) \in V_N$, $\lambda_N^{k+1}(\boldsymbol{\mu}) \in M_N$, $k \in \mathbb{I}$, that for all $v_N \in V_N$, $\eta_N \in M_N$ satisfy*

$$\frac{1}{\Delta t}\left(u_N^{k+1} - u_N^k, v_N\right)_{L^2(\Omega)} + a(u_N^{k+\theta}, v_N; \boldsymbol{\mu}) - b(\lambda_N^{k+1}, v_N) = f^{k+\theta}(v_N; \boldsymbol{\mu}), \tag{4.4.3a}$$

$$b(\eta_N - \lambda_N^{k+1}, u_N^{k+1}) \geq g^{k+1}(\eta_N - \lambda_N^{k+1}; \boldsymbol{\mu}). \tag{4.4.3b}$$

The initial value u_N^0 is chosen as the orthogonal projection of $u_{\mathcal{N}}^0$ on V_N, i.e., $(u_N^0 - u_{\mathcal{N}}^0, v_N)_V = 0$ for all $v_N \in V_N$.

4.4.2 Properties of the Reduced System

The well-posedness of the reduced saddle point problem (4.4.3) follows with identical arguments as for the detailed one. In particular, the properties of coercivity (Gårding inequality) and continuity of $a(\cdot, \cdot; \boldsymbol{\mu})$ on $V_N \times V_N$ and continuity of $b(\cdot, \cdot)$ on $W_N \times V_N$ are directly inherited from the corresponding properties on the high-fidelity spaces $V_{\mathcal{N}}$ and $W_{\mathcal{N}}$.

However, the same argumentation is not applicable for the inf-sup stability of $b(\cdot, \cdot)$ on $W_N \times V_N$. Hence, additional care should be taken for an appropriate construction of V_N, W_N, that guarantee the existence of $\beta_0 > 0$, such that

$$\beta_N := \inf_{\eta \in W_N} \sup_{v \in V_N} \frac{b(\eta, v)}{\|v\|_V \|\eta\|_W} \geq \beta_0 > 0. \tag{4.4.4}$$

To verify the condition (4.4.4), let us first introduce the following operator $T : W_{\mathcal{N}} \to V_{\mathcal{N}}$, defined as

$$(T\eta, v)_V := b(\eta, v), \quad \forall v \in V_{\mathcal{N}}. \tag{4.4.5}$$

Note that for $v \in V_{\mathcal{N}}$, $\eta \in W_{\mathcal{N}}$, $b(\eta, v) = \langle B\eta, v\rangle_{V' \times V}$, where $B : W \to V'$ is a linear continuous operator. Then by the Riesz representation theorem, $T\eta$ is, in fact, a Riesz representer of $B\eta \in V'$ and it holds

$$\|T\eta\|_V = \|B\eta\|_{V'} = \sup_{v \in V_{\mathcal{N}}} \frac{\langle B\eta, v\rangle_{V' \times V}}{\|v\|_V} = \sup_{v \in V_{\mathcal{N}}} \frac{b(\eta, v)}{\|v\|_V}. \tag{4.4.6}$$

The operator T is often referred to as the *supremizer* operator, since it is realizing the supremum in (4.4.6).

From (4.4.6) and (4.3.18) we obtain the following characterization of $\beta_{\mathcal{N}}$ for the detailed problem,

$$\beta_{\mathcal{N}} = \inf_{\eta \in W_{\mathcal{N}}} \frac{\|T\eta\|_V}{\|\eta\|_W}. \tag{4.4.7}$$

Then to form a stable pair of the reduced spaces V_N, W_N, a sufficient condition could be an "inclusion of the supremizers" in the primal space. The supremizers are the elements $T\xi_i \in V_N$, where $\xi_i \in W_N$, $1 \leq i \leq N_W$, is a basis of W_N.

In the context of the reduced basis method, this approach was first introduced in [Rov03], and subsequently widely applied for, e.g., non-coercive or Stokes problems, e.g., [GV11; NMR15; Rov03; RV07; VPR$^+$03]. Note that inclusion of the supremizers is not a unique way to obtain a stable pair of the reduced spaces. Alternatively, for variational inequalities an enrichment of the primal space by a-priori or unconstrained solutions can be considered, see for more details [HSW11; HSW12].

Let $\{\widetilde{\psi}_i\}_{i=1}^{N_S}$ denote a set of basis functions, which are built only from the set of the primal snapshots S_N^u. Then we consider the following "enriched" primal reduced space

$$V_N := \operatorname{span}\{\psi_i\}_{i=1}^{N_V} = \operatorname{span}\{\widetilde{\psi}_i, T\xi_j\}_{i,j=1}^{N_S,N_W} \subset V_{\mathcal{N}}. \tag{4.4.8}$$

The following lemma demonstrates that, with this choice, (V_N, W_N) satisfies the stability condition (4.4.4).

Lemma 4.4.1. *Let V_N be given by* (4.4.8)*, then $b(\cdot,\cdot)$ is inf-sup stable on $W_N \times V_N$,* (4.4.4)*, and hence the reduced problem admits a unique solution. Moreover, there exist $\beta^0 > 0$, such that the following inequalities holds*

$$\beta_N \geq \beta_{\mathcal{N}} \geq \beta^0 > 0. \tag{4.4.9}$$

Proof. The proof can be found in e.g., [HSW12; RV07]. For a self-contained presentation, we provide it here. Using the fact that $V_N \subset V_{\mathcal{N}}$, the definition of the supremizer operator (4.4.5), (4.4.6), and the enrichment of V_N by supremizers (4.4.8), we can derive that

$$\begin{aligned}\beta_{\mathcal{N}} &= \inf_{\eta \in W_{\mathcal{N}}} \sup_{v \in V_{\mathcal{N}}} \frac{b(\eta, v)}{\|v\|_V \|\eta\|_W} \leq \inf_{\eta \in W_N} \sup_{v \in V_{\mathcal{N}}} \frac{b(\eta, v)}{\|v\|_V \|\eta\|_W} \\ &= \inf_{\eta \in W_N} \frac{b(\eta, T\eta)}{\|T\eta\|_V \|\eta\|_W} \leq \inf_{\eta \in W_N} \sup_{v \in V_N} \frac{b(\eta, v)}{\|v\|_V \|\eta\|_W} = \beta_N. \end{aligned}$$

□

As the next step, similar to the linear case in Chapter 3, Proposition 3.4.1, we provide a consistency property of the reduced basis solution.

Proposition 4.4.2 (Reproduction of solutions)**.** *If for some $\boldsymbol{\mu} \in \mathcal{P}$, $\theta \in [1/2, 1]$ and all $k \in \mathbb{I}$, $u_{\mathcal{N}}^{k+1}(\boldsymbol{\mu}) \in V_N$, and $\lambda_{\mathcal{N}}^{k+1}(\boldsymbol{\mu}) \in M_N$ with $u_{\mathcal{N}}^0(\boldsymbol{\mu}) \in V_N$, then*

$$u_N^{k+1}(\boldsymbol{\mu}) = u_{\mathcal{N}}^{k+1}(\boldsymbol{\mu}), \quad \lambda_N^{k+1}(\boldsymbol{\mu}) = \lambda_{\mathcal{N}}^{k+1}(\boldsymbol{\mu}), \quad \forall k \in \mathbb{I}.$$

Proof. We prove this property by induction. For $k = 0$, $u_{\mathcal{N}}^0 \in V_N$ and for $u_N^0 \in V_N$ we have $(u_N^0 - u_{\mathcal{N}}^0, v_N)_V = 0$, for all $v_N \in V_N$. Set $v_N = u_N^0 - u_{\mathcal{N}}^0$, then

$$(u_N^0 - u_{\mathcal{N}}^0, u_N^0 - u_{\mathcal{N}}^0)_V = 0,$$

which is true only for $u_N^0 = u_{\mathcal{N}}^0$. For the induction step, we assume that $u_{\mathcal{N}}^k = u_N^k$, $\lambda_{\mathcal{N}}^k = \lambda_N^k$. Then, choosing $v = v_N \in V_N \subset V_{\mathcal{N}}$, $\eta = \eta_N \in M_N \subset M_{\mathcal{N}}$, we directly obtain

$$\begin{aligned}
&\frac{1}{\Delta t}\left(u_{\mathcal{N}}^{k+1} - u_N^k, v_N\right)_{L^2(\Omega)} + a(u_{\mathcal{N}}^{k+\theta}, v_N; \boldsymbol{\mu}) - b(\lambda_{\mathcal{N}}^{k+1}, v_N) = f^{k+\theta}(v_N; \boldsymbol{\mu}),\\
&b(\eta_N - \lambda_{\mathcal{N}}^{k+1}, u_{\mathcal{N}}^{k+1}) \geq g^{k+1}(\eta_N - \lambda_{\mathcal{N}}^{k+1}; \boldsymbol{\mu}),
\end{aligned}$$

which implies that $(u_{\mathcal{N}}^{k+1}, \lambda_{\mathcal{N}}^{k+1}) \in V_N \times M_N$ solves the reduced problem (4.4.3). Using the uniqueness of the solution, we obtain $u_N^{k+1} = u_{\mathcal{N}}^{k+1}$ and $\lambda_N^{k+1} = \lambda_{\mathcal{N}}^{k+1}$, $k \in \mathbb{I}$. □

We comment on the regularity of the solution w.r.t. the parameter. In particular, the solution of the reduced problem is Lipschitz continuous, if the data is also Lipschitz continuous, see, e.g., [HSW12].

4.5 A Posteriori Error Analysis

In this section we present an a posteriori error analysis of the reduced scheme (4.4.3). For the derivation we restrict ourselves to the implicit Euler time discretization scheme, i.e., $\theta = 1$.

4.5.1 Preliminaries

Recall that for linear parabolic problems, the error associated with the reduced basis approximation is controlled in terms of the equality residuals; see Section 3.4.2. By contrast, for the current problem an additional error associated with the inequality constraints should be also taken into account.

For every $\boldsymbol{\mu} \in \mathcal{P}$, $k \in \mathbb{I}$, we define the equality and inequality residuals associated with the reduced basis approximation as

$$\begin{aligned}
r^{k+1}(v; \boldsymbol{\mu}) := \frac{1}{\Delta t}(u_N^{k+1}(\boldsymbol{\mu}) - u_N^k(\boldsymbol{\mu}), v)_{L^2(\Omega)} + a(u_N^{k+1}(\boldsymbol{\mu}), v; \boldsymbol{\mu})\\
- b(\lambda_N^{k+1}(\boldsymbol{\mu}), v) - f^{k+1}(v; \boldsymbol{\mu}), \quad \forall v \in V_{\mathcal{N}}, \qquad (4.5.1)\\
s^{k+1}(\eta; \boldsymbol{\mu}) := b(\eta, u_N^{k+1}(\boldsymbol{\mu})) - g^{k+1}(\eta; \boldsymbol{\mu}). \quad \forall \eta \in M_{\mathcal{N}}. \qquad (4.5.2)
\end{aligned}$$

Note that for every $\boldsymbol{\mu} \in \mathcal{P}$, $\lambda_{\mathcal{N}}^{k+1} \in M_{\mathcal{N}}$ and $\lambda_N^{k+1} \in M_N$, we have

$$b(\lambda_{\mathcal{N}}^{k+1}, u_N^{k+1}(\boldsymbol{\mu})) - g^{k+1}(\lambda_{\mathcal{N}}^{k+1}; \boldsymbol{\mu}) = 0, \tag{4.5.3a}$$
$$b(\lambda_N^{k+1}, u_N^{k+1}(\boldsymbol{\mu})) - g^{k+1}(\lambda_N^{k+1}; \boldsymbol{\mu}) = 0. \tag{4.5.3b}$$

These properties (4.5.3) are obtained by simply taking $\eta = 0$, $\eta = 2\lambda_{\mathcal{N}}^{k+1}(\boldsymbol{\mu})$ in (4.3.16b) and $\eta = 0$, $\eta = 2\lambda_N^{k+1}(\boldsymbol{\mu})$ in (4.4.3b).

We also introduce the primal and dual errors associated with the reduced basis approximation as

$$e_u^k(\boldsymbol{\mu}) := u_N^k(\boldsymbol{\mu}) - u_{\mathcal{N}}^k(\boldsymbol{\mu}), \qquad e_N^u(\boldsymbol{\mu}) := \left(e_u^k(\boldsymbol{\mu})\right)_{k\in\mathbb{I}_0}, \tag{4.5.4a}$$
$$e_\lambda^k(\boldsymbol{\mu}) := \lambda_N^k(\boldsymbol{\mu}) - \lambda_{\mathcal{N}}^k(\boldsymbol{\mu}), \qquad e_N^\lambda(\boldsymbol{\mu}) := \left(e_\lambda^{k+1}(\boldsymbol{\mu})\right)_{k\in\mathbb{I}}. \tag{4.5.4b}$$

Using the linearity of $r^{k+1}(v;\boldsymbol{\mu})$ and (4.3.16), one has for all $v \in V_{\mathcal{N}}$ that

$$r^{k+1}(v;\boldsymbol{\mu}) = \frac{1}{\Delta t}(e_u^{k+1}(\boldsymbol{\mu}) - e_u^k(\boldsymbol{\mu}), v)_{L^2(\Omega)} + a(e_u^{k+1}(\boldsymbol{\mu}), v) - b(e_\lambda^{k+1}(\boldsymbol{\mu}), v). \tag{4.5.5}$$

For all $k \in \mathbb{I}$, we define the Riesz representer $\hat{r}^{k+1}(\boldsymbol{\mu}) \in V_{\mathcal{N}}$ of the equality residuals, and by $\hat{s}^{k+1}(\boldsymbol{\mu}) \in W_{\mathcal{N}}$ the Riesz representer of the inequality residuals:

$$(v, \hat{r}^{k+1}(\boldsymbol{\mu}))_V = r^{k+1}(v;\boldsymbol{\mu}), \qquad \forall v \in V_{\mathcal{N}}, \tag{4.5.6a}$$
$$(\eta, \hat{s}^{k+1}(\boldsymbol{\mu}))_W = s^{k+1}(\eta;\boldsymbol{\mu}), \qquad \forall \eta \in W_{\mathcal{N}}. \tag{4.5.6b}$$

In the error analysis, we make use of the following norm bound

$$\|v\|_{L^2(\Omega)} \le C_\Omega \|v\|_V, \qquad \forall v \in V_{\mathcal{N}}. \tag{4.5.7}$$

If $V = H_0^1(\Omega)$ with $\|\cdot\|_V = |\cdot|_{H^1}$, then (4.5.7) is the standard Friedrichs-Poincaré inequality with the Friedrichs-Poincaré constant C_Ω.

From now on we assume that $\Delta t < 1/(2\lambda_a^{\mathcal{N}}(\boldsymbol{\mu}))$, and recall, from Chapter 3, the discrete spatio-temporal norm (3.4.17)

$$|||v|||_{\boldsymbol{\mu}} := \left(\left(1 - 2\lambda_a^{\mathcal{N}}(\boldsymbol{\mu})\Delta t\right)^I \|v^I\|_{L^2(\Omega)}^2 + \alpha_a^{\mathcal{N}}(\boldsymbol{\mu})\Delta t \sum_{k=0}^{I-1} \left(1 - 2\lambda_a^{\mathcal{N}}(\boldsymbol{\mu})\Delta t\right)^k \|v^{k+1}\|_V^2\right)^{1/2}, \tag{4.5.8}$$

where $v =: \left(v^{k+1}\right)_{k\in\mathbb{I}} \in V_{\mathcal{N}}$.

Primal-Dual Error Relation

We recall the following result from [BHS+15], which establishes the connection between the primal and dual errors and is used later to derive the a posteriori error bounds.

Lemma 4.5.1 (Primal-dual error relation)**.** *For all $\boldsymbol{\mu} \in \mathcal{P}$, $k \in \mathbb{I}$, the dual error at each time step t^{k+1}, can be bounded by the primal error as*

$$\|e_\lambda^{k+1}(\boldsymbol{\mu})\|_W \leq \frac{1}{\beta_{\mathcal{N}}} \left(\frac{C_\Omega}{\Delta t} \|e_u^{k+1}(\boldsymbol{\mu}) - e_u^k(\boldsymbol{\mu})\|_{L^2(\Omega)} + \gamma_a^{\mathcal{N}}(\boldsymbol{\mu}) \|e_u^{k+1}(\boldsymbol{\mu})\|_V + \|r^{k+1}(\boldsymbol{\mu})\|_{V'} \right). \tag{4.5.9}$$

Proof. The inf-sup stability of $b(\cdot,\cdot)$ ensures that for all $\eta \in W_{\mathcal{N}}$ there exist an element $v^\star \in V_{\mathcal{N}}$, $v^\star \neq 0$ such that the following holds

$$\beta_{\mathcal{N}} \|v^\star\|_V \|\eta\|_W \leq b(\eta, v^\star).$$

Taking $\eta := e_\lambda^{k+1} \in W_{\mathcal{N}}$, using (4.5.5), the Cauchy-Schwarz inequality, and the continuity of $a(\cdot,\cdot)$, we obtain

$$\begin{aligned} \beta_{\mathcal{N}} \|v^\star\|_V \|e_\lambda^{k+1}\|_W &\leq \frac{1}{\Delta t}(e_u^{k+1} - e_u^k, v^\star)_{L^2(\Omega)} + a(e_u^{k+1}, v^\star) - r^{k+1}(v^\star) \\ &\leq \frac{1}{\Delta t}\|e_u^{k+1} - e_u^k\|_{L^2(\Omega)} \|v^\star\|_{L^2(\Omega)} + \gamma_a^{\mathcal{N}} \|e_u^{k+1}\|_V \|v^\star\|_V + \|r^{k+1}\|_{V'} \|v^\star\|_V. \end{aligned} \tag{4.5.10}$$

Applying the norm bound (4.5.7), we obtain the desired result. □

Projectors

The derivation of the a posteriori error estimates for saddle point problems with equality constraints, e.g., for the Stokes problem, [GRV12; GV11], includes the estimate of the norms of residuals $\|r^k\|_{V'}$ and $\|s^k\|_{W'}$. By contrast, in our setting, we are dealing with inequality constraints. Hence, the quantity $\|s^k\|_{W'} = \|\hat{s}^k\|_W$ is not a straightforward error estimator component. Estimating the norm of the residual $\|s^k\|_{W'}$ would lead to a penalization of both the positive and negative parts of s^k.

Hence, to treat the inherent nonlinearity induced by the inequalities, we consider a family[1] of projectors on the cone $\widetilde{M}_{\mathcal{N}} \subset W_{\mathcal{N}}$, $\pi^{k+1} : W_{\mathcal{N}} \to \widetilde{M}_{\mathcal{N}}$, $k \in \mathbb{I}$, where

$$\widetilde{M}_{\mathcal{N}} := \{\eta \in W_{\mathcal{N}} : \quad (\eta, \eta')_W \geq 0, \quad \eta' \in M_{\mathcal{N}}\}. \tag{4.5.11}$$

4.5.2 A Posteriori Error Estimators

For any $\boldsymbol{\mu} \in \mathcal{P}$, $k \in \mathbb{I}$, we define the following estimators:

$$\delta_r^{k+1}(\boldsymbol{\mu}) := \|r^{k+1}(\boldsymbol{\mu})\|_{V'} = \|\hat{r}^{k+1}(\boldsymbol{\mu})\|_V, \tag{4.5.12a}$$

$$\delta_s^{k+1}(\boldsymbol{\mu}) := \|\hat{s}^{k+1}(\boldsymbol{\mu}) - \pi^{k+1}(\hat{s}^{k+1}(\boldsymbol{\mu}))\|_W, \tag{4.5.12b}$$

$$\widetilde{\delta}_s^{k+1}(\boldsymbol{\mu}) := (\lambda_N^{k+1}(\boldsymbol{\mu}), \pi^{k+1}(\hat{s}^{k+1}(\boldsymbol{\mu})))_W. \tag{4.5.12c}$$

[1] In fact, the projectors π^{k+1} can be chosen invariant with respect to time and the index $k+1$ is redundant in this case. However, for convenience of further analysis we preserve this index.

The next result, which is a generalization of Theorem 4.2 in [BHS+15] to a non-coercive bilinear form $a(\cdot,\cdot;\boldsymbol{\mu})$, establishes an error bound in terms of the estimators (4.5.12).

Theorem 4.5.2. *For all $\boldsymbol{\mu} \in \mathcal{P}$, we obtain the following upper bound for the primal error:*

$$|||e_N^u(\boldsymbol{\mu})|||_{\boldsymbol{\mu}} \leq \Delta_N^u(\boldsymbol{\mu}) := \left(\|e_u^0\|_{L^2(\Omega)}^2 + \sum_{k=0}^{I-1} \left(1 - 2\lambda_a^{\mathcal{N}}(\boldsymbol{\mu})\Delta t\right)^k d^{k+1}(\boldsymbol{\mu}) \right)^{1/2}, \quad (4.5.13)$$

where

$$d^{k+1} = \frac{\Delta t}{\alpha_a^{\mathcal{N}}} \left(\delta_r^{k+1} + \frac{\delta_s^{k+1}\gamma_a^{\mathcal{N}}}{\beta_{\mathcal{N}}} \right)^2 + \left(\frac{C_\Omega \delta_s^{k+1}}{\beta_{\mathcal{N}}} \right)^2 + 2\Delta t \frac{\delta_s^{k+1}\delta_r^{k+1}}{\beta_{\mathcal{N}}} + 2\Delta t \widetilde{\delta}_s^{k+1}.$$

Proof. Taking the test function $v := e_u^{k+1}$ in (4.5.5) and using the Gårding inequality, we obtain

$$\frac{1}{\Delta t}\left(e_u^{k+1} - e_u^k, e_u^{k+1}\right)_{L^2(\Omega)} + \alpha_a^{\mathcal{N}}\|e_u^{k+1}\|_V^2 - \lambda_a^{\mathcal{N}}\|e_u^{k+1}\|_{L^2(\Omega)}^2 \leq r^{k+1}(e_u^{k+1}) + b(e_\lambda^{k+1}, e_u^{k+1}). \quad (4.5.14)$$

Using (3.4.11), the first term of the inequality (4.5.14) can be expressed as

$$\left(e_u^{k+1} - e_u^k, e_u^{k+1}\right)_{L^2(\Omega)} = \frac{1}{2}\|e_u^{k+1}\|_{L^2(\Omega)}^2 - \frac{1}{2}\|e_u^k\|_{L^2(\Omega)}^2 + \frac{1}{2}\|e_u^{k+1} - e_u^k\|_{L^2(\Omega)}^2. \quad (4.5.15)$$

Using (4.5.3), (4.5.6b), the definition of $s^{k+1}(\eta)$ and π^{k+1} (4.5.11), and the fact that $b(\lambda_N^{k+1}, u_{\mathcal{N}}^{k+1}) - g^{k+1}(\lambda_N^{k+1}) \geq 0$ from (4.3.16b), we can estimate the term $b(e_\lambda^{k+1}, e_u^{k+1})$ in (4.5.14):

$$\begin{aligned}
b(e_\lambda^{k+1}, e_u^{k+1}) &= b(\lambda_N^{k+1}, u_N^{k+1}) - b(\lambda_{\mathcal{N}}^{k+1}, u_N^{k+1}) - b(\lambda_N^{k+1}, u_{\mathcal{N}}^{k+1}) + b(\lambda_{\mathcal{N}}^{k+1}, u_{\mathcal{N}}^{k+1}) \\
&\leq g^{k+1}(\lambda_N^{k+1}) - s^{k+1}(\lambda_{\mathcal{N}}^{k+1}) - g^{k+1}(\lambda_{\mathcal{N}}^{k+1}) - g^{k+1}(\lambda_N^{k+1}) + g^{k+1}(\lambda_{\mathcal{N}}^{k+1}) \\
&= -s^{k+1}(\lambda_{\mathcal{N}}^{k+1}) = s^{k+1}(e_\lambda^{k+1}) = \left(e_\lambda^{k+1}, \hat{s}^{k+1}\right)_W \\
&= (e_\lambda^{k+1}, \hat{s}^{k+1} - \pi^{k+1}(\hat{s}^{k+1}))_W + (e_\lambda^{k+1}, \pi^{k+1}(\hat{s}^{k+1}))_W \\
&\leq \|e_\lambda^{k+1}\|_W \|\hat{s}^{k+1} - \pi^{k+1}(\hat{s}^{k+1})\|_W + (\lambda_N^{k+1}, \pi^{k+1}(\hat{s}^{k+1}))_W \\
&= \delta_s^{k+1}\|e_\lambda^{k+1}\|_W + \widetilde{\delta}_s^{k+1}.
\end{aligned}$$

This estimate combined with (4.5.15) and with the Cauchy-Schwarz inequality, applied to the first term on the right-hand side of (4.5.14), gives rise to:

$$\frac{1}{2\Delta t}\|e_u^{k+1}\|_{L^2(\Omega)}^2 + \frac{1}{2\Delta t}\|e_u^{k+1} - e_u^k\|_{L^2(\Omega)}^2 + \alpha_a^{\mathcal{N}}\|e_u^{k+1}\|_V^2 - \lambda_a^{\mathcal{N}}\|e_u^{k+1}\|_{L^2(\Omega)}^2 \leq \frac{1}{2\Delta t}\|e_u^k\|_{L^2(\Omega)}^2 + \delta_r^{k+1}\|e_u^{k+1}\|_V + \delta_s^{k+1}\|e_\lambda^{k+1}\|_W + \widetilde{\delta}_s^{k+1}. \quad (4.5.16)$$

Using Lemma 4.5.1 and Young's inequality (3.4.10) with $\varepsilon = 1$, we can bound the dual error $\|e_\lambda^{k+1}\|_W$ in (4.5.16) as

$$\delta_s^{k+1}\|e_\lambda^{k+1}\|_W \leq \frac{1}{2\Delta t}\left(\frac{C_\Omega \delta_s^{k+1}}{\beta_{\mathcal{N}}}\right)^2 + \frac{1}{2\Delta t}\|e_u^{k+1} - e_u^k\|^2_{L^2(\Omega)} + \frac{\delta_s^{k+1}}{\beta_{\mathcal{N}}}\left(\gamma_a^{\mathcal{N}}\|e_u^{k+1}\|_V + \delta_r^{k+1}\right).$$

With this estimate, (4.5.16) can be simplified to

$$\frac{1}{2\Delta t}\|e_u^{k+1}\|^2_{L^2(\Omega)} + \alpha_a^{\mathcal{N}}\|e_u^{k+1}\|_V^2 - \lambda_a^{\mathcal{N}}\|e_u^{k+1}\|^2_{L^2(\Omega)} \leq \frac{1}{2\Delta t}\|e_u^k\|^2_{L^2(\Omega)} + \frac{1}{2\Delta t}\left(\frac{C_\Omega \delta_s^{k+1}}{\beta_{\mathcal{N}}}\right)^2 + \left(\delta_r^{k+1} + \frac{\delta_s^{k+1}\gamma_a^{\mathcal{N}}}{\beta_{\mathcal{N}}}\right)\|e_u^{k+1}\|_V + \frac{\delta_s^{k+1}\delta_r^{k+1}}{\beta_{\mathcal{N}}} + \widetilde{\delta}_s^{k+1}. \quad (4.5.17)$$

Applying Young's inequality (3.4.10) with $\varepsilon = \sqrt{\alpha_a^{\mathcal{N}}}$ to the third term on the right-hand side of (4.5.17) gives:

$$\left(\delta_r^{k+1} + \frac{\delta_s^{k+1}\gamma_a^{\mathcal{N}}}{\beta_{\mathcal{N}}}\right)\|e_u^{k+1}\|_V \leq \frac{1}{2\alpha_a^{\mathcal{N}}}\left(\delta_r^{k+1} + \frac{\delta_s^{k+1}\gamma_a^{\mathcal{N}}}{\beta_{\mathcal{N}}}\right)^2 + \frac{1}{2}\alpha_a^{\mathcal{N}}\|e_u^{k+1}\|_V^2.$$

Combining the last estimates, we can write (4.5.17) as

$$\frac{1}{2\Delta t}\|e_u^{k+1}\|^2_{L^2(\Omega)} + \frac{1}{2}\alpha_a^{\mathcal{N}}\|e_u^{k+1}\|_V^2 - \lambda_a^{\mathcal{N}}\|e_u^{k+1}\|^2_{L^2(\Omega)} \leq \frac{1}{2\Delta t}\|e_u^k\|^2_{L^2(\Omega)} + \frac{1}{2\alpha_a^{\mathcal{N}}}\left(\delta_r^{k+1} + \frac{\delta_s^{k+1}\gamma_a^{\mathcal{N}}}{\beta_{\mathcal{N}}}\right)^2 + \frac{1}{2\Delta t}\left(\frac{C_\Omega \delta_s^{k+1}}{\beta_{\mathcal{N}}}\right)^2 + \frac{\delta_s^{k+1}\delta_r^{k+1}}{\beta_{\mathcal{N}}} + \widetilde{\delta}_s^{k+1}.$$

Multiplying the last inequality by $2\Delta t(1 - 2\lambda_a^{\mathcal{N}}\Delta t)^k$, $k \in \mathbb{I}$, we obtain

$$\left(1 - 2\lambda_a^{\mathcal{N}}\Delta t\right)^{k+1}\|e_u^{k+1}\|^2_{L^2(\Omega)} + \left(1 - 2\lambda_a^{\mathcal{N}}\Delta t\right)^k \Delta t\alpha_a^{\mathcal{N}}\|e_u^{k+1}\|_V^2 \leq \left(1 - 2\lambda_a^{\mathcal{N}}\Delta t\right)^k\|e_u^k\|^2_{L^2(\Omega)} + \left(1 - 2\lambda_a^{\mathcal{N}}\Delta t\right)^k d^{k+1},$$

where

$$d^{k+1} = \frac{\Delta t}{\alpha_a^{\mathcal{N}}}\left(\delta_r^{k+1} + \frac{\delta_s^{k+1}\gamma_a^{\mathcal{N}}}{\beta_{\mathcal{N}}}\right)^2 + \left(\frac{C_\Omega \delta_s^{k+1}}{\beta_{\mathcal{N}}}\right)^2 + 2\Delta t\frac{\delta_s^{k+1}\delta_r^{k+1}}{\beta_{\mathcal{N}}} + 2\Delta t\widetilde{\delta}_s^{k+1}$$

Making a summation of the resulting inequalities from $k = 0, \ldots, I-1$, we obtain a telescopic sum. Taking the square root provides us with the desired result. □

If $W = V'$, one may consider an equivalent choice for the family of projectors used in the a posteriori error estimators. In particular, consider the family of projectors $\Pi^{k+1} : V_{\mathcal{N}} \to V_{\mathcal{N}}^+$ on the cone $V_{\mathcal{N}}^+ = \{v \in V_{\mathcal{N}} : \ \langle v, \eta \rangle_{V \times V'} \geq 0, \ \eta \in M_{\mathcal{N}}\}$, $k \in \mathbb{I}$. Furthermore, introduce the following quantities:

$$\delta_s^{k+1}(\boldsymbol{\mu}) := \| s^{k+1}(\boldsymbol{\mu}) - \Pi^{k+1}(s^{k+1}(\boldsymbol{\mu})) \|_V, \tag{4.5.18a}$$

$$\widetilde{\delta}_s^{k+1}(\boldsymbol{\mu}) := \langle \lambda_N^{k+1}(\boldsymbol{\mu}), \Pi^{k+1}(s^{k+1}(\boldsymbol{\mu})) \rangle_{V' \times V}. \tag{4.5.18b}$$

In fact, for this specification, we obtain the same result for a posteriori error estimators.

Proposition 4.5.3. *For all $\boldsymbol{\mu} \in \mathcal{P}$, $k \in \mathbb{I}$, the error bounds from Theorem 4.5.2 holds true for the specification of $\delta_s^{k+1}(\boldsymbol{\mu})$ and $\widetilde{\delta}_s^{k+1}(\boldsymbol{\mu})$ in* (4.5.18).

Proof. The proof directly follows from the proof of Theorem 4.5.2, without using the Riesz representers of the residuals, by directly expressing $s^{k+1}(e_\lambda^{k+1})$ as $s^{k+1}(e_\lambda^{k+1}) = \langle s^{k+1}, e_\lambda^{k+1} \rangle_{W' \times W} = \langle e_\lambda^{k+1}, s^{k+1} \rangle_{V' \times V}$. □

Under an additional assumption we can further simplify the error bound, which is stated in the following result.

Proposition 4.5.4. *Under the conditions of Theorem 4.5.2, and additionally assuming that the projectors π^{k+1} satisfy the condition*

$$(\pi^{k+1}(\hat{s}^{k+1}), \lambda_N^{k+1})_W = 0, \quad k \in \mathbb{I}, \tag{4.5.19}$$

we obtain that $\widetilde{\delta}_s^{k+1} = 0$ and the error bounds simplifies accordingly.

Projectors satisfying (4.5.19) have been used in [BHS+15] in the context of the RBM. We also refer to [Woh11; WW09] where such techniques are applied for finite element based error estimators in contact mechanics and for obstacle problems.

If we assume that there exists computable (in an offine-online fashion) lower and upper bounds of the discrete coercivity $\alpha_a^{\mathcal{N}}(\boldsymbol{\mu})$, continuity $\gamma_a^{\mathcal{N}}(\boldsymbol{\mu})$, and Gårding $\lambda_a^{\mathcal{N}}(\boldsymbol{\mu})$ constants, and a lower bound of the inf-sup stability constant $\beta_{\mathcal{N}}$, that is,

$$0 < \alpha_a^{\mathrm{LB}} \leq \alpha_a^{\mathcal{N}}(\boldsymbol{\mu}), \quad \gamma_a^{\mathcal{N}}(\boldsymbol{\mu}) \leq \gamma_a^{\mathrm{UB}}, \quad \lambda_a^{\mathcal{N}}(\boldsymbol{\mu}) \leq \lambda_a^{\mathrm{UB}}, \quad \beta_{\mathcal{N}} \geq \beta^{\mathrm{LB}} > 0, \tag{4.5.20}$$

then, under the assumption $\Delta t < 1/(2\lambda_a^{\mathrm{UB}})$, the computationally expensive, discrete coercivity, continuity and inf-sup stability constants in the definition of an upper bound Δ_N^u can be replaced by their cheaper computable respective bounds. However, we still will have only a partial offline-online decomposition of the error bounds, see Section 4.7.4.

4.6 Reduced Basis Spaces Construction

In this section, we present an overview of the different methods to build the reduced primal $\Psi_N \subset V_{\mathcal{N}}$ and dual bases $\Xi_N \subset M_{\mathcal{N}}$. Since we are considering a time-dependent variational inequality, special care should be taken to appropriately construct the reduced cone M_N as well as to tackle the additional time dimension.

For stationary variational inequalities, one could employ the standard greedy procedure to iteratively build Ψ_N and Ξ_N from the set of snapshots [HSW12; ZBV16]. However, for time dependent variational inequalities, applying a greedy iteration in both parameter and time may result in a high computational cost. Alternatively, a POD procedure, Section 3.4.3, which is standard for linear time-dependent problems, can not be unified with the construction of the dual space, due to the possible disruption of the positivity of M_N.

In this section we describe several strategies which can be applied for a suitable reduced dual space construction. In particular, we consider the POD-Angle-Greedy algorithm, the Non-Negative Matrix Factorization (NNMF) algorithm and the standard greedy procedure. For the primal space, since it does not involve any constraints, we follow the POD-Greedy algorithm.

Let us also comment on time-dependent variational inequalities treated in a space-time framework. For this case, there is no need for an additional temporal compression, as the reduction approach is performed in both a time and space, and one can employ the same greedy strategy as for the stationary variational inequalities, see [GU14; GU15].

4.6.1 POD-Angle-Greedy Algorithm

The POD-Angle-Greedy algorithm, introduced in [BHS$^+$15; HSW13], consists in building iteratively and simultaneously the reduced primal and dual bases in a greedy fashion. In particular, the construction of the primal reduced basis is performed by the standard POD-Greedy Algorithm 3.1, while for the dual one we employ the so-called *Angle-Greedy* procedure, presented in Algorithm 4.1, see also [BHS$^+$15; HSW13].

We comment on the idea behind the POD-Angle-Greedy algorithm. As in Section 3.4.3, we consider a finite training set $\mathcal{P}_{\text{train}} \subset \mathcal{P}$. Given the initial (quite arbitrary) choice of the reduced basis spaces, we initiate a greedy loop (Step 5). The loop is repeated $N_{\max}$ times or until the desired tolerance ε_{tol} is reached (Step 7). Particularly, for given primal and dual spaces at the stage $N-1$, we identify the parameter vector $\boldsymbol{\mu}_N$ in the training set $\mathcal{P}_{\text{train}}$, that currently leads to the worst reduced basis approximation (Step 6). For this parameter, new primal and dual basis vectors are generated. In particular, the selection of new primal reduced basis vectors is based on the idea of the POD-Greedy procedure (Step 11), described in

Section 3.4.3. The dual reduced basis vectors are selected using an Angle-Greedy criterion (Step 9–10). The idea is to maximize the volume of the resulting cone, i.e., we include the snapshot showing the largest deviation from the current reduced dual space. That is, the vector $\lambda^{k_N}(\boldsymbol{\mu}_N)$ that maximizes $\measuredangle\left(\lambda^{k_N}(\boldsymbol{\mu}_N), W_{N-1}\right)$, where

$$\measuredangle(\eta, Y) := \arccos\left(\|\Pi_Y \eta\|_W / \|\eta\|_W\right) \tag{4.6.1}$$

denotes the angle between the vector $\eta \in W$ and the linear space $Y \subset W$, with $\Pi_Y \eta$ being an orthogonal projection of η on Y.

Algorithm 4.1 POD-Angle-Greedy Algorithm

Input: Maximum number of iterations $N_{\max} > 0$, training sample set $\mathcal{P}_{\text{train}} \subset \mathcal{P}$, target tolerance ε_{tol}

Output: RB bases Ψ_N, Ξ_N and RB spaces V_N, W_N

1: choose arbitrarily $\boldsymbol{\mu}_0 \in \mathcal{P}_{\text{train}}$ and $k' \in \mathbb{I}_0$
2: compute $\{u^k_{\mathcal{N}}(\boldsymbol{\mu}_0)\}_{k\in\mathbb{I}_0}$, $\{\lambda^{k+1}_{\mathcal{N}}(\boldsymbol{\mu})\}_{k\in\mathbb{I}}$
3: set $\xi_0 = \lambda^{k'}_{\mathcal{N}}(\boldsymbol{\mu}_0)/\|\lambda^{k'}_{\mathcal{N}}(\boldsymbol{\mu}_0)\|_W$, $\Xi_0 = \{\xi_0\}$, $W_0 = \operatorname{span}\{\Xi_0\}$
4: set $\Psi_0 = \text{orthonormalize}\left\{u^{k'}_{\mathcal{N}}(\boldsymbol{\mu}_0), T\xi_0\right\}$, $V_0 = \operatorname{span}\{\Psi_0\}$
5: **for** $N = 1, \ldots, N_{\max}$ **do**
6: $\quad[\varepsilon^{\text{train}}_N, \boldsymbol{\mu}_N] = \arg\max_{\boldsymbol{\mu}\in\mathcal{P}_{\text{train}}} E_{N-1}(\boldsymbol{\mu})$
7: $\quad$**if** $\varepsilon^{\text{train}}_N < \varepsilon_{\text{tol}}$ **then return**
8: $\quad$**end if**
9: $\quad k_N = \arg\max_{k\in\mathbb{I}}\left(\measuredangle\left(\lambda^{k+1}_{\mathcal{N}}(\boldsymbol{\mu}_N), W_{N-1}\right)\right)$
10: $\quad\xi_N = \lambda^{k_N}_{\mathcal{N}}(\boldsymbol{\mu}_N)/\|\lambda^{k_N}_{\mathcal{N}}(\boldsymbol{\mu}_N)\|_W$, $\Xi_N = \Xi_{N-1}\cup\{\xi_N\}$, $W_N = \operatorname{span}\{\Xi_N\}$
11: $\quad\psi_N = POD_1\left(\left\{u^k_{\mathcal{N}}(\boldsymbol{\mu}_N) - \Pi_{V_{N-1}}\left(u^k_{\mathcal{N}}(\boldsymbol{\mu}_N)\right)\right\}_{k\in\mathbb{I}_0}\right)$
12: $\quad\Psi_N = \text{orthonormalize}\{\Psi_{N-1}\cup\{\psi_N, T\xi_N\}\}$, $V_N = \operatorname{span}\{\Psi_N\}$
13: **end for**

As it was pointed out in Section 4.4.2, to ensure the stability of the reduced basis system (4.4.3), we need to guarantee that the reduced basis spaces V_N ,W_N form an inf-sup stable pair. For this, we enrich the primal reduced basis by the "supremizers" (Step 12). This results in $|\Psi_N| \leq 2N_{\max}$ and $|\Xi_N| \leq N_{\max}$.

In practice, to have smaller and faster reduced models, one may skip the "supremizer enrichment" procedure. However, in this case there is no proof of stability of the system, see for more details, e.g., [HSW12].

The selection of the "worst" parameter in the greedy loop requires a measure $E_N(\boldsymbol{\mu})$ (Step 6). This error estimator can be chosen similarly as for the POD-Greedy algorithm (Algorithm 3.1), i.e., a primal projection error or a true error, see (3.4.19a), (3.4.19b), (3.4.19c) or an a posteriori error bound (4.5.13), $E^{\text{apost}}_u(\boldsymbol{\mu}) :=$

$\Delta_N^u(\boldsymbol{\mu})$. A combination of the primal and dual errors could be also utilized, e.g., $E_N(\boldsymbol{\mu}) = \omega_u E_u^{\text{true}}(\boldsymbol{\mu}) + \omega_\lambda E_\lambda^{\text{true}}(\boldsymbol{\mu})$, where $\omega_u, \omega_\lambda \geq 0$ are some weights and

$$E_\lambda^{\text{true}}(\boldsymbol{\mu}) := \left(\Delta t \sum_{k=0}^{I-1} \|e_\lambda^{k+1}(\boldsymbol{\mu})\|_W^2 \right)^{1/2} = \left(\Delta t \sum_{k=0}^{I-1} \|\lambda_N^{k+1}(\boldsymbol{\mu}) - \lambda_{\mathcal{N}}^{k+1}(\boldsymbol{\mu})\|_W^2 \right)^{1/2}.$$

Remark 4.6.1. *For the European option case, due to the absence of the Lagrange multiplier, the system no longer has a saddle point structure. Hence, in Algorithm 4.1 we omit the supremizer enrichment in Step 12 and the Angle-Greedy routine in Step 9–10. Then the algorithm reduces to the classical (strong) POD-Greedy algorithm (Algorithm 3.1).*

4.6.2 POD-NNMF

Instead of the "angle-greedy" strategy in Algorithm 4.1, one may employ alternative algorithms which can preserve the positivity constraints for the dual space construction. One of the choices is the non-negative matrix factorization (NNMF) procedure.

NNMF is a matrix factorization algorithm, which uses non-negativity constraints. It was introduced in the context of face recognition problems [LS99]. Since then much research has been done for the theoretical study of the method as well as for the extension to the different fields of application, e.g, for sound object extraction [Sma04], image processing, e.g., [LHZ+01; LS99]. In combination with the reduced basis method, NNMF was recently applied to contact problems [BAF16] and compared to the SVD procedure.

Here we briefly describe the main idea behind the NNMF approach. We consider a non-negative snapshot matrix $\mathbf{X} \in \mathbb{R}^{m \times n}$, which consist of n data points in $\mathbb{R}^m$. Given a constant $r < m$, the non-negative matrix factorization algorithm is a procedure to find a non-negative matrix $\mathbf{Q} \in \mathbb{R}^{m \times r}$ and another non-negative matrix $\mathbf{H} \in \mathbb{R}^{r \times n}$, that solve the problem:

$$\begin{aligned} &\underset{\mathbf{Q} \in \mathbb{R}^{m \times r},\ \mathbf{H} \in \mathbb{R}^{r \times n}}{\text{minimize}} && \|\mathbf{X} - \mathbf{Q}\mathbf{H}\|_{\text{F}}^2 \\ &\text{subject to} && \mathbf{Q} \geq 0, \mathbf{H} \geq 0. \end{aligned} \tag{4.6.2}$$

Here, $\|\cdot\|_{\text{F}}$ is the Frobenius norm, i.e., for $\mathbf{X} \in \mathbb{R}^{m \times n}$, it is defined as $\|\mathbf{X}\|_{\text{F}} = \left(\sum_{i=1}^m \sum_{j=1}^n \mathbf{X}_{ij}^2 \right)^{1/2}$. We can interpret $\mathbf{Q}\mathbf{H}$ as a compressed from of $\mathbf{X}$, $\mathbf{X} \approx \mathbf{Q}\mathbf{H}$. The matrix $\mathbf{Q}$ is regarded as a basis matrix and $\mathbf{H}$ as an encoding matrix.

We remark that no closed form solutions exist for the minimization problem (4.6.2). Hence, an appropriate numerical approximation should be utilized to solve it. In addition, the objective functional is only convex with respect to $\mathbf{Q}$ or $\mathbf{H}$, but not in $\mathbf{Q}$ and $\mathbf{H}$ together. Hence, most iterative algorithms will converge to a local minima.

Popular algorithms for NNMF are based on multiplicative update rules, where $\mathbf{Q}, \mathbf{H}$ are defined iteratively following the rule, see [LS00; LS99]:

$$\mathbf{Q} \leftarrow \mathbf{Q} \circ \frac{\mathbf{X}\mathbf{H}^T}{\mathbf{Q}\mathbf{H}\mathbf{H}^T}, \qquad \mathbf{H} \leftarrow \mathbf{H} \circ \frac{\mathbf{Q}^T\mathbf{X}}{\mathbf{Q}^T\mathbf{Q}\mathbf{H}}. \tag{4.6.3}$$

Here, "$\circ$" denotes an element-wise multiplication (the Hadamard product) and "$\frac{\cdot}{\cdot}$" denotes an element-wise division. Different choices of the multiplicative update rule for $\mathbf{Q}$ and $\mathbf{H}$ lead to different variants of the NNMF algorithm, such as NNMF-orthogonal [Cho08], NNMF-convolutive [Sma04], NNMF-local [LHZ+01] etc.

The NNMF algorithm also has a geometric interpretation. It can be seen as a problem of finding a simplicial cone in the positive orthant, which contains the given data points. In, e.g, [DS04; HSS14] such problem was studied as well as the geometric conditions presented, under which the factorization is unique.

We incorporate the NNMF strategy for the reduced basis construction. In Algorithm 4.2 one of the variations how to apply NNMF for the dual reduced basis is presented.

Algorithm 4.2 POD-NNMF-Greedy Algorithm

Input: Maximum number of iterations $N_{\max} > 0$, training sample set $\mathcal{P}_{\text{train}} \subset \mathcal{P}$, target tolerance ε_{tol}, initial bases Ψ_0, Ξ_0, $V_0 = \operatorname{span}\{\Psi_0\}$,$W_0 = \operatorname{span}\{\Xi_0\}$

1: **for** $N = 1, \dots, N_{\max}$ **do**
2: $\quad[\varepsilon_N^{\text{train}}, \boldsymbol{\mu}_N] = \arg\max_{\boldsymbol{\mu} \in \mathcal{P}_{\text{train}}} E_{N-1}(\boldsymbol{\mu})$
3: $\quad$**if** $\varepsilon_N^{\text{train}} < \varepsilon_{\text{tol}}$ **then return**
4: $\quad$**end if**
5: $\quad$compute $\{u_{\mathcal{N}}^k(\boldsymbol{\mu}_i)\}_{k=0,i=1}^{I,N}$, $\{\lambda_{\mathcal{N}}^{k+1}(\boldsymbol{\mu}_i)\}_{k,i=1}^{I,N}$
6: $\quad\Xi_N = \text{NNMF}_N\left(\left\{\lambda_{\mathcal{N}}^{k+1}(\boldsymbol{\mu}_i)\right\}_{k,i=1}^{I,N}\right)$, $W_N = \operatorname{span}\{\Xi_N\}$
7: $\quad\Psi_N = \text{POD}_N\left(\left\{u_{\mathcal{N}}^k(\boldsymbol{\mu}_i)\right\}_{k=0,i=1}^{I,N}\right)$
8: $\quad\Psi_N = \text{orthonormalize}\,\{\Psi_N, T\Xi_N\}$, $V_N = \operatorname{span}\{\Psi_N\}$
9: **end for**

We use an "enrichment by supremizers" to obtain a stable pair of reduced basis spaces. Note that the algorithm requires given primal and dual initial bases, which, e.g., can be chosen as in Algorithm 4.1, Steps 1–4. Note, the abbreviation $\text{NNMF}_N\left(\{\lambda_{\mathcal{N}}^{k+1}(\boldsymbol{\mu}_i)\}_{k,i=1}^{I,N}\right)$ implies the application of the NNMF procedure (4.6.2) to the snapshot matrix, consisting of the coefficient vectors of $\lambda_{\mathcal{N}}^{k+1}(\boldsymbol{\mu})$, $\boldsymbol{\mu} \in \mathcal{P}$, $k \in \mathbb{I}$. That is, if $\boldsymbol{\lambda}^k(\boldsymbol{\mu}) := \left(\lambda_{\mathcal{N},i}^k(\boldsymbol{\mu})\right)_{i=1}^{\mathcal{N}_W}$ denotes the coefficient vector of $\lambda_{\mathcal{N}}^k(\boldsymbol{\mu})$, the snapshot matrix $\mathbf{X}$ is defined as

$$\mathbf{X} := \left[\boldsymbol{\lambda}^1(\boldsymbol{\mu}_1), \dots, \boldsymbol{\lambda}^I(\boldsymbol{\mu}_1), \dots, \boldsymbol{\lambda}^1(\boldsymbol{\mu}_N), \dots, \boldsymbol{\lambda}^I(\boldsymbol{\mu}_N)\right] \in \mathbb{R}^{\mathcal{N} \times (IN)}, \quad N \leq N_{\max}.$$

4.7 Implementation Aspects

In this section we present a method to solve the reduced problem (4.4.3). We describe several steps of the efficient offline-online computation procedure for the reduced solutions as well as the solver for the reduced system. We highlight the main ingredients for the computation of the a posteriori error bounds and describe an offline- online computational procedure.

4.7.1 Algebraic Saddle Point Formulation

We start by providing the algebraic formulation for the detailed and reduced problems.

Denote by $\mathbf{u}^{k+1}(\boldsymbol{\mu}) \in \mathbb{R}^{\mathcal{N}_V}$, $\boldsymbol{\lambda}^{k+1}(\boldsymbol{\mu}) \in \mathbb{R}^{\mathcal{N}_W}$ the coefficient vectors of the detailed solutions $u_{\mathcal{N}}^{k+1}(\boldsymbol{\mu}) \in V_{\mathcal{N}}$ and $\lambda_{\mathcal{N}}^{k+1}(\boldsymbol{\mu}) \in M_{\mathcal{N}}$, $k \in \mathbb{I}$, $\boldsymbol{\mu} \in \mathcal{P}$. Introduce the following high-fidelity matrices and vectors:

$$\mathbf{M} := \Big((\phi_j, \phi_i)_{L^2(\Omega)}\Big)_{i,j=1}^{\mathcal{N}_V}, \qquad \mathbf{A}(\boldsymbol{\mu}) := (a(\phi_j, \phi_i; \boldsymbol{\mu}))_{i,j=1}^{\mathcal{N}_V}, \quad \mathbf{B} := (b(\chi_j, \phi_i))_{i,j=1}^{\mathcal{N}_V, \mathcal{N}_W},$$
$$\mathbf{f}^{k+\theta}(\boldsymbol{\mu}) := \Big(f^{k+\theta}(\phi_i; \boldsymbol{\mu})\Big)_{i=1}^{\mathcal{N}_V}, \quad \mathbf{g}^{k+1}(\boldsymbol{\mu}) := \Big(g^{k+1}(\chi_i; \boldsymbol{\mu})\Big)_{i=1}^{\mathcal{N}_W}.$$

Note, if χ_j are the biorthogonal basis functions, the matrix $\mathbf{B}$ is a diagonal matrix or an identity after suitable rescaling of the basis functions. For $\tau \in \{\theta, (1-\theta)\}$, where $\theta \in [1/2, 1]$, we denote

$$\mathbf{S}^{\tau}(\boldsymbol{\mu}) := \frac{1}{\Delta t}\mathbf{M} + \tau \mathbf{A}(\boldsymbol{\mu}).$$

Then the algebraic form of the detailed saddle point problem (4.3.16) reads as follows.

Problem 4.7.1 (Algebraic detailed saddle point problem)**.** *For a given $\boldsymbol{\mu} \in \mathcal{P}$, $\theta \in [1/2, 1]$, to find a detailed pair of solutions $(u_{\mathcal{N}}^{k+1}(\boldsymbol{\mu}), \lambda_{\mathcal{N}}^{k+1}(\boldsymbol{\mu})) \in V_{\mathcal{N}} \times M_{\mathcal{N}}$ with the corresponding coefficient vectors $(\mathbf{u}^{k+1}(\boldsymbol{\mu}), \boldsymbol{\lambda}^{k+1}(\boldsymbol{\mu})) \in \mathbb{R}^{\mathcal{N}_V} \times \mathbb{R}^{\mathcal{N}_W}$, $k \in \mathbb{I}$, we need to solve the system of inequalities*

$$\mathbf{S}^{\theta}(\boldsymbol{\mu})\mathbf{u}^{k+1}(\boldsymbol{\mu}) - \mathbf{B}\boldsymbol{\lambda}^{k+1}(\boldsymbol{\mu}) = \mathbf{S}^{\theta-1}(\boldsymbol{\mu})\mathbf{u}^{k}(\boldsymbol{\mu}) + \mathbf{f}^{k+\theta}(\boldsymbol{\mu}), \tag{4.7.1a}$$
$$\boldsymbol{\lambda}^{k+1}(\boldsymbol{\mu}) \geq 0, \tag{4.7.1b}$$
$$\mathbf{B}^T\mathbf{u}^{k+1}(\boldsymbol{\mu}) - \mathbf{g}^{k+1}(\boldsymbol{\mu}) \geq 0, \tag{4.7.1c}$$
$$\Big(\boldsymbol{\lambda}^{k+1}(\boldsymbol{\mu})\Big)^T \Big(\mathbf{B}^T\mathbf{u}^{k+1}(\boldsymbol{\mu}) - \mathbf{g}^{k+1}(\boldsymbol{\mu})\Big) = 0. \tag{4.7.1d}$$

The equivalent representation (4.7.1b)–(4.7.1d) of the variational inequality is often referred to as a complementarity problem (CP) in the literature, see, e.g., [FP03].

Similarly, for the reduced problem, denote by $\mathbf{u}_N^{k+1}(\boldsymbol{\mu}) \in \mathbb{R}^{N_V}$, $\boldsymbol{\lambda}_N^{k+1}(\boldsymbol{\mu}) \in \mathbb{R}^{N_W}$ the coefficient vectors of the reduced solutions $u_N^{k+1}(\boldsymbol{\mu}) = \sum_{j=1}^{N_V} u_{N,j}\psi_j \in V_N$ and $\lambda_N^{k+1}(\boldsymbol{\mu}) = \sum_{j=1}^{N_W} \lambda_{N,j}\xi_j \in M_N$, $k \in \mathbb{I}$, $\boldsymbol{\mu} \in \mathcal{P}$. Define the following reduced basis matrices and vectors

$$\mathbf{M}_N := \Big((\psi_j, \psi_i)_{L^2(\Omega)}\Big)_{i,j=1}^{N_V}, \ \mathbf{A}_N(\boldsymbol{\mu}) := (a(\psi_j, \psi_i; \boldsymbol{\mu}))_{i,j=1}^{N_V}, \ \mathbf{B}_N := (b(\xi_j, \psi_i))_{i,j=1}^{N_V, N_W},$$
$$\mathbf{f}_N^{k+\theta}(\boldsymbol{\mu}) := \Big(f^{k+\theta}(\psi_i; \boldsymbol{\mu})\Big)_{i=1}^{N_V}, \quad \mathbf{g}_N^{k+1}(\boldsymbol{\mu}) := \Big(g^{k+1}(\xi_i; \boldsymbol{\mu})\Big)_{i=1}^{N_W}.$$

As previously, for $\tau \in \{\theta, (1-\theta)\}$, $\theta \in [1/2, 1]$, we introduce the reduced basis matrix

$$\mathbf{S}_N^{\tau}(\boldsymbol{\mu}) := \frac{1}{\Delta t}\mathbf{M}_N + \tau \mathbf{A}_N(\boldsymbol{\mu}).$$

Then, in the algebraic form the reduced basis saddle point problem (4.4.3) can be stated as follows.

Problem 4.7.2 (Algebraic reduced saddle point problem)**.** *For a given $\boldsymbol{\mu} \in \mathcal{P}$, $\theta \in [1/2, 1]$, to find a reduced pair of solutions $(u_N^{k+1}(\boldsymbol{\mu}), \lambda_N^{k+1}(\boldsymbol{\mu})) \in V_N \times M_N$ with the corresponding coefficient vectors $(\mathbf{u}_N^{k+1}(\boldsymbol{\mu}), \boldsymbol{\lambda}_N^{k+1}(\boldsymbol{\mu})) \in \mathbb{R}^{\mathcal{N}} \times \mathbb{R}^{\mathcal{N}}$, $k \in \mathbb{I}$, is equivalent to solve the following system of inequalities*

$$\mathbf{S}_N^{\theta}(\boldsymbol{\mu})\mathbf{u}_N^{k+1}(\boldsymbol{\mu}) - \mathbf{B}_N\boldsymbol{\lambda}_N^{k+1}(\boldsymbol{\mu}) = \mathbf{S}_N^{\theta-1}(\boldsymbol{\mu})\mathbf{u}_N^{k}(\boldsymbol{\mu}) + \mathbf{f}_N^{k+\theta}(\boldsymbol{\mu}), \tag{4.7.2a}$$
$$\boldsymbol{\lambda}_N^{k+1}(\boldsymbol{\mu}) \geq 0, \tag{4.7.2b}$$
$$\mathbf{B}_N^T\mathbf{u}_N^{k+1}(\boldsymbol{\mu}) - \mathbf{g}_N^{k+1}(\boldsymbol{\mu}) \geq 0, \tag{4.7.2c}$$
$$\Big(\boldsymbol{\lambda}_N^{k+1}(\boldsymbol{\mu})\Big)^T \Big(\mathbf{B}_N^T\mathbf{u}_N^{k+1}(\boldsymbol{\mu}) - \mathbf{g}_N^{k+1}(\boldsymbol{\mu})\Big) = 0, \tag{4.7.2d}$$

where $\mathbf{u}_N^0(\boldsymbol{\mu}) \in \mathbb{R}^{N_V}$ is obtained by solving $((u_N^0(\boldsymbol{\mu}) - u_{\mathcal{N}}^0(\boldsymbol{\mu}), \psi_p)_V)_{p=1}^{N_V} = 0$ (see Section 3.4.4).

4.7.2 Solution Algorithm

In this section we comment on the solution algorithm for the detailed and reduced problems. The approach is based on the Primal-Dual-Active-Set strategy (PDAS), see [HHW10; HIK02], and its adapted version for the reduced problem, see [BHS+15]. The PDAS algorithm is equivalent to a semi-smooth Newton method, which converges locally superlinearly; see for more details [HIK02].

Detailed problem

For generic coefficient vectors $\mathbf{U}, \boldsymbol{\Lambda} \in \mathbb{R}^n$, $n > 0$, we introduce a non-differentiable complementarity function $\mathcal{C}$, defined as follows, [FP03; HIK02],

$$\mathcal{C}(\mathbf{U}, \boldsymbol{\Lambda}) := \boldsymbol{\Lambda} - \max(0, \boldsymbol{\Lambda} + c\mathbf{U}), \tag{4.7.3}$$

where the max operation is understood pointwise with some arbitrary $c > 0$. For other choices of the NCP function $\mathcal{C}(\cdot,\cdot)$; see [FP03].

Then we reformulate the system of inequality constrains (4.7.1b)–(4.7.1d) as a non-linear system of equations or, as often referred to, a non-linear complementarity problem (NCP). We require:

$$\mathbf{S}^{\theta}(\boldsymbol{\mu})\mathbf{u}^{k+1}(\boldsymbol{\mu}) - \mathbf{B}\boldsymbol{\lambda}^{k+1}(\boldsymbol{\mu}) = \mathbf{S}^{\theta-1}(\boldsymbol{\mu})\mathbf{u}^{k}(\boldsymbol{\mu}) + \mathbf{f}^{k+\theta}(\boldsymbol{\mu}), \tag{4.7.4a}$$

$$\mathcal{C}(\mathbf{g}^{k+1}(\boldsymbol{\mu}) - \mathbf{B}^{T}\mathbf{u}^{k+1}(\boldsymbol{\mu}), \boldsymbol{\lambda}^{k+1}(\boldsymbol{\mu})) = 0. \tag{4.7.4b}$$

To solve (4.7.4), we employ a primal-dual active set strategy, [HIK02], which is described in Algorithm 4.3.

Algorithm 4.3 Primal-Dual Active Set Strategy for the Detailed Problem

Input: Initial condition $(\mathbf{u}^0, \boldsymbol{\lambda}^0)$, e.g., $\boldsymbol{\lambda}^0 = 0$, number of time steps I
Output: Detailed solution trajectory $(\mathbf{u}^{k+1}, \boldsymbol{\lambda}^{k+1})$, for all $k \in \mathbb{I}$

1: **for** $k = 0, \ldots, I-1$ **do**
2: set $(\mathbf{u}^{k+1,0}, \boldsymbol{\lambda}^{k+1,0}) = (\mathbf{u}^{k}, \boldsymbol{\lambda}^{k})$
3: **for** $m = 0, \ldots$ **do**
4: update the active $\mathcal{A}_m$ and inactive $\mathcal{I}_m$ sets

$$\mathcal{A}_m := \mathcal{A}(\mathbf{g}^{k+1} - \mathbf{B}^{T}\mathbf{u}^{k+1,m}, \boldsymbol{\lambda}^{k+1,m}),$$
$$\mathcal{I}_m := \mathcal{I}(\mathbf{g}^{k+1} - \mathbf{B}^{T}\mathbf{u}^{k+1,m}, \boldsymbol{\lambda}^{k+1,m})$$

5: **if** $m \geq 1$ and $\mathcal{A}_m = \mathcal{A}_{m-1}$ and $\mathcal{I}_m = \mathcal{I}_{m-1}$ **then**
6: $(\mathbf{u}^{k+1}, \boldsymbol{\lambda}^{k+1}) = (\mathbf{u}^{k+1,m}, \boldsymbol{\lambda}^{k+1,m})$ and go to Step 9
7: **end if**
8: compute $(\mathbf{u}^{k+1,m+1}, \boldsymbol{\lambda}^{k+1,m+1})$ by solving

$$\begin{aligned} \mathbf{S}^{\theta}\mathbf{u}^{k+1,m+1} - \mathbf{B}\boldsymbol{\lambda}^{k+1,m+1} &= \mathbf{S}^{\theta-1}\mathbf{u}^{k} + \mathbf{f}^{k+\theta} \\ \mathbf{B}^{T}\mathbf{u}^{k+1,m+1} &= \mathbf{g}^{k+1}, && \text{on} \quad \mathcal{A}_m \\ \boldsymbol{\lambda}^{k+1,m+1} &= 0, && \text{on} \quad \mathcal{I}_m. \end{aligned}$$

9: **end for**
10: **end for**

For generic coefficient vectors $\mathbf{U}, \boldsymbol{\Lambda} \in \mathbb{R}^n$, $n > 0$, the functions $\mathcal{A}$ and $\mathcal{I}$, which are used to update the active and inactive sets, are defined as follows:

$$\mathcal{A}(\mathbf{U}, \boldsymbol{\Lambda}) = \{i : \ 1 \leq i \leq n, \ (\boldsymbol{\Lambda} + c\mathbf{U})_i \geq 0\},$$
$$\mathcal{I}(\mathbf{U}, \boldsymbol{\Lambda}) = \{i : \ 1 \leq i \leq n, \ (\boldsymbol{\Lambda} + c\mathbf{U})_i < 0\}.$$

Reduced Problem

Analogously, we can rewrite the system of reduced complementarity inequalities (4.7.2) as a non-linear complementarity equation.

$$\mathbf{S}_N^{\theta}(\boldsymbol{\mu})\mathbf{u}_N^{k+1}(\boldsymbol{\mu}) - \mathbf{B}_N\boldsymbol{\lambda}_N^{k+1}(\boldsymbol{\mu}) = \mathbf{S}_N^{\theta-1}\mathbf{u}_N^{k}(\boldsymbol{\mu}) + \mathbf{f}_N^{k+\theta}(\boldsymbol{\mu}), \tag{4.7.5a}$$

$$\mathcal{C}(\mathbf{g}_N^{k+1}(\boldsymbol{\mu}) - \mathbf{B}_N^T\mathbf{u}_N^{k+1}(\boldsymbol{\mu}), \boldsymbol{\lambda}_N^{k+1}(\boldsymbol{\mu})) = 0. \tag{4.7.5b}$$

To solve the reduced system (4.7.5), we adapt Algorithm 4.3 to the reduced system, which comprises Algorithm 4.4.

Algorithm 4.4 Primal-Dual Active Set Strategy for the Reduced Problem

Input: Initial condition $(\mathbf{u}_N^0, \boldsymbol{\lambda}_N^0)$, e.g., $\boldsymbol{\lambda}_N^0 = 0$, number of time steps I
Output: Reduced solution trajectory $(\mathbf{u}_N^{k+1}, \boldsymbol{\lambda}_N^{k+1})$, for all $k \in \mathbb{I}$

1: **for** $k = 0, \dots, I-1$ **do**
2: set $(\mathbf{u}_N^{k+1,0}, \boldsymbol{\lambda}_N^{k+1,0}) = (\mathbf{u}_N^k, \boldsymbol{\lambda}_N^k)$
3: **for** $m = 0, \dots$ **do**
4: update the active $\mathcal{A}_m$ and inactive $\mathcal{I}_m$ sets

$$\mathcal{A}_m := \mathcal{A}(\mathbf{g}_N^{k+1} - \mathbf{B}_N^T\mathbf{u}_N^{k+1,m}, \boldsymbol{\lambda}_N^{k+1,m}),$$
$$\mathcal{I}_m := \mathcal{I}(\mathbf{g}_N^{k+1} - \mathbf{B}_N^T\mathbf{u}_N^{k+1,m}, \boldsymbol{\lambda}_N^{k+1,m})$$

5: **if** $m \geq 1$ and $\mathcal{A}_m = \mathcal{A}_{m-1}$ and $\mathcal{I}_m = \mathcal{I}_{m-1}$ **then**
6: $(\mathbf{u}_N^{k+1}, \boldsymbol{\lambda}_N^{k+1}) = (\mathbf{u}_N^{k+1,m}, \boldsymbol{\lambda}_N^{k+1,m})$ and go to Step 9
7: **end if**
8: compute $(\mathbf{u}_N^{k+1,m+1}, \boldsymbol{\lambda}_N^{k+1,m+1})$ by solving

$$\begin{aligned} \mathbf{S}_N^{\theta}\mathbf{u}_N^{k+1,m+1} - \mathbf{B}_N\boldsymbol{\lambda}_N^{k+1,m+1} &= \mathbf{S}_N^{\theta-1}\mathbf{u}_N^k + \mathbf{f}_N^{k+\theta} \\ \mathbf{B}_N^T\mathbf{u}_N^{k+1,m+1} &= \mathbf{g}_N^{k+1}, && \text{on} \quad \mathcal{A}_m \\ \boldsymbol{\lambda}_N^{k+1,m+1} &= 0, && \text{on} \quad \mathcal{I}_m. \end{aligned}$$

9: **end for**
10: **end for**

We comment on the difference between Algorithm 4.3 and Algorithm 4.4. As mentioned before, by an appropriate choice of the dual basis, the matrix $\mathbf{B}$ in (4.7.1) can be an identity matrix. Consequently, the algebraic detailed saddle point problem in Step 8 in Algorithm 4.3 can be simplified to a system of linear equations on the inactive set. By contrast, for the reduced problem the matrix $\mathbf{B}_N$ is full and not diagonal, which does not allow to perform similar simplification for solving the algebraic reduced saddle point problem (Step 8 in Algorithm 4.4).

4.7.3 Offline-Online Computational Procedure

In this section we comment on the efficient offline-online computational procedure for solving the reduced saddle point problem. Since the steps are very similar to those outlined in Section 3.4.4, to avoid redundancy, we provide only a brief explanation.

The same as before, we require an assumption of affine parameter dependence of the parameter dependent bilinear and linear forms. That is, there exist $\Theta_q^a : \mathcal{P} \to \mathbb{R}$, $\Theta_q^{f,k} : \mathcal{P} \to \mathbb{R}$, such that, for all $v \in V$, $\boldsymbol{\mu} \in \mathcal{P}$,

$$a(u, v; \boldsymbol{\mu}) = \sum_{q=1}^{Q_a} \Theta_q^a(\boldsymbol{\mu}) a_q(u, v), \quad f^k(v; \boldsymbol{\mu}) = \sum_{q=1}^{Q_f} \Theta_q^{f,k}(\boldsymbol{\mu}) f_q^k(v).$$

In addition, we assume an affine parameter dependence of the obstacle functional, i.e, there exist $\Theta_q^{g,k} : \mathcal{P} \to \mathbb{R}$, such that for all $\eta \in W$, $\boldsymbol{\mu} \in \mathcal{P}$,

$$g^k(\eta; \boldsymbol{\mu}) = \sum_{q=1}^{Q_g} \Theta_q^{g,k}(\boldsymbol{\mu}) g_q^k(\eta).$$

Note that the bilinear form $b(\cdot, \cdot)$ in (4.4.3) is parameter independent. The computation of the initial condition $u_N^0(\boldsymbol{\mu})$ follows the same routine as in Section 3.4.4, and we will omit its representation here.

Using these assumptions, the offline-online procedure for Problem 4.7.2 can be summarized as follows. In the offline stage we compute all parameter independent matrices and vectors,

$$\begin{aligned}
\mathbf{M}_N &:= \Big((\psi_j, \psi_i)_{L^2(\Omega)}\Big)_{i,j=1}^{N_V} \in \mathbb{R}^{N_V \times N_V}, & \mathbf{f}_{N,q}^k &:= \Big(f_q^k(\psi_i)\Big)_{i=1}^{N_V} \in \mathbb{R}^{N_V}, \\
\mathbf{A}_{N,q} &:= (a_q(\psi_j, \psi_i))_{i,j=1}^{N_V} \in \mathbb{R}^{N_V \times N_V}, & \mathbf{g}_{N,q}^k &:= \Big(g_q^k(\xi_i)\Big)_{i=1}^{N_W} \in \mathbb{R}^{N_W}, \\
\mathbf{B}_N &:= (b(\xi_j, \psi_i))_{i,j=1}^{N_V, N_W} \in \mathbb{R}^{N_V \times N_W}.
\end{aligned}$$

Then for a given $\boldsymbol{\mu} \in \mathcal{P}$, we perform an online routine, where we assemble all parameter dependent matrices and vectors and solve the reduced problem (4.7.2) using, e.g., Algorithm 4.4,

$$\mathbf{A}_N(\boldsymbol{\mu}) = \sum_{q=1}^{Q_a} \Theta_q^a(\boldsymbol{\mu}) \mathbf{A}_{N,q}, \quad \mathbf{f}_N^k(\boldsymbol{\mu}) = \sum_{q=1}^{Q_f} \Theta_q^{f,k}(\boldsymbol{\mu}) \mathbf{f}_{N,q}^k, \quad \mathbf{g}_N^k(\boldsymbol{\mu}) = \sum_{q=1}^{Q_g} \Theta_q^{g,k}(\boldsymbol{\mu}) \mathbf{g}_{N,q}^k.$$

Using the conformity of the reduced spaces, we can expand the reduced basis functions ψ_j, ξ_j, with respect to the basis functions of $V_\mathcal{N}$ and $W_\mathcal{N}$. That is, $\psi_j = \sum_{i=1}^{\mathcal{N}_V} \psi_{j,i} \phi_i$, $\xi_j = \sum_{i=1}^{\mathcal{N}_W} \xi_{j,i} \chi_i$. Denote by $\boldsymbol{\Psi}_N$ and $\boldsymbol{\Xi}_N$ the transformation matrices for the primal and dual bases respectively,

$$\boldsymbol{\Psi}_N = (\psi_{i,j})_{i,j=1}^{\mathcal{N}_V, N_V} \in \mathbb{R}^{\mathcal{N}_V \times N_V}, \quad \boldsymbol{\Xi}_N = (\xi_{i,j})_{i,j=1}^{\mathcal{N}_W, N_V} \in \mathbb{R}^{\mathcal{N}_W \times N_W}. \tag{4.7.6}$$

Then the reduced matrices and vectors, can be represented via the high-fidelity ones,

$$\mathbf{M}_N = \mathbf{\Psi}_N^T \mathbf{M} \mathbf{\Psi}_N, \quad \mathbf{A}_{N,g} = \mathbf{\Psi}_N^T \mathbf{A}_q \mathbf{\Psi}_N, \quad \mathbf{B}_N = \mathbf{\Psi}_N^T \mathbf{B} \mathbf{\Xi}_N,$$
$$\mathbf{f}_{N,q}^k = \mathbf{\Psi}_N^T \mathbf{f}_{N,q}^k, \qquad \mathbf{g}_{N,q}^k = \mathbf{\Xi}_N^T \mathbf{g}_{N,q}^k.$$

Note that for our computations we require an evaluation of $f^{k+\theta}(\boldsymbol{\mu})$ instead of $f^k(\boldsymbol{\mu})$. We refer to Section 3.4.4 where it has been discussed in detail.

Let us comment on the affine parameter dependence for the particular case of the Black-Scholes or Heston models. For both models, as it was shown in Section 3.4.4, the bilinear and linear forms admit an affine decomposition. An affine decomposition of the linear forms $f^k(\cdot;\boldsymbol{\mu})$, $g^k(\cdot;\boldsymbol{\mu})$ depends on the affine decomposition of the boundary data and an obstacle functional. Note that in the present case these quantities are parameter-independent, cf. (4.2.2).

4.7.4 A Posteriori Estimates

In this section we comment on the computational procedure of the a posteriori error bounds presented in Section 4.5. We remark, that in contrast to the RBM for linear problems, a posteriori error bounds for variational inequalities involve the computation of the non-linear projection, which admits only a partial offline-online decomposition.

Recall, that the discrete spaces $V_\mathcal{N}$ and $W_\mathcal{N}$ can be written in terms of their bases,

$$V_\mathcal{N} = \operatorname{span}\{\phi_p,\ p = 1, \dots, \mathcal{N}_V\}, \quad W_\mathcal{N} = \operatorname{span}\{\chi_q,\ q = 1, \dots, \mathcal{N}_W\}.$$

As before, for all $\boldsymbol{\mu} \in \mathcal{P}$, $k \in \mathbb{I}$, let $\mathbf{u}_N^{k+1}(\boldsymbol{\mu})$, $\boldsymbol{\lambda}_N^{k+1}(\boldsymbol{\mu})$ be the coefficient vectors of $u_N^{k+1}(\boldsymbol{\mu})$ and $\lambda_N^{k+1}(\boldsymbol{\mu})$ respectively.

Denote by $\boldsymbol{\eta}, \boldsymbol{\eta}' \in \mathbb{R}^{\mathcal{N}_W}$ and $\mathbf{v}, \mathbf{v}' \in \mathbb{R}^{\mathcal{N}_V}$ the coefficient vectors of $\eta, \eta' \in W_\mathcal{N}$ and $v, v' \in V_\mathcal{N}$, respectively. The computation of a posteriori quantities requires the evaluation of the inner products on $V_\mathcal{N}$ and $W_\mathcal{N}$, i.e.,

$$(v, v')_V = \mathbf{v}^T \mathbf{M}_V \mathbf{v}', \qquad (\eta, \eta')_W = \boldsymbol{\eta}^T \mathbf{M}_W \boldsymbol{\eta}', \tag{4.7.7}$$

with inner product matrices $\mathbf{M}_V$ and $\mathbf{M}_W$,

$$\mathbf{M}_V := ((\phi_i, \phi_j)_V)_{i,j=1}^{\mathcal{N}_V}, \quad \mathbf{M}_W := ((\chi_i, \chi_j)_W)_{i,j=1}^{\mathcal{N}_W}. \tag{4.7.8}$$

In some cases, the primal and dual inner product matrices can be related, see, e.g., [HSW11, Appendix A.2], which is stated in the following proposition.

Proposition 4.7.1. *If $W = V'$ and taking the dual basis functions for $W_\mathcal{N}$ we have that $\mathbf{M}_W = \mathbf{M}_V^{-1}$. Moreover, if $\mathbf{M}_V$ is an M-matrix, then for all $\eta, \eta' \in M_\mathcal{N}$, one obtains the additional property*

$$(\eta, \eta')_W \geq 0. \tag{4.7.9}$$

Proof. By taking the dual basis functions on the same mesh as primal ones, one has $\mathcal{N}_V = \mathcal{N}_W = \mathcal{N}$. Recall, that for $\eta \in W_\mathcal{N}$, by the Riesz representation theorem, there exist an element $\hat{\eta} \in V_\mathcal{N}$, such that for all $v \in V_\mathcal{N}$, $(\hat{\eta}, v)_V = \eta(v)$. Let $\hat{\boldsymbol{\eta}}$ be the coefficient vector of $\hat{\eta}$, then

$$(\hat{\eta}, v)_V = \hat{\boldsymbol{\eta}}^T \mathbf{M}_V \mathbf{v} = \boldsymbol{\eta}^T \mathbf{v},$$

and hence $\hat{\boldsymbol{\eta}} = \mathbf{M}_V^{-1}\boldsymbol{\eta}$. Then for $\eta, \eta' \in W_\mathcal{N}$,

$$\boldsymbol{\eta}^T \mathbf{M}_W \boldsymbol{\eta}' = (\eta, \eta')_W = (\hat{\eta}, \hat{\eta}')_V = \hat{\boldsymbol{\eta}}^T \mathbf{M}_V \hat{\boldsymbol{\eta}}' = (\mathbf{M}_V^{-1}\boldsymbol{\eta})^T \mathbf{M}_V (\mathbf{M}_V^{-1}\boldsymbol{\eta}') = \boldsymbol{\eta}^T \mathbf{M}_V^{-1} \boldsymbol{\eta}'.$$

If $\mathbf{M}_V$ is an M-matrix, that is, the matrix with positive diagonal and negative off-diagonal elements, then its inverse, $\mathbf{M}_V^{-1}$, has positive entries. Then choosing $\eta, \eta' \in M_\mathcal{N}$, by the definition of $M_\mathcal{N}$, we have $\boldsymbol{\eta}, \boldsymbol{\eta}' \geq 0$ and (4.7.9) follows directly. □

Remark 4.7.1. *For some cases, e.g., for the finite element formulation of the Laplace operator on a triangular mesh with "well-shaped" elements, one obtains an M-matrix [Ber03]. "Well-shaped" means, that the sum of two angles, which are opposite to each interior edge, should be not more than* 180°.

Computation of the Equality Residual Norm

In this section we discuss the computational procedure for the a posteriori error bounds. For simplicity of representation, in this section we restrict our consideration to the case of the implicit Euler time-stepping scheme, i.e., $\theta = 1$.

The computation of the error bounds involves the computation of the norm of the equality residual $\delta_r^{k+1} := \|r^{k+1}(\boldsymbol{\mu})\|_{V'}$, defined in (4.5.12a). We comment on the procedure, which allows to perform this computation in the offline-online manner.

Using affine parameter dependence of the bilinear and linear forms, the residual (4.5.1) can be written as follows

$$\begin{aligned} r^{k+1}(v;\boldsymbol{\mu}) :=& \frac{1}{\Delta t}\sum_{i=1}^{N_V}(u_{N,i}^{k+1}(\boldsymbol{\mu}) - u_{N,i}^{k}(\boldsymbol{\mu}))(\psi_i, v)_{L^2(\Omega)} + \sum_{q=1}^{Q_a}\sum_{i=1}^{N_V}\Theta_q^a(\boldsymbol{\mu})u_{N,i}^{k+1}(\boldsymbol{\mu})a_q(\psi_i, v) \\ &- \sum_{i=1}^{N_W}\lambda_{N,i}^{k+1}(\boldsymbol{\mu})b(\xi_i, v) - \sum_{q=1}^{Q_f}\Theta_q^{f,k+1}(\boldsymbol{\mu})f_q^{k+1}(v), \qquad v \in V_\mathcal{N}. \end{aligned}$$

Introduce the coefficient vector with $Q_r = N_V + Q_a N_V + N_W + Q_f$ components,

$$\begin{aligned} &\boldsymbol{\Theta}^{r,k+1}(\boldsymbol{\mu}) := \left(\Theta_1^{r,k+1}(\boldsymbol{\mu}), \ldots, \Theta_{Q_r}^{r,k+1}(\boldsymbol{\mu})\right)^T \\ &:= \left(\frac{1}{\Delta t}(\mathbf{u}_N^{k+1} - \mathbf{u}_N^k)^T, (\mathbf{u}_N^{k+1})^T\Theta_1^a, \ldots, (\mathbf{u}_N^{k+1})^T\Theta_{Q_a}^a, -(\boldsymbol{\lambda}_N^{k+1})^T, -\Theta_1^{f,k+1}, \ldots, -\Theta_{Q_f}^{f,k+1}\right)^T. \end{aligned}$$

Following a similar ordering we define

$$\begin{aligned}\Big(r_1^{k+1}(\cdot),\dots,r_{Q_r}^{k+1}(\cdot)\Big)^T :=\Big((\psi_1,\cdot)_{L^2(\Omega)},\dots,(\psi_{N_V},\cdot)_{L^2(\Omega)},\dots\\ a_1(\psi_1,\cdot),\dots,a_1(\psi_{N_V},\cdot),\dots,a_{Q_a}(\psi_1,\cdot),\dots,a_{Q_a}(\psi_{N_V},\cdot),\dots\\ b(\xi_1,\cdot),\dots,b(\xi_{N_W},\cdot),f_1^{k+1}(\cdot),\dots,f_{Q_f}^{k+1}(\cdot)\Big)^T.\end{aligned}$$

It follows, that the residual admits an affine decomposition, i.e.,

$$r^{k+1}(v;\boldsymbol{\mu}) = \sum_{q=1}^{Q_r} \Theta_q^{r,k+1} r_q^{k+1}(v).$$

Denote by $\hat{r}_q^{k+1}$ the Riesz representer of r_q^{k+1}, i.e, $r_q^{k+1}(v) = (v,\hat{r}_q^{k+1})_V$, then we obtain

$$(v,\hat{r}^{k+1}(\boldsymbol{\mu}))_V = r^{k+1}(v;\boldsymbol{\mu}) = \sum_{q=1}^{Q_r} \Theta_q^{r,k+1}(\boldsymbol{\mu}) r_q^{k+1}(v) = \sum_{q=1}^{Q_r} \Theta_q^{r,k+1}(\boldsymbol{\mu})(v,\hat{r}_q^{k+1})_V, \tag{4.7.10}$$

hence, we recover the affine decomposition of the Riesz representer,

$$\hat{r}^{k+1}(\boldsymbol{\mu}) = \sum_{q=1}^{Q_r} \Theta_q^{r,k+1}(\boldsymbol{\mu})\hat{r}_q^{k+1}.$$

Then the computation of the norm of the residual leads to the computation

$$\|r^{k+1}(\boldsymbol{\mu})\|_{V'}^2 = \sum_{q=1}^{Q_r}\sum_{q'=1}^{Q_r} \Theta_q^{r,k+1}(\boldsymbol{\mu})(\hat{r}_q^{k+1},\hat{r}_{q'}^{k+1})_V,$$

or in matrix form

$$\|r^{k+1}(\boldsymbol{\mu})\|_{V'}^2 = (\boldsymbol{\Theta}^{r,k+1}(\boldsymbol{\mu}))^T \mathbf{G}_r^{k+1} \boldsymbol{\Theta}^{r,k+1}(\boldsymbol{\mu}), \tag{4.7.11}$$

where $\mathbf{G}_r^{k+1} := \Big((\hat{r}_q^{k+1},\hat{r}_{q'}^{k+1})_V\Big)_{q,q'=1}^{Q_r} \in \mathbb{R}^{Q_r\times Q_r}$. Then an offline-online procedure looks as follows: in the offline stage, for each $k\in\mathbb{I}$, we compute the Gramian matrix $\mathbf{G}_r^k$ with the cost $\mathcal{O}(IQ_rN_V^2+IQ_r^2N_V)$. In the parameter dependent online routine, we evaluate (4.7.11) for each time step $k\in\mathbb{I}$, with the cost $\mathcal{O}(IQ_r^2)$, which is independent of $\mathcal{N}_V$.

Computation of the Inequality Residual Norm

Next, we describe the computation of the quantities, associated with the inequality residual. Depending on the choice of the projection π^{k+1} or Π^{k+1}, $k \in \mathbb{I}$, we require the evaluation of δ_s^{k+1}, $\widetilde{\delta}_s^{k+1}$, defined in (4.5.12) or (4.5.18), respectively.

We define $\pi^{k+1} : W_{\mathcal{N}} \to \widetilde{M}_{\mathcal{N}}$ as in [BHS+15; HSW11; HSW12],

$$\pi^{k+1}(\eta) = \pi(\eta) = \sum_{i=1}^{\mathcal{N}_W} \pi_i \chi_i, \quad \boldsymbol{\pi} = (\pi_i)_{i=1}^{\mathcal{N}_W} := \mathbf{M}_W^{-1}[\mathbf{M}_W \boldsymbol{\eta}]_+, \tag{4.7.12}$$

where $[\cdot]_+$ denotes the component-wise positive part of the vector. Additionally, to ensure the validity of the assumption (4.5.19), we denote by $\widetilde{\boldsymbol{\lambda}}_N^{k+1}(\boldsymbol{\mu}) \in \mathbb{R}^{\mathcal{N}_W}$, $k \in \mathbb{I}$, $\boldsymbol{\mu} \in \mathcal{P}$, the coefficient vector of the reduced solution $\lambda_N^{k+1}(\boldsymbol{\mu})$ represented in the detailed basis, and define the family of projections π^{k+1} as

$$\pi^{k+1}(\eta) = \sum_{i=1}^{\mathcal{N}_W} \pi_i^{k+1} \chi_i, \quad \boldsymbol{\pi}^{k+1} = (\pi_i^{k+1})_{i=1}^{\mathcal{N}_W} := \mathbf{M}_W^{-1} \left([\mathbf{M}_W \boldsymbol{\eta}]_+ \circ \mathbf{I}_{\{\widetilde{\boldsymbol{\lambda}}_N^{k+1}=0\}} \right). \tag{4.7.13}$$

Here, "$\circ$" denotes the Hadamard product and $\mathbf{I}_{\{\widetilde{\boldsymbol{\lambda}}_N^{k+1}=0\}} = \left(I_{\{\widetilde{\lambda}_{N,i}^{k+1}=0\}} \right)_{i=1}^{\mathcal{N}_W}$ is defined as

$$I_{\{\widetilde{\lambda}_{N,i}^{k+1}=0\}} = \begin{cases} 0 & \text{if } \widetilde{\lambda}_{N,i}^{k+1} \neq 0, \\ 1 & \text{else,} \end{cases} \tag{4.7.14}$$

where $\widetilde{\lambda}_{N,i}^{k+1}$ denotes the i-th component of the vector $\widetilde{\boldsymbol{\lambda}}_N^{k+1}$.

Taking into account that $\hat{\mathbf{s}}^{k+1}(\boldsymbol{\mu}) = \mathbf{M}_W^{-1}\mathbf{s}^{k+1}(\boldsymbol{\mu})$, the error estimators $\delta_s^{k+1}(\boldsymbol{\mu})$, $\widetilde{\delta}_s^{k+1}(\boldsymbol{\mu})$, as in (4.5.12), can be expressed as follows:

$$\begin{aligned}
(\delta_s^{k+1}(\boldsymbol{\mu}))^2 &= \left(\hat{\mathbf{s}}^{k+1}(\boldsymbol{\mu}) - \mathbf{M}_W^{-1}[\mathbf{M}_W \hat{\mathbf{s}}^{k+1}(\boldsymbol{\mu})]_+\right)^T \mathbf{M}_W \left(\hat{\mathbf{s}}^{k+1}(\boldsymbol{\mu}) - \mathbf{M}_W^{-1}[\mathbf{M}_W \hat{\mathbf{s}}^{k+1}(\boldsymbol{\mu})]_+\right) \\
&= \left(\mathbf{M}_W^{-1}\mathbf{s}^{k+1}(\boldsymbol{\mu}) - \mathbf{M}_W^{-1}[\mathbf{s}^{k+1}(\boldsymbol{\mu})]_+\right)^T \mathbf{M}_W \left(\mathbf{M}_W^{-1}\mathbf{s}^{k+1}(\boldsymbol{\mu}) - \mathbf{M}_W^{-1}[\mathbf{s}^{k+1}(\boldsymbol{\mu})]_+\right) \\
&= \left(\mathbf{s}^{k+1}(\boldsymbol{\mu}) - [\mathbf{s}^{k+1}(\boldsymbol{\mu})]_+\right)^T \mathbf{M}_W^{-1} \left(\mathbf{s}^{k+1}(\boldsymbol{\mu}) - [\mathbf{s}^{k+1}(\boldsymbol{\mu})]_+\right). \\
\widetilde{\delta}_s^{k+1}(\boldsymbol{\mu}) &= \left(\widetilde{\boldsymbol{\lambda}}_N^{k+1}(\boldsymbol{\mu})\right)^T \mathbf{M}_W \left(\mathbf{M}_W^{-1}[\mathbf{M}_W \hat{\mathbf{s}}^{k+1}(\boldsymbol{\mu})]_+\right) = \left(\widetilde{\boldsymbol{\lambda}}_N^{k+1}(\boldsymbol{\mu})\right)^T [\mathbf{s}^{k+1}(\boldsymbol{\mu})]_+.
\end{aligned}$$

With the choice of the projection (4.7.13), we directly arrive in the following,

$$\begin{aligned}
(\delta_s^{k+1}(\boldsymbol{\mu}))^2 &= \left(\mathbf{s}^{k+1}(\boldsymbol{\mu}) - [\mathbf{s}^{k+1}(\boldsymbol{\mu})]_+ \circ \mathbf{I}_{\{\widetilde{\boldsymbol{\lambda}}_N^{k+1}=0\}}\right)^T \mathbf{M}_W^{-1} \left(\mathbf{s}^{k+1}(\boldsymbol{\mu}) - [\mathbf{s}^{k+1}(\boldsymbol{\mu})]_+ \circ \mathbf{I}_{\{\widetilde{\boldsymbol{\lambda}}_N^{k+1}=0\}}\right). \\
\widetilde{\delta}_s^{k+1}(\boldsymbol{\mu}) &= \left(\widetilde{\boldsymbol{\lambda}}_N^{k+1}(\boldsymbol{\mu})\right)^T [\mathbf{s}^{k+1}(\boldsymbol{\mu})]_+ \circ \mathbf{I}_{\{\widetilde{\boldsymbol{\lambda}}_N^{k+1}=0\}} = 0.
\end{aligned}$$

Both projections (4.7.12) and (4.7.13) are associated to a similar computational cost, and numerically we did not observe significant differences in the quality of the error estimator with either choice of the projection. Therefore, in the following numerical experiments we focus on the case (4.7.12).

In the specific case $W = V'$ we can base our error estimate on the alternative derivation in Proposition 4.5.3. In this case, we define $\Pi^{k+1} : V_{\mathcal{N}} \to V_{\mathcal{N}}$ as follows:

$$\Pi^{k+1}(v) = \Pi(v) = \sum_{i=1}^{\mathcal{N}_V} \Pi_i \phi_i, \quad \mathbf{\Pi} = (\Pi_i)_{i=1}^{\mathcal{N}_V} := [\mathbf{v}]_+. \tag{4.7.15}$$

Then we directly obtain the following expressions for the quantities (4.5.18):

$$\begin{aligned}(\delta_s^{k+1}(\boldsymbol{\mu}))^2 &= \left(\mathbf{s}^{k+1}(\boldsymbol{\mu}) - [\mathbf{s}^{k+1}(\boldsymbol{\mu})]_+\right)^T \mathbf{M}_V \left(\mathbf{s}^{k+1}(\boldsymbol{\mu}) - [\mathbf{s}^{k+1}(\boldsymbol{\mu})]_+\right). \\ \widetilde{\delta}_s^{k+1}(\boldsymbol{\mu}) &= \left(\widetilde{\boldsymbol{\lambda}}_N^{k+1}(\boldsymbol{\mu})\right)^T [\mathbf{s}^{k+1}(\boldsymbol{\mu})]_+.\end{aligned}$$

Assuming that dual basis functions are employed, we have that $\mathbf{M}_V = \mathbf{M}_W^{-1}$; see Proposition 4.7.1. Comparing now the estimator quantities derived with the projections (4.7.12) and (4.7.15), we observe that in both cases we obtain an equivalent result. This provides an approach with a simpler derivation in this specific setting.

In contrast to the offline-online decomposition of the equality residual norm, we can observe that the computation of the inequality residual norm is not offline-online decomposable. The online computation remain dependent on the dimension of a high-fidelity problem $\mathcal{N}_W$. However, since the evaluation of the specific choice of π^{k+1} requires only a coordinate-wise application of the max function and a multiplication with $\mathbf{M}_V$ (no "solution" operation), the computational cost of this operation is very low. Alternatively, one may treat inequality constraints by the primal-dual approach by introducing an auxiliary dual (or slack) variable, see [ZBV16]. The advantage of this transformation is the possibility of obtaining a fully offline-online decomposable error bounds. However, this approach imposes additional restrictions and requires a solution of a supplementary reduced basis problem.

4.8 Numerical Results

For our numerical simulation we chose $X = H^1(\Omega)$, $V = H^1_{\Gamma_\mathrm{D}} = \{v \in X : v|_{\Gamma_\mathrm{D}} = 0\}$ with $\|\cdot\|_V = |\cdot|_{H^1}$, and $W = V'$. The polygonal domain $\Omega \subset \mathbb{R}^d$, $d = 1, 2$, is resolved by a triangulation $\mathcal{T}_{\mathcal{N}}$, consisting of J simplices $T_{\mathcal{N}}^j$, $j = 1, \ldots, J$. The discrete spaces are defined as in Chapter 3, that is,

$$X_{\mathcal{N}} := \{v \in X : \quad v_{|T_{\mathcal{N}}^j} \in \mathbb{P}^1(T_{\mathcal{N}}^j), 1 \le j \le J\}, \quad V_{\mathcal{N}} = X_{\mathcal{N}} \cap V.$$

We can represent $X_{\mathcal{N}} = \operatorname{span}\{\phi_p,\ p = 1,\dots,\mathcal{N}+\mathcal{N}_{\mathrm{D}}\}$ and $V_{\mathcal{N}} = \operatorname{span}\{\phi_p,\ p = 1,\dots,\mathcal{N}\}$, where ϕ_i are the nodal Lagrange basis functions and $\mathcal{N}$ stands for the number of inner nodes and $\mathcal{N}_X = \mathcal{N}+\mathcal{N}_{\mathrm{D}}$ for the number of all nodes.

For the discretization of the dual space W, we use discontinuous piecewise linear biorthogonal basis functions, which are defined on the same mesh as the basis functions of $V_{\mathcal{N}}$, [Woh00; Woh01; Woh11]. That is, $W_{\mathcal{N}} := \operatorname{span}\{\chi_q,\ q = 1,\dots,\mathcal{N}\}$, where χ_q satisfy a local biorthogonality relation:

$$\int_{T_{\mathcal{N}}^j} \chi_q \phi_p = \delta_{p,q} \int_{T_{\mathcal{N}}^j} \phi_p \geq 0, \quad p,q = 1,\dots,\mathcal{N}.$$

Recall, that the discrete cone $M_{\mathcal{N}} \subset W_{\mathcal{N}}$ is given as

$$M_{\mathcal{N}} = \operatorname{span}_+\{\chi_q\}_{q=1}^{\mathcal{N}_W} := \Big\{\eta \in W_{\mathcal{N}} : \quad \eta = \sum_{q=1}^{\mathcal{N}_W} \alpha_q \chi_q, \quad \alpha_q \geq 0\Big\}. \tag{4.8.1}$$

We can observe that $\chi_q \notin M$, i.e., $M_{\mathcal{N}} \not\subset M$, and we obtain a non-conforming approach with respect to the Lagrange multiplier; see Remark 4.3.1.

If not specified, we establish the following setting to perform the numerical simulations. The computational domain Ω is set to $\Omega = (x_{\min}, x_{\max}) = (-5, 5)$ for the Black-Scholes model and to $\Omega = (\nu_{\min}, \nu_{\max}) \times (x_{\min}, x_{\max}) = (10^{-5}, 3) \times (-5, 5)$ for the Heston model. For the Black-Scholes model we set $\mathcal{N}_X = 500$ nodes and for Heston $\mathcal{N}_X = 49 \times 97 = 4753$ nodes. The time domain $[0, T]$ with $T = 2$ is discretized with a uniform mesh with $\Delta t = 0.008$ and $I = 250$. We consider the implicit Euler discretization, i.e., $\theta = 1$.

Recall the model parameter $\boldsymbol{\mu} = (\sigma, q, r) \in \mathcal{P}$ for the Black-Scholes model and $\boldsymbol{\mu} = (\xi, \rho, \gamma, \kappa, r) \in \mathcal{P}$ for the Heston model. We consider the following specifications of $\mathcal{P}$ for the Black-Scholes model:

$$\mathcal{P} \equiv [0.2, 0.6] \times [0.014, 0.06] \times [0.001, 0.06] \subset \mathbb{R}^3, \tag{4.8.2a}$$

$$\mathcal{P} \equiv [0.2, 0.6] \times [0, 0.02] \times [0.001, 0.06] \subset \mathbb{R}^3, \tag{4.8.2b}$$

and for the Heston model

$$\mathcal{P} \equiv [0.1, 0.9] \times [-0.95, 0.95] \times [0.01, 0.5] \times [0.1, 5] \times [0.0001, 0.8] \subset \mathbb{R}^5. \tag{4.8.2c}$$

Since the purpose of this section is to study the approximation qualities and the properties of the reduced basis method for large variations of the parameters, we do not restrict ourselves only to the financially meaningful ranges of the parameter and allow, e.g., cases when the Feller condition (2.6.2) is not fulfilled.

To generate the basis we consider a finite set $\mathcal{P}_{\mathrm{train}}$ composed of values, which are equidistantly distributed in $\mathcal{P}$. The size $|\mathcal{P}_{\mathrm{train}}|$ will be specified in each particular case. The strike K is set to $K = 1$.

4.8.1 Detailed Solution

Based on the discretization described above, the detailed solution of an American option price in the Black-Scholes and Heston models are depicted in Figure 4.1 and Figure 4.2 respectively.

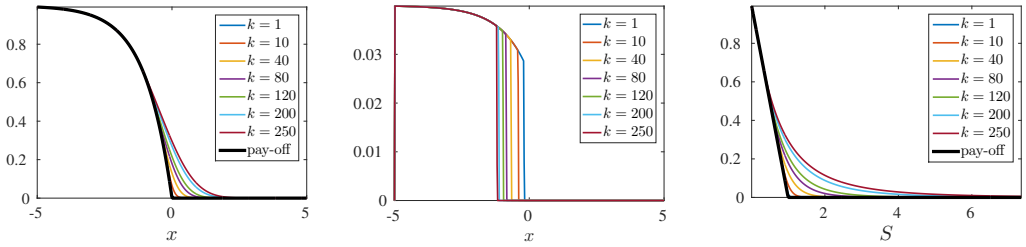

Figure 4.1: A time evolution of the American put option in the Black-Scholes model $u^k_{\mathcal{N}}(\boldsymbol{\mu})$ for $\boldsymbol{\mu}^\star = (06, 0.014, 0.04)$ (left), and the corresponding Lagrange multiplier $\lambda^k_{\mathcal{N}}(\boldsymbol{\mu})$ (middle). The price of the option in the original stock price variable S, $S = Ke^x$, (right, zoomed in view).

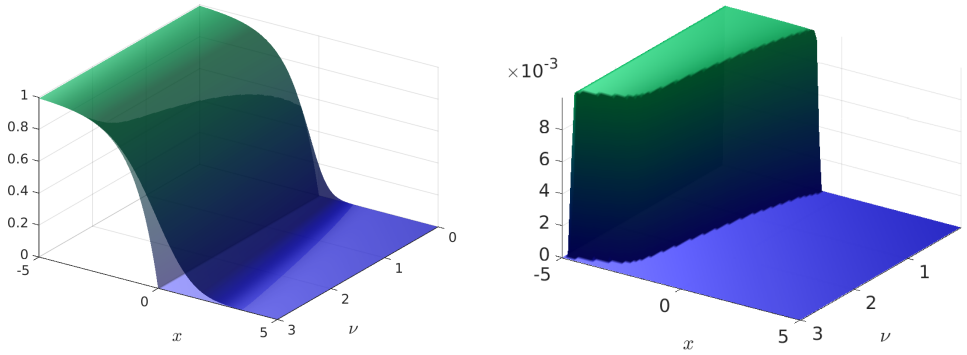

Figure 4.2: The value of the American put option $u^I_{\mathcal{N}}(\boldsymbol{\mu})$ and its pay-off (left) and the corresponding Lagrange multiplier $\lambda^I_{\mathcal{N}}(\boldsymbol{\mu})$ (right) in the Heston model at $t = T = 2$ and corresponding to $\boldsymbol{\mu}^\star = (0.9, 0.21, 0.16, 3, 0.01)$.

To motivate the application of the reduced basis method, we demonstrate the variability of the solution with respect to the parameter $\boldsymbol{\mu} \in \mathcal{P}$. In Figure 4.3, the variation of the primal and dual solutions of the Black-Scholes model for different parameter values is visualized. While one of the parameters is varying, the rest are fixed and take the values of the reference parameter $\boldsymbol{\mu}^\star = (0.6, 0.06, 0.06)$. We observe, that biggest alteration of the solution corresponds to the volatility parameter σ.

Analogously for the Heston model, the snapshots of the solution for different parameter values are presented in Figure 4.4. Overall, for both models we can observe that the parameter dependence is significant and non-trivial.

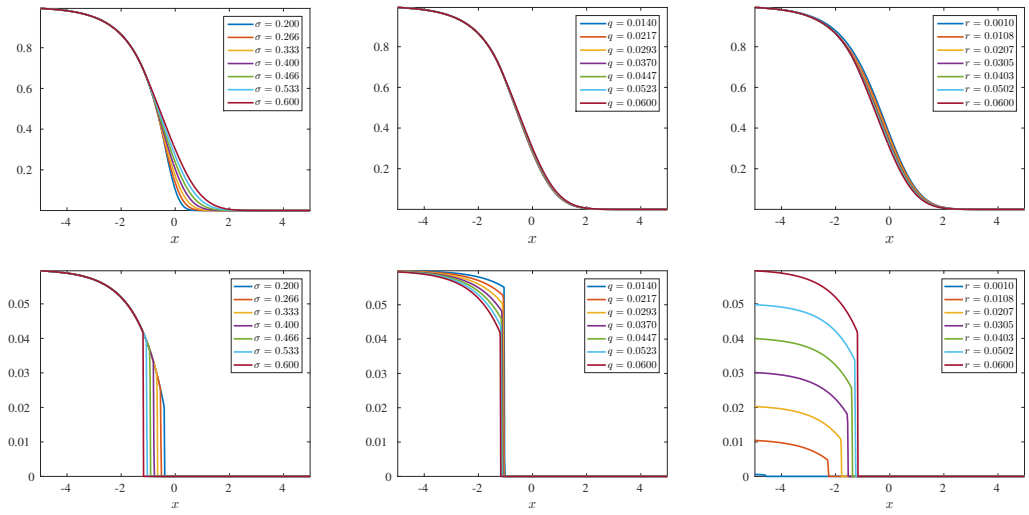

Figure 4.3: Snapshots of the primal solutions (top) and corresponding Lagrange multipliers (bottom) in the Black-Scholes model at $T = 2$ for different values of σ, q, and r.

4.8.2 Reduced Basis Spaces Construction

Since the approximation quality of the reduced basis method depends on many factors, such as the smoothness of the parameter manifold and the complexity of the underlying model, we first study the influence of the parameter complexity of each model. We consider different dimensions of the parameter domain $\mathcal{P}$. In particular, we consider for the Black-Scholes model the following cases:

$(B1)$ $\boldsymbol{\mu} = \sigma \in \mathcal{P}$, $\mathcal{P} := [0.2, 0.6] \subset \mathbb{R}^1$, cf. (4.8.2b);

$(B2)$ $\boldsymbol{\mu} = (\sigma, q, r) \in \mathcal{P}$, $\mathcal{P} := [0.2, 0.6] \times [0.014, 0.06] \times [0.001, 0.06] \subset \mathbb{R}^3$, cf. (4.8.2a).

Accordingly, for the Heston model we choose:

$(H1)$ $\boldsymbol{\mu} = (\gamma, \kappa) \in \mathcal{P}$, $\mathcal{P} := [0.01, 0.5] \times [0.1, 5] \subset \mathbb{R}^2$, cf. (4.8.2c);

$(H2)$ $\boldsymbol{\mu} = (\xi, \rho, \gamma) \in \mathcal{P}$, $\mathcal{P} := [0.1, 0.9] \times [-0.95, 0.95] \times [0.01, 0.5] \subset \mathbb{R}^3$, cf. (4.8.2c).

The remaining parameters we fix to the values of the reference parameter vector $\boldsymbol{\mu}^\star = (0.4, 0, 0.001)$ for the Black-Scholes model and $\boldsymbol{\mu}^\star = (0.9, 0.21, 0.16, 0.1, 0.007)$

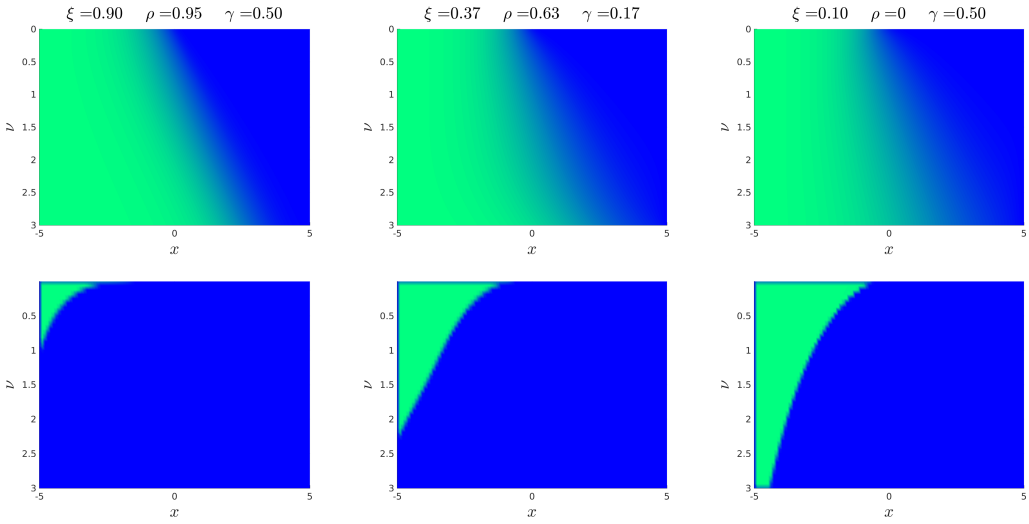

Figure 4.4: Snapshots of the primal solutions (top) and corresponding Lagrange multipliers (bottom) in the Heston model for different values of ξ, ρ, and γ at $T = 2$. The remaining parameters are set to $r = 0.007$, $\kappa = 0.1$.

for the Heston model. If not stated otherwise, we always follow the enrichment by supremizers strategy to guarantee the stability of the reduced spaces. Recall, that in this case we obtain $N_V \leq 2N_{\max}$ and $N_W \leq N_{\max}$.

For the case $(B1)$ of the Black-Scholes model, we consider $|\mathcal{P}_{\text{train}}| = 50$ equidistantly distributed points. For the construction of the reduced bases, we apply POD-Angle-Greedy (Algorithm 4.1), with the true error $E_N(\boldsymbol{\mu}) = \omega_u E_u^{\text{true}}(\boldsymbol{\mu}) + \omega_\lambda E_\lambda^{\text{true}}(\boldsymbol{\mu})$ as the selection criterion, for some weights ω_u, $\omega_\lambda \in \mathbb{R}_+$. The evolution of the error produced by the algorithm using different weights for the error indicators is depicted in Figure 4.5. We observe, that in all cases the error is decaying with growing value of $N_{\max}$. Moreover, it can be seen, that despite the choice of the weights ω_u, ω_λ of the error indicator, we obtain the same convergence order of the error.

Now, we consider the reduced basis performance for the Heston model. First, we consider the case $(H1)$. Using $\mathcal{P}_{\text{train}}$ with $|\mathcal{P}_{\text{train}}| = 64$, we build the reduced bases using Algorithm 4.1 with $E_N(\boldsymbol{\mu}) = E_u^{\text{true}}(\boldsymbol{\mu})$. The evolution of the error is presented in Figure 4.6 (left). In addition, in the same figure (right) we plot the parameters which were selected during the iterations of the algorithm. As before, the diameter of the circles corresponds to the "frequency of the selection" of the parameters.

Next, we consider the remaining case $(B2)$ for the Black-Scholes model and the case $(H2)$ for the Heston model. For both models we use $\mathcal{P}_{\text{train}}$ of $|\mathcal{P}_{\text{train}}| = 7^3 = 343$ uniformly distributed points. The reduced bases are built with Algorithm 4.1 using $E_N(\boldsymbol{\mu}) = E_u^{\text{true}}(\boldsymbol{\mu})$. The evolution of the error is presented in Figure 4.7 (left) and

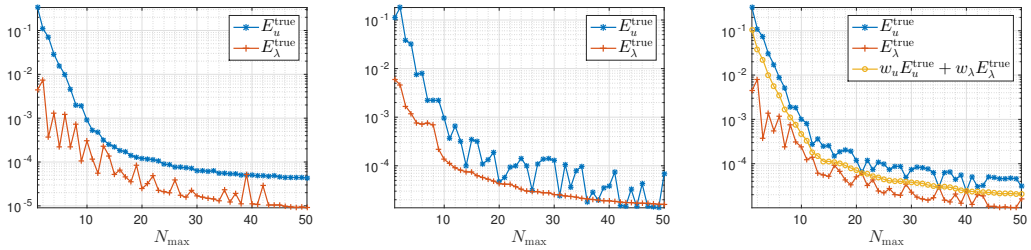

Figure 4.5: Evolution of $\max_{\boldsymbol{\mu}\in\mathcal{P}_{\text{train}}} E_{u/\lambda}^{\text{true}}(\boldsymbol{\mu})$ for the American put option in the Black-Scholes model (case $(B1)$) during the iterations of Algorithm 4.1 using the error estimator $E_N(\boldsymbol{\mu}) = \omega_u E_u^{\text{true}}(\boldsymbol{\mu}) + \omega_\lambda E_\lambda^{\text{true}}(\boldsymbol{\mu})$ as a selection criterion with $\omega_u = 1$, $\omega_\lambda = 0$ (left), $\omega_u = 0$, $\omega_\lambda = 1$ (middle) and $\omega_u = \omega_\lambda = 0.5$ (right).

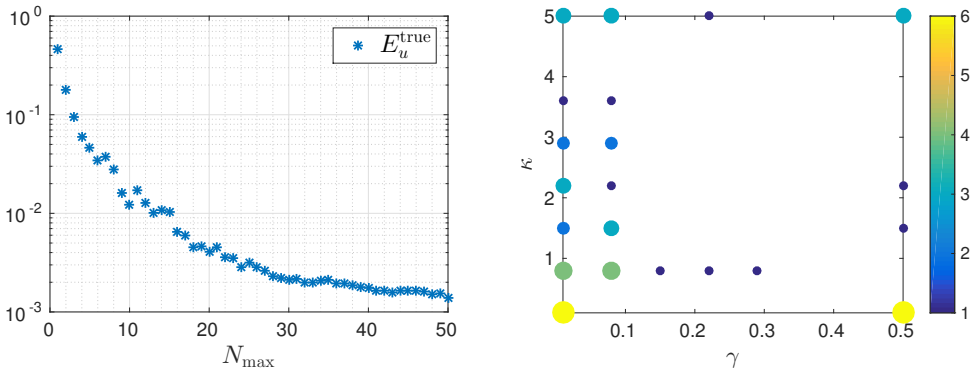

Figure 4.6: Left: Evolution of $\max_{\boldsymbol{\mu}\in\mathcal{P}_{\text{train}}} E_u^{\text{true}}(\boldsymbol{\mu})$ for the American put option in the Heston model produced by Algorithm 4.1 with $\boldsymbol{\mu} = (\gamma, \kappa)$. Right: Plot of the selected parameters $\boldsymbol{\mu}_1, \ldots, \boldsymbol{\mu}_{N_{\max}} \in \mathcal{P}_{\text{train}}$ and their frequency of the selection. The training set consists of $|\mathcal{P}_{\text{train}}| = 8^2 = 64$ equidistantly distributed points.

Figure 4.8 (left) for the Black-Scholes and Heston models respectively. For both cases we observe an error decay with increasing dimension of the reduced system. However, it can be observed that the convergence of the error for the Heston model is much slower than for the Black-Scholes model. The RBM requires more than twice the number of basis functions to reach a similar accuracy. This can be explained by, e.g., the non-trivial parameter dependence as well as the complexity of the Heston model. Due to a non-linearity of the variational inequality problem we can clearly observe that the error decay for American put options is much slower than for European put options, see Section 3.5. To achieve a similar accuracy for American options, one

clearly needs to work with the larger dimension of the reduced problem.

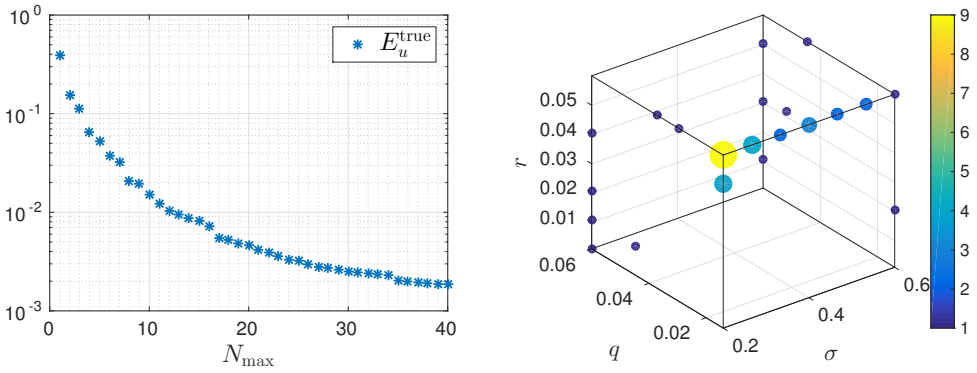

Figure 4.7: Left: Evolution of $\max_{\boldsymbol{\mu}\in\mathcal{P}_{\text{train}}} E_u^{\text{true}}(\boldsymbol{\mu})$ for the American put option in the Black-Scholes model produced by Algorithm 4.1 with $\boldsymbol{\mu} = (\sigma, q, r)$. Right: Plot of the selected parameters $\boldsymbol{\mu}_1, \ldots, \boldsymbol{\mu}_{N_{\max}} \in \mathcal{P}_{\text{train}}$ and their frequency of the selection. The training set consists of $|\mathcal{P}_{\text{train}}| = 7^3 = 343$ equidistantly distributed points.

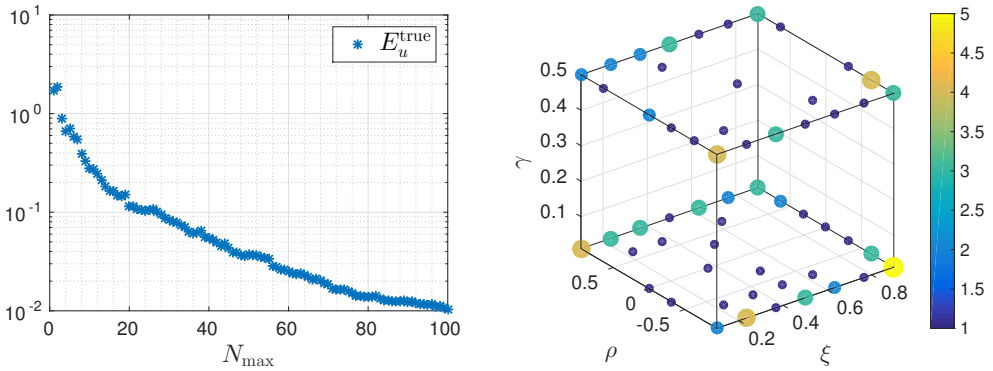

Figure 4.8: Left: Evolution of $\max_{\boldsymbol{\mu}\in\mathcal{P}_{\text{train}}} E_u^{\text{true}}(\boldsymbol{\mu})$ for the American put option in the Heston model produced by Algorithm 4.1 with $\boldsymbol{\mu} = (\xi, \rho, \gamma)$. Right: Plot of the selected parameters $\boldsymbol{\mu}_1, \ldots, \boldsymbol{\mu}_{N_{\max}} \in \mathcal{P}_{\text{train}}$ and their frequency of the selection. The training set consists of $|\mathcal{P}_{\text{train}}| = 7^3 = 343$ equidistantly distributed points.

Using the computed reduced basis sets Ψ_N, Ξ_N (constructed as described above, for the cases $(B2)$ and $(H2)$), we construct reduced basis spaces V_N and W_N of dimension $N_V = 80$, $N_W = 40$ for the Black-Scholes model and $N_V = 200$, $N_W = 100$ for the Heston model. We consider the performance of the RB approach for a random

parameter $\boldsymbol{\mu}^\star \in \mathcal{P} \setminus \mathcal{P}_{\text{train}}$. The results are depicted in Figure 4.9 and Figure 4.10 for the Black-Scholes and Heston models respectively. We observe that in both cases the detailed primal and reduced solutions are hardly distinguishable and the relative error in the maximum norm is of order 10^{-4}, which reveals a good RB approximation. The illustration of the RB basis vectors for the Black-Scholes model are presented in Figure 4.11.

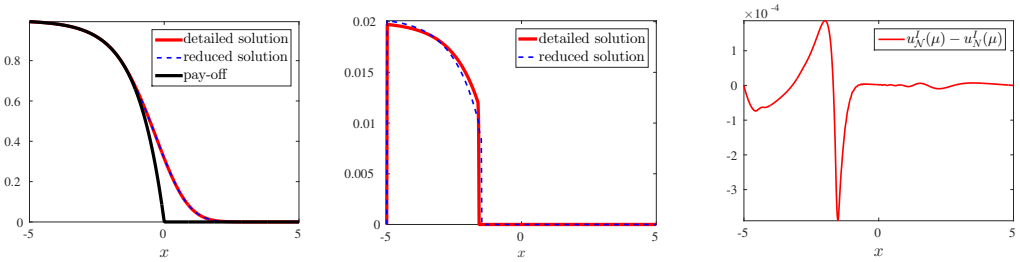

Figure 4.9: Detailed and reduced primal solutions (left) and the corresponding detailed and reduced dual solutions (middle) of the American put option in the Black-Scholes model at $T = 2$ and for $\boldsymbol{\mu}^\star = (0.57, 0.04, 0.02) \notin \mathcal{P}_{\text{train}}$. The difference of the primal detailed and reduced solutions (right).

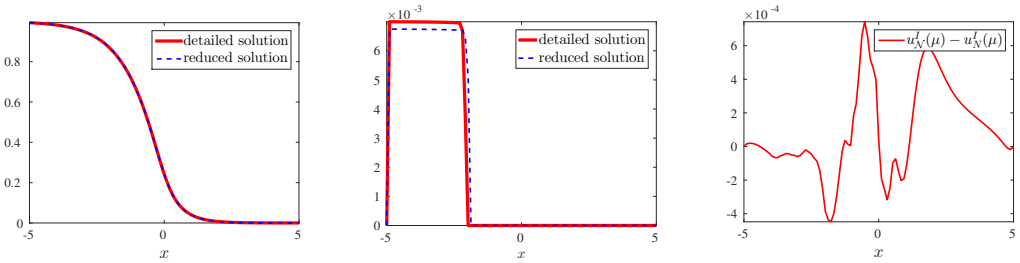

Figure 4.10: Detailed and reduced primal solutions (left) and the corresponding detailed and reduced dual solutions (middle) of the American put option in the Heston model at $T = 2$, extracted at $\nu = 0.25$, and for $\boldsymbol{\mu}^\star = (0.7, 0.2, 0.16, 0.1, 0.007) \notin \mathcal{P}_{\text{train}}$. The difference of the primal detailed and reduced solutions (right).

4.8.3 Comparison of Different RB Spaces

In our previous test we exploit the POD-Angle-Greedy, Algorithm 4.1. Now, we present numerical tests for the alternative approaches. That is, we investigate the combination of the NNMF algorithm with POD-Greedy algorithm, described in Section 4.6.2.

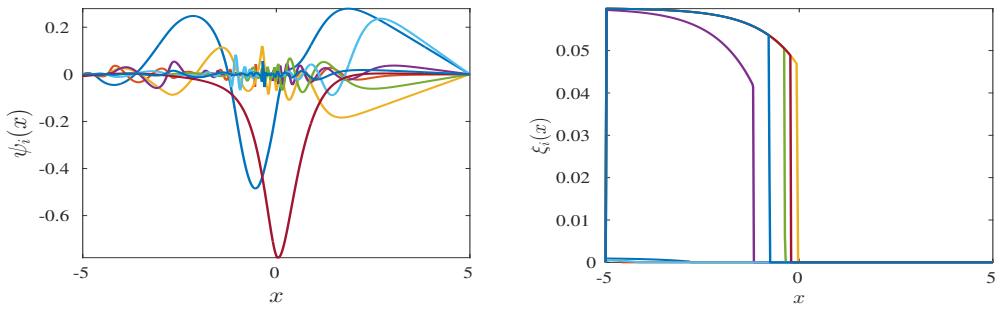

Figure 4.11: The first eight vectors of the primal (left) and dual (right) reduced bases obtained with Algorithm 4.1 using $E_u^{\text{true}}(\boldsymbol{\mu})$ as a selection criterion for the American put option in the Black-Scholes model.

We restrict ourselves to the Heston model and consider the following settings: $\Omega = (0.0025, 0.5) \times (-5, 5)$, $\mathcal{N}_X = 4753$, $T = 1$, $I = 20$. The parameter specifications are chosen as in the case $(H1)$ with $|\mathcal{P}_{\text{train}}| = 10^2 = 100$ equidistantly distributed points. For the primal space construction we apply POD-Greedy, Algorithm 4.1, and for the dual one we explore and compare different approaches, such as NNMF, greedy or Angle-Greedy. Furthermore, using different multiplicative update rules for the NNMF algorithm we consider several variants of NNMF, such as NNMF-orthogonal, NNMF-local and NNMF-convolutive. The corresponding simulations for NNMF are performed using the NMFlib (v0.1.3) [Gri10] library. We consider Algorithm 4.2 with $E_N(\boldsymbol{\mu}) = E_u^{\text{true}}(\boldsymbol{\mu})$, and we build the reduced basis spaces with $N_{\max} = 5, 10, 15, 25, 35$. As before, for stability reasons, we enrich the reduced primal space with the supremizers, which results in $N_V \leq 2N_{\max}$ and $N_W \leq N_{\max}$. The values of $\max_{\boldsymbol{\mu} \in \mathcal{P}_{\text{train}}} E_N(\boldsymbol{\mu})$ obtained during the iterations of the basis construction algorithm for different $N_{\max}$ and different strategies for the construction of W_N are reported in Table 4.1.

Method	$N_{\max} = 5$	$N_{\max} = 10$	$N_{\max} = 15$	$N_{\max} = 25$	$N_{\max} = 35$
Angle-Greedy	1.163e − 01	5.764e − 02	2.452e − 02	1.192e − 02	8.944e − 03
NNMF	1.374e − 01	5.565e − 02	2.647e − 02	1.330e − 02	1.057e − 02
NNMF-orthogonal	1.174e − 01	5.621e − 02	3.218e − 02	1.880e − 02	2.164e − 02
NNMF-local	1.178e − 01	5.004e − 02	3.060e − 02	2.351e − 02	1.652e − 02
NNMF-convolutive	1.173e − 01	5.413e − 02	2.692e − 02	1.357e − 02	1.172e − 02
Greedy	1.170e − 01	5.630e − 02	2.459e − 02	1.641e − 02	1.251e − 02

Table 4.1: Comparison of the maximal training errors produced by the different basis construction algorithms.

Overall, we observe that all algorithms produce a similar accuracy for the approximation. The graphical representation of these results is given in Figure 4.12. The corresponding selected parameters, obtained during the basis generation routine are presented in Figure 4.13. We can observe that Angle-Greedy, NNMF-convolutive, and greedy procedures provide the most stable and sharp approximations. Comparing the distribution of the parameters in Figure 4.13 we can conclude that the Angle-Greedy tends to exploit more of the parameter variation of the model than the other approaches.

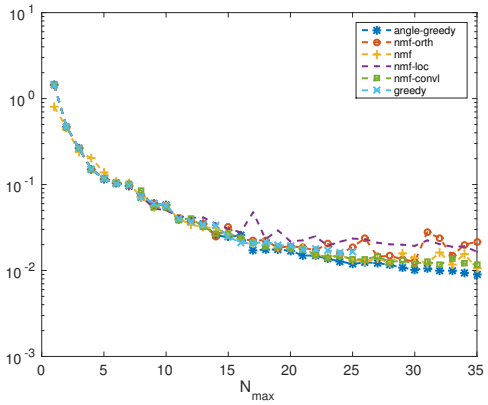

Figure 4.12: Evolution of $\max_{\boldsymbol{\mu}\in\mathcal{P}_{\text{train}}} E^{\text{true}}(\boldsymbol{\mu})$ with respect to the different dimension $N_{\max}$ using different algorithms for the the dual reduced space construction.

4.8.4 A Posteriori Error Estimates

We now turn to the numerical investigation of the error estimates derived in Section 4.5 using the example of American put options in the Black-Scholes and Heston models. For the Heston model we consider the same settings, introduced at the beginning of this section. Namely, the computational domain Ω is set to $\Omega = (10^{-5}, 3) \times (-5, 5)$ with $\mathcal{N}_X = 49 \times 97 = 4753$ nodes. We recall the time domain $[0, T] = [0, 2]$ and $\Delta t = 0.008$, $I = 250$, $\theta = 1$.

We consider POD-Angle-Greedy algorithm (Algorithm 4.1) for basis construction, and use alternatively $E_N(\boldsymbol{\mu}) = E_u^{\boldsymbol{\mu}}(\boldsymbol{\mu}) = |||e_N^u(\boldsymbol{\mu})|||_{\boldsymbol{\mu}}$ or $E_N(\boldsymbol{\mu}) = E_u^{\text{apost}}(\boldsymbol{\mu}) = \Delta_N^u(\boldsymbol{\mu})$, with the error bound $E_u^{\text{apost}}(\boldsymbol{\mu})$ defined as in (4.5.13) and $E_u^{\boldsymbol{\mu}}(\boldsymbol{\mu})$ as in (4.5.8). To measure the rate of overestimation of the a posteriori error bounds, we define the effectivity $\eta_N(\boldsymbol{\mu})$, associated with the error bound as

$$\eta_N(\boldsymbol{\mu}) = \frac{E_u^{\text{apost}}(\boldsymbol{\mu})}{E_u^{\boldsymbol{\mu}}(\boldsymbol{\mu})}. \tag{4.8.3}$$

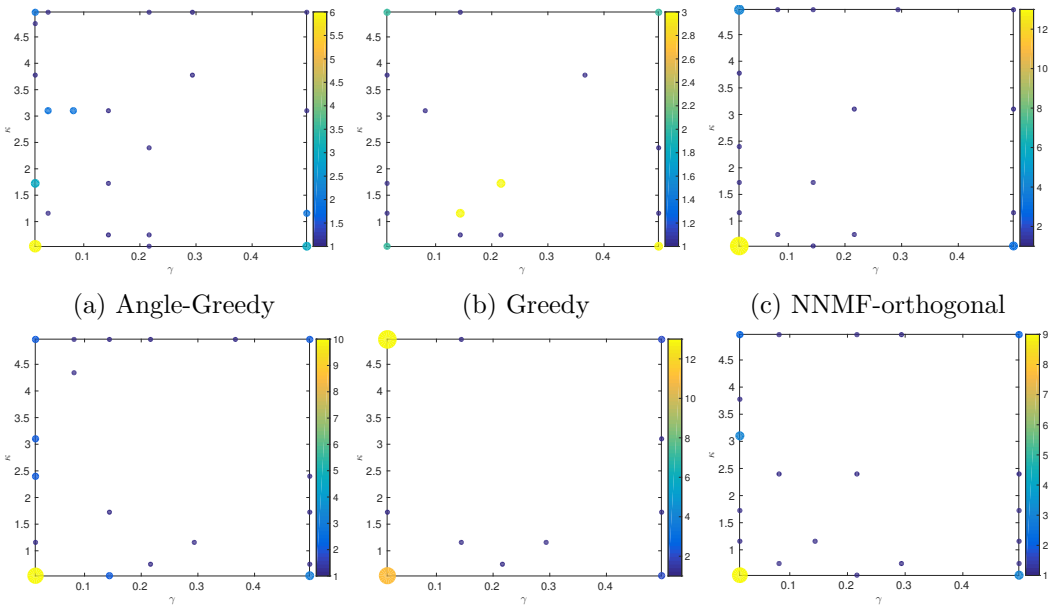

(a) Angle-Greedy (b) Greedy (c) NNMF-orthogonal

(d) NNMF (e) NNMF-local (f) NNMF-convolutive

Figure 4.13: The selected parameters $\boldsymbol{\mu}_1, \ldots, \boldsymbol{\mu}_{N_{\max}} \in \mathcal{P}_{\text{train}}$ and their frequency of the selection using different algorithms for the dual reduced space construction.

We consider the values of the quantity $\max_{\boldsymbol{\mu} \in \mathcal{P}_{\text{train}}} E_N(\boldsymbol{\mu})$ along the iterations of Algorithm 4.1, with $E_N(\boldsymbol{\mu}) = E_u^{\text{apost}}(\boldsymbol{\mu})$.

Single Parameter Case

To study the effect of the error estimator, first, we consider $\mathcal{P}_{\text{train}}$, composed of only a single parameter $\boldsymbol{\mu}$, $|\mathcal{P}_{\text{train}}| = 1$, with $\boldsymbol{\mu} = (0.6, 0.0217, 0.001)$ for the Black-Scholes model, and $\boldsymbol{\mu} = (0.9, -0.6333, 0.01, 0.1, 0.007)$ for the Heston model. The corresponding results for both models are presented in Figure 4.14. We can observe that the error bound is tighter in the case of the Black-Scholes model. In fact, the effectivity $\eta_N(\boldsymbol{\mu})$ for the Black-Scholes model is, on average, one order of magnitude smaller as for the Heston model. This can be explained by the more complex structure of the model. Taking a look on the constants contributing to the error estimator $E_u^{\text{apost}}(\boldsymbol{\mu})$ for a given $\boldsymbol{\mu}$, we obtain the following values: $\alpha_a^{\mathcal{N}}(\boldsymbol{\mu}) = 0.18$, $\gamma_a^{\mathcal{N}}(\boldsymbol{\mu}) = 0.3717$, $\lambda_a^{\mathcal{N}}(\boldsymbol{\mu}) = 0$, $\gamma_a^{\mathcal{N}}(\boldsymbol{\mu})/\alpha_a^{\mathcal{N}}(\boldsymbol{\mu}) \approx 2.065$ for the Black-Scholes model and $\alpha_a^{\mathcal{N}}(\boldsymbol{\mu}) = 0.0226$, $\gamma_a^{\mathcal{N}}(\boldsymbol{\mu}) = 2.447$, $\lambda_a^{\mathcal{N}}(\boldsymbol{\mu}) = 24.909$, $\gamma_a^{\mathcal{N}}(\boldsymbol{\mu})/\alpha_a^{\mathcal{N}}(\boldsymbol{\mu}) \approx 108.27$ for the Heston model. We observe that, for instance, the quotient $\gamma_a^{\mathcal{N}}(\boldsymbol{\mu})/\alpha_a^{\mathcal{N}}(\boldsymbol{\mu})$, which certainly influences the effectivity of the error bound, is much larger for the Heston model.

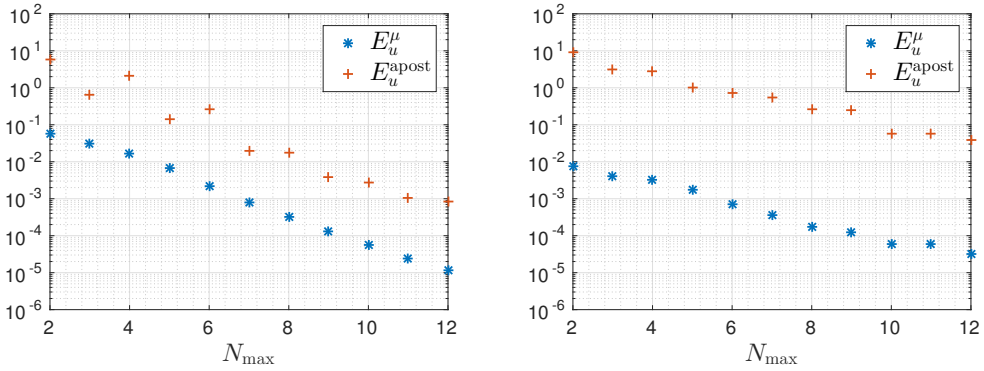

Figure 4.14: Evolution of $\max_{\boldsymbol{\mu}\in\mathcal{P}_{\text{train}}} E_u^{\boldsymbol{\mu}/\text{apost}}(\boldsymbol{\mu})$ for the American put option in the Black-Scholes (left) and Heston (right) models during the iterations of Algorithm 4.1 with the error estimator $E(\boldsymbol{\mu}) = E_u^{\text{apost}}(\boldsymbol{\mu})$ as a selection criterion, using $\mathcal{P}_{\text{train}} \equiv \{\boldsymbol{\mu}\} = \{(0.6, 0.0217, 0.001)\}$ for the Black-Scholes and $\mathcal{P}_{\text{train}} \equiv \{\boldsymbol{\mu}\} = \{(0.9, -0.6333, 0.01, 0.1, 0.007)\}$ for the Heston models.

General Parameter Case

Next, we extend our consideration to the general case. Namely, we consider the settings $(B1)$–$(B2)$ for the Black-Scholes model and $(H2)$ for the Heston model (described in Section 4.8.2). As before, we study the evolution of $\max_{\boldsymbol{\mu}\in\mathcal{P}_{\text{train}}} E_N(\boldsymbol{\mu})$ during the iterations of Algorithm 4.1, choosing either $E_N(\boldsymbol{\mu}) = E_u^{\boldsymbol{\mu}}(\boldsymbol{\mu})$ or $E_N(\boldsymbol{\mu}) = E_u^{\text{apost}}(\boldsymbol{\mu})$ as the selection criterion. The results are presented in Figure 4.15 and Figure 4.16 for the Black-Scholes model, and in Figure 4.17 for the Heston model. Note that the choice of the error measure $E_N(\boldsymbol{\mu})$ does not have a significant impact on the effectivities.

We notice that for both models, using $E_N(\boldsymbol{\mu}) = E_u^{\boldsymbol{\mu}}(\boldsymbol{\mu})$ as an error measure in Algorithm 4.1, results in less monotone error convergence of $E_u^{\text{apost}}(\boldsymbol{\mu})$ with respect to $N_{\max}$, and vice versa. However, overall we obtain similar order of convergence when using either of these error indicators. From this we can conclude that the rigorous upper bound of the error is confirmed in the numerical experiments and reflects the error behavior, hence provides the certification of the reduced basis method. As we have already observed, the sharpness of an error bound can be model dependent, which could be investigated in greater detail in a future work.

In addition, we investigate the effect of the maturity T (length of the time interval) on the effectivities. To this purpose, for the same reduced bases computed above, we also evaluate the error indicators with $\widetilde{T} = \Delta t \widetilde{I}$ where $\widetilde{I} \in \mathbb{N}$, $\widetilde{I} \leq I$. It is clear that the result from Theorem 4.5.2 remains valid if we replace I by $\widetilde{I}$ in the definition of

the error $E_u^{\boldsymbol{\mu}}(\boldsymbol{\mu})$ and the estimator $E_u^{\text{apost}}(\boldsymbol{\mu})$. Numerical values of the corresponding effectivities are reported in Table 4.2 and Table 4.3.

We point out that the error bound (4.5.13) includes the term $(C_\Omega \delta_s^{k+1}/\beta_{\mathcal{N}})^2$, which does not have a multiplicative factor Δt. This suggest a possible growth of an error in the number of the time steps. However, empirically this behavior can be observed rather weakly (see Table 4.2 and Table 4.3).

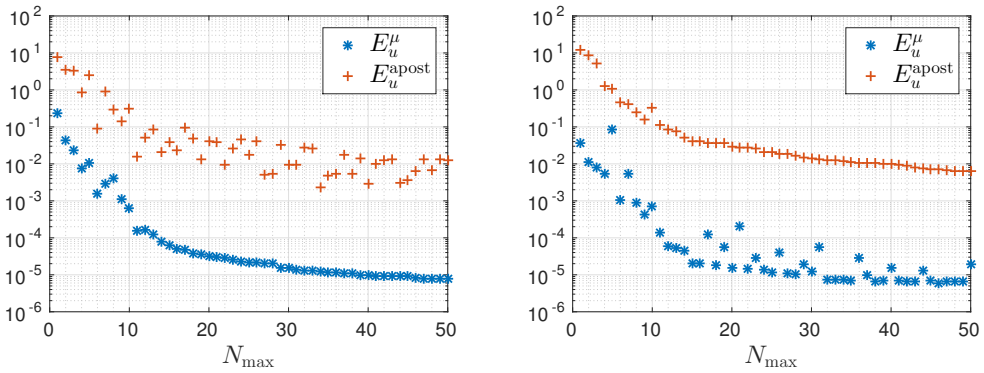

Figure 4.15: Evolution of $\max_{\boldsymbol{\mu}\in\mathcal{P}_{\text{train}}} E_u^{\boldsymbol{\mu}/\text{apost}}(\boldsymbol{\mu})$ for the American put option in the Black-Scholes model during the iterations of Algorithm 4.1 with the error estimator $E_N(\boldsymbol{\mu}) = E_u^{\boldsymbol{\mu}}(\boldsymbol{\mu})$ (left) and $E_N(\boldsymbol{\mu}) = E_u^{\text{apost}}(\boldsymbol{\mu})$ (right) as a selection criterion. The training set consists of $|\mathcal{P}_{\text{train}}| = 50$ equidistantly distributed points and $\boldsymbol{\mu} = \sigma$.

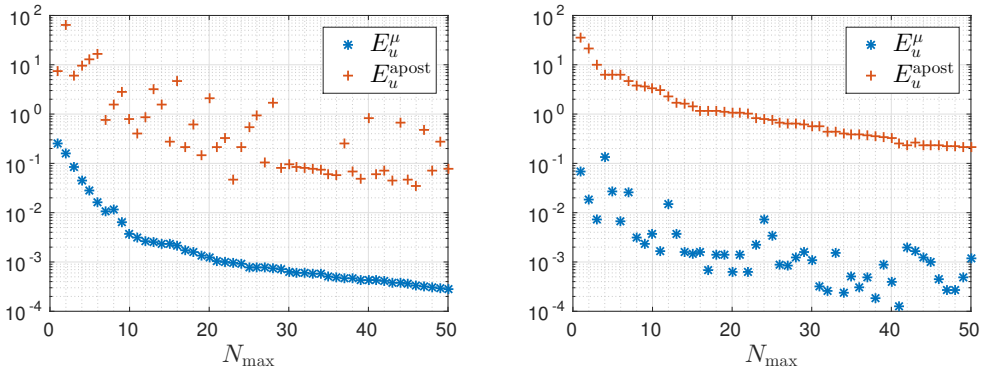

Figure 4.16: Evolution of $\max_{\boldsymbol{\mu}\in\mathcal{P}_{\text{train}}} E_u^{\boldsymbol{\mu}/\text{apost}}(\boldsymbol{\mu})$ for the American put option in the Black-Scholes model during the iterations of Algorithm 4.1 with the error estimator $E_N(\boldsymbol{\mu}) = E_u^{\boldsymbol{\mu}}(\boldsymbol{\mu})$ (left) and $E_N(\boldsymbol{\mu}) = E_u^{\text{apost}}(\boldsymbol{\mu})$ (right) as a selection criterion. The training set consists of $|\mathcal{P}_{\text{train}}| = 343$ equidistantly distributed points and $\boldsymbol{\mu} = (\sigma, q, r)$.

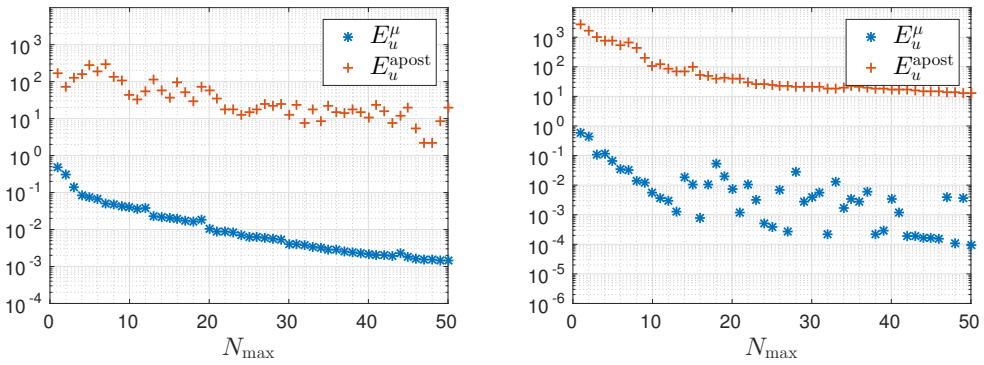

Figure 4.17: Evolution of $\max_{\boldsymbol{\mu}\in\mathcal{P}_{\text{train}}} E_u^{\boldsymbol{\mu}/\text{apost}}(\boldsymbol{\mu})$ for the American put option in the Heston model during the iterations of Algorithm 4.1 with the error estimator $E_N(\boldsymbol{\mu}) = E_u^{\boldsymbol{\mu}}(\boldsymbol{\mu})$ (left) and $E_N(\boldsymbol{\mu}) = E_u^{\text{apost}}(\boldsymbol{\mu})$ (right) as a selection criterion. The training set consists of $|\mathcal{P}_{\text{train}}| = 343$ equidistantly distributed points and $\boldsymbol{\mu} = (\xi, \rho, \gamma)$.

	$\widetilde{I} = 30$	$\widetilde{I} = 60$	$\widetilde{I} = 120$	$\widetilde{I} = 180$	$\widetilde{I} = 250$
$N_{\max} = 5$	1.74e+01	2.44e+01	2.98e+01	3.82e+01	4.48e+01
$N_{\max} = 15$	7.32e+01	8.81e+01	9.94e+01	1.19e+02	1.36e+02
$N_{\max} = 25$	1.10e+02	1.21e+02	1.54e+02	2.33e+02	2.55e+02
$N_{\max} = 30$	9.42e+01	2.26e+02	2.86e+02	3.09e+02	3.72e+02
$N_{\max} = 35$	1.06e+02	1.37e+02	1.52e+02	1.84e+02	2.32e+02
$N_{\max} = 45$	9.63e+01	9.06e+01	1.00e+02	1.79e+02	1.68e+02
$N_{\max} = 50$	3.47e+02	4.59e+02	4.87e+02	8.65e+02	1.16e+03

(a) $E_N(\boldsymbol{\mu}) = E_u^{\boldsymbol{\mu}}(\boldsymbol{\mu})$

	$\widetilde{I} = 30$	$\widetilde{I} = 60$	$\widetilde{I} = 120$	$\widetilde{I} = 180$	$\widetilde{I} = 250$
$N_{\max} = 5$	1.07e+01	1.45e+01	1.70e+01	2.06e+01	2.32e+01
$N_{\max} = 15$	3.91e+02	5.49e+02	5.53e+02	5.37e+02	6.79e+02
$N_{\max} = 25$	5.50e+02	5.01e+02	4.93e+02	7.06e+02	9.60e+02
$N_{\max} = 30$	4.01e+02	4.27e+02	5.81e+02	7.81e+02	8.30e+02
$N_{\max} = 35$	6.29e+02	2.46e+02	3.35e+02	8.04e+02	9.24e+02
$N_{\max} = 45$	2.37e+02	4.27e+01	8.85e+02	1.30e+03	1.19e+03
$N_{\max} = 50$	1.06e+02	1.13e+02	1.47e+02	1.25e+02	1.78e+02

(b) $E_N(\boldsymbol{\mu}) = E_u^{\text{apost}}(\boldsymbol{\mu})$

Table 4.2: Maximum effectivities for the American put option in the Black-Scholes model for different maturities $\widetilde{T} = \widetilde{I}\Delta t$, with a fixed $\Delta t = 0.008$ and for different values of $N_{\max}$, using the error measure $E_N(\boldsymbol{\mu}) = E_u^{\boldsymbol{\mu}}(\boldsymbol{\mu})$ or $E_N(\boldsymbol{\mu}) = E_u^{\text{apost}}(\boldsymbol{\mu})$ as a selection criterion (always for $\widetilde{I} = I = 250$). The training set consists of $|\mathcal{P}_{\text{train}}| = 50$ equidistantly distributed points and $\boldsymbol{\mu} = \sigma$.

	$\widetilde{I} = 30$	$\widetilde{I} = 60$	$\widetilde{I} = 120$	$\widetilde{I} = 180$	$\widetilde{I} = 250$
$N_{\max} = 5$	1.54e+02	2.24e+02	2.83e+02	3.89e+02	4.89e+02
$N_{\max} = 15$	1.95e+02	2.64e+02	3.22e+02	4.38e+02	5.55e+02
$N_{\max} = 25$	2.51e+02	3.90e+02	4.97e+02	6.52e+02	7.58e+02
$N_{\max} = 30$	1.64e+02	2.34e+02	2.90e+02	3.88e+02	4.52e+02
$N_{\max} = 35$	1.16e+02	1.49e+02	1.77e+02	2.27e+02	2.84e+02
$N_{\max} = 45$	2.80e+02	4.33e+02	5.47e+02	6.90e+02	8.20e+02
$N_{\max} = 50$	2.42e+02	2.28e+02	2.21e+02	2.23e+02	2.36e+02

(a) $E_N(\boldsymbol{\mu}) = E_u^{\boldsymbol{\mu}}(\boldsymbol{\mu})$

	$\widetilde{I} = 30$	$\widetilde{I} = 60$	$\widetilde{I} = 120$	$\widetilde{I} = 180$	$\widetilde{I} = 250$
$N_{\max} = 5$	1.18e+03	1.75e+03	2.22e+03	3.04e+03	3.70e+03
$N_{\max} = 15$	4.82e+02	7.86e+02	9.76e+02	1.16e+03	1.24e+03
$N_{\max} = 25$	5.49e+03	9.57e+03	8.43e+03	8.20e+03	9.11e+03
$N_{\max} = 30$	1.58e+03	1.92e+03	2.19e+03	2.67e+03	3.05e+03
$N_{\max} = 35$	6.33e+02	6.72e+02	7.66e+02	8.74e+02	8.64e+02
$N_{\max} = 45$	2.65e+03	3.93e+03	3.41e+03	2.90e+03	3.23e+03
$N_{\max} = 50$	5.94e+03	4.05e+03	3.40e+03	3.22e+03	3.64e+03

(b) $E_N(\boldsymbol{\mu}) = E_u^{\text{apost}}(\boldsymbol{\mu})$

Table 4.3: Maximum effectivities for the American put option in the Heston model for different maturities $\widetilde{T} = \widetilde{I}\Delta t$, with a fixed $\Delta t = 0.008$ and for different values of $N_{\max}$, using the error measure $E_N(\boldsymbol{\mu}) = E_u^{\boldsymbol{\mu}}(\boldsymbol{\mu})$ or $E_N(\boldsymbol{\mu}) = E_u^{\text{apost}}(\boldsymbol{\mu})$ as a selection criterion (always for $\widetilde{I} = I = 250$). The training set consists of $|\mathcal{P}_{\text{train}}| = 343$ equidistantly distributed points and $\boldsymbol{\mu} = (\xi, \rho, \gamma)$.

4.8.5 Efficiency of the Method

Now we turn to the study of the efficiency of the reduced basis method. The runtime performance of the reduced basis scheme compared to the computation of the detailed solution is reflected in Table 4.4. We compare different model settings, as described in Section 4.8.2. We measure the computational times of the offline and online phases, similarly as in Section 3.5. We briefly recall the following quantities:

- t_1: Computation time for a single detailed solution for a given parameter $\boldsymbol{\mu} \in \mathcal{P}$.

Online phase

- t_2: Computation time to assemble the reduced system and to solve the reduced problem for a given $\boldsymbol{\mu} \in \mathcal{P}$.

Offline phase

- t_3: Computation time for the construction of the reduced bases using Algorithm 4.1 with $E_N(\boldsymbol{\mu}) = E_u^{\text{true}}(\boldsymbol{\mu})$.
- t_4: Computation time to construct the parameter independent reduced data, e.g., $\mathbf{A}_N^q$, $\mathbf{B}_N$ etc.
- t_5: Computation time for evaluation of the snapshots, that is the time for computing the detailed solutions $(u_{\mathcal{N}}^k(\boldsymbol{\mu}), \lambda_{\mathcal{N}}^k(\boldsymbol{\mu}))$, for all $\boldsymbol{\mu} \in \mathcal{P}_{\text{train}}$. The cost is influenced by the dimension of $\mathcal{P}_{\text{train}}$, which is $|\mathcal{P}_{\text{train}}| = 50$ for the case $(B1)$, $|\mathcal{P}_{\text{train}}| = 343$ for $(B2)$ and $(H2)$, and $|\mathcal{P}_{\text{train}}| = 64$ for $(H1)$.
- t_1/t_2: Asymptotic speed-up of the online routine obtained using the reduced basis method.

	$N_{\max}$	t_1	t_2	t_3	t_4	t_5	t_1/t_2
Black-Sholes, $(B1)$	50	1.971	0.331	1661	0.0268	80.46	5.954
Black-Sholes, $(B2)$	35	1.798	0.1471	1810	0.0054	529.1	12.22
Heston, $(H1)$	50	270.3	0.2545	3155	0.0425	46830	1006
Heston, $(H2)$	100	264.6	0.5008	13471	0.1073	138901	528.3

Table 4.4: Runtime measurements (in seconds) of the reduced basis method for different $N_{\max}$ and for different model parameter settings.

We observe a significant speed-up, in particular, when dealing with the more complex Heston model, where the complexity of the two dimensional detailed problem prevails the complexity of the one-dimensional Black-Scholes model. We also can notice that

the costly offline routine does not suggest to apply the reduced basis method for a single parameter evaluation only. However, this cost will pay off in the case when we are performing multi-query simulations. A situation where the need for multi-query simulations arises naturally will be studied in the next chapter in the context of the calibration to market data.

We also note that similarly to the case of European options, in the multi-query context it makes sense to neglect the assembly time in t_1, when computing the asymptotic speed up. However, in the present case this does not have a significant effect, since t_1 is not dominated by the assembly time, but by the detailed solution procedure, i.e., the PDAS strategy. For the Heston model the contribution of the assembly time to t_1 is less than 10% for the given numerical examples.

5 Application to the Calibration on Option Prices

> "But the days of closed-form solutions are numbered because models are increasingly complex. Numerical algorithms will have to be more efficient because speed is becoming a dominant factor with high-frequency trading..."
>
> O. Pironneau, "Pricing futures by deterministic methods", *Acta Numerica*, 21 (2012), pp. 577–671

5.1 Introduction

To calculate the price of an option (European or American) in a specific model, one needs to provide the respective input data. These data consist of the current stock price S_0, the maturity time T, the strike price K, and the set of the input parameters, which we previously denoted by $\boldsymbol{\mu} \in \mathcal{P}$. Whereas the first three components, S_0, K, T, are known and provided by the market data, the input parameter vector $\boldsymbol{\mu}$ is not known a priori, except for the interest rate r, and needs to be estimated from the market. These types of problems are referred to as parameter identification problems or, among practitioners, calibration problems. That is, given a set of observations of market option prices, we are searching for the parameter $\boldsymbol{\mu}$ that provides the best fit of the given data to the model one.

Generally, the market data is characterized by:

1. The spot price today S_0
2. The market option prices $P_i^{\text{obs}} = P^{\text{obs}}(S_0, T_i, K_i)$ (for American or European options, put or call) for different maturities T_i and for different strikes K_i, $i = 1, \ldots\ldots, M$.

Mathematically, the calibration on option prices can be stated as a least squares minimization problem: find $\boldsymbol{\mu} \in \mathcal{P}_{\text{opt}} \subset \mathcal{P}$ that solves

$$\min_{\boldsymbol{\mu}} J(\boldsymbol{\mu}), \qquad J(\boldsymbol{\mu}) := \frac{1}{M} \sum_{i=1}^{M} |P_i^{\text{obs}} - P_i(\boldsymbol{\mu})|^2, \tag{5.1.1}$$

where $P_i(\boldsymbol{\mu}) = P(S_0, T_i, K_i; \boldsymbol{\mu})$ are the model prices, which can be computed by, e.g., solving the PDE corresponding to the particular model. In Chapter 2 we saw that for European options, P_i solves

$$\frac{\partial P_i(\boldsymbol{\mu})}{\partial \tau} + \mathcal{L}(\boldsymbol{\mu}) P_i(\boldsymbol{\mu}) = 0, \qquad \text{in} \quad [0, T_i) \times \mathbb{R}^n_+, \tag{5.1.2a}$$

$$P_i(T_i; \boldsymbol{\mu}) = \mathcal{H}_i, \qquad \text{in} \quad \mathbb{R}^n_+, \tag{5.1.2b}$$

where $\mathcal{H}_i = (K_i - S)_+$ for the put and $\mathcal{H}_i = (S - K_i)_+$ for the call options and $n = 1, 2$. For the case of American put options we have

$$\frac{\partial P_i(\boldsymbol{\mu})}{\partial \tau} + \mathcal{L}(\boldsymbol{\mu}) P_i(\boldsymbol{\mu}) \leq 0, \qquad \text{in} \quad [0, T_i) \times \mathbb{R}^n_+, \tag{5.1.3a}$$

$$P_i(\boldsymbol{\mu}) \geq \mathcal{H}_i, \qquad \text{in} \quad [0, T_i) \times \mathbb{R}^n_+, \tag{5.1.3b}$$

$$\left(\frac{\partial P_i(\boldsymbol{\mu})}{\partial \tau} + \mathcal{L}(\boldsymbol{\mu}) P_i(\boldsymbol{\mu}) \right) (P_i(\boldsymbol{\mu}) - \mathcal{H}_i) = 0, \qquad \text{in} \quad [0, T_i) \times \mathbb{R}^n_+, \tag{5.1.3c}$$

$$P_i(T_i; \boldsymbol{\mu}) = \mathcal{H}_i, \qquad \text{in} \quad \mathbb{R}^n_+, \tag{5.1.3d}$$

with $\mathcal{H}_i := (K_i - S)_+$. Both models are subject to suitable boundary conditions. As before, the partial differential operator $\mathcal{L}$ is defined by the model used to price the option; see Chapter 2 for more details.

We note that, alternatively, one can work directly in the stochastic framework and compute P_i, e.g., by the Monte Carlo method or by the (binomial) tree method, see e.g., [CRR79]. For European options, one can also use analytic techniques such as closed-form solutions or FFT. However, since for complex options, such as American puts, in general, one can not expect to derive an analytic formula to value an option, this framework remains still restrictive. Therefore, to maintain the generality of our approach we focus on the calibration problem within the PDE framework.

The problem of type (5.1.1) is also referred in the literature as a PDE constrained optimization problem or an optimal control problem (in a reduced form). For American options, it is also interpreted as an optimal control problem constrained by parabolic variational inequalities. These problems have been extensively studied in the literature, cf. [Hin01; HR86; IK00; Mig76; MP84]. In the context of option pricing, we refer to, e.g., [Ach05; AIP04; AP05a; AP05b; BI97].

The solvability of (5.1.1) is accomplished by the construction of an appropriate numerical optimization algorithm coupled with the numerical approximation of the underlying PDE problem. The performance and the choice of the algorithm is directly connected to the properties of $J(\boldsymbol{\mu})$, such as differentiability, convexity etc. At each iteration of the optimization algorithm we evaluate several times the least square objective $J(\boldsymbol{\mu})$, which requires to solve M times a PDE. However, if one performs the usual log-transformation of the stock variable, $S = Ke^x$ (see Section 2.7), this reduces to a single solution of the underlying PDE. Indeed, in the new variable

$x = \log(S/K)$, the strike price K enters as a scaling factor in the PDE. Hence, taking $T = \max(T_i)$ and choosing some reference value of K, e.g., $K = 1$, for each $\boldsymbol{\mu}$, to find $P_i(\boldsymbol{\mu})$, $i = 1, \ldots, M$, reduces to solve the problem (5.1.2) or (5.1.3) only once.

Even though we can reduce the number of the PDE computations from M to a single evaluation, we still have to solve a high-fidelity problem, the cost of which, especially for complex options, can be very high. And since the market data is changing rapidly, there is a high demand to provide fast and efficient calibration routines. Accordingly, the use of model order reduction techniques to accelerate the optimization process are of high interest. One of the approaches is to replace the underlying complex model by the reduced-order surrogate one, which is constructed by, e.g., the POD or the reduced basis method. The employment of POD techniques for calibration gained its popularity in recent years, e.g., [SS08; SS14; SSS14]. The reduced basis method was studied in [CLP11; Pir09].

We also mention the application of model order reduction techniques in the general context of PDE constrained optimization problems. This comprises the works [SV10] using the POD method and recent work [DH15] for the reduced basis method. For inverse problems the method was applied in [GHH16].

For European options, the efficiency can be improved by using closed form solutions, see e.g., [GGM+12; MPS14; SST04]. The availability and fairly easy and cheap computations of these solutions make this approach very popular in applications.

In turn, for American options, which do not admit an analytic expansion, one can consider, the so called de-Americanization approach [BGG+16; CW10], which is frequently used among practitioners. This method translates American prices into European ones and then performs the calibration on the respective European prices by directly using the closed-form solutions for European options.

As we can see there is a high demand of fast, accurate and reliable techniques to calibration on option prices. Motivated by this example, the goal of this chapter is twofold. From one side, we seek to apply the previously developed methodology to the calibration on American options. And from another side, we introduce alternative techniques, such as the de-Americanization method and provide a numerical comparison of both approaches.

Due to the richer parameter nature of the Heston model and its ability to replicate closer the market behavior than the standard Black-Scholes model does, we restrict our consideration in this chapter to this model only. It is worth to mention that the reduced basis method as well as the other approaches investigated here are general enough that they can be easily adapted to different models.

The content of the chapter is structured as follows: We start in Section 5.2.1 by describing the optimization problem with the detailed model. In Section 5.2.2 and Section 5.2.3 we consider the optimization with the surrogate models, obtained by the RBM and the de-Americanization methods. In Section 5.2.4 we briefly comment on the optimization algorithms to solve the problems. Eventually, in Section 5.3

we supply the reader with numerous numerical examples of the calibration with the reduced-order models. We start in Section 5.3.1 by demonstrating the performance of the reduced basis method for calibrating on American and European options. Next, in Section 5.3.2, we take a look on the numerical study of the de-Americanization method. Then the comparison of both techniques is presented in Section 5.3.3 on the synthetic and in Section 5.3.3 on the real market data sets.

5.2 Calibration Procedure

5.2.1 Problem Setting

We describe the calibration problem for the Heston model. Recall the model parameter $\boldsymbol{\mu} = (\xi, \rho, \gamma, \kappa, r) \in \mathcal{P} \subset \mathbb{R}^5$. Apart from the interest rate r, the remaining parameters need to be identified. Given S_0 and the set of observations P_i^{obs} at (T_i, K_i), $i = 1, \dots, M$, we need to compute the corresponding prices in the Heston model $P_i(\nu_0, S_0, T_i, K_i)$, where $\nu_0 \in \mathbb{R}_+$ is the initial volatility. The value of ν_0 is not known and needs to be estimated together with the other parameters. We collect all parameters to be identified in the single vector $\boldsymbol{\Theta} = (\Theta_1, \dots, \Theta_5) = (\xi, \rho, \gamma, \kappa, \nu_0) \in \mathcal{P}_{\text{opt}}$, where

$$\mathcal{P}_{\text{opt}} := \left\{ \boldsymbol{\Theta} \in \mathbb{R}^5 : \Theta_{\min,i} \leq \Theta_i \leq \Theta_{\max,i}, \quad i = 1, \dots, 5 \right\}. \tag{5.2.1}$$

We replace the PDE constraints with the corresponding weak discrete problem in a log-transformed variable. To avoid repetition, we do not present the full procedure here and refer to Chapter 3 and Chapter 4, where the weak and discrete weak formulations for European and American options have been derived in detail. We remain in the same functional analytic settings as introduced in the aforementioned chapters. Recall, that suitably chosen discrete approximation spaces to price European and American options are denoted by $X_{\mathcal{N}} \subset X$, $V_{\mathcal{N}} \subset V$ and $(V_{\mathcal{N}}, W_{\mathcal{N}}) \subset (V, W)$ and the discrete cone by $M_{\mathcal{N}} \subset W_{\mathcal{N}}$. Let $t := T - \tau$ and denote by T the maximal maturity time, $T = \max(T_i)$, $i = 1, \dots, M$. The time interval $[0, T]$ is subdivided into I subintervals of equal length, $t^k = k\Delta t$, $0 < k \leq I$ with $\Delta t = T/I$. We consider the θ-weighted scheme for the time integration, in particular, $\theta = 1/2$. Recall the definition of the Dirichlet lift function $u_{L\mathcal{N}}^k(\nu, x; \boldsymbol{\mu})$ with $(\nu, x) \in \Omega$, where $\Omega = (\nu_{\min}, \nu_{\max}) \times (x_{\min}, x_{\max}) \subset \mathbb{R}^2$. For a given $\boldsymbol{\mu} \in \mathcal{P}$ we approximate $P(\nu, Ke^x, t^k; \boldsymbol{\mu})$ by $w_{\mathcal{N}}^k(\nu, x; \boldsymbol{\mu})$, where $w_{\mathcal{N}}^k(\nu, x; \boldsymbol{\mu}) := u_{\mathcal{N}}^k(\nu, x; \boldsymbol{\mu}) + u_{L\mathcal{N}}^k(\nu, x; \boldsymbol{\mu})$.

The detailed solution $u_{\mathcal{N}}^k(\boldsymbol{\mu}) \in V_{\mathcal{N}}$ for the European option problem solves the following discrete problem (see Problem 3.3.1)

$$\mathbb{E}_{\mathcal{N}}^{\text{EO}}(\boldsymbol{\mu}) = \begin{cases} \frac{1}{\Delta t} \left(u_{\mathcal{N}}^{k+1} - u_{\mathcal{N}}^k, v \right)_{L^2(\Omega)} + a(u_{\mathcal{N}}^{k+\theta}, v; \boldsymbol{\mu}) = f^{k+\theta}(v; \boldsymbol{\mu}), \\ (u_{\mathcal{N}}^0 - u^0, v)_V = 0, \qquad v \in V_{\mathcal{N}}. \end{cases}$$

Respectively, the solution pair $(u_{\mathcal{N}}^k(\boldsymbol{\mu}), \lambda_{\mathcal{N}}^k(\boldsymbol{\mu})) \in V_{\mathcal{N}} \times M_{\mathcal{N}}$ for the American option problem satisfies (see Problem 4.3.4)

$$\mathbb{E}_{\mathcal{N}}^{\mathrm{AO}}(\boldsymbol{\mu}) = \begin{cases} \frac{1}{\Delta t}\left(u_{\mathcal{N}}^{k+1} - u_{\mathcal{N}}^k, v\right)_{L^2(\Omega)} + a(u_{\mathcal{N}}^{k+\theta}, v; \boldsymbol{\mu}) - b(\lambda_{\mathcal{N}}^{k+1}, v) = f^{k+\theta}(v; \boldsymbol{\mu}), \\ b(\eta - \lambda_{\mathcal{N}}^{k+1}, u_{\mathcal{N}}^{k+1}) \geq g^{k+1}(\eta - \lambda_{\mathcal{N}}^{k+1}; \boldsymbol{\mu}), \qquad \eta \in M_{\mathcal{N}},\ v \in V_{\mathcal{N}}, \\ (u_{\mathcal{N}}^0 - u^0, v)_V = 0. \end{cases}$$

For $i = 1, \ldots, M$ we denote the approximate model price

$$P_i^{\mathcal{N},\mathrm{s}}(\boldsymbol{\Theta}) := w_{\mathcal{N}}^{k_i}(\log(S_0/K_i), \nu_0; \boldsymbol{\mu}),$$

where $w_{\mathcal{N}}^{k_i}(\boldsymbol{\mu}) := u_{\mathcal{N}}^{k_i}(\boldsymbol{\mu}) + u_{L\mathcal{N}}^{k_i}(\boldsymbol{\mu})$, and $u_{\mathcal{N}}^{k_i}(\boldsymbol{\mu})$ solves $\mathbb{E}_{\mathcal{N}} := \mathbb{E}_{\mathcal{N}}^s$, $s \in \{\mathrm{EO}, \mathrm{AO}\}$. By abuse of notation, we often omit the index s in the notation of $P_i^{\mathcal{N},s}$, if it is clear from the context. Then the minimization problem (5.1.1) can be written in the following form (often referred to as a reduced problem in the optimal control theory),

$$\min_{\boldsymbol{\Theta} \in \mathcal{P}_{\mathrm{opt}}} J_{\mathcal{N}}(\boldsymbol{\Theta}), \quad J_{\mathcal{N}}(\boldsymbol{\Theta}) := \frac{1}{M} \sum_{i=1}^{M} |P_i^{\mathrm{obs}} - P_i^{\mathcal{N}}(\boldsymbol{\Theta})|^2. \tag{5.2.2}$$

We comment on the solvability of the above finite dimensional minimization problem. Since for a given $\boldsymbol{\mu} \in \mathcal{P}$ under appropriate conditions there exist a unique solution $u_{\mathcal{N}}^k(\boldsymbol{\mu})$ of $\mathbb{E}_{\mathcal{N}}^{\mathrm{EO}}(\boldsymbol{\mu})$ or $\mathbb{E}_{\mathcal{N}}^{\mathrm{AO}}(\boldsymbol{\mu})$ (see Section 3.3.4 and Section 4.3.2), invoking the continuity of the solution map, we then can guarantee the existence of the global solution $\boldsymbol{\Theta} \in \mathcal{P}_{\mathrm{opt}}$ of (5.2.2). The uniqueness is more involved and studied depending on the particular properties of $J(\boldsymbol{\Theta})$, which is not convex, in the present case.

5.2.2 Reduced Basis Approximation

As it has been pointed out previously, the high-fidelity discrete problem $\mathbb{E}_{\mathcal{N}}$ is computationally expensive and significantly slows down the calibration procedure. To reduce the complexity we apply the reduced basis method and substitute the detailed model $\mathbb{E}_{\mathcal{N}}$ with the reduced-order surrogate one $\mathbb{E}_N$. The detailed procedure of the construction of the efficient reduced basis method is reported in Chapter 3 and Chapter 4 and omitted here to avoid redundancy.

Using a suitable basis generation procedure, see Section 3.4.3 and Section 4.6, we construct the low-dimensional reduced spaces $V_N \subset V_{\mathcal{N}}$ for European options and $V_N \subset V_{\mathcal{N}}$, $W_N \subset W_{\mathcal{N}}$, $M_N \subset M_{\mathcal{N}}$ for American options with $\dim(V_N) \ll \dim(V_{\mathcal{N}})$, $\dim(W_N) \ll \dim(W_{\mathcal{N}})$. The reduced surrogate models to price European

and American options are defined as follows

$$\mathbb{E}_N^{\mathrm{EO}}(\boldsymbol{\mu}) = \begin{cases} \frac{1}{\Delta t}\left(u_N^{k+1} - u_N^k, v\right)_{L^2(\Omega)} + a(u_N^{k+\theta}, v; \boldsymbol{\mu}) = f^{k+\theta}(v; \boldsymbol{\mu}), \\ (u_N^0 - u^0, v)_V = 0, \qquad v \in V_N. \end{cases}$$

$$\mathbb{E}_N^{\mathrm{AO}}(\boldsymbol{\mu}) = \begin{cases} \frac{1}{\Delta t}\left(u_N^{k+1} - u_N^k, v\right)_{L^2(\Omega)} + a(u_N^{k+\theta}, v; \boldsymbol{\mu}) - b(\lambda_N^{k+1}, v) = f^{k+\theta}(v; \boldsymbol{\mu}), \\ b(\eta - \lambda_N^{k+1}, u_N^{k+1}) \geq g^{k+1}(\eta - \lambda_N^{k+1}; \boldsymbol{\mu}), \qquad \eta \in M_N,\ v \in V_N, \\ (u_N^0 - u^0, v)_V = 0. \end{cases}$$

Analogously, for $i = 1, \ldots, M$ we denote the reduced basis approximation of the model price as

$$P_i^{N,s}(\boldsymbol{\Theta}) := w_N^{k_i}(\log(S_0/K_i), \nu_0; \boldsymbol{\mu}),$$

where $w_N^{k_i}(\boldsymbol{\mu}) := u_N^{k_i}(\boldsymbol{\mu}) + u_{L\mathcal{N}}^{k_i}(\boldsymbol{\mu})$, and $u_N^{k_i}(\boldsymbol{\mu})$ solves $\mathbb{E}_N := \mathbb{E}_N^s$, $s \in \{\mathrm{EO}, \mathrm{AO}\}$. Then we approximate $J_{\mathcal{N}}(\boldsymbol{\Theta}) \approx J_N(\boldsymbol{\Theta})$, and obtain the following minimization problem for the reduced model

$$\min_{\boldsymbol{\Theta} \in \mathcal{P}_{\mathrm{opt}}} J_N(\boldsymbol{\Theta}), \quad J_N(\boldsymbol{\Theta}) := \frac{1}{M} \sum_{i=1}^{M} |P_i^{\mathrm{obs}} - P_i^N(\boldsymbol{\Theta})|^2. \tag{5.2.3}$$

Remark 5.2.1. *Since the interest rate r is not a calibrated parameter and it is provided by the data set, for the construction of the reduced basis spaces, one may consider the variation of only four parameters $\boldsymbol{\mu} = (\xi, \rho, \gamma, \kappa) \in \mathcal{P} \subset \mathbb{R}^4$. However, this choice is restrictive and for new market data one needs to construct a new reduced basis set. Therefore, to conserve generality in our approach, we consider the variation of all parameters, $\boldsymbol{\mu} = (\xi, \rho, \gamma, \kappa, r)$, and consequently the constructed reduced basis will be entirely market-independent.*

5.2.3 De-Americanization Method (DAS)

The de-Americanization approach, which is frequently applied by practitioners, can also be considered as a model order reduction technique for calibration on American options. However, in contrast to the reduced basis framework, where the reduction was performed towards the underlying PDE constraints, in the de-Americanization method we substitute the original minimization problem by means of a perturbation of the given input data set. That is, given an input data of American put options, we consider minimization problem (5.2.2) with $J_{\mathcal{N}}(\boldsymbol{\Theta}) \approx \widetilde{J}_{\mathcal{N}}(\boldsymbol{\Theta})$,

$$\min_{\boldsymbol{\Theta} \in \mathcal{P}_{\mathrm{opt}}} \widetilde{J}_{\mathcal{N}}(\boldsymbol{\Theta}), \quad \widetilde{J}_{\mathcal{N}}(\boldsymbol{\Theta}) := \frac{1}{M} \sum_{i=1}^{M} |\widetilde{P}_i^{\mathrm{obs}} - P_i^{\mathcal{N}}(\boldsymbol{\Theta})|^2, \tag{5.2.4}$$

where the prices $\widetilde{P}_i^{\mathrm{obs}}$ are the pseudo-European put prices. These are obtained by perturbing American put prices P_i^{obs}, i.e., $\widetilde{P}_i^{\mathrm{obs}} := D(P_i^{\mathrm{obs}})$, where $D : \mathbb{R} \to \mathbb{R}$, and

the corresponding model prices are $P_i^{\mathcal{N}}(\boldsymbol{\Theta}) = P_i^{\mathcal{N},\mathrm{EO}}(\boldsymbol{\Theta})$, $i = 1, \dots, M$. Following the approach as in [BGG+16], we use the binomial tree method, see [CRR79], to transform American put option prices into pseudo-European ("de-Americanized") put prices.

The advantage of this method is that the complexity of the non-linear model for pricing American options can be reduced to that of the linear model for pricing European options. To perform a further reduction, one may consider instead of solving linear, but still high-dimensional problem $\mathbb{E}_{\mathcal{N}}^{EO}$, to use the closed-form solutions to evaluate the model prices. Denote the model prices, obtained by the closed-form solutions, by P_i^{CF}. For the European call option in the Heston model it is defined in (2.6.19). Using the put-call parity (2.4.15) the respective European put prices can be obtained.

Then we are dealing with the following minimization problem

$$\min_{\boldsymbol{\Theta}\in\mathcal{P}_{\mathrm{opt}}} \widetilde{J}_{\mathrm{CF}}(\boldsymbol{\Theta}), \quad \widetilde{J}_{\mathrm{CF}}(\boldsymbol{\Theta}) := \frac{1}{M}\sum_{i=1}^{M} |\widetilde{P}_i^{\mathrm{obs}} - P_i^{\mathrm{CF}}(\boldsymbol{\Theta})|^2. \tag{5.2.5}$$

As it was remarked previously, closed-form solutions can have limited applicability and in some cases, e.g., for the Heston model, one should make use of suitable numerical approximation techniques to approximate the integrals.

Being simple in implementation and efficient, the de-Americanization method, to the best of our knowledge, is lacking a rigorous theoretical framework. In [BGG+16] the de-Americanization error is numerically investigated for different models (CEV, Heston and Merton) and the settings, in which the application of the de-Americanization method leads to pitfalls, are explored. From the computational point of view, the method is very attractive, especially in combination with the closed-form solutions. However, for each set of observations, it requires an additional pre-processing time to transform the American data into European one, and, as we will see later, this cost can dominate significantly the computational cost of the entire calibration routine.

One could also consider a combination of the RBM with the de-Americanization strategy, i.e., applying the RBM to approximate $\mathbb{E}_{\mathcal{N}}^{\mathrm{EO}}$ by $\mathbb{E}_{N}^{\mathrm{EO}}$. The corresponding minimization problem can be stated as follows

$$\min_{\boldsymbol{\Theta}\in\mathcal{P}_{\mathrm{opt}}} \widetilde{J}_N(\boldsymbol{\Theta}), \quad \widetilde{J}_N(\boldsymbol{\Theta}) := \frac{1}{M}\sum_{i=1}^{M} |\widetilde{P}_i^{\mathrm{obs}} - P_i^{N}(\boldsymbol{\Theta})|^2, \tag{5.2.6}$$

with $P_i^N(\boldsymbol{\Theta}) = P_i^{N,\mathrm{EO}}(\boldsymbol{\Theta})$.

5.2.4 Optimization Algorithms

The minimization problems we have introduced belong to the class of finite dimensional optimization problems with box constraints. To solve such problems one needs

to employ an appropriate numerical optimization algorithm, which, ideally, would satisfy some basic requirements, e.g., to be robust, efficient and to identify the solution with sufficient accuracy. Among a wide variety of the existing algorithms, see, e.g., [NW06] for an overview, there is no general approach fulfilling all these requirements. The choice and construction of the algorithm is solely based on the structure and properties of the objective $J(\boldsymbol{\mu})$, such as convexity and differentiability, as well as the structure of the admissible set $\mathcal{P}_{\text{opt}}$. In general, the fastest algorithms, such as gradient-based ones, provide only a local solution. Global optimization algorithms, e.g., probabilistic methods as simulated annealing or genetic algorithms, do not require any information of the gradient. However, they are known to be computationally demanding.

For the particular case of the calibration with European options, the most popular algorithms are the gradient-based optimization methods; see, e.g., [AIP04; AP05a; AP05b; SS14]. By contrast, for American options, the situation is more involved not only due to the non-linearity of the underlying PDE model, but also due to the fact that one can not guarantee the differentiability of the solution map. The remedy is to apply regularization techniques, e.g., by adding penalty terms or smoothing the inequality constraints, e.g., [Ach05; Ach08; AP05a; Hin01; IK00; SW13].

Since the purpose of this chapter is to apply the reduced basis method to real-world examples and to compare it to alternative model reduction techniques, we do not consider this issues as a main focus of the work and leave a detailed study of the impact of the numerical solver of the optimization problem for future investigation.

For our numerical experiments we use the MATLAB Optimization Toolbox [Mat]. In particular, the built-in "black-box" optimization solver *lsqnonlin* or *fmincon*, in which the gradients are approximated by finite differences.

5.3 Numerical Results

For the numerical experiments we consider the setting for the Heston model as in Section 4.8. In particular, we set $X = H^1(\Omega)$, $V = H^1_{\Gamma_{\text{D}}}(\Omega)$ and $W = V'$. The approximate spaces $X_{\mathcal{N}}$, $V_{\mathcal{N}}$ are the standard conforming nodal first order finite elements. The dual space $W_{\mathcal{N}}$ is composed of the dual biorthogonal basis functions. We set $T = 2$ and $I = 250$, $\Delta t = T/I = 0.008$. The computational domain $\Omega = (\nu_{\min}, \nu_{\max}) \times (x_{\min}, x_{\max}) = (10^{-5}, 3) \times (-5, 5)$ is resolved by a triangulation with $\mathcal{N}_X = 4753$ nodes. For $\boldsymbol{\mu} = (\xi, \rho, \gamma, \kappa, r) \in \mathcal{P} \subset \mathbb{R}^5$ and $\boldsymbol{\Theta} = (\xi, \rho, \gamma, \kappa, \nu_0) \in \mathcal{P}^{\text{opt}} \subset \mathbb{R}^5$, we define

$$\mathcal{P} \equiv [0.1, 0.9] \times [-0.95, 0.95] \times [0.01, 0.5] \times [0.1, 5] \times [0.0001, 0.8], \tag{5.3.1}$$

$$\mathcal{P}^{\text{opt}} \equiv [0.1, 0.9] \times [-0.95, 0.3] \times [0.01, 0.5] \times [0.1, 5] \times [10^{-5}, 1]. \tag{5.3.2}$$

5.3.1 Calibration on Options with the RBM

For the detailed problem of pricing European, $\mathbb{E}_{\mathcal{N}}^{\mathrm{EO}}(\boldsymbol{\mu})$, and American put options, $\mathbb{E}_{\mathcal{N}}^{\mathrm{AO}}(\boldsymbol{\mu})$, in the Heston model the boundary conditions are chosen as in (2.7.10) and (2.7.14) respectively. We consider $\mathcal{P}_{\mathrm{train}}$ composed of uniformly distributed points in $\mathcal{P}$ with $|\mathcal{P}_{\mathrm{train}}| = 1024$ for the European put and $|\mathcal{P}_{\mathrm{train}}| = 3125$ for the American put options. The basis generations are conducted by using POD-Greedy algorithm (Algorithm 3.1), and POD-Angle-Greedy algorithm (Algorithm 4.1) with $E_u^{\mathrm{true}}(\boldsymbol{\mu})$ as a selection criterion for both models. In addition, for American options, we enrich V_N with supremizers to guarantee the stability of the reduced system. Accordingly, we obtain the dimensions of the reduced system as $N_{\max} = 100$ for European put and $N_{\max} = 125$ for American put options.

Unless otherwise stated, the calibration routine is performed with *lsqnonlin*, which uses a Trust-Region-Reflective algorithm, and the stopping criterion is set as $J(\boldsymbol{\Theta}) - J(\boldsymbol{\Theta}^\star) \leq 10^{-12}$, $\|\boldsymbol{\Theta} - \boldsymbol{\Theta}^\star\|_2 \leq 10^{-5}$, where $\boldsymbol{\Theta}^\star$ is a locally optimal solution.

Calibration on the Synthetic Data Set

First, we consider a performance of the RBM on a synthetic data set composed of option prices for different maturities and strikes under the following settings:

$$
\begin{aligned}
&S_0 = 1, \quad r = 5\%, \\
&T_1 = \frac{2}{12}, && K_1 = \{0.95, 0.975, 1, 1.025, 1.05\}, \\
&T_2 = \frac{6}{12}, && K_2 = K_1 \cup \{0.9, 0.925, 1.075, 1.1\}, \\
&T_3 = \frac{9}{12}, && K_3 = K_2 \cup \{0.85, 0.875, 1.125, 1.15\}, \\
&T_4 = 1, && K_4 = K_3 \cup \{0.8, 0.825, 1.175, 1.2\}, \\
&T_5 = 2, && K_5 = K_4 \cup \{0.75, 0.775, 1.225, 1.25\}.
\end{aligned}
\tag{5.3.3}
$$

For each pair $(T_i, K_i)_{i=1,\dots,5}$, we generate two artificial sets of observations P^{obs} which consist of 65 European and American put options computed at $\boldsymbol{\Theta} = \boldsymbol{\Theta}_{\mathrm{ex}} = (0.7, -0.8, 0.3, 1.4, 0.3)$. That is, we solve the detailed problems (5.2.2) with $\mathbb{E}_{\mathcal{N}}^{\mathrm{AO}}$ and $\mathbb{E}_{\mathcal{N}}^{\mathrm{EO}}$ for the parameter $\boldsymbol{\mu} = (0.7, -0.8, 0.3, 1.4, 0.3)$ and $K = 1$ and interpolate the corresponding solutions $K_i u_{\mathcal{N}}^{k_i}(\nu, x; \boldsymbol{\mu})$ at $\nu^\star = \nu_0$, $x_i^\star = \log(S_0/K_i)$.

We perform the optimization routine with the reduced surrogate model (5.2.3). To verify the approach, we also carry out the optimization with the high-fidelity detailed problem (5.2.2). For both procedures we use the same initial guess $\boldsymbol{\Theta}_{\mathrm{in}}$ for the numerical optimization routine. The results of the calibration for two different data sets of American and European options are presented in Table 5.1a. We observe that using the detailed models $\mathbb{E}_{\mathcal{N}}^{s}$, $s \in \{\mathrm{AO}, \mathrm{EO}\}$ we can recover the exact parameter

$\boldsymbol{\Theta}_{\text{ex}}$ up to the parameter tolerance. For the reduced surrogate models we observe a slight deviation of the parameters from the exact one, however the results remain still accurate enough.

The graphical illustration of the results can be found in Figure 5.1 and Figure 5.3 for American and European put options respectively. In the plots, we hardly can observe any differences in the option price obtained from the synthetic and the calibrated data with the detailed problem and with the reduced problem. To quantify the differences between the reduced and detailed calibration, we plot the pointwise absolute relative errors $|P_i^{\text{obs}} - P_i^s(\boldsymbol{\Theta}^\star)|/P_i^{\text{obs}}$, $s \in \{\mathcal{N}, N\}$, $i = 1, \ldots, M$, in Figure 5.2 and in Figure 5.4. We observe that the reduced models produce very good fit to the observed synthetic data with the relative error within the 0.5% margin.

The run-time performance is reported in Table 5.1b. We notice that the optimization routine with the surrogate reduced model is about 100 times faster for American put options and about 350 times faster for European put options.

In addition, one can observe that the reduced model for American options recovers the parameter slightly better than the European one, which intuitively would seem surprising. This fact can be explained by the larger dimension of the reduced system for American options and the larger training set, which is is also reflected in the run-time performance. Consequently, depending on the priority of the task, i.e., accuracy vs. efficiency, one can always manually adjust the dimension of the reduced system.

It is well known that optimization algorithms are sensitive to the initial guess. To study the robustness of the algorithm w.r.t. an initial guess, we consider a sample of 30 initial values $\boldsymbol{\Theta}_{\text{in}}$, randomly distributed in $\mathcal{P}^{\text{opt}}$ for both cases of American and European put options. We averaged the results and for American (European) options these are: $\boldsymbol{\Theta}^\star = (0.6940, -0.8314, 0.2983, 1.4466, 0.3013)$ ($\boldsymbol{\Theta}^\star = (0.6162, -0.8858, 0.2926, 1.3063, 0.3003)$), the average number of iterations is 18 (17), the average number of function evaluations $\#J$ is 114 (108), the average time for calibration is 12.56 min (2.58 min). These results are similar to the ones reported in Table 5.1, which suggests that the optimization algorithm is robust with respect to an initial guess.

5.3.2 Numerical Study of the de-Americanization Approach

Next, we turn to the numerical investigation of the de-Americanization method as an alternative model reduction approach to calibrate with American put options, which was briefly described in Section 5.2.3. Since we are not aware of any theoretical study on the approximation quality of the method, we try to examine it numerically in various scenarios. For a more detailed parameter study of the de-Americanization effect we refer to [BGG$^+$16].

First, we study the approach and the errors caused by transforming from American to European options. In particular we investigate the discrepancy of the de-Americanized put options with the corresponding American ones. We consider the

Method	$\mathbb{E}(\boldsymbol{\mu})$	$\boldsymbol{\Theta}$	ξ	ρ	γ	κ	ν_0	$\|\boldsymbol{\Theta}_{\text{ex}} - \boldsymbol{\Theta}^\star\|_2$
		$\boldsymbol{\Theta}_{\text{ex}}$	0.700	−0.800	0.300	1.400	0.300	
		$\boldsymbol{\Theta}_{\text{in}}$	0.601	−0.682	0.487	2.020	0.496	
$J_{\mathcal{N}}(\boldsymbol{\Theta})$	$\mathbb{E}_{\mathcal{N}}^{\text{AO}}$	$\boldsymbol{\Theta}^\star$	0.700	−0.800	0.300	1.399	0.300	2.14e − 05
$J_N(\boldsymbol{\Theta})$	$\mathbb{E}_N^{\text{AO}}$	$\boldsymbol{\Theta}^\star$	0.694	−0.831	0.298	1.447	0.303	5.62e − 02
$J_{\mathcal{N}}(\boldsymbol{\Theta})$	$\mathbb{E}_{\mathcal{N}}^{\text{EO}}$	$\boldsymbol{\Theta}^\star$	0.700	−0.800	0.300	1.399	0.300	2.05e − 05
$J_N(\boldsymbol{\Theta})$	$\mathbb{E}_N^{\text{EO}}$	$\boldsymbol{\Theta}^\star$	0.616	−0.886	0.293	1.306	0.300	1.52e − 01

(a) Parameters obtained by the calibration routine.

Method	$\mathbb{E}(\boldsymbol{\mu})$	# iter.	# J	calib. time	$J(\boldsymbol{\Theta}^\star)$
$J_{\mathcal{N}}(\boldsymbol{\Theta})$	$\mathbb{E}_{\mathcal{N}}^{\text{AO}}$	7	48	15.59 hrs	1.698e − 16
$J_N(\boldsymbol{\Theta})$	$\mathbb{E}_N^{\text{AO}}$	8	54	9.50 min	9.515e − 09
$J_{\mathcal{N}}(\boldsymbol{\Theta})$	$\mathbb{E}_{\mathcal{N}}^{\text{EO}}$	7	48	11.67 hrs	1.242e − 16
$J_N(\boldsymbol{\Theta})$	$\mathbb{E}_N^{\text{EO}}$	11	72	1.996 min	1.157e − 08

(b) Calibration results in terms of the run-time performance. The number "# iter." corresponds to the number of iterations and "# J" is the total number of function evaluations performed by the optimization routine.

Table 5.1: Calibration results for the synthetic data set of American and European put options in the Heston model using different approaches.

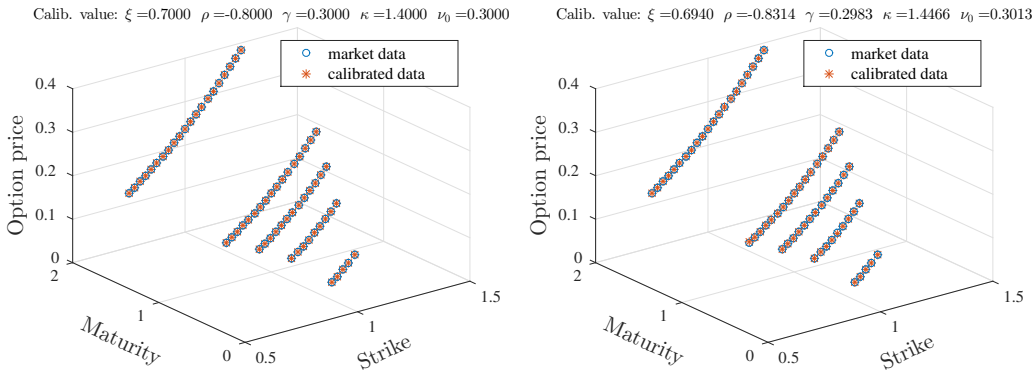

Figure 5.1: Results of the calibration to the synthetic data set of American put options in the Heston model using the detailed model $\mathbb{E}_{\mathcal{N}}(\boldsymbol{\mu})$ (left) and the reduced surrogate model $\mathbb{E}_N(\boldsymbol{\mu})$ (right). The circles are the synthetic prices and the stars are the prices in the calibrated model.

following settings

$$
\begin{aligned}
S_0 &= 1 \\
K &= \{0.80, 0.85, 0.90, 0.95, 1.00, 1.05, 1.10, 1.15, 1.20\} \\
T &= \left\{\frac{1}{12}, \frac{2}{12}, \frac{3}{12}, \frac{4}{12}, \frac{6}{12}, \frac{9}{12}, \frac{12}{12}, \frac{24}{12}\right\} \\
r &= \{0, 0.01, 0.02, 0.05, 0.07\}\,.
\end{aligned}
$$

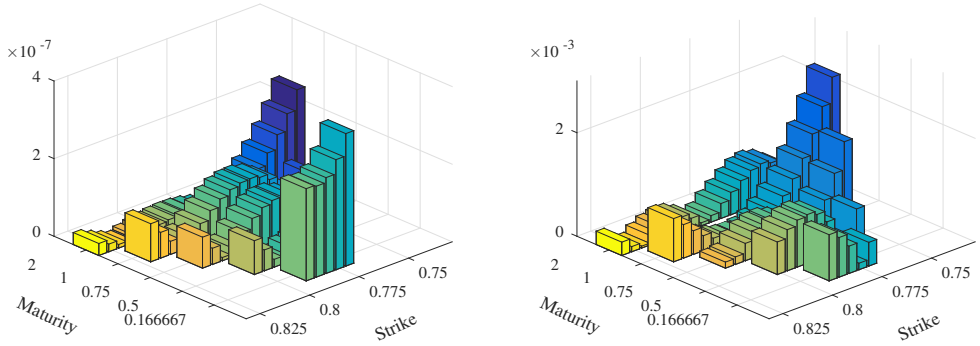

Figure 5.2: Calibration results for the synthetic data set of American put options in terms of pointwise absolute relative errors, $|P_i^{\text{obs}} - P_i^{s,\text{AO}}(\boldsymbol{\Theta}^\star)|/P_i^{\text{obs}}$, $i = 1, \ldots, M$, using the Heston model. Left: calibration with the detailed model $\mathbb{E}_{\mathcal{N}}(\boldsymbol{\mu})$, $s = \mathcal{N}$. Right: calibration with the reduced surrogate model $\mathbb{E}_N(\boldsymbol{\mu})$, $s = N$.

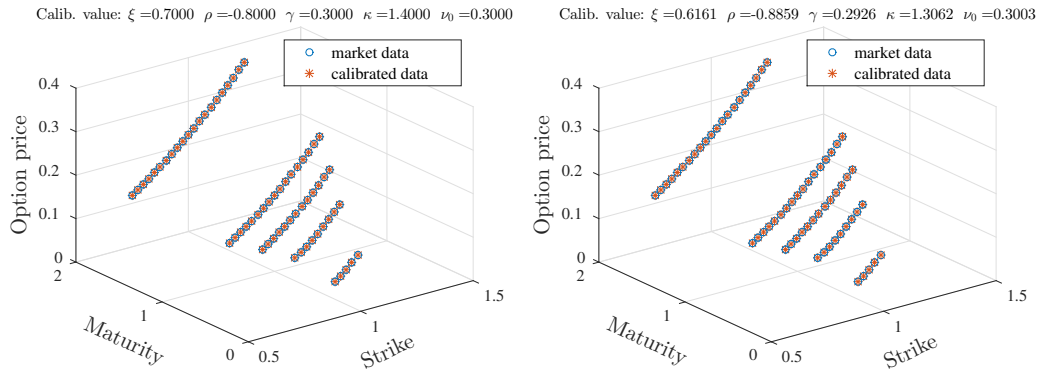

Figure 5.3: Results of the calibration to the synthetic data set of European put options in the Heston model using the detailed model $\mathbb{E}_{\mathcal{N}}(\boldsymbol{\mu})$ (left) and the reduced surrogate model $\mathbb{E}_N(\boldsymbol{\mu})$ (right). The circles are the synthetic prices and the stars are the prices in the calibrated model.

We consider different scenarios that correspond to the different values of the parameter $\boldsymbol{\Theta}$, presented in Table 5.2. We comment on the choice of these parameters. Since, in statistical tests it is commonly observed that the correlation between stocks and their volatilities is negative (the leverage effect), we exclude positive values of the parameter ρ in our scenarios. Starting from scenario p_1, we increase the volatility of volatility parameter ξ and decrease the correlation ρ, and accordingly increase

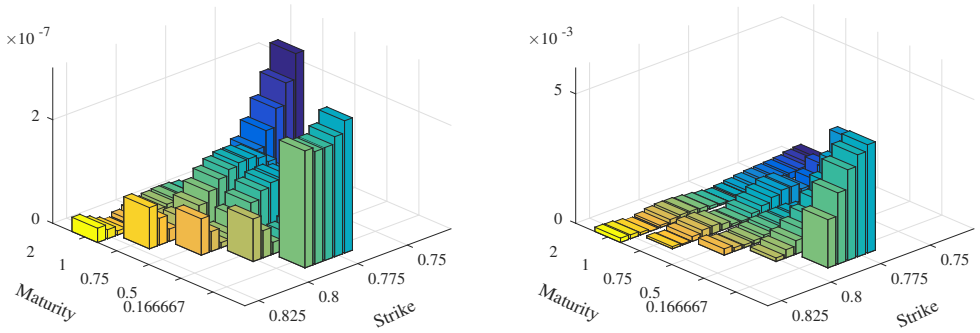

Figure 5.4: Calibration results for the synthetic data set of European put options in terms of pointwise absolute relative errors, $|P_i^{\text{obs}} - P_i^{s,\text{EO}}(\boldsymbol{\Theta}^\star)|/P_i^{\text{obs}}$, $i = 1, \ldots, M$, using the Heston model. Left: calibration with the detailed model $\mathbb{E}_{\mathcal{N}}(\boldsymbol{\mu})$, $s = \mathcal{N}$. Right: calibration with the reduced surrogate model $\mathbb{E}_N(\boldsymbol{\mu})$, $s = N$.

the long-run variance γ and the mean reversion speed κ. In all scenarios the initial volatility is set to the value of the mean reversion γ, i.e., $\nu_0 = \gamma$.

Scenario	ξ	ρ	γ	κ	ν_0
p_1	0.10	−0.20	0.07	0.1	0.07
p_2	0.25	−0.50	0.10	0.4	0.10
p_3	0.40	−0.50	0.15	0.6	0.15
p_4	0.55	−0.45	0.20	1.2	0.20
p_5	0.70	−0.80	0.30	1.4	0.30

Table 5.2: Overview of the parameter sets for the Heston model, used to study the de-Americanization approach.

For these parameter scenarios we construct different synthetic data sets, i.e., the data sets corresponding to the different values of the parameters $\boldsymbol{\Theta}_i$ and interest rates r_j, $i, j = 1, \ldots, 5$. Each data set is composed of the respective American put option prices in the Heston model, $P_i^{\mathcal{N},\text{AO}}$, $i = 1, \ldots, 72$, computed for each pair (T_i, K_j), $i = 1, \ldots, 8$, $j = 1, \ldots, 9$. Then, applying the de-Americanized approach, we translate these option prices into the corresponding European put prices $\widetilde{P}_i^{\mathcal{N},\text{EO}} := D(P_i^{\mathcal{N},\text{AO}})$. To investigate the error produced by this transformation, we compare the European put prices produced by the de-Americanization method $\widetilde{P}_i^{\mathcal{N},\text{EO}}$ with the European put prices obtained by solving the Heston PDE directly, $P_i^{\mathcal{N},\text{EO}}$. The values of maximal error ($\max_i |\widetilde{P}_i^{\mathcal{N},\text{EO}}(\boldsymbol{\Theta}) - P_i^{\mathcal{N},\text{EO}}(\boldsymbol{\Theta})|$) are presented in Table 5.3. The reference values

$(\max_i P_i^{\mathcal{N},\mathrm{EO}}(\boldsymbol{\Theta}))$ are presented in the second column of the table.

		Maximal absolute difference								Maximal European price							
		T_1	T_2	T_3	T_4	T_5	T_6	T_7	T_8	T_1	T_2	T_3	T_4	T_5	T_6	T_7	T_8
p_1	$r = 0\%$	1e−6	8e−7	7e−7	2e−7	7e−7	6e−7	2e−6	2e−6	0.200	0.202	0.205	0.209	0.217	0.229	0.240	0.278
	$r = 1\%$	3e−4	1e−4	1e−4	9e−5	7e−5	6e−5	5e−5	6e−5	0.199	0.200	0.202	0.205	0.212	0.222	0.231	0.261
	$r = 2\%$	3e−4	1e−4	2e−4	1e−4	1e−4	8e−5	5e−5	1e−4	0.198	0.198	0.200	0.202	0.207	0.214	0.221	0.244
	$r = 5\%$	5e−4	2e−3	2e−4	1e−4	2e−4	2e−4	9e−5	3e−4	0.195	0.193	0.191	0.191	0.192	0.194	0.195	0.198
	$r = 7\%$	6e−4	3e−3	7e−3	3e−5	8e−5	3e−4	2e−4	2e−4	0.194	0.189	0.186	0.184	0.182	0.180	0.179	0.171
p_2	$r = 0\%$	5e−7	5e−7	4e−7	5e−7	7e−7	7e−7	1e−6	2e−7	0.201	0.204	0.208	0.214	0.224	0.238	0.251	0.293
	$r = 1\%$	1e−4	7e−5	8e−5	5e−5	2e−5	1e−5	5e−5	2e−4	0.200	0.202	0.206	0.210	0.219	0.231	0.242	0.277
	$r = 2\%$	7e−4	1e−4	1e−4	6e−5	2e−5	3e−5	9e−5	4e−4	0.199	0.200	0.203	0.207	0.214	0.224	0.233	0.261
	$r = 5\%$	8e−4	6e−5	3e−4	9e−5	2e−5	2e−5	7e−5	4e−4	0.196	0.195	0.195	0.197	0.200	0.204	0.208	0.217
	$r = 7\%$	1e−3	5e−3	3e−6	1e−4	4e−5	6e−5	7e−5	5e−5	0.194	0.191	0.190	0.190	0.191	0.192	0.193	0.192
p_3	$r = 0\%$	1e−6	2e−6	1e−6	7e−7	6e−7	6e−7	5e−7	3e−6	0.202	0.208	0.216	0.224	0.238	0.256	0.273	0.326
	$r = 1\%$	8e−5	5e−5	4e−5	1e−5	2e−5	6e−5	1e−4	3e−4	0.201	0.207	0.213	0.220	0.233	0.250	0.264	0.309
	$r = 2\%$	2e−4	7e−5	7e−5	8e−6	5e−5	1e−4	2e−4	6e−4	0.200	0.205	0.211	0.217	0.228	0.243	0.255	0.294
	$r = 5\%$	2e−4	1e−4	1e−4	1e−5	1e−4	3e−4	4e−4	1e−3	0.197	0.199	0.203	0.207	0.215	0.224	0.231	0.250
	$r = 7\%$	2e−3	1e−4	2e−4	2e−5	2e−4	3e−4	4e−4	8e−4	0.195	0.196	0.198	0.201	0.206	0.212	0.216	0.225
p_4	$r = 0\%$	4e−8	8e−7	2e−6	4e−8	2e−6	2e−6	3e−6	2e−6	0.204	0.214	0.224	0.234	0.252	0.275	0.295	0.362
	$r = 1\%$	7e−5	3e−5	2e−5	2e−6	3e−5	6e−5	9e−5	3e−4	0.203	0.212	0.221	0.231	0.247	0.268	0.287	0.345
	$r = 2\%$	1e−4	4e−5	4e−5	2e−5	7e−5	1e−4	2e−4	6e−4	0.202	0.210	0.219	0.227	0.243	0.262	0.278	0.329
	$r = 5\%$	3e−4	6e−5	7e−5	8e−5	2e−4	3e−4	4e−4	1e−3	0.199	0.205	0.211	0.218	0.229	0.243	0.255	0.286
	$r = 7\%$	3e−4	6e−5	9e−5	1e−4	3e−4	4e−4	5e−4	1e−3	0.197	0.202	0.207	0.212	0.221	0.231	0.240	0.259
p_5	$r = 0\%$	5e−7	4e−7	2e−7	4e−7	8e−7	4e−6	6e−6	4e−6	0.207	0.222	0.234	0.248	0.270	0.297	0.322	0.400
	$r = 1\%$	6e−5	3e−5	2e−5	9e−6	6e−5	2e−4	3e−4	1e−3	0.206	0.220	0.232	0.245	0.265	0.291	0.314	0.384
	$r = 2\%$	1e−4	5e−5	5e−5	1e−5	1e−4	3e−4	5e−4	2e−3	0.205	0.218	0.230	0.242	0.261	0.285	0.306	0.369
	$r = 5\%$	2e−4	1e−4	1e−4	3e−5	1e−4	4e−4	9e−4	3e−3	0.202	0.213	0.223	0.233	0.249	0.268	0.283	0.326
	$r = 7\%$	3e−4	1e−4	2e−4	9e−5	6e−5	4e−4	8e−4	3e−3	0.201	0.210	0.219	0.227	0.241	0.257	0.269	0.300

Table 5.3: Summary of the de-Americanization effects for the Heston model.

We observe that for each parameter setting the de-Americanization error tends to increase with increasing interest rate r. We can also see that for $r = 0\%$ the de-Americanization has the weakest effect. Another observation is that, for scenarios p_4 and p_5, where the volatility of volatility ξ and correlation ρ have high magnitudes, the de-Americanization has the strongest effect. These findings can be traced also in the reconstruction of these parameters in the calibration routine, as we will see in the next section. Additionally, we notice that for short maturities the de-Americanized price is lower than the according European price, whereas for high maturities the de-Americanized price is higher than the European one.

5.3.3 Comparison of Different Model Reduction Approaches

In this section we perform a numerical comparison of the calibration with American put options using different model reduction techniques: the reduced basis method, the de-Americanization approach and the combination of both techniques. That is, we consider the minimization problems (5.2.3), (5.2.4) and (5.2.6). For the purposes of comparison, we also carry out the calibration with the detailed solver (5.2.2).

First, we generated a synthetic set of observations P^{obs} with the settings as in (5.3.3). We consider different parameter scenarios corresponding to different values of $\boldsymbol{\Theta} \in \mathcal{P}_{\mathrm{opt}}$; see Table 5.4. For each scenario, we construct an artificial set of observations

$P_i^{\text{obs}} := P_i^{\mathcal{N},\text{AO}}$, $i = 1, \ldots, 65$. We note that, in general, the parameter κ is price-insensitive, see, e.g. [JKW+11], and thus it can not be reconstructed. Therefore, for each scenario we fix the parameter κ to its exact value and do the parameter estimation only for the remaining parameters ξ, ρ, γ, and ν_0.

Scenario	ξ	ρ	γ	κ	ν_0
p_1	0.10	−0.20	0.07	0.5	0.07
p_2	0.25	−0.50	0.10	0.5	0.10
p_3	0.40	−0.50	0.15	0.6	0.15
p_4	0.55	−0.45	0.20	1.2	0.20
p_5	0.70	−0.80	0.30	1.4	0.30
p_6	0.2928	−0.7571	0.0707	0.6067	0.0707

Table 5.4: Overview of the parameter sets used to generate the synthetic data set.

The results of the calibration are summarized in Table 5.5. We observe that, overall, all methods provide a good reconstruction of the parameters. The optimization routine with the detailed solver identifies the parameter up to the optimization tolerance, that demonstrates the robustness of the optimization algorithm.

For clarity, the graphical illustration of these scenarios using different model reduction techniques is depicted in Figure 5.5. To eliminate the effect of different scaling we also present the value of each parameter in Figure 5.6. It can be seen that for all approaches the main difficulty lies in identifying ξ and ρ. In fact, this tendency has been also observed for the detailed solver (see cases p_1, p_4, Table 5.5). The remaining parameters γ and ν_0 are recovered almost exactly. We also note that for scenarios p_1–p_3, which correspond to the cases when the magnitudes of ξ, ν_0 and ρ are the smallest, the calibration with the de-Americanized approach is able to provide a better reconstruction of the parameter ξ than the reduced basis method. By contrast, in the scenarios p_4 and p_5, which correspond to large magnitude of the correlation parameter, the de-Americanization gives poorer results for ξ and ρ. This is consistent with the observation made in Section 5.3.2, where we noticed that the errors caused by de-Americanization are the largest in the cases where the absolute values of ξ and ρ are large (see Table 5.3, scenario p_5, maturity T_8).

To summarize, we can say that the cases with "extreme" parameter values have a significant impact on the performance of the optimization routine, in both the detailed and the reduced problems. In the case of the reduced basis method, this difficulty may be overcome by considering, e.g., an adaptive parameter domain partition, see [HDO11], in particular for ξ and ρ or by increasing the number of snapshots, and furthermore increasing the dimension of the reduced system.

As the next step we study the efficiency of both methods. The statistical data about the run-time performance is given in Table 5.6. We observe that all reduction

Scenario	Method	$\mathbb{E}(\boldsymbol{\mu})$	$\boldsymbol{\Theta}$	ξ	ρ	γ	ν_0	$J(\boldsymbol{\Theta}^\star)$
			$\boldsymbol{\Theta}_{\text{ex}}$	0.1	−0.2	0.07	0.07	
	$J_{\mathcal{N}}(\boldsymbol{\Theta})$	$\mathbb{E}_{\mathcal{N}}^{\text{AO}}$	$\boldsymbol{\Theta}^\star$	0.1002	−0.1997	0.07	0.07	7.8806e−14
p_1	$\widetilde{J}_{\mathcal{N}}(\boldsymbol{\Theta})$	$\mathbb{E}_{\mathcal{N}}^{\text{EO}}$	$\boldsymbol{\Theta}^\star$	0.1000	−0.3003	0.0701	0.0688	1.0248e−07
	$J_N(\boldsymbol{\Theta})$	$\mathbb{E}_N^{\text{AO}}$	$\boldsymbol{\Theta}^\star$	0.1477	−0.0788	0.0697	0.0700	4.3440e−08
	$\widetilde{J}_N(\boldsymbol{\Theta})$	$\mathbb{E}_N^{\text{EO}}$	$\boldsymbol{\Theta}^\star$	0.1849	−0.1801	0.0772	0.0634	3.2571e−07
			$\boldsymbol{\Theta}_{\text{ex}}$	0.25	−0.5	0.1	0.1	
	$J_{\mathcal{N}}(\boldsymbol{\Theta})$	$\mathbb{E}_{\mathcal{N}}^{\text{AO}}$	$\boldsymbol{\Theta}^\star$	0.25	−0.5	0.1	0.1	6.4756e−17
p_2	$\widetilde{J}_{\mathcal{N}}(\boldsymbol{\Theta})$	$\mathbb{E}_{\mathcal{N}}^{\text{EO}}$	$\boldsymbol{\Theta}^\star$	0.2404	−0.5388	0.1001	0.0991	1.1363e−08
	$J_N(\boldsymbol{\Theta})$	$\mathbb{E}_N^{\text{AO}}$	$\boldsymbol{\Theta}^\star$	0.2860	−0.4824	0.0968	0.1015	9.9148e−08
	$\widetilde{J}_N(\boldsymbol{\Theta})$	$\mathbb{E}_N^{\text{EO}}$	$\boldsymbol{\Theta}^\star$	0.2973	−0.4104	0.1087	0.0959	1.1681e−07
			$\boldsymbol{\Theta}_{\text{ex}}$	0.4	−0.5	0.15	0.15	
	$J_{\mathcal{N}}(\boldsymbol{\Theta})$	$\mathbb{E}_{\mathcal{N}}^{\text{AO}}$	$\boldsymbol{\Theta}^\star$	0.4	−0.5	0.15	0.15	2.9834e−18
p_3	$\widetilde{J}_{\mathcal{N}}(\boldsymbol{\Theta})$	$\mathbb{E}_{\mathcal{N}}^{\text{EO}}$	$\boldsymbol{\Theta}^\star$	0.4282	−0.4620	0.1544	0.1492	2.2003e−09
	$J_N(\boldsymbol{\Theta})$	$\mathbb{E}_N^{\text{AO}}$	$\boldsymbol{\Theta}^\star$	0.3537	−0.5731	0.1456	0.1504	6.2085e−09
	$\widetilde{J}_N(\boldsymbol{\Theta})$	$\mathbb{E}_N^{\text{EO}}$	$\boldsymbol{\Theta}^\star$	0.4576	−0.4155	0.1519	0.1484	4.4351e−08
			$\boldsymbol{\Theta}_{\text{ex}}$	0.55	−0.45	0.2	0.2	
	$J_{\mathcal{N}}(\boldsymbol{\Theta})$	$\mathbb{E}_{\mathcal{N}}^{\text{AO}}$	$\boldsymbol{\Theta}^\star$	0.5502	−0.4499	0.2	0.2	4.8235e−14
p_4	$\widetilde{J}_{\mathcal{N}}(\boldsymbol{\Theta})$	$\mathbb{E}_{\mathcal{N}}^{\text{EO}}$	$\boldsymbol{\Theta}^\star$	0.5801	−0.4220	0.2044	0.1989	1.5377e−09
	$J_N(\boldsymbol{\Theta})$	$\mathbb{E}_N^{\text{AO}}$	$\boldsymbol{\Theta}^\star$	0.5048	−0.4980	0.1989	0.1995	1.6681e−08
	$\widetilde{J}_N(\boldsymbol{\Theta})$	$\mathbb{E}_N^{\text{EO}}$	$\boldsymbol{\Theta}^\star$	0.5359	−0.4473	0.2013	0.1989	1.9256e−08
			$\boldsymbol{\Theta}_{\text{ex}}$	0.7	−0.8	0.3	0.3	
	$J_{\mathcal{N}}(\boldsymbol{\Theta})$	$\mathbb{E}_{\mathcal{N}}^{\text{AO}}$	$\boldsymbol{\Theta}^\star$	0.7	−0.8	0.3	0.3	3.4388e−18
p_5	$\widetilde{J}_{\mathcal{N}}(\boldsymbol{\Theta})$	$\mathbb{E}_{\mathcal{N}}^{\text{EO}}$	$\boldsymbol{\Theta}^\star$	0.8433	−0.6668	0.3170	0.2990	1.8369e−08
	$J_N(\boldsymbol{\Theta})$	$\mathbb{E}_N^{\text{AO}}$	$\boldsymbol{\Theta}^\star$	0.6881	−0.8259	0.2994	0.3006	1.0533e−08
	$\widetilde{J}_N(\boldsymbol{\Theta})$	$\mathbb{E}_N^{\text{EO}}$	$\boldsymbol{\Theta}^\star$	0.7718	−0.7136	0.3102	0.2991	2.3145e−08
			$\boldsymbol{\Theta}_{\text{ex}}$	0.2928	−0.7571	0.0707	0.0707	
	$J_{\mathcal{N}}(\boldsymbol{\Theta})$	$\mathbb{E}_{\mathcal{N}}^{\text{AO}}$	$\boldsymbol{\Theta}^\star$	0.2928	−0.7571	0.0707	0.0707	6.5746e−18
p_6	$\widetilde{J}_{\mathcal{N}}(\boldsymbol{\Theta})$	$\mathbb{E}_{\mathcal{N}}^{\text{EO}}$	$\boldsymbol{\Theta}^\star$	0.3690	−0.6026	0.0736	0.0685	1.6179e−07
	$J_N(\boldsymbol{\Theta})$	$\mathbb{E}_N^{\text{AO}}$	$\boldsymbol{\Theta}^\star$	0.3096	−0.7049	0.0700	0.0718	9.6369e−08
	$\widetilde{J}_N(\boldsymbol{\Theta})$	$\mathbb{E}_N^{\text{EO}}$	$\boldsymbol{\Theta}^\star$	0.3527	−0.5209	0.0814	0.0638	3.5672e−07

Table 5.5: Calibration results on American put options in the Heston model with different model reduction techniques.

approaches provide a significant speed-up compared to the expensive detailed solver, which on average takes about eight hours for each scenario. We also note that, despite the computational efficiency of the de-Americanization method in the calibration process, it requires an additional time to pre-process the data, i.e., to transform the American prices into the corresponding pseudo-European ones. This deteriorates

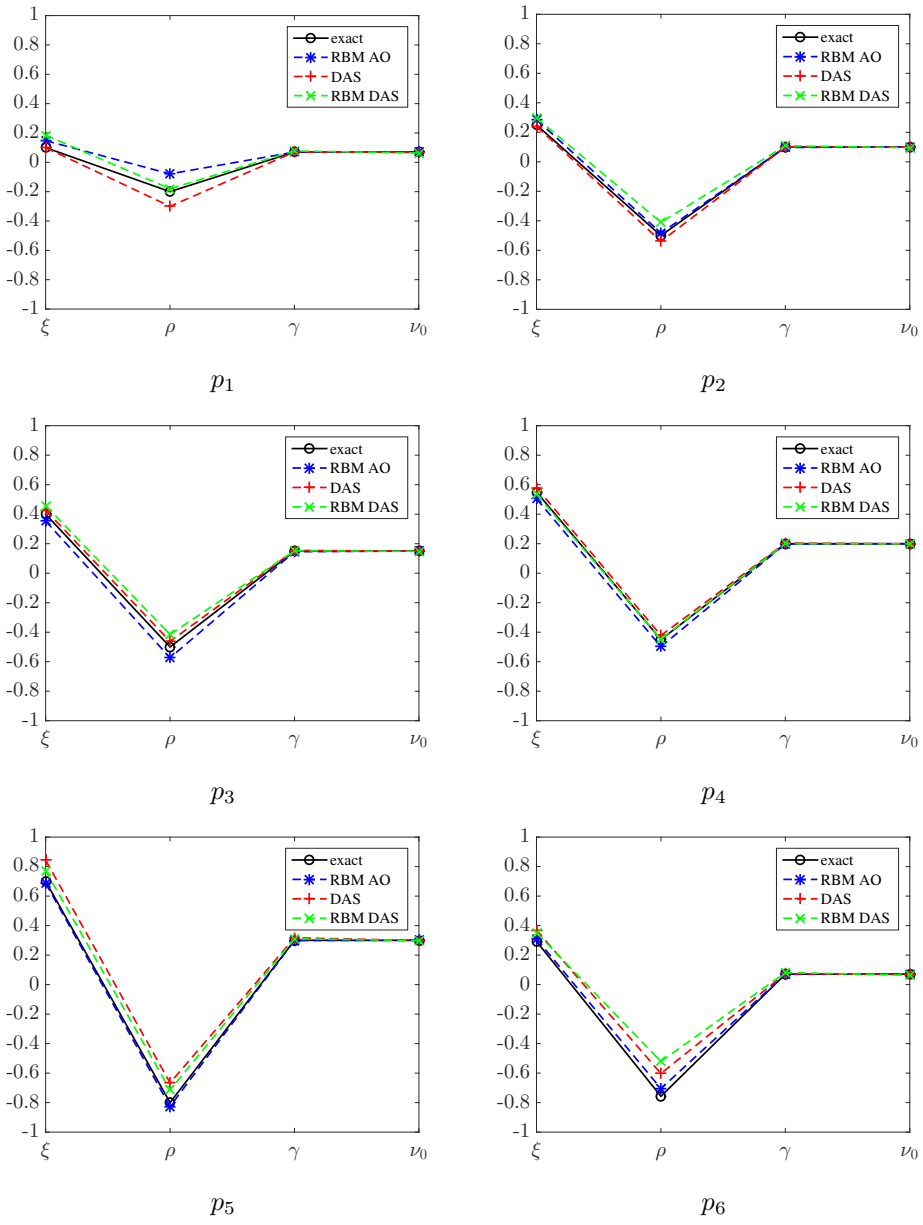

Figure 5.5: Graphical illustration of the reconstructed parameters for different scenarios obtained by calibrating on American put options in the Heston model using different model reduction approaches.

significantly the overall efficiency of the method.

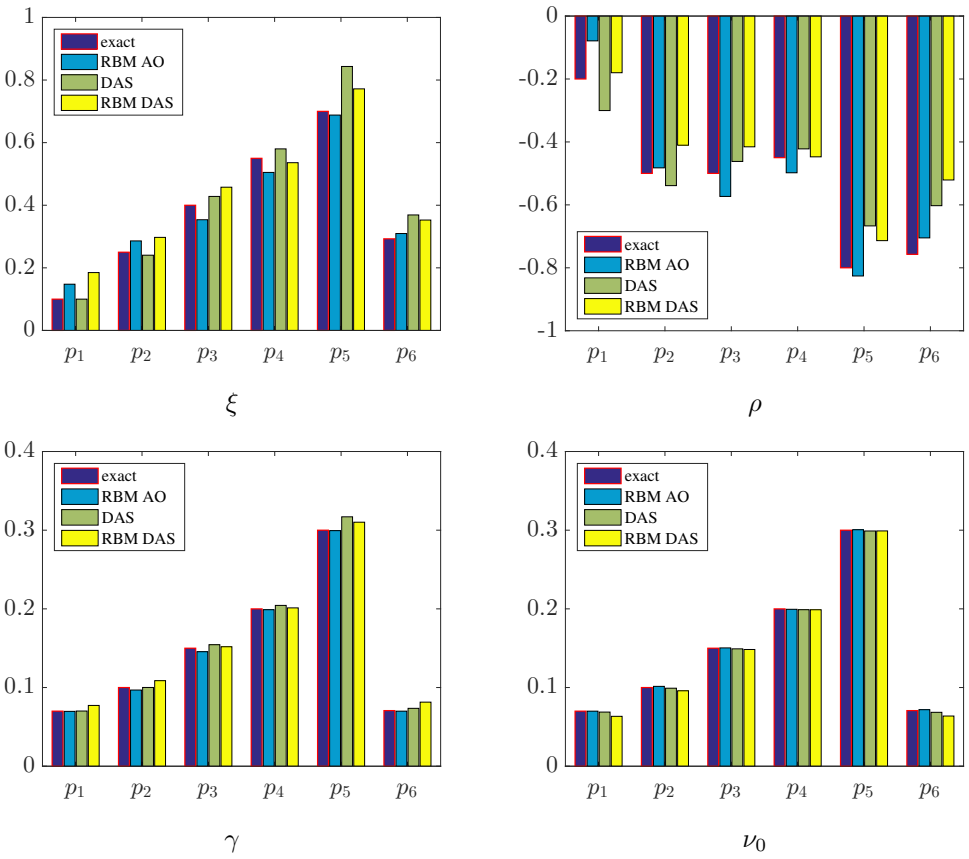

Figure 5.6: Graphical illustration of the reconstructed parameters obtained by calibrating on American put options in the Heston model using different model reduction approaches.

We note that the combined approach (5.2.6), i.e., a combination of RBM with the de-Americanization method, also provides promising results, especially in terms of efficiency, where it seems to be the fastest. However, in terms, of the reconstruction of the parameter, the method is inferior to other approaches, which could be explained by the "double" reduction error, caused, first by the de-Americanization method and, secondly by the RBM (scenarios p_5, p_6).

Calibration on Google Options

Finally, we extend our consideration to the calibration on a real market data set, provided by options on the Google stock. Since the Google stock does not pay dividends, the American call options can be priced the same as the European call options,

Scenario	Method	$\mathbb{E}(\boldsymbol{\mu})$	$\#J$	calib. time	pre-process. time for P^{obs}
p_1	$J_{\mathcal{N}}(\boldsymbol{\Theta})$	$\mathbb{E}_{\mathcal{N}}^{\text{AO}}$	75	8.524 hrs	
	$\widetilde{J}_{\mathcal{N}}(\boldsymbol{\Theta})$	$\mathbb{E}_{\mathcal{N}}^{\text{EO}}$	145	18.018 min	36.045 min
	$J_N(\boldsymbol{\Theta})$	$\mathbb{E}_N^{\text{AO}}$	70	3.912 min	
	$\widetilde{J}_N(\boldsymbol{\Theta})$	$\mathbb{E}_N^{\text{EO}}$	170	4.855 min	36.045 min
p_2	$J_{\mathcal{N}}(\boldsymbol{\Theta})$	$\mathbb{E}_{\mathcal{N}}^{\text{AO}}$	65	8.035 hrs	
	$\widetilde{J}_{\mathcal{N}}(\boldsymbol{\Theta})$	$\mathbb{E}_{\mathcal{N}}^{\text{EO}}$	70	8.895 min	36.830 min
	$J_N(\boldsymbol{\Theta})$	$\mathbb{E}_N^{\text{AO}}$	70	3.489 min	
	$\widetilde{J}_N(\boldsymbol{\Theta})$	$\mathbb{E}_N^{\text{EO}}$	70	2.050 min	36.830 min
p_3	$J_{\mathcal{N}}(\boldsymbol{\Theta})$	$\mathbb{E}_{\mathcal{N}}^{\text{AO}}$	60	8.341 hrs	
	$\widetilde{J}_{\mathcal{N}}(\boldsymbol{\Theta})$	$\mathbb{E}_{\mathcal{N}}^{\text{EO}}$	60	8.083 min	35.374 min
	$J_N(\boldsymbol{\Theta})$	$\mathbb{E}_N^{\text{AO}}$	70	3.574 min	
	$\widetilde{J}_N(\boldsymbol{\Theta})$	$\mathbb{E}_N^{\text{EO}}$	80	2.353 min	35.374 min
p_4	$J_{\mathcal{N}}(\boldsymbol{\Theta})$	$\mathbb{E}_{\mathcal{N}}^{\text{AO}}$	50	7.0877 hrs	
	$\widetilde{J}_{\mathcal{N}}(\boldsymbol{\Theta})$	$\mathbb{E}_{\mathcal{N}}^{\text{EO}}$	45	6.031 min	36.660 min
	$J_N(\boldsymbol{\Theta})$	$\mathbb{E}_N^{\text{AO}}$	55	2.813 min	
	$\widetilde{J}_N(\boldsymbol{\Theta})$	$\mathbb{E}_N^{\text{EO}}$	75	2.189 min	36.660 min
p_5	$J_{\mathcal{N}}(\boldsymbol{\Theta})$	$\mathbb{E}_{\mathcal{N}}^{\text{AO}}$	40	6.3318 hrs	
	$\widetilde{J}_{\mathcal{N}}(\boldsymbol{\Theta})$	$\mathbb{E}_{\mathcal{N}}^{\text{EO}}$	65	8.607 min	36.574 min
	$J_N(\boldsymbol{\Theta})$	$\mathbb{E}_N^{\text{AO}}$	45	2.271 min	
	$\widetilde{J}_N(\boldsymbol{\Theta})$	$\mathbb{E}_N^{\text{EO}}$	65	1.933 min	36.574 min
p_6	$J_{\mathcal{N}}(\boldsymbol{\Theta})$	$\mathbb{E}_{\mathcal{N}}^{\text{AO}}$	70	9.6656 hrs	
	$\widetilde{J}_{\mathcal{N}}(\boldsymbol{\Theta})$	$\mathbb{E}_{\mathcal{N}}^{\text{EO}}$	70	9.555 min	36.960 min
	$J_N(\boldsymbol{\Theta})$	$\mathbb{E}_N^{\text{AO}}$	90	4.503 min	
	$\widetilde{J}_N(\boldsymbol{\Theta})$	$\mathbb{E}_N^{\text{EO}}$	100	3.055 min	36.960 min

Table 5.6: Computational time for calibrating American put options using different model reduction techniques.

[Hul03]. Hence, we restrict consideration to only American put options. Namely, we consider the data P^{obs} of 401 American put options with $S_0 = 523.755$, $r = 0.15\%$ on February 2nd, 2015. The data is pre-processed by using the methodology applied to the volatility index (VIX) by the Chicago board of exchange [CBO09]:

- For each option with the strike price K_i, we consider the midpoint of the bid-ask spread.
- Options with zero bid prices are neglected.
- If two puts with consecutive strike prices have zero bid prices, no puts with lower strike prices are included.

The used data is given in Table 5.7. In terms of the moneyness, we consider all types, out-of-the money ($K_i < S_0$), at-the-money ($K_i = S_0$) and in-the-money ($K_i > S_0$) options.

In our synthetic test scenarios, the Feller condition (2.6.2) was automatically satisfied. However, this does not hold for general calibration processes. Thus, we incorporate the following additional constraint on $\boldsymbol{\Theta} = (\xi, \rho, \gamma, \kappa, \nu_0) \in \mathcal{P}_{\text{opt}}$

$$\mathcal{P}_{\text{opt}} := \left\{ \boldsymbol{\Theta} \in \mathbb{R}^5 : \Theta_{\min,i} \leq \Theta_i \leq \Theta_{\max,i},\ 2\Theta_3\Theta_4 - \Theta_1^2 < 0,\ i = 1, \ldots, 5 \right\}. \quad (5.3.4)$$

As optimization algorithm, we take the MATLAB function *fmincon* based on the Interior-Point method and which, in contrast to *lsqnonlin*, allows the inclusion of inequality constraints. We consider the same termination condition for the optimization routine as previously.

To calibrate the parameters, we consider the detailed minimization problem (5.2.2) and, as previously, the reduced models: the RBM (5.2.3), the de-Americanization method (5.2.4) and the combination of both (5.2.6). For completeness, we also consider the calibration of the de-Americanized data using the closed-form solutions (2.6.19) for the problem (5.2.5).

The results of the calibration are presented in Table 5.8. At the first glance, we observe that all approaches provide a very similar reconstructed parameter. In particular, γ and ν_0 seem to be easily identified, which has been already noted in our previous experiments. The rate of mean reversion κ appears to be a non-identifiable parameter, and all models provide quite different results. For the remaining parameters ξ and ρ, we observe that the de-Americanization method tends to underestimate the volatility of volatility ξ and the correlation ρ, compared to the detailed and reduced approach. This is clearly reflected in all models that use the perturbed de-Americanized data, i.e., $\widetilde{J}_{\mathcal{N}}(\boldsymbol{\Theta})$, $\widetilde{J}_{N}(\boldsymbol{\Theta})$, and $\widetilde{J}_{\text{CF}}(\boldsymbol{\Theta})$. This is in good agreement with our observations for the synthetic data sets (see scenario p_5 and p_6), where for large absolute values of the correlation parameters the de-Americanization method was unable to provide a good reconstruction of the parameters ξ and ρ.

The graphical illustrations of the results are presented in Figure 5.7 for the detailed and reduced models using the calibration on the actual market data. In Figure 5.8, the results corresponding to the calibration on the de-Americanized data with detailed model and closed-form solutions are also reported. The relative error for all approaches does not exceed 60% and increases in the out-of-the money region, which corresponds to the smallest option prices. To reduce this effect, one may consider different weights in the objective functional, e.g., imposing more weights for small option price values.

The results of the run-time performance of the different methods are given in Table 5.8b. We notice that the detailed approach requires an extensive amount of time, which might be fully impractical for industrial applications. The reduction

$K\backslash T$	0.2027	0.3753	0.6247	0.9507	1.9671
250					2.50
260				1.20	2.90
265			0.55		
270			0.62	1.30	3.30
275			0.68	1.50	
280			0.75	1.62	3.80
285			0.80	1.73	
290			0.88	1.80	4.65
295			0.97	1.95	
300		0.28	1.00	2.10	5.35
305		0.40	1.12	2.27	
310		0.40	1.20	2.45	6.25
315		0.40	1.30	2.67	
320		0.47	1.38	2.85	7.40
325		0.57	1.50	3.12	
330		0.65	1.60	3.40	8.10
335		0.72	1.75	3.60	
340		0.78	1.90	3.85	9.65
345		0.82	2.05	4.20	
350		0.88	2.23	4.55	10.90
355		0.97	2.40	4.90	
360		1.05	2.70	5.30	12.55
365		1.12	2.90	5.65	
370		1.25	3.17	6.15	14.30
375		1.38	3.45	6.65	
380		1.52	3.75	7.15	16.45
385		1.65	4.10	7.65	
390		2.05	4.45	8.15	18.30
395	0.93	2.25	4.85	8.80	
400	1.05	2.50	5.30	9.45	20.85
405		2.73	5.75	10.10	
410	1.40	3.08	6.30	10.75	22.85
415	1.48	3.35	6.85	11.55	
420	1.65	3.75	7.45	12.40	25.55
425	1.93	4.10	8.15	13.40	
430	2.10	4.55	8.80	14.20	28.30
435	2.33	5.05	9.55	15.35	
440	2.70	5.55	10.40	16.25	31.35
445	3.10	6.10	11.25	17.35	
450	3.50	6.80	12.30	18.65	34.00
455	3.92	7.50	13.25	19.80	
460	4.25	8.35	14.25	21.20	37.80
465	5.20	9.20	15.45	22.60	
470	5.85	10.20	16.70	23.90	41.45
475	6.65	11.25	18.00	25.30	
480	7.60	12.40	19.45	27.15	45.20
485	8.65	13.70	20.95	28.55	
490	9.85	15.10	22.55	30.75	49.20
495	11.15	16.55	24.25	32.60	
500	12.65	18.25	26.00	34.60	53.50
505	14.05	20.00	27.90	36.80	
510	16.05	21.95	30.00	38.70	58.15
515	17.75	23.90	32.15	41.45	
520	19.90	26.20	34.40	43.65	62.90
525	22.50	28.55	36.70	46.05	
530	24.70	31.05	39.20	48.55	67.90
535	27.40	33.50	41.85	50.85	

$K\backslash T$	0.2027	0.3753	0.6247	0.9507	1.9671
540	30.20	36.40	44.45	52.70	72.65
545	33.25	39.25	47.60	56.10	
550	37.15	42.30	50.25	58.95	78.50
555	40.80	45.45	53.15	61.85	
560	44.30	49.00	56.55	64.80	84.05
565	48.25	52.35	59.40	67.50	
570	51.95	56.00	63.50	71.10	90.40
575	55.90	59.80	66.70	73.90	
580	60.20	63.70	69.85	77.25	96.45
585	64.50	67.10	74.25	81.30	
590	68.80	71.60	77.85	84.45	103.00
595	73.35	76.30	81.70	88.20	
600	77.35	80.65	85.10	91.55	108.85
605	82.35	84.80	89.65	95.20	
610	87.30	89.65	93.20	99.10	116.45
615	92.50	94.05	97.40	102.90	
620	96.65	98.45	101.85	106.80	123.75
625	101.30	103.00	106.40	111.80	
630	106.50	107.25	110.60	116.00	130.65
635	111.75	112.95	115.00	120.25	
640	117.20	117.25	119.85	124.40	138.10
645	121.45	122.30	124.40	128.55	
650	127.25	126.70	128.90	132.55	
655		131.45	133.70	137.15	
660		136.45	138.15	141.80	153.70
665		141.45	143.05	146.10	
670		146.65	147.35	150.50	
675		151.80	152.05	154.90	
680		156.20	158.25	159.45	169.45
685		161.20	161.60	164.05	
690		166.30	166.55	168.65	
695		171.30	171.45	173.15	
700		176.20	176.45	178.15	186.40
705		181.10	181.75		
710		186.15	186.25	188.40	
715		191.10	191.35		
720		196.05	195.85	197.15	203.70
725		201.05	201.80		
730		205.85	206.50	206.95	
735		211.00	211.05		
740		216.80	216.80	216.20	222.30
745		221.80	221.90		
750		226.55	226.85	226.20	
755		231.80			
760		236.80		236.15	240.60
765		241.95			
770		246.95		246.05	
775		251.80			
780		256.80		256.05	258.90
790		267.00		265.70	
800		276.95		276.05	277.70
810		287.25		286.05	
820				296.05	
830				306.05	
840				316.05	
860				336.05	
880				356.05	

Table 5.7: Google market data consisting of 401 American put options with $S_0 = 523,755$ on February 2nd, 2015.

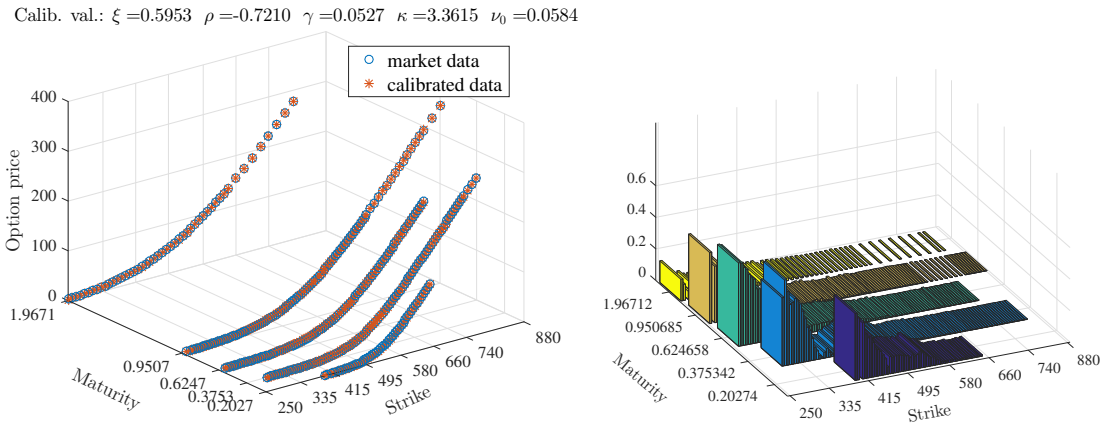

(a) Detailed problem, $J_{\mathcal{N}}(\boldsymbol{\Theta})$

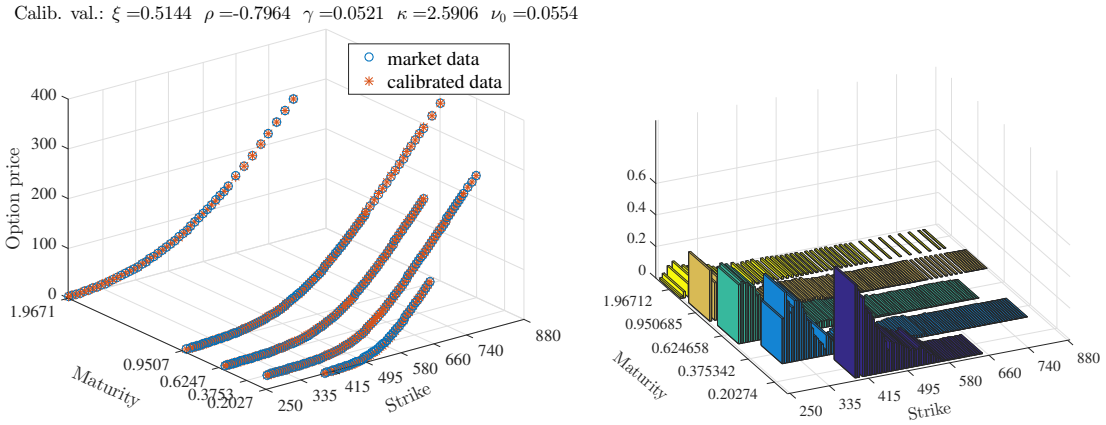

(b) Reduced problem, $J_N(\boldsymbol{\Theta})$

Figure 5.7: Left: the Google data set of American put options (circles) and the calibrated model data in the Heston model (stars). Right: the relative error of the market and calibrated data, $|P_i^{\text{obs}} - P_i^{s,\text{AO}}(\boldsymbol{\Theta}^\star)|/P_i^{\text{obs}}$, $i = 1, \ldots, M$, $s \in \{\mathcal{N}, N\}$.

approaches in this case seem to be powerful and necessary tools, which allow to reduce significantly the cost from a couple of days to less than an hour. Notably, we observe the substantial speed-up obtained by evaluating model prices with the closed-form solutions. This approach appears to us the most efficient when dealing with European options. However, taking into consideration the additional time for pre-processing the data in the de-Americanization approach, the total time for calibration with this method can be much slower than the calibration with American options

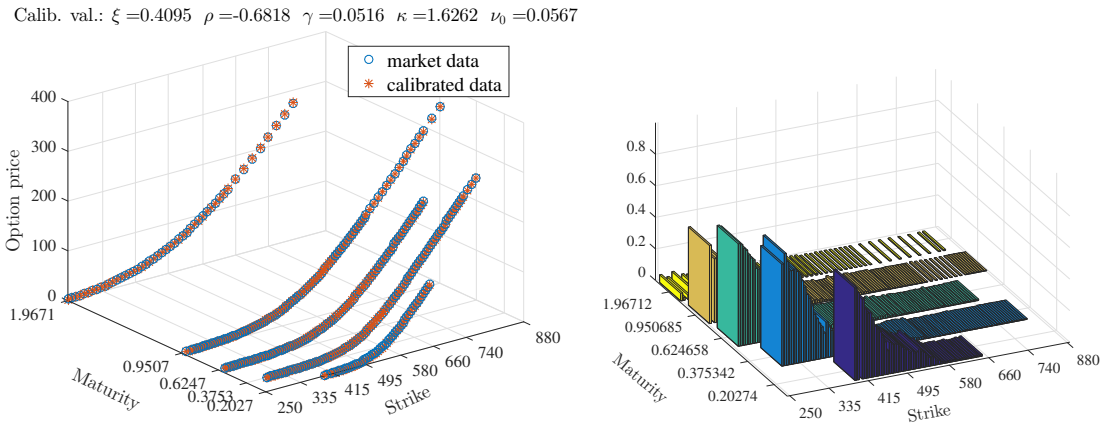

(a) De-Americanized problem, $\widetilde{J}_{\mathcal{N}}(\boldsymbol{\Theta})$

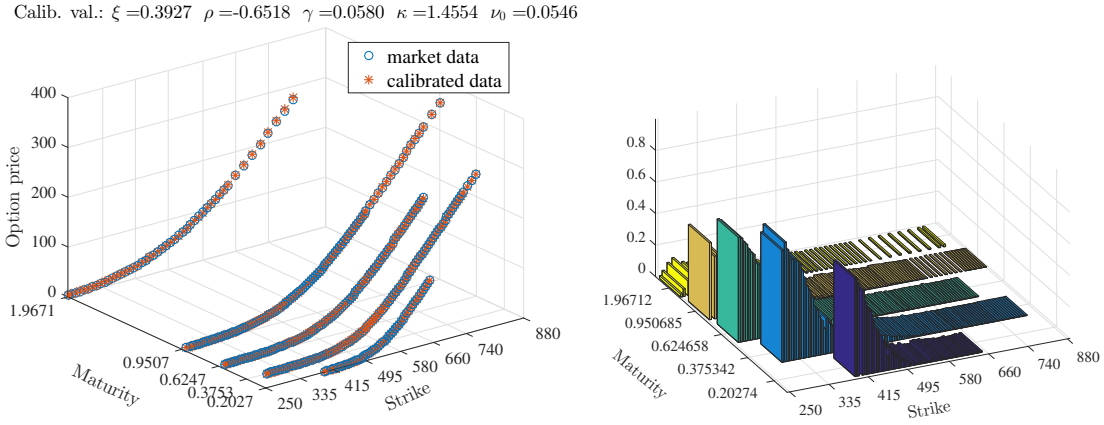

(b) De-Americanized problem with the closed-form solutions, $\widetilde{J}_{\mathrm{CF}}(\boldsymbol{\Theta})$

Figure 5.8: Left: the Google data set of the de-Americanized American put options (circles) and the calibrated model data in the Heston model (stars). Right: the relative error of the market and calibrated data, $|P_i^{\mathrm{obs}} - P_i^{s,\mathrm{EO}}(\boldsymbol{\Theta}^\star)|/P_i^{\mathrm{obs}}$, $i = 1, \ldots, M$, $s \in \{\mathcal{N}, \mathrm{CF}\}$.

using the RBM, depending how often the calibration has to be performed with new market data. We point out, that for the cases of multiple usage of the same data set the de-Americanization strategy with the closed form solutions could seem to be more attractive from the performance point of view than the reduced basis method. However, the de-Americanization method introduces an additional error. Together with the lack of a rigorous theoretical analysis of the de-Americanization approach, the combination of the calibration with American options and the RBM appears to

Method	$\mathbb{E}(\boldsymbol{\mu})$	$\boldsymbol{\Theta}$	ξ	ρ	γ	κ	ν_0
		$\boldsymbol{\Theta}_{\text{in}}$	0.6005	−0.6815	0.4867	2.02	0.4961
$J_{\mathcal{N}}(\boldsymbol{\Theta})$	$\mathbb{E}_{\mathcal{N}}^{\text{AO}}$	$\boldsymbol{\Theta}^\star$	0.5953	−0.7210	0.0527	3.3615	0.0584
$J_N(\boldsymbol{\Theta})$	$\mathbb{E}_N^{\text{AO}}$	$\boldsymbol{\Theta}^\star$	0.5144	−0.7964	0.0521	2.5906	0.0554
$\widetilde{J}_{\mathcal{N}}(\boldsymbol{\Theta})$	$\mathbb{E}_{\mathcal{N}}^{\text{EO}}$	$\boldsymbol{\Theta}^\star$	0.4095	−0.6818	0.0516	1.6262	0.0567
$\widetilde{J}_N(\boldsymbol{\Theta})$	$\mathbb{E}_N^{\text{EO}}$	$\boldsymbol{\Theta}^\star$	0.3785	−0.9469	0.0500	4.9822	0.0717
$\widetilde{J}_{\text{CF}}(\boldsymbol{\Theta})$	—	$\boldsymbol{\Theta}^\star$	0.3927	−0.6518	0.0580	1.4554	0.0546

(a) Parameters obtained by the calibration routine.

Method	$\mathbb{E}(\boldsymbol{\mu})$	# iter.	# J	calib. time	pre-process. time for P^{obs}
$J_{\mathcal{N}}(\boldsymbol{\Theta})$	$\mathbb{E}_{\mathcal{N}}^{\text{AO}}$	35	219	68.72 hrs	
$J_N(\boldsymbol{\Theta})$	$\mathbb{E}_N^{\text{AO}}$	38	260	44.20 min	
$\widetilde{J}_{\mathcal{N}}(\boldsymbol{\Theta})$	$\mathbb{E}_{\mathcal{N}}^{\text{EO}}$	34	207	56.47 min	4.96 hrs
$\widetilde{J}_N(\boldsymbol{\Theta})$	$\mathbb{E}_N^{\text{EO}}$	35	228	37.40 min	4.96 hrs
$\widetilde{J}_{\text{CF}}(\boldsymbol{\Theta})$	—	43	265	4.30 min	4.96 hrs

(b) Calibration results in terms of the run-time performance. The number "# iter." corresponds to the number of iterations and "# J" is the total number of function evaluations performed by the optimization routine.

Table 5.8: Calibration results for the market data set of American put options given on the Google stock in the Heston model using different approaches.

be an attractive choice for this application.

6 Conclusions and Outlook

In this thesis we have developed a framework of the reduced basis method which enables an efficient evaluation of finance products, such as option prices. The deduced theoretical results are supported by numerical studies. In addition, we have applied the method to financial applications and compared its efficiency to commonly used methods. In conclusion, we can say that the RBM method can be considered as an efficient, reliable and competitive method for option pricing problems, especially for the evaluation of complex options, such as American puts.

The main objective of the present work was to develop the methodology of the RBM for parabolic variational inequalities and to adapt it in the context of option pricing problems. The theoretical results for the reduced variational inequality problem have been presented in the second part of the thesis. The well-posedness of the reduced system and a posteriori error estimates have been derived. The latter ones have been also extended to cover the cases of weakly coercive problems. One of the challenges, caused by the non-linearity of the problem is reflected in the approximation of the reduced space of Lagrange multipliers, where one needs to preserve the positivity constraint. Here we have compared different algorithms which could tackle this difficulty, such as the Angle-Greedy and the NNMF strategies. With the developed framework we have been able to treat realistic examples for the variational inequalities which concern the pricing of American options. We have observed a significant speedup with the RBM compared to the FEM.

In order to evaluate the practical efficiency of the method, we have extended the RBM to the application of a calibration on option prices. Here, we have studied the performance of the RBM for both linear and nonlinear models, that is, pricing European and American options. However, our primary focus was on the RBM for American options, due to the fact that for calibration on European options, one can already gain a significant speed up by using, e.g., closed-form solutions. We have compared the RBM to some reduction approaches which are common in practice, such as the de-Americanization method. The empirical study demonstrated a high efficiency of the RBM method and its competitiveness to other model reduction approaches. One of the main advantages of the RBM is in its independence on the given market data set, i.e., the method does not require an additional online computational time to pre-process the given data. Additionally, the RBM framework allows to control the reduction error, by enlarging the dimension of the RB space, in contrast to, e.g., the de-Americanization method, where the approximation error

remains fixed.

During the development of the current RBM methodology, we encountered several open questions and problems which can serve as potential extensions to our approach.

With the use of the RBM we have been able to perform the reduction of the spatial complexity only. To reduce the complexity further, i.e., in the temporal direction, one may consider space-time discretization schemes. These schemes in combination with the RBM have been already successfully applied in [GU14; MU14; Ste14; UP14; Yan14; YPU14], however only in the context of the tensor product spaces. One can consider a more general approach, that is, a full space-time method [Kar15; NS11; NS13; Ste15], which does not restrict us to the tensor-product structure. Here, the time variable is treated as an additional spatial variable. This approach can be considered as a general framework to perform more sophisticated adaptive local refinement in a whole space-time cylinder. This feature could be beneficial for the detailed solver for American options, where one can provide an adaptive refinement in the early exercise region that constitutes the area of actual interest. It also allows to apply the RBM without loss of its consistency property.

The online efficiency of the RBM applied to the time-stepping schemes mostly depends on the three ingredients, which are the RB dimension, the number of time steps and the computational cost of the reduced solver. The first two, which provide the most contribution to the online computational cost, are adjustable depending on the model problem and desired accuracy of the reduced basis approximation. The reduced solver is dependent on the nature of the problem. In our computational study for parabolic variational inequalities we have limited ourselves to the solution algorithm based on the primal-dual active set strategy (PDAS). A competitive studies of the different reduced and detailed solvers and their efficiency could be a potential topic of interest.

In the present work, we did not attempt to reduce the cost of the offline stage. However, as we could observe from the numerical results, there are situations when the accuracy of the RBM does not seem to be sufficient or the method is lacking in recovering some of the parameters. This can be improved in several ways. The natural choice would be to enlarge the dimension of the reduced space. Additionally, one can conduct an empirical study by using a richer training set or an adaptive parameter domain partitioning, see, e.g., [HDO11; HO08a]. However this could lead to a significant increase of the offline computational cost. To overcome this difficulty, additional techniques from HPC, such as parallelization, could be applied.

Another open question concerns the optimization problem for the calibration on the American put options. The main difficulty here comes from the fact that one can not guarantee the differentiability of the objective functional with respect to the parameter. Hence, in order to theoretically justify the application of gradient based optimization algorithms, the problem needs to be regularized. This can be achieved by, e.g., smoothing the inequality constrains or by adding a penalty term,

see, e.g., [Ach05; Ach08; AP05a]. Although this topic has been discussed actively in the literature, in particular in the context of the optimal control problems, e.g, [Hin01; HR86; IK00; Mig76; MP84; SW13], in the RBM framework this remains an interesting and new perspective for future research.

Bibliography

[Ach05] Y. Achdou. "An inverse problem for a parabolic variational inequality arising in volatility calibration with American options." In: *SIAM J. Control Optim.* 43.5 (2005), 1583–1615 (electronic).

[Ach08] Y. Achdou. "Calibration of Lévy processes with American options." In: *Partial differential equations*. Vol. 16. Comput. Methods Appl. Sci. Springer, Dordrecht, 2008, pp. 259–277.

[AGG10] F. AitSahlia, M. Goswami, and S. Guha. "American option pricing under stochastic volatility: an empirical evaluation." In: *Comput. Manag. Sci.* 7.2 (2010), pp. 189–206.

[AIP04] Y. Achdou, G. Indragoby, and O. Pironneau. "Volatility calibration with American options." In: *Methods Appl. Anal.* 11.4 (2004), pp. 533–556.

[AP05a] Y. Achdou and O. Pironneau. "Numerical Procedure for Calibration of Volatility with American Options." In: *Appl. Math. Finance* 12.3 (2005), pp. 201–241.

[AP05b] Y. Achdou and O. Pironneau. *Computational methods for option pricing*. Vol. 30. Frontiers in Applied Mathematics. Society for Industrial and Applied Mathematics (SIAM), Philadelphia, PA, 2005.

[ASB78] B. O Almroth, P. Stern, and F. A. Brogan. "Automatic choice of global shape functions in structural analysis." In: *AIAA Journal* 16.5 (1978), pp. 525–528.

[Bac00] L. Bachelier. "Théorie de la spéculation." In: *Ann. Sci. École Norm. Sup. (3)* 17 (1900), pp. 21–86.

[BAF16] M. Balajewicz, D. Amsallem, and C. Farhat. "Projection-based model reduction for contact problems." In: *Internat. J. Numer. Methods Engrg.* 106.8 (2016), pp. 644–663.

[Ber03] M. Bern. "Adaptive mesh generation." In: *Error estimation and adaptive discretization methods in computational fluid dynamics*. Vol. 25. Lect. Notes Comput. Sci. Eng. Springer, Berlin, 2003, pp. 1–46.

[BFB13] D. Boffi, M. Fortin, and F. Brezzi. *Mixed finite element methods and applications*. Springer series in computational mathematics. Berlin, Heidelberg: Springer, 2013.

[BGG+16] O. Burkovska, K. Glau, M. Gaß, M. Mahlstedt, W. Schoutens, and B. Wohlmuth. "Calibration to American Options: Numerical Investigation of the de-Americanization." In: *ArXiv e-prints* (2016).

[BHR78] F. Brezzi, W. W. Hager, and P.-A. Raviart. "Error estimates for the finite element solution of variational inequalities. II. Mixed methods." In: *Numer. Math.* 31.1 (1978/79), pp. 1–16.

[BHS+15] O. Burkovska, B. Haasdonk, J. Salomon, and B. Wohlmuth. "Reduced basis methods for pricing options with the Black-Scholes and Heston models." In: *SIAM J. Financial Math.* 6.1 (2015), pp. 685–712.

[BI97] I. Bouchouev and V. Isakov. "The inverse problem of option pricing." In: *Inverse Problems* 13.5 (1997), pp. L11–L17.

[BKG+15] E. Bader, M. Kärcher, M. Grepl, and K. Veroy. "A Certified Reduced Basis Approach for Parametrized Linear-Quadratic Optimal Control Problems with Control Constraints." In: *IFAC-Papers Online* 48.1 (2015). 8th Vienna International Conference on Mathematical Modelling – MATHMOD 2015, pp. 719–720.

[BL82] A. Bensoussan and J.-L. Lions. *Applications of variational inequalities in stochastic control*. Vol. 12. Studies in Mathematics and its Applications. Translated from the French. North-Holland Publishing Co., Amsterdam-New York, 1982.

[BMN+04] M. Barrault, Y. Maday, N. C. Nguyen, and A. T. Patera. "An 'empirical interpolation' method: application to efficient reduced-basis discretization of partial differential equations." In: *C. R. Math. Acad. Sci. Paris* 339.9 (2004), pp. 667 –672.

[BMP+12] A. Buffa, Y. Maday, A. T. Patera, C. Prud'homme, and G. Turinici. "*A priori* convergence of the greedy algorithm for the parametrized reduced basis method." In: *ESAIM Math. Model. Numer. Anal.* 46.3 (2012), pp. 595–603.

[BS73] F. Black and M. Scholes. "The pricing of options and corporate liabilities." In: *J. Polit. Econ.* 81.3 (1973), pp. 637–654.

[CBO09] CBOE. *The CBOE volatility index – VIX*. 2009.

[Cho08] S. Choi. "Algorithms for orthogonal nonnegative matrix factorization." In: *2008 IEEE International Joint Conference on Neural Networks (IEEE World Congress on Computational Intelligence)*. 2008, pp. 1828–1832.

[CLP11] R. Cont, N. Lantos, and O. Pironneau. "A reduced basis for option pricing." In: *SIAM J. Financial Math.* 2.1 (2011), pp. 287–316.

[CP99] N. Clarke and K. Parrott. "Multigrid for American option pricing with stochastic volatility." In: *Appl. Math. Finance* 6.3 (1999), pp. 177–195.

[CRR79] J. C. Cox, S. A. Ross, and M. Rubinstein. "Option pricing: A simplified approach." In: *J. Financ. Econ.* 7.3 (1979), pp. 229–263.

[CS09] S. Chaturantabut and D. C. Sorensen. "Discrete Empirical Interpolation for nonlinear model reduction." In: *Proceedings of the 48h IEEE Conference on Decision and Control (CDC) held jointly with 2009 28th Chinese Control Conference*. 2009, pp. 4316–4321.

[CS10] S. Chaturantabut and D. C. Sorensen. "Nonlinear model reduction via discrete empirical interpolation." In: *SIAM J. Sci. Comput.* 32.5 (2010), pp. 2737–2764.

[CW10] P. Carr and L. Wu. "Stock options and credit default swaps: A joint framework for valuation and estimation." In: *Journal of Financial Econometrics* 8.4 (2010), pp. 409–449.

[DF12] B. Düring and M. Fournié. "High-order compact finite difference scheme for option pricing in stochastic volatility models." In: *J. Comput. Appl. Math.* 236.17 (2012), pp. 4462–4473.

[DH15] M. A. Dihlmann and B. Haasdonk. "Certified PDE-constrained parameter optimization using reduced basis surrogate models for evolution problems." In: *Comput. Optim. Appl.* 60.3 (2015), pp. 753–787.

[DHK+12] M. Drohmann, B. Haasdonk, S. Kaulmann, and M. Ohlberger. "Advances in DUNE: Proceedings of the DUNE User Meeting, Held in October 6th–8th 2010 in Stuttgart, Germany." In: Berlin, Heidelberg: Springer Berlin Heidelberg, 2012. Chap. A Software Framework for Reduced Basis Methods Using Dune-RB and RBmatlab, pp. 77–88.

[DHO12] M. Drohmann, B. Haasdonk, and M. Ohlberger. "Reduced basis approximation for nonlinear parametrized evolution equations based on empirical operator interpolation." In: *SIAM J. Sci. Comput.* 34.2 (2012), A937–A969.

[DL00] R. Dautray and J.-L. Lions. *Mathematical analysis and numerical methods for science and technology. Vol. 5.* Evolution problems. I. Springer-Verlag, Berlin, 2000.

[DL72] G. Duvaut and J.-L. Lions. *Les inéquations en mécanique et en physique.* Travaux et Recherches Mathématiques, No. 21. Dunod, Paris, 1972.

[DS04] D. Donoho and V. Stodden. "When Does Non-Negative Matrix Factorization Give a Correct Decomposition into Parts?" In: *Adv. Neural Inf. Process. Syst. 16.* MIT Press, 2004, pp. 1141–1148.

[FCG06] A. Falcó, F. Chinesta, and M. González. *Model Reduction Methods In Option Pricing.* Working Papers. Serie AD 2006-16. Instituto Valenciano de Investigaciones Económicas, S.A. (Ivie), 2006.

[Fic63] G. Fichera. "Sul problema elastostatico di Signorini con ambigue condizioni al contorno." In: *Atti Accad. Naz. Lincei Rend. Cl. Sci. Fis. Mat. Natur. (8)* 34 (1963), pp. 138–142.

[FLM+11] L. Feng, V. Linetsky, J. L. Morales, and J. Nocedal. "On the solution of complementarity problems arising in American options pricing." In: *Optim. Methods Softw.* 26.4-5 (2011), pp. 813–825.

[FP03] F. Facchinei and J.-S. Pang. *Finite-dimensional variational inequalities and complementarity problems. Vol. I.* Springer Series in Operations Research. Springer-Verlag, New York, 2003.

[Gal08] V. Galiotos. *Stochastic Volatility and the Volatility Smile.* Tech. rep. 15. Uppsala University, Department of Mathematics, 2008, pp. 1–32.

[Gar76] M. Garman. *A General Theory of Asset Valuation under Diffusion State Processes.* Research Program in Finance Working Papers 50. University of California at Berkeley, 1976.

[Gat06] J. Gatheral. *The Volatility Surface: A Practitioner's Guide.* Vol. 357. John Wiley & Sons, 2006.

[GGM+12] F. Gerlich, A. M. Giese, J. H. Maruhn, and E. W. Sachs. "Parameter identification in financial market models with a feasible point SQP algorithm." In: *Comput. Optim. Appl.* 51.3 (2012), pp. 1137–1161.

[GHH16] D. Garmatter, B. Haasdonk, and B. Harrach. "A reduced basis Landweber method for nonlinear inverse problems." In: *Inverse Problems* 32.3 (2016), pp. 035001, 21.

[Glo08] R. Glowinski. *Numerical Methods for Nonlinear Variational Problems.* Scientific Computation. Springer, 2008.

[GLT81] R. Glowinski, J.-L. Lions, and R. Trémolières. *Numerical analysis of variational inequalities*. Vol. 8. Studies in Mathematics and its Applications. Translated from the French. North-Holland Publishing Co., Amsterdam-New York, 1981.

[GMN+07] M. A. Grepl, Y. Maday, N. C. Nguyen, and A. T. Patera. "Efficient reduced-basis treatment of nonaffine and nonlinear partial differential equations." In: *M2AN Math. Model. Numer. Anal.* 41.3 (2007), pp. 575–605.

[GP05] M. Grepl and A. Patera. "A posteriori error bounds for reduced-basis approximations of parametrized parabolic partial differential equations." In: *M2AN, Math. Model. Numer. Anal.* 39.1 (2005), pp. 157–181.

[Gre05] M. A. Grepl. "Reduced-basis approximation and a posteriori error estimation for parabolic partial differential equations." PhD thesis. Massachusetts Institute of Technology, 2005.

[Gri10] G. Grindlay. *NMFlib Matlab library*. `http://www.ee.columbia.edu/~grindlay/code.html#NMFlib`. Version 0.1.3. 2010.

[GRV12] A.-L. Gerner, A. Reusken, and K. Veroy. "Reduced Basis A Posteriori Error Bounds for the Instationary Stokes Equations." In: *ArXiv e-prints* (2012).

[GU14] S. Glas and K. Urban. "On noncoercive variational inequalities." In: *SIAM J. Numer. Anal.* 52.5 (2014), pp. 2250–2271.

[GU15] S. Glas and K. Urban. "Numerical Investigations of an Error Bound for Reduced Basis Approximations of Noncoercice Variational Inequalities." In: *IFAC-Papers Online* 48.1 (2015). 8th Vienna International Conference on Mathematical Modelling – MATHMOD 2015, pp. 721–726.

[GV11] A.-L. Gerner and K. Veroy. "Reduced Basis A Posteriori Error Bounds For The Stokes Equations In Parametrized Domains: A Penalty Approach." In: *Math. Models Methods Appl. Sci.* 21.10 (2011), 2103–2134.

[Haa11] B. Haasdonk. *Reduzierte-Basis-Methoden, Vorlesungsskript SS 2011*. Tech. rep. 2011-004. 2011.

[Haa13] B. Haasdonk. "Convergence rates of the POD-greedy method." In: *ESAIM Math. Model. Numer. Anal.* 47.3 (2013), pp. 859–873.

[Haa16] B. Haasdonk. *Reduced Basis Methods for Parametrized PDEs – A Tutorial Introduction for Stationary and Instationary Problems*. Tech. rep. Chapter to appear in P. Benner, A. Cohen, M. Ohlberger and K. Will-

cox: "Model Reduction and Approximation for Complex Systems", Society for Industrial and Applied Mathematics (SIAM), Philadelphia, PA. 2016.

[HDO11] B. Haasdonk, M. Dihlmann, and M. Ohlberger. "A training set and multiple bases generation approach for parameterized model reduction based on adaptive grids in parameter space." In: *Math. Comput. Model. Dyn. Syst.* 17.4 (2011), pp. 423–442.

[Hes93] S. L. Heston. "A Closed-Form Solution for Options with Stochastic Volatility with Applications to Bond and Currency Options." In: *Rev. Financ. Stud.* 6.2 (1993), pp. 327–43.

[HF10] K. J. In 't Hout and S. Foulon. "ADI finite difference schemes for option pricing in the Heston model with correlation." In: *Int. J. Numer. Anal. Model.* 7.2 (2010), pp. 303–320.

[HH15] T. Haentjens and K. J. In 't Hout. "ADI Schemes for Pricing American Options under the Heston Model." In: *Appl. Math. Finance* 22.3 (2015), pp. 207–237.

[HHW10] C. Hager, S. Hüeber, and B. Wohlmuth. "Numerical techniques for the valuation of basket options and its Greeks." In: *J. Comput. Finance* 13.4 (2010), pp. 1–31.

[HIK02] M. Hintermüller, K. Ito, and K. Kunisch. "The Primal-Dual Active Set Strategy as a Semismooth Newton Method." In: *SIAM J. Optim.* 13.3 (2002), pp. 865–888.

[Hin01] M. Hintermüller. "Inverse coefficient problems for variational inequalities: optimality conditions and numerical realization." In: *M2AN Math. Model. Numer. Anal.* 35.1 (2001), pp. 129–152.

[HO08a] B. Haasdonk and M. Ohlberger. "Adaptive basis enrichment for the reduced basis method applied to finite volume schemes." In: *Finite volumes for complex applications V*. ISTE, London, 2008, pp. 471–478.

[HO08b] B. Haasdonk and M. Ohlberger. "Reduced basis method for finite volume approximations of parametrized linear evolution equations." In: *M2AN Math. Model. Numer. Anal.* 42.2 (2008), pp. 277–302.

[HR86] J. Haslinger and T. Roubíček. "Optimal control of variational inequalities. Approximation theory and numerical realization." In: *Appl. Math. Optim.* 14.3 (1986), pp. 187–201.

[HRS16] J. S. Hesthaven, G. Rozza, and B. Stamm. *Certified reduced basis methods for parametrized partial differential equations.* SpringerBriefs in Mathematics. BCAM SpringerBriefs. Springer, Cham; BCAM Basque Center for Applied Mathematics, Bilbao, 2016.

[HRS+13] N. Hilber, O. Reichmann, C. Schwab, and C. Winter. *Computational methods for quantitative finance. Finite element methods for derivative pricing.* Springer Finance, 2013.

[HSS14] K. Huang, N. D. Sidiropoulos, and A. Swami. "Non-negative matrix factorization revisited: uniqueness and algorithm for symmetric decomposition." In: *IEEE Trans. Signal Process.* 62.1 (2014), pp. 211–224.

[HSW11] B. Haasdonk, J. Salomon, and B. Wohlmuth. *A Reduced Basis Method for Parametrized Variational Inequalities.* SimTech preprint 2011–17, University of Stuttgart. 2011.

[HSW12] B. Haasdonk, J. Salomon, and B. Wohlmuth. "A reduced basis method for parametrized variational inequalities." In: *SIAM J. Numer. Anal.* 50.5 (2012), pp. 2656–2676.

[HSW13] B. Haasdonk, J. Salomon, and B. Wohlmuth. "A Reduced Basis Method for the Simulation of American Options." In: *Numerical Mathematics and Advanced Applications 2011: Proceedings of ENUMATH 2011, the 9th European Conference on Numerical Mathematics and Advanced Applications, Leicester, September 2011.* Berlin, Heidelberg: Springer Berlin Heidelberg, 2013, pp. 821–829.

[Hul03] J. C. Hull. *Options, Futures, and Other Derivative Securities.* Fifth. Prentice-Hall, 2003.

[HW87] J. Hull and A. White. "The Pricing of Options on Assets with Stochastic Volatilities." In: *J. Finance* 42.2 (1987), pp. 281–300.

[IK00] K. Ito and K. Kunisch. "Optimal control of elliptic variational inequalities." In: *Appl. Math. Optim.* 41.3 (2000), pp. 343–364.

[IK08] K. Ito and K. Kunisch. *Lagrange multiplier approach to variational problems and applications.* Vol. 15. Advances in Design and Control. Society for Industrial and Applied Mathematics (SIAM), Philadelphia, PA, 2008.

[IM91] J. M. Ingram and M. M. Marsh. "Projections onto convex cones in Hilbert space." In: *J. Approx. Theory* 64.3 (1991), pp. 343–350.

[IT08] S. Ikonen and J. Toivanen. "Efficient numerical methods for pricing American options under stochastic volatility." In: *Numer. Methods Partial Differential Equations* 24.1 (2008), pp. 104–126.

[IT09] S. Ikonen and J. Toivanen. "Operator splitting methods for pricing American options under stochastic volatility." In: *Numer. Math.* 113.2 (2009), pp. 299–324.

[Jam03] P. James. *Option theory*. John Wiley & Sons, 2003.

[JKW+11] A. Janek, T. Kluge, R. Weron, and U. Wystup. "FX smile in the Heston model." In: *Statistical tools for finance and insurance*. Springer, Heidelberg, 2011, pp. 133–162.

[JLL90] P. Jaillet, D. Lamberton, and B. Lapeyre. "Variational inequalities and the pricing of American options." In: *Acta Appl. Math.* 21.3 (1990), pp. 263–289.

[JS87] H. Johnson and D. Shanno. "Option Pricing when the Variance is Changing." In: *J. Finan. Quant. Anal.* 22.2 (1987), pp. 143–151.

[Kar15] E. Karabelas. "Space-Time Discontinuous Galerkin Methods for Cardiac Electro-Mechanics." PhD thesis. Technische Universität Graz, 2015.

[KO88] N. Kikuchi and J. T. Oden. *Contact problems in elasticity: a study of variational inequalities and finite element methods*. Vol. 8. SIAM Studies in Applied Mathematics. Society for Industrial and Applied Mathematics (SIAM), Philadelphia, PA, 1988.

[KS00] D. Kinderlehrer and G. Stampacchia. *An introduction to variational inequalities and their applications*. Vol. 31. Classics Appl. Math. Reprint of the 1980 original. Society for Industrial and Applied Mathematics (SIAM), Philadelphia, PA, 2000.

[KS91] I. Karatzas and S. E. Shreve. *Brownian motion and stochastic calculus*. Second. Vol. 113. Grad. Texts in Math. Springer-Verlag, New York, 1991.

[KSW12] A. Kunoth, C. Schneider, and K. Wiechers. "Multiscale methods for the valuation of American options with stochastic volatility." In: *Int. J. Comput. Math.* 89.9 (2012), pp. 1145–1163.

[LHZ+01] S. Z. Li, X. Hou, H. Zhang, and Q. Cheng. "Learning spatially localized, parts-based representation." In: *Computer Vision and Pattern Recognition, 2001. CVPR 2001. Proceedings of the 2001 IEEE Computer Society Conference on*. Vol. 1. 2001, I–207–I–212 vol.1.

[Lio72] J.-L. Lions. "Partial Differential Inequalities." In: *Russian Math. Surveys* 27.2 (1972), p. 91.

[LL96] D. Lamberton and B. Lapeyre. *Introduction to stochastic calculus applied to finance*. Translated from the 1991 French original by Nicolas Rabeau and François Mantion. Chapman & Hall, London, 1996.

[LM72a] J.-L. Lions and E. Magenes. *Non-homogeneous boundary value problems and applications. Vol. I.* Translated from the French by P. Kenneth, Die Grundlehren der mathematischen Wissenschaften, Band 181. Springer-Verlag, New York-Heidelberg, 1972.

[LM72b] J.-L. Lions and E. Magenes. *Non-homogeneous boundary value problems and applications. Vol. II.* Translated from the French by P. Kenneth, Die Grundlehren der mathematischen Wissenschaften, Band 182. Springer-Verlag, New York-Heidelberg, 1972.

[LS00] D. D. Lee and H. S. Seung. "Algorithms for Non-negative Matrix Factorization." In: *NIPS*. MIT Press, 2000, pp. 556–562.

[LS67] J.-L. Lions and G. Stampacchia. "Variational inequalities." In: *Comm. Pure Appl. Math.* 20 (1967), pp. 493–519.

[LS99] D. D. Lee and H. S. Seung. "Learning the parts of objects by non-negative matrix factorization." In: *Nature* 401.6755 (1999), pp. 788–791.

[Mat] *MATLAB*. `http://www.mathworks.com/`. Version R2015a. The Mathworks, Inc., 2015.

[Mig76] F. Mignot. "Contrôle dans les inéquations variationelles elliptiques." In: *J. Funct. Anal.* 22.2 (1976), pp. 130–185.

[MNP+09] Y. Maday, N. C. Nguyen, A. T. Patera, and G. S. H. Pau. "A general multipurpose interpolation procedure: the magic points." In: *Commun. Pure Appl. Anal.* 8.1 (2009), pp. 383–404.

[MP84] F. Mignot and J.-P. Puel. "Optimal control in some variational inequalities." In: *SIAM J. Control Optim.* 22.3 (1984), pp. 466–476.

[MPS14] M. Mrázek, J. Pospíšil, and T. Sobotka. "On Optimization Techniques for Calibration of Stochastic Volatility Models." In: *AMCM 2015, November 28–30, 2014, Athens, Greece*. 2014, pp. 34–40.

[MQR08] R. Milani, A. Quarteroni, and G. Rozza. "Reduced basis method for linear elasticity problems with many parameters." In: *Comput. Methods Appl. Mech. Engrg.* 197.51-52 (2008), pp. 4812–4829.

[MU14] A. Mayerhofer and K. Urban. *A Reduced Basis Method for Parabolic Partial Differential Equations with Parameter Functions and Application to Option Pricing*. Preprint, University of Ulm. Accepted for publication in J. Comput. Finance. 2014.

[NMR15] F. Negri, A. Manzoni, and G. Rozza. "Reduced basis approximation of parametrized optimal flow control problems for the Stokes equations." In: *Comput. Math. Appl.* 69.4 (2015), pp. 319–336.

[Noo81] A. K. Noor. "Recent advances in reduction methods for nonlinear problems." In: *Comput. & Structures* 13.1-3 (1981), pp. 31–44.

[NP80] A. K. Noor and J. M. Peters. "Reduced basis technique for nonlinear analysis of structures." In: *AIAA Journal* 18.4 (1980), pp. 455–462.

[NS11] M. Neumüller and O. Steinbach. "Refinement of flexible space-time finite element meshes and discontinuous Galerkin methods." In: *Comput. Vis. Sci.* 14.5 (2011), pp. 189–205.

[NS13] M. Neumüller and O. Steinbach. "A DG space-time domain decomposition method." In: *Domain decomposition methods in science and engineering XX*. Vol. 91. Lect. Notes Comput. Sci. Eng. Springer, Heidelberg, 2013, pp. 623–630.

[NW06] J. Nocedal and S. J. Wright. *Numerical optimization*. Second. Springer Series in Operations Research and Financial Engineering. Springer, New York, 2006.

[OO13] C. O'Sullivan and S. O'Sullivan. "Pricing European and American options in the Heston model with accelerated explicit finite differencing methods." In: *Int. J. Theor. Appl. Finance* 16.3 (2013), pp. 1350015, 35.

[Oos03] C. W. Oosterlee. "On multigrid for linear complementarity problems with application to American-style options." In: *Electron. Trans. Numer. Anal* (2003), pp. 165–185.

[PGB15] B. Peherstorfer, P. Gómez, and H.-J. Bungartz. "Reduced models for sparse grid discretizations of the multi-asset Black-Scholes equation." In: *Adv. Comput. Math.* 41.5 (2015), pp. 1365–1389.

[Pir09] O. Pironneau. "Calibration of options on a reduced basis." In: *J. Comput. Appl. Math.* 232.1 (2009), pp. 139–147.

[Pir11] O. Pironneau. "Reduced basis for vanilla and basket options." In: *Risk and Decision Analysis* 2.4 (2011), pp. 185–194.

[Pir12] O. Pironneau. "Proper orthogonal decomposition for pricing options." In: *J. Comput. Finance* 16.1 (2012), pp. 33–46.

[PR06] A. T. Patera and G. Rozza. *Reduced Basis Approximation and A Posteriori Error Estimation for Parametrized Partial Differential Equations*. Tech. rep. Version 1.0, MIT 2006–2007, to appear in (tentative rubric) MIT Pappalardo Graduate Monographs in Mechanical Engineering. Massachusetts Institute of Technology, 2006.

[PRV+02] C. Prud'homme, D. V. Rovas, K. Veroy, and A. T. Patera. "A mathematical and computational framework for reliable real-time solution of parametrized partial differential equations." In: *M2AN Math. Model. Numer. Anal.* 36.5 (2002), pp. 747–771.

[QMN16] A. Quarteroni, A. Manzoni, and F. Negri. *Reduced basis methods for partial differential equations*. Vol. 92. Unitext. An introduction, La Matematica per il 3+2. Springer, Cham, 2016.

[QV94] A. Quarteroni and A. Valli. *Numerical approximation of partial differential equations*. Vol. 23. Springer Series in Computational Mathematics. Springer-Verlag, Berlin, 1994.

[RBm13] RBmatlab. *Matlab library, University of Stuttgart, University of Münster, University of Ulm*. `http://www.morepas.org`. Version 1.13.10. 2013.

[Rov03] D. Rovas. "Reduced-basis output bound methods for parametrized partial differential equations." PhD thesis. Massachusetts Institute of Technology, 2003.

[Roz05] G. Rozza. *Shape design by optimal flow control and reduced basis techniques: applications to bypass configurations in haemodynamics*. PhD thesis, EPFL, Lausanne, 2005.

[RV07] G. Rozza and K. Veroy. "On the stability of the reduced basis method for Stokes equations in parametrized domains." In: *Comput. Methods Appl. Mech. Engrg.* 196.7 (2007), pp. 1244–1260.

[Sco97] L. O. Scott. "Pricing stock options in a jump-diffusion model with stochastic volatility and interest rates: applications of Fourier inversion methods." In: *Math. Finance* 7.4 (1997), pp. 413–426.

[Sey09] R. U. Seydel. *Tools for computational finance*. Fourth. Universitext. Springer-Verlag, Berlin, 2009.

[Sig59] A. Signorini. "Questioni di elasticità non linearizzata e semilinearizzata." In: *Rend. Mat. e Appl. (5)* 18 (1959), pp. 95–139.

[Sma04] P. Smaragdis. “Non-negative Matrix Factor Deconvolution; Extraction of Multiple Sound Sources from Monophonic Inputs.” In: *Independent Component Analysis and Blind Signal Separation*. Vol. 3195. Lecture Notes in Comput. Sci. Springer Berlin Heidelberg, 2004, pp. 494–499.

[SS08] E. W. Sachs and M. Schu. “Reduced Order Models (POD) for Calibration Problems in Finance.” In: *Numerical Mathematics and Advanced Applications: Proceedings of ENUMATH 2007, the 7th European Conference on Numerical Mathematics and Advanced Applications, Graz, Austria, September 2007*. Berlin, Heidelberg: Springer Berlin Heidelberg, 2008, pp. 735–742.

[SS14] E. W. Sachs and M. Schneider. “Reduced-order models for the implied variance under local volatility.” In: *Int. J. Theor. Appl. Finance* 17.8 (2014), pp. 1450053, 23.

[SS91] E. M. Stein and J. C. Stein. “Stock Price Distributions with Stochastic Volatility: An Analytic Approach.” In: *Rev. Financ. Stud.* 4 (1991), pp. 727–752.

[SSS14] E. W. Sachs, M. Schneider, and M. Schu. “Adaptive trust-region POD methods in PIDE-constrained optimization.” In: *Trends in PDE constrained optimization*. Vol. 165. Internat. Ser. Numer. Math. Birkhäuser/Springer, Cham, 2014, pp. 327–342.

[SST04] W. Schoutens, E. Simons, and J. Tistaert. “A perfect calibration! Now what?” In: *Wilmott Magazine* (2004), pp. 66–78.

[Ste14] K. Steih. “Reduced basis methods for time-periodic parametric partial differential equations.” PhD thesis. University of Ulm, 2014.

[Ste15] O. Steinbach. “Space-time finite element methods for parabolic problems.” In: *Comput. Methods Appl. Math.* 15.4 (2015), pp. 551–566.

[SV10] E. W. Sachs and S. Volkwein. “POD-Galerkin approximations in PDE-constrained optimization.” In: *GAMM-Mitt.* 33.2 (2010), pp. 194–208.

[SW13] A. Schiela and D. Wachsmuth. “Convergence analysis of smoothing methods for optimal control of stationary variational inequalities with control constraints.” In: *ESAIM Math. Model. Numer. Anal.* 47.3 (2013), pp. 771–787.

[Top05] J. Topper. *Financial engineering with finite elements*. Vol. 319. John Wiley & Sons, 2005.

[UP14] K. Urban and A. T. Patera. "An improved error bound for reduced basis approximation of linear parabolic problems." In: *Math. Comp.* 83.288 (2014), pp. 1599–1615.

[Ver03] K. Veroy. "Reduced-Basis Methods Applied to Problems in Elasticity: Analysis and Applications." PhD thesis. Massachusetts Institute of Technology, 2003.

[VPR+03] K. Veroy, C. Prud'homme, D. V. Rovas, and A. T. Patera. "A Posteriori Error Bounds for Reduced-Basis Approximation of Parametrized Noncoercive and Nonlinear Elliptic Partial Differential Equations." In: *Proceedings of 16th AIAA computational fluid dynamics conference*. Paper 2003-3847. 2003.

[WAW01] G. Winkler, T. Apel, and U. Wystup. "Valuation of options in Heston's stochastic volatility model using finite element methods." In: *Foreign Exchange Risk*. Risk Publications, London, 2001, pp. 283–303.

[WDH93] P. Wilmott, J. Dewynne, and J. Howison. *Option Pricing: Mathematical Models and Computation*. Oxford: Oxford Financial Press, 1993.

[Wig87] J. B. Wiggins. "Option values under stochastic volatility: Theory and empirical estimates." In: *J. Financ. Econ.* 19.2 (1987), pp. 351–372.

[Wil01] P. Wilmott. *Paul Wilmott Introduces Quantitative Finance*. John Wiley & Sons, 2001.

[Woh00] B. I. Wohlmuth. "A mortar finite element method using dual spaces for the Lagrange multiplier." In: *SIAM J. Numer. Anal.* 38.3 (2000), pp. 989–1012.

[Woh01] B. Wohlmuth. *Discretization methods and iterative solvers based on domain decomposition*. Vol. 17. Lect. Notes Comput. Sci. Eng. Springer-Verlag, Berlin, 2001.

[Woh11] B. Wohlmuth. "Variationally consistent discretization schemes and numerical algorithms for contact problems." In: *Acta Numer.* 20 (2011), pp. 569–734.

[WW09] A. Weiss and B. Wohlmuth. "A posteriori error estimator and error control for contact problems." In: *Math. Comp.* 78.267 (2009), pp. 1237–1267.

[Yan14] M. Yano. "A space-time Petrov-Galerkin certified reduced basis method: application to the Boussinesq equations." In: *SIAM J. Sci. Comput.* 36.1 (2014), A232–A266.

[YPU14] M. Yano, A. T. Patera, and K. Urban. "A space-time *hp*-interpolation-based certified reduced basis method for Burgers' equation." In: *Math. Models Methods Appl. Sci.* 24.9 (2014), pp. 1903–1935.

[ZBV16] Z. Zhang, E. Bader, and K. Veroy. "A slack approach to reduced-basis approximation and error estimation for variational inequalities." In: *C. R. Math. Acad. Sci. Paris* 354.3 (2016), pp. 283–289.

[Zei90] E. Zeidler. *Nonlinear functional analysis and its applications. II/A*. Linear monotone operators. Springer-Verlag, New York, 1990.

[ZFV98] R. Zvan, P. Forsyth, and K. Vetzal. "Penalty methods for American options with stochastic volatility." In: *Journal of Computational and Applied Mathematics* 91.2 (1998), pp. 199 –218.